



HAL
open science

Ensemble density-functional theory : an ensemble perspective to target excited states and to palliate infamous deficiencies of standard ab initio methods

Clotilde Marut

► **To cite this version:**

Clotilde Marut. Ensemble density-functional theory : an ensemble perspective to target excited states and to palliate infamous deficiencies of standard ab initio methods. Material chemistry. Université Paul Sabatier - Toulouse III, 2023. English. NNT : 2023TOU30312 . tel-04585481

HAL Id: tel-04585481

<https://theses.hal.science/tel-04585481>

Submitted on 23 May 2024

HAL is a multi-disciplinary open access archive for the deposit and dissemination of scientific research documents, whether they are published or not. The documents may come from teaching and research institutions in France or abroad, or from public or private research centers.

L'archive ouverte pluridisciplinaire **HAL**, est destinée au dépôt et à la diffusion de documents scientifiques de niveau recherche, publiés ou non, émanant des établissements d'enseignement et de recherche français ou étrangers, des laboratoires publics ou privés.



THÈSE

En vue de l'obtention du
DOCTORAT DE L'UNIVERSITÉ DE TOULOUSE
Délivré par l'Université Toulouse 3 - Paul Sabatier

Présentée et soutenue par
Clotilde MARUT

Le 22 novembre 2023

La théorie de la fonctionnelle de la densité d'ensemble : une alternative pour décrire les états excités et pour pallier aux limitations des méthodes ab initio standard.

Ecole doctorale : **SDM - SCIENCES DE LA MATIERE - Toulouse**

Spécialité : **Physique**

Unité de recherche :
CEMES - Centre d'Elaboration de Matériaux et d'Etudes Structurales

Thèse dirigée par
Xavier BOUJU

Jury

Mme Lucia REINING, Rapporteur
M. Matthieu SAUBANÈRE, Rapporteur
Mme Maria HELLGREN, Examinatrice
M. Emmanuel FROMAGER, Examinateur
Mme Nadine HALBERSTADT, Examinatrice
M. Xavier BOUJU, Directeur de thèse

Ensemble Density-Functional Theory

An Ensemble Perspective to Target Excited States and to Palliate Infamous
Deficiencies of Standard Ab Initio Methods

Clotilde MARUT

2019-2023

Ensemble Density-Functional Theory

An Ensemble Perspective to Target Excited States and to Palliate Infamous Deficiencies of Standard Ab Initio Methods

Clotilde MARUT

Short abstract

This thesis is devoted to the implementation of ensemble density-functional theory (eDFT). Various formalisms of eDFT are explored and applied to small atomic and molecular systems: PPLB ensembles for the description of systems with fractional number of electrons, GOK ensembles to access neutrally excited states, and N -centered ensembles, which allow for the extraction of charged excitation energies, with no alteration of the number of electrons of the system. We will assess the performance of commonly used exchange-correlation functionals regarding the extraction of excitation energies, within the scope of eDFT. In particular, we will address some infamous deficiencies of standard approximations, such as the lack of derivative discontinuity, the violation of the piecewise-linearity exact-condition, the description of systems with fractional charge and fractional spin, and their practical implications on dissociation processes.

Keywords: Quantum chemistry, electronic structure, ensemble density-functional theory, Hartree-Fock theory, excitation energy, PPLB-DFT, GOK-DFT, N -centered eDFT, fractional spin, fractional charge

Résumé court

Cette thèse est consacrée à l'étude de la théorie de la fonctionnelle de la densité d'ensemble (eDFT) à travers différents formalismes et leur application à des systèmes atomiques et moléculaires : les ensembles PPLB pour la description de systèmes avec un nombre fractionnaire d'électrons, les ensembles GOK pour accéder aux états excités, et les ensembles N -centrés qui permettent d'extraire des énergies d'excitation chargée, sans altération du nombre d'électrons. Nous évaluerons la performance des fonctionnelles standard d'échange-corrélation vis-à-vis de l'extraction d'énergies d'excitation à travers l'eDFT. En particulier, nous discuterons certaines des limitations les plus connues de ces approximations standard, telles que l'absence de dérivée discontinue, la violation de la condition exacte de linéarité par morceaux, la description des systèmes avec charge ou spin fractionnaires et leur impact dans les processus de dissociation.

Mots-clés: Chimie quantique, structure électronique, théorie de la fonctionnelle de la densité d'ensemble, méthode de Hartree-Fock, énergie d'excitation, PPLB-DFT, GOK-DFT, eDFT N -centrée, spin fractionnaire, charge fractionnaire

*I'm not a man of too many faces
The mask I wear is one
But those who speak know nothing
And find out to their cost*

Sting
(Shape of My Heart)

Remerciements

Je voudrais tout d'abord remercier les membres du jury d'avoir accepté de prendre part à l'évaluation de mon travail de thèse et d'avoir fait le déplacement jusqu'à Toulouse pour assister à ma soutenance de thèse, les échanges qui en ont découlé ont été grandement appréciés. Je souhaiterais également remercier Nadine Halberstadt et Pierre Pujol pour leurs prises de position et le soutien qu'ils m'ont témoigné.

Enfin, j'adresse mes remerciements sincères et appuyés à Xavier Bouju avec qui j'ai d'abord eu le plaisir de travailler lors d'un stage de fin d'études et qui m'a ensuite soutenue et accompagnée durant ma thèse.

Pour moi, me consacrer à de longues études scientifiques parachevées par un travail de thèse long et rigoureux relevait avant tout d'une exigence personnelle et d'un besoin de m'accomplir intellectuellement. Mais faire une thèse ne se résume pas à un travail scientifique, c'est aussi un séjour de plusieurs années dans un monde très fermé et exagérément fantasmé.

Beaucoup s'imaginent, souvent naïvement, que le milieu de la recherche et, de fait, le métier de chercheur vont nécessairement de pair avec une certaine exemplarité, un haut sens déontologique et une incarnation sans faille de valeurs et de principes nobles en toutes circonstances, mais la réalité de ce milieu s'avère bien moins reluisante.

Alors que je débutais mes études et m'interrogeais déjà sur la réalité du métier de chercheur et ma légitimité à poursuivre dans cette voie, un enseignant-chercheur avait alors accepté de témoigner avec beaucoup de sincérité de son parcours personnel dans ce milieu, et avait terminé son propos par une mise en garde qui, des années plus tard, prend tout son sens maintenant que j'ai pu constater par moi-même cette même réalité :

“Le monde de la recherche (ou le champ de la recherche comme dirait Bourdieu) est un monde comme les autres, avec :

- ses petits chefs ;
- ses luttes de pouvoir ;
- ses égos surdimensionnés (beaucoup dans la recherche) ;
- ses coups bas ;
- etc.

Bien que les gens se consacrent à une cause noble, la science avec un grand S, beaucoup se comportent comme le commun des mortels. Cette découverte fût ma première désillusion quand j’ai débuté.”

Pour compléter ce propos, j’ajouterais qu’à une époque où il est pourtant de bon ton de condamner publiquement toute forme de harcèlement moral et de comportements inappropriés et sexistes, en interne ce sont plutôt l’opacité, l’impunité et la connivence qui prévalent, et l’usage d’intimidation et de représailles sont des pratiques qui ne choquent personne. Après tout, quoi de plus commode que d’utiliser le diplôme de quelqu’un pour faire pression et pour le ou la contraindre au silence, tant que cela permet de ne pas “perdre la face” et les financements qui vont avec. . .

*Des élites autoproclamées
Qui confondent privilèges et mérite
Se parent de leurs plus beaux tweets
Mais ne s’encombrent pas de principes*

Abstract

Over the last few decades, density-functional theory (DFT) has proved to be a rigorous approach for describing the ground-state of any electronic system. Due to a relatively low computational cost and the elaboration of sophisticated density-functional approximations (DFAs), DFT became the prevailing method used in electronic-structure calculations. Still, there remain numerous challenges that standard DFAs fail to overcome. These limitations are not attributed to failures of the theory itself but are rather due to deficiencies of the currently used approximate exchange-correlation (xc) functionals. There exists a generalization of ground-state DFT to fractional occupation numbers which allows for the description of systems with fractional number of electrons, PPLB-DFT. Such grand canonical extension of DFT can be achieved through the use of the ensemble formalism and enables direct extraction of charged excitation energies and other properties from a single DFT-like calculation. Unfortunately, the inability of commonly used exchange-correlation DFAs to mimic the infamous derivative discontinuity (DD) has proved to be highly detrimental to the prediction of charged excitations such as ionization potentials and electron affinities, yielding substantial errors, and known as the fundamental-gap problem. Regarding this matter, ensemble DFT (eDFT) offers a very appealing alternative benefiting from the possibility for explicitly weight-dependent xc-functionals to mimic the infamous DD through their derivatives with respect to the ensemble weights. DFT is known to possess deficiencies when it comes to computing charged and neutral excitations. The most popular way to access neutrally excited states within the scope of DFT is through its time-dependent extension, TD-DFT. Indeed, one would usually turn to TD-DFT to get accurate transition energies for low-lying excited-states with a relatively moderate computational cost. Although TD-DFT has been incredibly successful to access neutral excitation energies, it still suffers from some limitations and fails to provide accurate descriptions of some phenomena and properties. eDFT constitutes a promising alternative to TD-DFT for computing electronic excitation energies. In eDFT, it is possible to extract any neutral excitation energies of a N -electron system from a single calculation through the use of a Gross-Oliveira-Kohn (GOK) ensemble, with a similar computational cost and level of approximation for the xc-functional than in an usual DFT calculation. GOK-DFT is a less well-known but comparably rigorous alternative to TD-DFT where the large choice of ensemble weights and the weight-dependence of DFAs can significantly impact the accuracy of the energies. In DFT, it is well-known that the HOMO-LUMO gap can be a very poor estimation of the fundamental gap of the system, whereas eDFT may provide better predictions. Nevertheless, accessing charged excitations

usually require to vary the number of electrons of the system, which can be problematic for some systems. Very recently, a new canonical eDFT formalism has been developed, the N -centered formalism, which allows for the extraction of charged excitation energies without any alteration of the number of electrons of the system. The behaviour of standard approximations in the scope of eDFT may provide additional insight into the intrinsic systematic errors of DFAs, such as the violation of the piecewise-linearity and constancy-condition exact properties. Indeed, poor descriptions of systems with fractional charges and fractional spins have shown to have major implications on the description of strongly correlated systems, which are known to suffer from large static-correlation errors, as well as on the prediction of asymptotic integer dissociations and band-gap predictions. These considerations may lead the way to further development and refinement of the DFT scheme towards both current and emerging applications.

Résumé

Au cours des dernières décennies, la théorie de la fonctionnelle de la densité (DFT) s'est imposée comme une approche rigoureuse pour la description de l'état fondamental des systèmes électroniques. Grâce à son faible coût computationnel et à l'élaboration d'approximations sophistiquées pour la fonctionnelle d'échange-corrélation (xc-DFA), la DFT est devenue la méthode de choix pour le calcul de structure électronique. Néanmoins, il subsiste nombre de défis que la DFT ne parvient pas à surmonter. En réalité, ces carences ne sont pas le fruit de la théorie elle-même mais plutôt du fait de défauts intrinsèques des approximations utilisées. Il existe une formulation plus générale de la DFT pour les nombres fractionnaires d'occupation qui permet la description de systèmes avec nombre fractionnaire d'électrons, la PPLB-DFT. Cette formulation grand canonique de la DFT peut être mise en place à l'aide d'un formalisme d'ensemble et permet une extraction directe d'énergies d'excitation chargée et d'autres propriétés à partir d'un seul calcul de type DFT. Malheureusement, l'incapacité des DFAs à reproduire la fameuse dérivée discontinue (DD) s'est avérée être particulièrement préjudiciable pour la prédiction d'énergies d'excitation chargée, telles que les potentiels d'ionisation et les affinités électroniques, donnant lieu à des erreurs conséquentes, et connue comme le problème du gap fondamental. Dans ce contexte, la DFT d'ensemble (eDFT) offre une alternative très attrayante du fait de sa capacité à user de DFAs dépendantes du poids de l'ensemble pour reproduire la DD via leur dérivée. La DFT est connue pour montrer des limites vis-à-vis du calcul d'énergies d'excitation chargée et neutre. La procédure standard pour accéder aux états excités neutralement dans le cadre de la DFT est à travers son extension dépendante du temps, la TD-DFT. En effet, l'usage est de recourir à la TD-DFT pour obtenir des prédictions acceptables pour les énergies de transition des niveaux excités les plus bas, cela avec un coût computationnel relativement modéré. Bien que la TD-DFT se soit avérée incroyablement fructueuse pour accéder aux énergies d'excitation neutre, elle a également montré certaines limites lors de la description de certains phénomènes et propriétés physiques. En cela, l'eDFT constitue une alternative prometteuse à la TD-DFT pour le calcul des énergies d'excitation électroniques. En eDFT, il est possible d'extraire n'importe quelle énergie d'excitation neutre d'un système électronique en un seul calcul à l'aide d'un ensemble Gross-Oliveira-Kohn (GOK), et cela avec un coût computationnel et un niveau d'approximation pour la fonctionnelle d'xc, similaires à ceux de la DFT standard. La GOK-DFT est une alternative moins connue mais tout autant rigoureuse que la TD-DFT, où le large choix de poids de l'ensemble et la dépendance en poids de la fonctionnelle xc peuvent significativement influencer sur la qualité des énergies calculées. En temps normal,

accéder aux énergies d'excitation chargée nécessite de faire varier le nombre d'électrons du système, ce qui peut s'avérer problématique dans certains cas. Très récemment, un nouveau formalisme canonique a été développé, l'eDFT N -centrée, rendant possible l'extraction d'énergies d'excitation chargée sans altération du nombre d'électrons. Le comportement des DFAs standard dans le cadre de l'eDFT peut offrir une compréhension plus poussée de la nature intrinsèque des erreurs systématiques dont elles souffrent, telles que la violation des conditions exactes de linéarité par morceaux et de constance de l'énergie. En outre, la mauvaise description des systèmes avec charge et spin fractionnaires a prouvé avoir un impact majeur dans la description des systèmes fortement corrélés ainsi que dans les processus de dissociation et la prédiction de gaps d'énergie. Tout cela pourrait donner un nouvel essor au développement futur de la DFT et à des applications émergentes jusqu'alors inaccessibles.

Contents

List of Acronyms	XIII
Introduction	1
Ensemble Density-Functional Theory	1
Numerical Details	3
Thesis Structure	3
I Quantum Chemistry, Context and Standard Methods	5
1 Quantum Chemistry	7
1.1 Electronic-Structure Theory	7
1.2 The Many-Electron Problem	14
2 Hartree-Fock Theory	25
2.1 The Hartree-Fock Ansatz for the Wave function	25
2.2 The Hartree-Fock Approximation	28
2.3 The Basis-Set Formulation	35
2.4 The Self-Consistent-Field Scheme	45
3 Density-Functional Theory	47
3.1 Early Stages of Density-Functional Theory	48
3.2 Density-Functional Theory Fundamental Idea	51
3.3 Kohn and Sham Approach	54
3.4 The Basis-Set Formulation of DFT	58
3.5 Spin Density-Functional Theory	60
3.6 Exchange-Correlation Energy	63
II eDFT: an Alternative Approach to Access Excitation Energies and to Palliate Infamous Deficiencies of Standard Methods	67

4	PPLB Ensembles to Target Charged Excitations	69
4.1	Introduction: DFT for Open Systems	70
4.2	Perdew-Parr-Levy-Balduz Density-Functional Theory Formalism	83
4.3	Numerical Implementation of PPLB-DFT	95
5	GOK Ensembles to Target Neutral Excitations	129
5.1	Introduction: Excited States in Quantum Chemistry	129
5.2	Gross-Oliveira-Kohn Density-Functional Theory Formalism	131
5.3	Numerical Implementation of GOK-DFT	141
6	N-centered Ensembles: a Canonical Formalism for Charged Excitations	161
6.1	Introduction: Charged Excitations	161
6.2	N -centered Ensemble Density-Functional Theory	163
6.3	Numerical Implementation of N -centered Density-Functional Theory	174
6.4	Extended N -centered Ensembles: Combining Charged and Neutral Excitation Energies	200
7	Fractional-Charge Error, Fractional-Spin Error and How They Can Emerge from Dissociation Processes	209
7.1	Introduction: Fractional-Charge and Fractional-Spin Errors	209
7.2	Fractional-Dissociation Problem	210
7.3	Fractional-Spin Error	217
	Conclusion	231
A	Experimental Ionization Potentials, Electron Affinities and Fundamental Gaps of Neutral Atomic Systems	233
B	PPLB-DFT Supplementary Material	235
B.1	PPLB-DFT Code Testing	235
B.2	Overview of PPLB-DFT Results with CC-functionals	238
C	GOK-DFT Supplementary Material	243
C.1	GOK-DFT Code Testing	243
C.2	Proof of Correctness of the GOK-DFT Numerical Results	246
D	N-centered eDFT Supplementary Material	247
D.1	N -centered eDFT Code Testing	247
D.2	Overview of Left and Right N -centered Results with CC-Functionals	250
E	Résumé substantiel en français	253
	Bibliography	279

List of Acronyms

AO Atomic Orbital.

CC Curvature-Corrected.

CI Configuration Interaction.

DD Derivative Discontinuity.

DDE Density-Driven Error.

DFA Density-Functional Approximation.

DFT Density-Functional Theory.

EA Electron Affinity.

eDFT Ensemble Density-Functional Theory.

EEXX Ensemble Exact Exchange.

EXX Exact Exchange.

FCI Full Configuration Interaction.

FDE Functional-Driven Error.

FUEG Finite Uniform Electron Gas.

GGA Generalized Gradient Approximation.

GHF Generalized Hartree-Fock.

GKS Generalized Kohn-Sham.

GOK Gross-Oliveira-Kohn.

HF Hartree-Fock.

- HOMO** Highest-Occupied Molecular Orbital.
- Hxc** Hartree-Exchange-Correlation.
- IP** Ionization Potential.
- KS** Kohn-Sham.
- LDA** Local Density Approximation.
- LIM** Linear Interpolation Method.
- LSDA** Local Spin Density Approximation.
- LUMO** Lowest-Unoccupied Molecular Orbital.
- LZ** Levy-Zahariev.
- MO** Molecular Orbital.
- OEP** Optimized Effective Potential.
- PPLB** Perdew-Parr-Levy-Balduz.
- RHF** Restricted Hartree-Fock.
- SCF** Self-Consistent Field.
- STO** Slater-Type Orbital.
- TD-DFT** Time-Dependent Density-Functional Theory.
- TD-HF** Time-Dependent Hartree-Fock.
- TF** Thomas-Fermi.
- TFD** Thomas-Fermi-Dirac.
- UEG** Uniform Electron Gas.
- UHF** Unrestricted Hartree-Fock.
- XC** Exchange-Correlation.

Introduction

Ensemble Density-Functional Theory

Over the last few decades, density-functional theory (DFT), in its Kohn-Sham (KS) formulation, has proved to be a rigorous approach for describing the ground-state of any electronic system. Due to a relatively low computational cost and the elaboration of sophisticated functional approximations, DFT became the prevailing method used in electronic-structure calculations. This plebiscite stems from the practical observation that simple approximations perform remarkably well for a wide range of problems in chemistry and physics. As a matter of fact, the success or failures of DFT is based on the quality of the density-functional approximation (DFA).

There exists a formally-exact generalization of ground-state Kohn-Sham DFT (KS-DFT) for electronic states with fractional occupation numbers which allows for the description of open-systems with fractional number of electrons, PPLB-DFT. Such grand canonical extension of KS-DFT can be achieved through the use of the ensemble formalism and enables direct extraction of charged excitation energies and other properties from a single DFT-like calculation.

Unfortunately, the inability of commonly used exchange-correlation (xc) approximate functionals to mimic the famous derivative discontinuity of the exact potential has proved to be highly detrimental to the accurate prediction of charged excitations such as ionization potentials and electron affinities, yielding substantial errors and known as the fundamental-gap problem.

Regarding this matter, ensemble DFT (eDFT) offers a very appealing alternative benefiting from the possibility for explicitly weight-dependent xc-functionals to mimic the infamous derivative discontinuity through their derivatives with respect to the weights of the ensemble. In that sense, eDFT functionals may offer more stable and accurate predictions for excitation energies.

DFT is known to possess deficiencies when it comes to computing charged and neutral excitations. The most popular way to access neutral excited states within the scope of DFT is through its time-dependent (TD) extension, TD-DFT. Indeed, to circumvent these limitations, one would usually turn to TD-DFT to get accurate transition energies for low-lying excited-states with a relatively moderate computational cost.

Although TD-DFT has been incredibly successful to access neutral excitation energies, it still suffers from some limitations and fails to provide accurate descriptions of some phenomena and properties. For instance, within this time-dependent formalism, double excitations are completely absent from the spectra of TD-DFT and the quality of the excitation energies highly depends on the choice of the exchange-correlation functional which is usually treated in the standard adiabatic approximation.

Ensemble density-functional theory constitutes a promising alternative to TD-DFT for computing electronic excitation energies. In eDFT, it is possible to extract any neutral excitation energies of a N -electron system from a single calculation through the use of a Gross-Oliveira-Kohn (GOK) ensemble, with a similar computational cost and level of approximation for the exchange-correlation functional than in an usual pure-state DFT calculation.

GOK-DFT is a less well-known but comparably rigorous alternative to TD-DFT where the large choice of ensemble weights and the weight-dependence of approximate functionals can significantly impact the accuracy of the energies. These considerations are essential for the development of accurate functionals for ensemble applications.

In DFT (and PPLB-DFT), it is well-known that the Kohn-Sham gap (or HOMO-LUMO gap) can be a very poor estimation of the fundamental gap of the physical system but, within the scope of eDFT, it is possible to significantly improve the quality of this estimation through the infamous derivative discontinuity which can be directly connected to the weight-dependence of the xc-functional.

While this improvement can be quite consequent for small finite systems, it is still problematic when it comes to large periodic systems, like crystalline solids. Indeed, for such systems, extracting charged excitations will require to induce a same small variation of the number of electrons in every unit cell of the system which will inexorably lead to an infinitely large charge for the whole system.

Very recently, a new canonical eDFT formalism has been developed, the N -centered formalism, which allows for the extraction of charged excitation energies without any alteration of the number of electrons of the physical open system.

The extension of DFT to fractional charges and fractional spins has led to the development of exact conditions such as the piecewise linearity of the energy and the constancy condition that must be satisfied by exchange-correlation functionals. Exact conditions have helped unravel and understand limitations of commonly used DFAs that still exhibit large systematic errors such as localization or delocalization errors and static correlation errors. As a matter of fact, the tendency of commonly used functionals to fail to obey those two exact-constraint has been proven to have widespread implications.

Many massive failures of DFAs can be formalized and understood through the concept of fractional charges and fractional spins whose descriptions lead to errors that manifest themselves in a wide range of applications, from the simplest atomic and molecular systems to more challenging systems. Indeed, poor descriptions of fractional spins and fractional charges have shown to have major implications on the description of strongly correlated systems, which are known to suffer from large static-correlation errors, as well as on the prediction of asymptotic

integer dissociations and band-gap predictions.

Present-day DFAs already make DFT widely applicable to a variety of many-electron systems in physics, chemistry and material science, but there remain numerous challenges that common DFAs fail to overcome. These limitations are not attributed to failures of the theory itself but are rather due to deficiencies of the currently used approximate exchange-correlation functionals and, therefore, designing functionals that would properly encompass exact-conditions while remaining universally applicable constitutes a challenging task.

We believe that the behaviour of current standard approximations in the scope of ensemble applications may provide additional insight into the intrinsic systematic errors of approximate functionals and lead the way to further development and refinement of the DFT scheme towards both current and emerging applications. We will discuss and present those various eDFT formalisms through their application to very simple systems.

Numerical Details

In order to perform self-consistent ensemble calculations at both Hartree-Fock and DFT levels, an ensemble DFT code was implemented in Fortran during this PhD: the QuAcK eDFT code. The QuAcK software is a quantum chemistry package written in Fortran that includes an eDFT module which can perform self-consistent ensemble calculations with a large variety of approximations.

All results were computed using the QuAcK eDFT Fortran Code and/or Mathematica 12.0 and 13.0. Unless otherwise stated, calculations were performed in an unrestricted formalism with the QuAcK eDFT software and the convergence threshold of the self-consistent calculations was set to 10^{-5} . Atomic units are used throughout.

Thesis Structure

The thesis is organized as follows.

Part **I** discusses the foundations of quantum chemistry and focuses on the development of two of the major ab initio methods that form cornerstones of computational chemistry.

Chapter **1** gives a brief overview of the main problematics and fundamental concepts of quantum chemistry regarding electronic-structure calculations. Concepts such as the many-body wave function, the Schrödinger equation and the many-body problem are discussed.

The Hartree-Fock theory and its formalism, which is a pillar of quantum chemistry computational methods, are extensively introduced in Chapter **2**.

Chapter **3** is devoted to density-functional theory which became over the last decades the prevailing post-Hartree-Fock approach for calculation of physical and chemical properties of matter.

Part II of this manuscript is devoted to ensemble DFT and its numerical implementation and application to simple real atomic and molecular systems.

Chapter 4 makes the connection between standard DFT and ensemble DFT through its extension to systems with fractional numbers of electrons, PPLB-DFT, and its performance regarding charged excitation energies.

As for neutral excitation energies, Chapter 5 presents a second ensemble DFT formalism dedicated to neutrally excited states, GOK-DFT.

Turning back to charged excitations, Chapter 6 presents a quite-recent eDFT canonical ensemble formalism which benefits from the practical advantage to give access to charged excitations with no alteration of the number of electrons of the physical system.

Finally, Chapter 7 details the concept of fractional-charge and fractional-spin errors which can be formalized by use of the ensemble formalism, and have shown to have widespread implications in electronic-structure calculations.

For each ensemble formalism discussed in this work, supplementary materials, such as additional results and numerical proof of correctness of the eDFT computational code, are available in the Appendix of this manuscript (see Appendices B, C and D), as well as experimental references (see Appendix A) of the properties of interest.

Part I

Quantum Chemistry, Context and Standard Methods

Chapter 1

Quantum Chemistry

Contents

1.1 Electronic-Structure Theory	7
1.1.1 Some Context	7
1.1.2 Description of the State of the System	8
1.1.3 The Dirac Notation	9
1.1.4 The Schrödinger Equation	12
1.2 The Many-Electron Problem	14
1.2.1 The “Exact” versus “Approximate” Dilemma	14
1.2.2 The Variation Method	17
1.2.3 The Born-Oppenheimer Approximation	19

1.1 Electronic-Structure Theory

1.1.1 Some Context

The aim of Quantum Chemistry [39, 35, 58] is to accurately predict the behavior and properties of atoms, molecules or materials which are composed of interacting electrons and nuclei. Many important properties and phenomena can be explained and predicted through knowledge and good comprehension of those interactions. Electronic-structure theory is one of the central topics of quantum chemistry and focuses on the behavior of the electrons in order to explain and predict the reactivity or chemical and physical properties of matter. Whereas we use Newton’s equations when we need to study the motion of classical particles, when it comes to quantum particles, like electrons, it is quantum mechanics that one must resort to. First, let us recall some basic principles of the quantum mechanics formalism that we will need in that study.

1.1.2 Description of the State of the System

The wave function

In quantum mechanics [84], all the information about the physical state of an electronic system is encompassed into a mathematical object known as the “wave function” Ψ of the system. For a given electronic system, in the non-relativistic framework, the wave function will be a complex-valued function and will depend on all the space and spin coordinates of the N electrons of the system.

$$\Psi \equiv \Psi(\mathbf{x}_1, \mathbf{x}_2, \dots, \mathbf{x}_N) = \Psi(\mathbf{r}_1, \sigma_1, \mathbf{r}_2, \sigma_2, \dots, \mathbf{r}_N, \sigma_N), \quad (1.1)$$

where $\mathbf{r}_i \in \mathbb{R}^3$, $\sigma_i \in \{\uparrow; \downarrow\} \equiv \{+\frac{1}{2}; -\frac{1}{2}\}$ and $\mathbf{x}_i = (\mathbf{r}_i, \sigma_i)$ are respectively the space-coordinate vector, the spin coordinate and the combined space-spin coordinate vector of electron $i \in \llbracket 1; N \rrbracket$. Hence, the wave function fully describing the quantum state of the system depends on $4N$ coordinates, $3N$ space coordinates and N spin coordinates. The set of all realizable wave functions accessible to the system is called a “Hilbert space” \mathcal{H} .

The Pauli exclusion principle

Since electrons are fermions, which are particles with half-integer spins, the electronic wave function must obey the “Pauli exclusion principle” which states that two electrons cannot occupy the same quantum state simultaneously. Thus, the electronic wave function must be antisymmetric with respect to the permutation of any pair of electrons, meaning permutation of both space and spin coordinates

$$\Psi(\mathbf{x}_1, \mathbf{x}_2, \dots, \mathbf{x}_i, \dots, \mathbf{x}_j, \dots, \mathbf{x}_N) = -\Psi(\mathbf{x}_1, \mathbf{x}_2, \dots, \mathbf{x}_j, \dots, \mathbf{x}_i, \dots, \mathbf{x}_N). \quad (1.2)$$

Although this abstract quantity does not actually possess any physical meaning and is rather a purely statistical object, it can be seen as a probability amplitude and therefore must be square integrable and normalized

$$\int \dots \int |\Psi(\mathbf{x}_1, \mathbf{x}_2, \dots, \mathbf{x}_N)|^2 d\mathbf{x}_1 d\mathbf{x}_2 \dots d\mathbf{x}_N = 1. \quad (1.3)$$

Note that the previous integration includes integration over all space coordinates plus summation over all spin values. The knowledge of the wave function unravel the path to many other quantities, some of which contain much more physical meaning.

The electron density

The primary quantity that we will use in this work is the “electron density” of the system

$$n(\mathbf{r}) = N \int \dots \int |\Psi(\mathbf{r}, \sigma, \mathbf{x}_2, \dots, \mathbf{x}_N)|^2 d\sigma d\mathbf{x}_2 \dots d\mathbf{x}_N, \quad (1.4)$$

which represents the probability density of finding any electron in an infinitesimal element of volume $d\mathbf{r}$ at position \mathbf{r} .

Note that the electron density is a much simpler quantity than the wave function since it only depends on 3 coordinates, $\mathbf{r} \in \mathbb{R}^3$, no matter the size of the system (meaning the total number of electrons).

Since we know that there are N electrons spread out over all the accessible space region, it is only logical that if one extends the search to all this space one will ultimately find the N electrons. For that reason, the electron density must be normalized to the number of electrons of the system

$$\int_{\mathbb{R}^3} n(\mathbf{r})d\mathbf{r} = N. \quad (1.5)$$

But for now let us stay with the wave function Ψ .

In this chapter, we chose to first introduce the notion of wave function in the space-spin representation as it is a simple mathematical function $\Psi(\mathbf{r}, \sigma)$. Actually, there exists a much general representation of the wave function which is based on linear algebra and which we will need in order to proceed through the following sections: the “Dirac notation”.

For the sake of clarity we will restrict the following explanation to the case of a single-electron system and will also neglect its spin coordinate.

1.1.3 The Dirac Notation

Bra and ket

In quantum mechanics, the state Ψ of an electronic system will be represented by a “ket” vector $|\Psi\rangle$, which is a column vector. Similarly, there also will be a “bra” vector $\langle\Psi|$, which is a row vector and whose components are the complex conjugates of the ones of the corresponding ket $|\Psi\rangle$. Similarly to the wavefunction $\Psi(\mathbf{r}, \sigma)$, which was normalized in the space-spin representation, those two vectors will also be normalized

$$\langle\Psi|\Psi\rangle = 1. \quad (1.6)$$

This operation can be applied to any bra $\langle\Psi|$ and ket $|\Phi\rangle$ of the Hilbert space defined previously and is called an “inner product”. In the space representation, it is equivalent to a simple integral formulation

$$\langle\Psi|\Phi\rangle = \int_{\mathbb{R}^3} \Psi^*(\mathbf{r})\Phi(\mathbf{r})d\mathbf{r}. \quad (1.7)$$

Moreover, the wave function $\Psi(\mathbf{r})$ defined previously is just the component, or projection, of the ket $|\Psi\rangle$ into the space representation

$$\Psi(\mathbf{r}) = \langle\mathbf{r}|\Psi\rangle. \quad (1.8)$$

So far we have seen the formalism used to describe the state of the system but what about its properties?

Observable and operator

In quantum mechanics, any physical measurable property \mathcal{A} is called an “observable” and is associated with a linear and hermitian, or self-adjoint, “operator” \hat{A} which must verify the following property

$$\hat{A}^\dagger = \hat{A}. \quad (1.9)$$

If the system was originally in the state $|\Psi\rangle$, measuring the property \mathcal{A} will consist in applying the hermitian operator \hat{A} associated with that property to the left-side of $|\Psi\rangle$.

One of the most infamous oddities of quantum mechanics is that any measurement will influence the state of the system. Therefore it may result for the system to be in a new quantum state $|\Psi'\rangle$, meaning different than the initial state, once measurement is done

$$\hat{A}|\Psi\rangle = |\Psi'\rangle. \quad (1.10)$$

Eigenvalue equation

The only realizable values that one can observe during a measurement of the property \mathcal{A} are the “eigenvalues” $\{a_i\}$ associated with the operator \hat{A} , and are the solutions of the following “eigenvalue equation”

$$\hat{A}|\varphi_i\rangle = a_i|\varphi_i\rangle. \quad (1.11)$$

Since we want to measure real physical properties, meaning classical properties, it may not seem surprising to state that any hermitian operators associated with those observables must possess real eigenvalues $\{a_i\} \in \mathbb{R}$.

The states $\{|\varphi_i\rangle\}$ that satisfy this equation are called “eigenstates” of the operator \hat{A} and can be chosen to form an orthonormal basis

$$\langle\varphi_i|\varphi_j\rangle = \int_{\mathbb{R}^3} \varphi_i^*(\mathbf{r})\varphi_j(\mathbf{r})d\mathbf{r} = \delta_{ij}, \quad (1.12)$$

where δ_{ij} is the “Kronecker delta symbol”, which has the value $\delta_{ij} = 1$ when $i = j$ and $\delta_{ij} = 0$ when $i \neq j$.

For the sake of simplicity, we will only consider the case of non-degenerate solutions which implies that for each eigenvalue a_i there will exist only one eigenstate $|\varphi_i\rangle$, solution of the eigenvalue equation.

Note that the number of solutions of the eigenvalue equation of an hermitian operator can be infinite, thus the orthonormal basis formed by its eigenstates $\{|\varphi_i\rangle\}$ would be of infinite dimension. The basis $\{|\varphi_i\rangle\}$ is said to be “complete” in the sense that any state of the Hilbert space $|\Psi\rangle \in \mathcal{H}$ can be uniquely expanded in terms of the normalized eigenstates such that

$$|\Psi\rangle = \sum_{i=1}^{\infty} c_i |\varphi_i\rangle, \quad (1.13)$$

where $\{c_i\}$ is a unique set of complex coefficients.

Those eigenstates are in fact the only physical states of the system that will not be changed

due to measurement. If the system were initially in one of the eigenstate $|\varphi_i\rangle$ of the operator \hat{A} , it would still be in that same eigenstate after measurement. One of the specificities of the eigenstates of a hermitian operator is that in this particular basis, $\{|\varphi_i\rangle\}$, the matrix representation \mathbf{A} of the operator \hat{A} will be diagonal and its main diagonal elements will actually be the eigenvalues $\{a_i\}$

$$\mathbf{A} = \begin{pmatrix} a_1 & 0 & \dots & 0 \\ 0 & a_2 & & \vdots \\ \vdots & & \ddots & 0 \\ 0 & \dots & 0 & a_\infty \end{pmatrix}_{\{|\varphi_i\rangle\} \times \{|\varphi_i\rangle\}} . \quad (1.14)$$

In that sense, solving an eigenvalue problem will often consist in finding the orthonormal basis in which the matrix representation of the operator is diagonal.

At this point, there is still one last notion that we need to discuss before moving on to the next subsection: the “expectation value”.

Expectation value

We have seen that the only possible outcomes for the measurement of a property are the eigenvalues associated with its hermitian operator. But because the quantum world is a probabilistic world, the fact is that the result of the measurement would still be totally random and one would not be able to predict with certainty which of the eigenvalues one would obtain.

The expectation value of an observable \mathcal{A} is the statistical average value that one would expect to obtain if one were to do a large amount of measurements on the same quantum state $|\Psi\rangle$. Using the Dirac notation and the corresponding space representation, the expectation value of an observable \mathcal{A} is defined as follows

$$\langle \hat{A} \rangle_\Psi \equiv \frac{\langle \Psi | \hat{A} | \Psi \rangle}{\langle \Psi | \Psi \rangle} = \frac{\int \Psi^*(\mathbf{r}) \hat{A} \Psi(\mathbf{r}) d\mathbf{r}}{\int \Psi^*(\mathbf{r}) \Psi(\mathbf{r}) d\mathbf{r}} . \quad (1.15)$$

As a matter of fact, the electron density (1.4) introduced in the previous section is itself the expectation value of an observable associated with a hermitian operator.

For a N -electron system in the normalized state $|\Psi\rangle$, the electron density $n(\mathbf{r})$ is defined as the expectation value of the observable associated with the density operator $\hat{n}(\mathbf{r})$ such that

$$n(\mathbf{r}) = \langle \Psi | \hat{n}(\mathbf{r}) | \Psi \rangle , \quad (1.16)$$

with

$$\hat{n}(\mathbf{r}) = \sum_k^N \delta(\mathbf{r} - \mathbf{r}_k) , \quad (1.17)$$

where $\{\mathbf{r}_k\}$ are the space coordinate vectors of the N electrons, and $\delta(x)$ is the “Dirac delta function” which has the value $\delta(x) = 1$ when $x = 0$, and $\delta(x) = 0$ when $x \neq 0$.

There exist numerous properties, and so as many observables, that quantum chemists and physicists are interested in and would like to accurately predict depending on their field of work: position, spin, electric dipole momentum... but the one for which they would probably all share a common interest would be the total energy of the system.

1.1.4 The Schrödinger Equation

The time-independent Schrödinger equation

The hermitian operator associated with the total-energy observable of an electronic system is called the “Hamiltonian” \hat{H} and will take different forms depending on the characteristics of the system, the nature of the interactions involved, the environment in which it is placed... If one applies the formalism introduced in the previous subsection 1.1.3, one deduces that the only possible outcomes for a measurement of the total energy E of an electronic system will be the sets of eigenvalues associated with the hermitian energy operator, the Hamiltonian \hat{H} . Moreover, the eigenvalue equation associated with the Hamiltonian operator is a very crucial equation in quantum mechanics and is known as the “time-independent Schrödinger equation”

$$\hat{H} |\Psi\rangle = E |\Psi\rangle , \quad (1.18)$$

where Ψ is the wave function associated with the quantum state of the electronic system. The eigenstates and eigenvalues of the time-independent Schrödinger equation are usually referred to as the “stationary states” and “energy levels” of the system, respectively.

The energy spectrum

When we have introduced the notion of eigenvalues in 1.1.3, we have assumed that they were discrete quantities but, as a matter of fact, there exist situations and operators for which the eigenvalues form a continuous set. For an electronic system, the set of eigenvalues associated with the Hamiltonian operator is called the “energy spectrum” and represents all the realizable values for the total energy of the system. There are three possible scenarios [88, 5] to consider:

- The energy spectrum of the system is discrete which means that the eigenvalues of the time-independent Schrödinger equation will consist of a discontinuous, possibly infinite, set of values $\{E_n\}$, with $n \in \mathbb{N}$. Furthermore, the corresponding eigenstates can be normalized in order to form an orthonormal basis and the physical stationary states are called “bound states”. Bound states are usually associated with negative energy levels. For example, the quantum harmonic oscillator is a well-known example of systems with a fully discrete energy spectrum.
- The energy spectrum of the system is continuous which means that the eigenvalues can take a continuous range of values and the corresponding eigenstates have an infinite norm. Therefore, they cannot be normalized although they can be made orthonormal

in a more general sense. Those states are often called “unbound states” or “scattering states” and are usually associated with positive energies.

- The energy spectrum of the system is partly discrete and partly continuous in the sense that there are bound states as well as unbound states among the eigenstates of the time-independent Schrödinger equation. However, it is possible to study each part separately. A well-known example of systems with a mixed discrete-continuous energy spectrum is the hydrogen atom and all the hydrogen-like systems.

From now on we will only consider systems with a discrete energy spectrum.

Excitation energies

When a quantum system possesses a discrete energy spectrum, the state with the lowest energy level is referred to as the “ground state” while all the other states are called “excited states”. Although the ground state is defined as the more energetically stable state of the system, it is yet possible for an electron to be promoted from an initial low-energy level to a higher excited state by absorbing a specific amount of energy, from a photon for example. During an electronic-transition process, the promoted electron will usually very briefly exist in the higher energy state until relaxing back to a more energetically stable state and, along this relaxation, will in turn release photon energy.

The specific amount of energy required in order to promote an electron from an initial energy level E_n to another energy level E_m is simply the energy difference between those two levels and is called “excitation energy”

$$\Omega_{nm} = E_m - E_n. \quad (1.19)$$

When one changes the electronic configuration of the system by promoting one or many electrons from an initial state to another state, one talks about “neutral excitations” since one only rearranges the electron configuration without changing the total number of electrons of the system.

- One famous example of neutral excitation energies, which will be discussed in this work, is called the “optical gap” [7] Ω_{opt}^N and corresponds to the lowest energy transition accessible for the system via absorption of a single photon. The optical gap is usually assumed to be the transition from the ground state E_0^N to the lowest excited state E_1^N

$$\Omega_{\text{opt}}^N \equiv \Omega_{01}^N = E_1^N - E_0^N. \quad (1.20)$$

Another type of excitation energies are the ones corresponding to processes during which one adds (or removes) electrons to (or from) an initial electronic configuration. In that case, since one is changing the total number of electrons of the system, one will denote those excitations as “charged excitations”.

- The first charged excitation energy that we will mention in this work is the one corresponding to the removal of an electron from its ground-state electronic configuration. It corresponds to the electronic transition from the ground state of the N -electron system to the ground state of the $(N - 1)$ -electron system and is known as the “ionization potential”. The ionization potential represents the cost in energy that one must pay in order to remove an electron from the system. Actually, each removal of an electron from the system will be associated with a ionization potential which will be referred to as “first ionization potential”, “second ionization potential”...

The first ionization potential of the N -electron system is defined as follows

$$I_0^N = E_0^{N-1} - E_0^N . \quad (1.21)$$

- Similarly, we will also be interested in the charged excitation corresponding to the addition of an electron to the ground state of the N -electron system. In that case, the property of interest would be the “electron affinity” which represents the amount of energy which is released by the system due to the addition of a new electron

$$A_0^N = E_0^N - E_0^{N+1} . \quad (1.22)$$

- Finally, based on those two properties, one can also define the last useful notion that one will need in order to discuss charged excitations: the “fundamental gap”. The fundamental gap of a N -electron system is defined as the difference between its ionization potential and its electron affinity

$$\Omega_{\text{fun}}^N = I_0^N - A_0^N . \quad (1.23)$$

In the previous definitions, the subscript “0” and the superscript “ N ” emphasize the fact that the reference state is the ground state of the N -electron system.

So far, we have covered all the basic formalism of quantum mechanics required to properly describe and study an electronic system but the fact is that real materials, like atoms, molecules or solids, are never composed of only electrons. They actually consist of a dynamical environment formed by an arrangement of nuclei through which the electron distribution spreads out and interacts with.

To get a realistic and accurate description of such a system can be very challenging as we shall see in the next section.

1.2 The Many-Electron Problem

1.2.1 The “Exact” versus “Approximate” Dilemma

Approximate solution and exact constraints

In the previous section, we have seen that the key to accurately describe and predict the behavior and properties of an electronic system was to solve the famous time-independent

Schrödinger equation

$$\hat{H} |\Psi\rangle = E |\Psi\rangle . \quad (1.24)$$

Unfortunately, there exist only very few systems, essentially one-electron systems, for which we actually can analytically solve this equation. Most of the time, for more complicated systems, we must rely on approximations and numerical computation.

Indeed, for a N -electron system, in the space-spin representation, the time-independent Schrödinger equation takes the form

$$H(\mathbf{x}_1, \mathbf{x}_2, \dots, \mathbf{x}_N) \Psi(\mathbf{x}_1, \mathbf{x}_2, \dots, \mathbf{x}_N) = E \Psi(\mathbf{x}_1, \mathbf{x}_2, \dots, \mathbf{x}_N) , \quad (1.25)$$

where we see that both the Hamiltonian and the wave function depend on all space and spin coordinates of the system.

The first difficulty would be to properly describe the Hamiltonian of the system which must encompass all the information about the motion of the system and the nature of its interactions. As we shall see later, the main problematic part of the Hamiltonian would be the one describing the interacting nature of the electrons.

The second difficulty, and not the least, comes from the wave function itself since it must describe the correlated motion of interacting electrons which is a very complex system. The fact is that we simply do not know the form of the “exact” wave function of an interacting many-electron system.

Hopefully, we do know some of the “exact constraints” and properties that the exact wave function must verify. For instance, we have already introduced in the previous section the anti-symmetry property, due to the Pauli exclusion principle 1.1.2, as well as the normalization constraint (1.5).

Since the exact wave function seemed unreachable, even now despite the great advances achieved over the last decades in numerical computation, many methods in quantum chemistry were based on the simpler idea of finding the best “approximate solution” for the time-independent Schrödinger equation.

Basis set expansion

Many methods use the concept of “basis set” in order to expand approximate wave functions and optimize them with respect to a set of specific constraints.

For a given finite basis $\{|f_i\rangle\}$ of size $M \in \mathbb{N}$, the idea would be to find the best expansion coefficients $\{c_i\}$ from which we could build the best approximate solution $|\tilde{\Psi}\rangle$

$$|\Psi\rangle \approx |\tilde{\Psi}\rangle = \sum_{i=1}^M c_i |f_i\rangle . \quad (1.26)$$

As we have seen before, the exact wave function of the system can be written as an infinite expansion within the orthonormal basis of its eigenstates (1.13). From a computationally perspective, infinite basis are impossible to achieve, however we can still lean on the idea that the larger the basis the more accurate the result. Of course, using a larger basis would

also result in increasing the computational effort required in order to achieve the wanted accuracy.

All those considerations must be taken into account whenever one needs to perform quantum chemistry calculations.

Hartree-Fock ansatz

In quantum chemistry, many different ansatz have been proposed for the form of the approximate wave function, engendering various methods. The simplest one was probably the idea of using a single “Slater determinant” approximation to mimic the exact wave function which might seem a very crude approximation since Slater determinants are usually associated with the description of non-interacting electrons

$$|\Psi\rangle \approx |\tilde{\Psi}\rangle_{\text{HF}} = |\Phi_0\rangle, \quad (1.27)$$

where Φ_0 is a Slater determinant describing the ground state of a non-interacting N -electron system.

This particular ansatz is typical of the “Hartree-Fock” method (HF) which will be thoroughly introduced in the next chapter.

Post-Hartree-Fock methods

Many other methods (Configuration Interaction, Coupled Cluster, Møller-Plesset Perturbation Theory, Density-Functional Theory...) have actually been developed based on the Hartree-Fock formalism and are then referred to as “post-Hartree-Fock” methods.

In order to go beyond the scope of Hartree-Fock theory, some of them rather use a multi-determinantal ansatz in order to get a better approximation for the exact wave function of the interacting N -electron system, and thus a better prediction of its total energy

$$|\Psi\rangle \approx |\tilde{\Psi}\rangle = c_0 |\Phi_0\rangle + \sum_{I=1} c_I |\Phi_I\rangle, \quad (1.28)$$

where Φ_I represents any other determinant, other than the ground state determinant Φ_0 , associated with a N -electron system.

For instance, the “Configuration Interaction” (CI) method defines the approximate wave function as a linear combination of Slater determinants, not only including the Hartree-Fock ground state determinant but also all (or some) of the excited determinants that one can obtain when exciting one or many electrons from the Hartree-Fock configuration (singly excited, doubly excited...)

$$|\Psi\rangle \approx |\tilde{\Psi}\rangle_{\text{CI}} = c_0 |\Phi_0\rangle + \sum_{\text{S}} c_{\text{S}} |\Phi_{\text{S}}\rangle + \sum_{\text{D}} c_{\text{D}} |\Phi_{\text{D}}\rangle + \dots \quad (1.29)$$

where the summations are over all determinants that are singly (S), doubly (D)... excited relative to the Hartree-Fock determinant Φ_0 .

If the CI expansion (1.29) takes into account all the possible excited determinants, the method is called “Full CI” (FCI) and the resulting energy and wave function should converge towards the exact ones. If one chooses to only take into account a finite number of determinants, for computational cost considerations for instance, the CI expansion is said to be truncated.

Another post-Hartree-Fock method which was widely used over the past decades is the “Density-Functional Theory” (DFT). Density-functional theory is indeed based on the Hartree-Fock frameworks but doesn’t use a multi-determinantal form for the approximate wave function in order to go beyond the Hartree-Fock result. Instead, it relies on the electron density (1.4) as we shall see in a few chapters.

In this work, we will strictly focus on Hartree-Fock and Density-Functional Theory methods.

1.2.2 The Variation Method

The variation principle

We have seen that solving exactly the time-independent Schrödinger equation was not a realistic objective but that one could instead try to find the best approximate solution. We shall discuss now what we mean by “best” approximation.

We recall that the total energy associated with a given state of the system is defined as the expectation value 1.1.3 of the Hamiltonian operator. Let us call Ψ_0 the normalized exact ground-state wave function of the system and E_0 the associate exact ground-state energy so that

$$E_0 \equiv \langle \hat{H} \rangle_{\Psi_0} = \langle \Psi_0 | \hat{H} | \Psi_0 \rangle . \quad (1.30)$$

Since we do not know the exact ground-state wave function Ψ_0 , we will use instead a normalized approximate wave function, which will be referred to as “trial wave function” $\tilde{\Psi}$, and in which we can retain some of the known exact characteristics of the exact ground-state wave function, like the normalization constraint (1.5) and the antisymmetry property 1.1.2 for instance.

The expectation value of the energy associated with this trial wave function is then

$$\tilde{E} \equiv \langle \hat{H} \rangle_{\tilde{\Psi}} = \langle \tilde{\Psi} | \hat{H} | \tilde{\Psi} \rangle . \quad (1.31)$$

The variation principle [84] states that any trial wave function will have a total energy higher than the exact total energy and the only possibility to obtain the exact energy would be if the trial wave function were actually the exact wave function of the system

$$E_0 \leq \langle \tilde{\Psi} | \hat{H} | \tilde{\Psi} \rangle = \tilde{E} . \quad (1.32)$$

Note that the variation principle, although applied to the energy in this work, is a much more general approach which consists in finding approximate solutions to any eigenvalue problem

1.1.3.

In practice, one often has to restrict the search to a specific subset of trial wave functions with a specific form, obeying a specific set of constraints that one would have imposed, with a targeted symmetry. . . If one applies the variation principle to a specific subset of trial wave functions, the minimum of the energy that one would obtain would be a variational estimate of the exact ground-state energy for this particular class of trial wave functions.

Hence, if one could extend the search to all possible trial wave functions, one would ultimately find that the minimizing trial wave function would be the exact ground-state wave function of the system, and that the associated minimum of the energy would be the exact ground-state energy.

Linear expansion and matrix eigenvalue problem

We have seen in 1.2.1 that one could use a finite basis set $\{f_i\}$, with a fixed number M of basis functions, to linearly expand a trial wave function

$$|\tilde{\Psi}\rangle = \sum_{i=1}^M c_i |f_i\rangle . \quad (1.33)$$

Linear expansions of trial wave functions allow one to reformulate the variation method in a more general matrix formulation: the “linear variational method”.

The linear variational method not only provides an approximate solution for the ground state $\{\Psi_0; E_0\}$ of the system but also a whole set of approximations for a given number of eigenstates $\{\Psi_i; E_i\}$.

If one chooses to work with a finite basis set of real orthonormal basis functions $\{f_i\}$, so that

$$\langle f_i | f_j \rangle = \langle f_j | f_i \rangle = \delta_{ij} , \quad (1.34)$$

one can replace all the terms of the eigenvalue equation 1.1.3 by their matrix representations

$$\mathbf{H}\mathbf{c} = E\mathbf{c} . \quad (1.35)$$

The trial wave function would then be replaced by a column vector \mathbf{c} whose elements would be its expansion coefficients with respect to the orthonormal basis $\{f_i\}$

$$\mathbf{c} \equiv \begin{pmatrix} c_1 \\ c_2 \\ \vdots \\ c_M \end{pmatrix}_{\{f_i\}} , \quad (1.36)$$

and, similarly, the Hamiltonian operator \hat{H} would be replaced by its matrix representation

\mathbf{H} in the same basis

$$\mathbf{H} = \begin{pmatrix} H_{11} & H_{12} & \dots & H_{1M} \\ H_{21} & H_{22} & & \vdots \\ \vdots & & \ddots & \vdots \\ H_{M1} & \dots & \dots & H_{MM} \end{pmatrix}_{\{|f_i\rangle\} \times \{|f_i\rangle\}}. \quad (1.37)$$

Since we have chosen to work with a real basis and since the Hamiltonian is an hermitian operator (1.9), it would be a $M \times M$ symmetric matrix such that

$$H_{ij} = H_{ji} = \langle f_i | \hat{H} | f_j \rangle, \quad (1.38)$$

where H_{ij} is the matrix element of \mathbf{H} of row i and column j .

Because of its dimensionality, solving the linear variational problem (1.35) consists in solving M distinct eigenvalue equations and, for each equation, in finding the column vector \mathbf{c} which only changes by a scalar multiplication by some scalar energy E after left-multiplication by the Hamiltonian matrix.

For a hermitian operator, the matrix eigenvalue problem has exactly M orthonormal solutions $\tilde{\Psi}_n$, with the associated real eigenvalues \tilde{E}_n , with $\tilde{E}_0 < \tilde{E}_1 < \dots < \tilde{E}_{M-1}$.

When one works out the variational principle in a M -dimensional vector space, one obtains a set of M solutions $\{\tilde{\Psi}_n; \tilde{E}_n\}$, with $n \in \llbracket 0, M-1 \rrbracket$, which can be interpreted as variational estimates of the M lowest exact electronic states of the system $\{\Psi_n; E_n\}$ [35, 84].

- In the case of linear expansions of the trial wave function (see equation (1.33)), the set of approximate solutions will be upper bounds to the set of the exact lowest energies and, in the limit of a complete basis set $M \rightarrow \infty$, these solutions will converge from above towards the exact solutions.
- Conversely, for nonlinear expansions of the trial wave function, the lowest approximate solution $\{\tilde{\Psi}_0; \tilde{E}_0\}$ would still be an upper bound to the exact ground state $\{\Psi_0; E_0\}$ of the system but it would no longer be guaranteed for the approximations of the excited states.

1.2.3 The Born-Oppenheimer Approximation

Molecular system

We have seen how one could describe and predict the behavior and properties of electronic systems but when one does quantum chemistry one needs to describe real systems, atoms, molecules, condensed matter... which are not limited to a sole electronic environment.

Such systems are usually modeled as two sets of different particles, a set of electrons with space-coordinates $\{\mathbf{r}_i\}$, mass m_e and charge $-e$, with $i \in \llbracket 1; N \rrbracket$, and a set of nuclei with space-coordinates $\{\mathbf{R}_A\}$, mass $\{M_A\}$, atomic numbers $\{Z_A\}$ and nuclear charges $\{Z_A e\}$, with

$A \in \llbracket 1; M_{\text{nucl}} \rrbracket$.

In the non-relativistic and time-independent framework, the wave function associated with the quantum state of a molecular system will only depend on all the spatial-coordinates (or spin-coordinates if one does not neglect the spin of the electrons and nuclei)

$$\Psi(\{\mathbf{r}_i\}, \{\mathbf{R}_A\}). \quad (1.39)$$

By “only” we mean that it will only depend explicitly on the position coordinates of the particles, not their momenta.

As we have seen in this chapter, in order to get a proper description of this system one must solve the time-independent Schrödinger equation

$$\hat{H} |\Psi\rangle = E |\Psi\rangle, \quad (1.40)$$

where the Hamiltonian of the whole molecular system will also depend on the space-coordinates of all the electrons and nuclei $\hat{H}(\{\mathbf{r}_i\}, \{\mathbf{R}_A\})$.

In the absence of any external electric or magnetic field, the non-relativistic time-independent molecular Hamiltonian [39] can be decomposed as follows

$$\begin{aligned} \hat{H} = & \boxed{-\frac{\hbar^2}{2m_e} \sum_{i=1}^N \nabla_i^2 + \frac{1}{2} \sum_{i=1}^N \sum_{\substack{j=1 \\ j \neq i}}^N \frac{e^2}{|\mathbf{r}_i - \mathbf{r}_j|} - \sum_{i=1}^N \sum_{A=1}^{M_{\text{nucl}}} \frac{Z_A e^2}{|\mathbf{r}_i - \mathbf{R}_A|}} \\ & + \frac{1}{2} \sum_{A=1}^{M_{\text{nucl}}} \sum_{\substack{B=1 \\ B \neq A}}^{M_{\text{nucl}}} \frac{Z_A Z_B e^2}{|\mathbf{R}_A - \mathbf{R}_B|} - \sum_{A=1}^{M_{\text{nucl}}} \frac{\hbar^2}{2M_A} \nabla_A^2 \\ & = \underbrace{\hat{T}_e + \hat{V}_{ee} + \hat{V}_{en}}_{\hat{H}_{\text{elec}}} + \hat{V}_{nn} + \hat{T}_n. \end{aligned} \quad (1.41)$$

where \hbar is the reduced Planck's constant.

In the previous decomposition, one has to distinguish two subsets.

The first three terms represent the electronic part of the molecular Hamiltonian since they are the only terms which depend on the electronic characteristics and positions.

They consist of the operators for the kinetic energy of the electrons \hat{T}_e , the Coulomb repulsion between electrons \hat{V}_{ee} and the coulombic attraction between electrons and nuclei \hat{V}_{en} , respectively, and will be gathered in order to form the electronic Hamiltonian \hat{H}_{elec} of the molecular system.

The last two terms in the previous molecular Hamiltonian expression only depend on the nuclei characteristics and positions and represent the operator associated with the coulombic repulsion between nuclei \hat{V}_{nn} and the operator for the kinetic energy of the nuclei \hat{T}_n , respectively.

Atomic units and accuracy

In Sciences, people usually work and perform calculations using the “International System of Units” (S.I.) but in the context of computational chemistry there exists a much more convenient metric system for atomic and molecular calculations, the “Atomic Units System” (a.u.).

The atomic units system [84] is based on fundamental constants from which one can derived many more:

- The atomic unit of mass is the electron mass $m_e \equiv 1$;
- The atomic unit of charge is the elementary charge $e \equiv 1$;
- The reduced Planck’s constant \hbar is equal to unity $\hbar \equiv 1$;
- The atomic unit of length is the Bohr radius (or just “Bohr”) $a_0 = \frac{4\pi\epsilon_0\hbar^2}{m_e e^2} \equiv 1$, where ϵ_0 is the vacuum permittivity;
- Coulomb’s constant is equal to unity $k_e = \frac{1}{4\pi\epsilon_0} \equiv 1$;
- The atomic unit of energy is the Hartree $E_h = \frac{m_e e^4}{(4\pi\epsilon_0\hbar)^2} \equiv 1$.

Besides the atomic units system, quantum chemists and physicists sometimes prefer to work with other units in order to express energy estimates. In this work, we may sometimes express the energy in “electron-volt” or in “kilocalorie per mole”

$$E_h = 27.2116 \text{ eV} = 627.509 \text{ kcal mol}^{-1}. \quad (1.42)$$

In order to evaluate the accuracy of a numerical result, it may be compared to a reference value obtained from another method, or from experiments. In quantum chemistry, the energy difference between the approximate energy and the reference value is usually said acceptable if it is less than a specific amount of energy, the “chemical accuracy”

$$\epsilon \approx 9.5 \times 10^{-4} \text{ a.u.} \approx 0.026 \text{ eV} \approx 0.599 \text{ kcal mol}^{-1}, \quad (1.43)$$

but it may also depend on the nature of the problem one is working on and it may partly determine, along with the computational cost, the appropriate method to use.

The use of the atomic units system enables one to completely recast the time-independent Schrödinger equation into a dimensionless form

$$\hat{H} = \boxed{-\frac{1}{2} \sum_{i=1}^N \nabla_i^2 + \frac{1}{2} \sum_{i=1}^N \sum_{\substack{j=1 \\ j \neq i}}^N \frac{1}{r_{ij}} - \sum_{i=1}^N \sum_{A=1}^{M_{\text{nuc}}} \frac{Z_A}{r_{iA}}} + \frac{1}{2} \sum_{A=1}^{M_{\text{nuc}}} \sum_{\substack{B=1 \\ B \neq A}}^{M_{\text{nuc}}} \frac{Z_A Z_B}{R_{AB}} - \sum_{A=1}^{M_{\text{nuc}}} \frac{1}{2M_A} \nabla_A^2}, \quad (1.44)$$

where we have used shorter notations to express the distances between particles such that r_{ij} represents the distance between electrons i and j , r_{iA} , the distance between electron i and nucleus A and R_{AB} , the distance between nuclei A and B .

The Born-Oppenheimer approximation

The “Born-Oppenheimer approximation” [39] stems from the practical observation that electrons are much more lighter than nuclei and, hence, have much smaller mass $m_e \ll M_A$. Since the kinetic operator describing the motion of a particle is proportional to the inverse of its mass, a very intuitive approximation consists in stating that, since electrons are much faster than nuclei, they do not “see” the motion of the nuclei and instantaneously react to any change of the nuclear configuration. This is the Born-Oppenheimer approximation.

As a first consequence, one can choose to completely neglect the nuclear kinetic term \hat{T}_n in the molecular Hamiltonian defined previously. Furthermore, since the electrons do not see the motion of the nuclei, they perceive them like simple point charges, in the sense that the electrons will move in the field of frozen nuclei.

Another consequence of the Born-Oppenheimer approximation will be that, since the nuclei are considered fixed, the distance between two nuclei is also a constant. For that reason the operator describing the coulombic repulsion between nuclei \hat{V}_{nn} will be a constant operator and will only result in adding a constant shift in the eigenvalues of the total Hamiltonian, with no change in the eigenvectors.

If one applies the Born-Oppenheimer approximation to the molecular Hamiltonian defined previously in equation (1.44), one obtains that

$$\hat{H} \approx \hat{H}_{\text{tot}} \equiv \hat{H}_{\text{elec}} + \hat{V}_{nn}, \quad (1.45)$$

which is now the total Hamiltonian \hat{H}_{tot} of a molecular system with fixed nuclei.

Solving the Schrödinger equation associated with \hat{H}_{tot} is known as “the electronic problem” and will be our sole concern in this work.

Nevertheless, if one’s interest were also to describe and predict the nuclear motion and properties of the molecular system such as the vibrational, rotational or translational energies, it would still be achievable in the Born-Oppenheimer framework.

In a sense, the Born-Oppenheimer approximation decouples the motions of the electrons and the nuclei and allow to treat both separately. Indeed, the Born-Oppenheimer approximation for the total molecular wave function of the system is

$$\Psi(\{\mathbf{r}_i\}, \{\mathbf{R}_A\}) \approx \underbrace{\Psi_{\text{elec}}(\{\mathbf{r}_i\}, \{\mathbf{R}_A\})}_{\substack{\text{motion of the electrons} \\ \text{in the field of “fixed” nuclei}}} \overbrace{\Psi_{\text{nucl}}(\{\mathbf{R}_A\})}^{\substack{\text{motion of the nuclei in the} \\ \text{“average” field of the electrons}}, \quad (1.46)$$

where Ψ_{nucl} describes the vibrational, rotational and translational motion and energy of the system while Ψ_{elec} describes the electronic behavior and properties.

First, one would have to solve the electronic problem,

$$\hat{H}_{\text{elec}} |\Psi_{\text{elec}}\rangle = E_{\text{elec}} |\Psi_{\text{elec}}\rangle, \quad (1.47)$$

in order to find out the electronic eigenstates and energies $\{\Psi_{\text{elec}}, E_{\text{elec}}\}$ which would only depend parametrically on the nuclear configurations $\{\mathbf{R}_A\}$. This means that, for each nuclear configuration, there will be a different set of electronic eigenstates $\Psi_{\text{elec}}(\{\mathbf{r}_i\}, \{\mathbf{R}_A\})$ and energies $E_{\text{elec}}(\{\mathbf{R}_A\})$.

Once the electronic problem is resolved, one would have to average all the positions and characteristics of the electrons over the electronic wave function in order to solve the nuclear equation describing the motion of the nuclei in the “average” field of the electrons

$$\hat{H}_{\text{nucl}} |\Psi_{\text{nucl}}\rangle = E_{\text{nucl}} |\Psi_{\text{nucl}}\rangle . \quad (1.48)$$

A commonly used description consists in saying that the nuclei move on a “potential energy surface” $E_{\text{tot}}(\{\mathbf{R}_A\})$ which is obtained by solving the electronic problem.

Hence, one would obtain a complete description, yet approximated, of all the molecular and electronic behaviors and properties of the molecular system.

Chapter 2

Hartree-Fock Theory

Contents

2.1	The Hartree-Fock Ansatz for the Wave function	25
2.1.1	Spin Orbitals, Molecular Orbitals and Atomic Orbitals	26
2.1.2	Hartree Product and Slater Determinant	27
2.2	The Hartree-Fock Approximation	28
2.2.1	Mean-Field Theory	28
2.2.2	The Hartree-Fock Energy	29
2.2.3	The Hartree-Fock Equations	31
2.2.4	Solutions to the Hartree-Fock equations	33
2.3	The Basis-Set Formulation	35
2.3.1	Restricted Hartree-Fock	35
2.3.2	Unrestricted Hartree-Fock	40
2.3.3	Hartree-Fock Limit and Correlation Energy	44
2.4	The Self-Consistent-Field Scheme	45

2.1 The Hartree-Fock Ansatz for the Wave function

Hartree-Fock theory is a computational method which aims to solve approximately the time-independent Schrödinger equation for many-body electronic systems under the non-relativistic Born-Oppenheimer approximation. It is the simplest wave function method and can be a very useful approximation for qualitative studies of molecular systems but also a very convenient starting point for more accurate methods.

Although Hartree-Fock method is often not accurate enough, it has the advantage of being applicable to large systems where other methods usually fail and often constitutes a good

choice when one wants to have a qualitative description of molecular systems. When Hartree-Fock is insufficient to provide accurate predictions, it can still be used as a convenient first guess that more accurate methods will improve by adding corrections.

To do so, Hartree-Fock relies on the concept of “orbitals” to give a proper, yet approximate, description of electronic structure of atomic and molecular systems.

2.1.1 Spin Orbitals, Molecular Orbitals and Atomic Orbitals

An orbital is a wave function associated with a single electron. As we have seen in the previous chapter, the quantum state of an electron include informations about the spatial distribution of the electron but also its spin σ , an intrinsic quantum property (we will use the compact notation \mathbf{x} for the combined space-spin coordinate). Hence, orbitals must reflect those two aspects.

In this work, we must distinguish three different classes of orbitals: “spin orbitals”, “molecular orbitals” (MOs) and “atomic orbitals” (AOs).

Spin orbitals and molecular orbitals

A spin orbital $\chi_i(\mathbf{x})$ gives the complete description of an electron and usually takes the form of a product of a spatial function, a spatial orbital $\varphi_i(\mathbf{r})$ which is also referred to as a molecular orbital, and a spin function which can be of two types, α or β depending on the spin value of the electron

$$\chi_i(\mathbf{x}) \equiv \begin{cases} \varphi_i(\mathbf{r})\alpha(\sigma) \\ \varphi_i(\mathbf{r})\beta(\sigma) \end{cases} . \quad (2.1)$$

Hence, if we have a finite set of molecular orbitals at our disposal, we can form twice as much spin orbitals.

Since the spin functions are orthonormal, if one chooses to build spin orbitals from a set of orthonormal molecular orbitals, the resulting spin orbitals will also be orthonormal

$$\langle \chi_i | \chi_j \rangle = \int \chi_i^*(\mathbf{x}) \chi_j(\mathbf{x}) d\mathbf{x} = \delta_{ij} . \quad (2.2)$$

Note that it is not mandatory to build all spin-orbitals with the same set of molecular orbitals. One could choose to use different sets of molecular orbitals to build the spin orbitals for electrons with spin α and electrons with spin β . The choice of using a unique set or two different sets of molecular orbitals depending on the spin of the electrons will give rise to two different Hartree-Fock formalisms: “Restricted” and “Unrestricted” Hartree-Fock, which will be discussed in detail in subsequent sections.

Atomic orbitals

The last class of orbitals that we will need are atomic orbitals $\phi_\mu(\mathbf{r})$. Atomic orbitals do not have physical meaning but are rather mathematical basis functions that we will use in order

to expand linearly the molecular orbitals

$$\varphi_i(\mathbf{r}) = \sum_{\mu} C_{\mu i} \phi_{\mu}(\mathbf{r}). \quad (2.3)$$

There exist multiple possible functions to use as atomic orbitals (Slater-type function, Gaussian-type function...) but they should reflect the nature of the system in order to get a proper description. The nature of the atomic orbitals can affect the accuracy and the computational cost of the method.

For molecular systems, a common choice is to use atom-centered Gaussian functions because Gaussians functions possess very convenient calculus properties which make integrals, especially two-electron integrals, much easier to compute with Gaussian-Type Orbitals (GTO) than with Slater-Type orbitals (STO).

For extended periodic systems, for instance, one can rather choose to use plane wave basis functions to expand the spatial orbitals.

2.1.2 Hartree Product and Slater Determinant

Hartree product

Originally, Hartree [34] proposed to describe N-electron wave functions as simple product of one-electron orbitals. In that sense, he assumed that electrons behave like independent particles so that they do not “see” each other and are totally “uncorrelated”. This particular form of wave function is known as a “Hartree product”

$$\Psi_{\text{HP}}(\mathbf{x}_1, \mathbf{x}_2, \dots, \mathbf{x}_N) \equiv \chi_i(\mathbf{x}_1) \chi_j(\mathbf{x}_2) \dots \chi_k(\mathbf{x}_N). \quad (2.4)$$

Unfortunately, Hartree products are not consistent with the indistinguishability requirement of electrons nor with the antisymmetry exact constraint imposed by the Pauli exclusion principle [80] and [23].

Slater determinant

Hopefully, we can correct the antisymmetry and indistinguishability failure of the Hartree product by taking precise linear combinations of Hartree products and forming what is called a “Slater determinant”

$$\Phi(\mathbf{x}_1, \mathbf{x}_2, \dots, \mathbf{x}_N) = \frac{1}{\sqrt{N!}} \begin{vmatrix} \chi_i(\mathbf{x}_1) & \chi_j(\mathbf{x}_1) & \dots & \chi_k(\mathbf{x}_1) \\ \chi_i(\mathbf{x}_2) & \chi_j(\mathbf{x}_2) & \dots & \chi_k(\mathbf{x}_2) \\ \vdots & \vdots & \ddots & \vdots \\ \chi_i(\mathbf{x}_N) & \chi_j(\mathbf{x}_N) & \dots & \chi_k(\mathbf{x}_N) \end{vmatrix}. \quad (2.5)$$

The previous definition represents a general normalized Slater determinant formed from a random set of N occupied spin orbitals $\{\chi_i, \chi_j, \dots, \chi_k\}$.

In the particular case where the determinant must represent a ground state, the N electrons would be placed in the spin orbitals which possess the lowest orbital energies $\{\varepsilon_i\}$ and the ground state Slater determinant would be formed from these particular subset of spin orbitals

$$\Phi_0(\mathbf{x}_1, \mathbf{x}_2, \dots, \mathbf{x}_N) = \frac{1}{\sqrt{N!}} \begin{vmatrix} \chi_1(\mathbf{x}_1) & \chi_2(\mathbf{x}_1) & \dots & \chi_N(\mathbf{x}_1) \\ \chi_1(\mathbf{x}_2) & \chi_2(\mathbf{x}_2) & \dots & \chi_N(\mathbf{x}_2) \\ \vdots & \vdots & \ddots & \vdots \\ \chi_1(\mathbf{x}_N) & \chi_2(\mathbf{x}_N) & \dots & \chi_N(\mathbf{x}_N) \end{vmatrix}, \quad (2.6)$$

where we have chosen to sort the spin orbitals so that $\varepsilon_1 < \varepsilon_2 < \dots < \varepsilon_N$. Any other Slater determinant would be associated with an excited state of the system.

There exists a shorter notation for representing a Slater determinant which consist in only representing its diagonal elements, the occupied spin orbitals, in a ket vector

$$\Phi_0(\mathbf{x}_1, \mathbf{x}_2, \dots, \mathbf{x}_N) \equiv |\chi_1(\mathbf{x}_1)\chi_2(\mathbf{x}_2) \dots \chi_N(\mathbf{x}_N)\rangle = |\chi_1\chi_2 \dots \chi_N\rangle. \quad (2.7)$$

From now on, we will use this compact notation when working with Slater determinants.

Using a single Slater determinant to represent a many-electron wave function is analogous to treating the electron-electron interaction in an average way as we will see in the next section.

2.2 The Hartree-Fock Approximation

2.2.1 Mean-Field Theory

We have seen in 1.2.3 that, in the non-relativistic Born-Oppenheimer approximation, the exact electronic Hamiltonian of the system may be written in the form

$$\hat{H}_{\text{elec}} = -\frac{1}{2} \sum_{i=1}^N \nabla_i^2 - \sum_{i=1}^N \sum_{A=1}^{M_{\text{nucl}}} \frac{Z_A}{r_{iA}} + \frac{1}{2} \sum_{i=1}^N \sum_{\substack{j=1 \\ j \neq i}}^N \frac{1}{r_{ij}}. \quad (2.8)$$

The first two terms are usually gathered together in order to form the “core” Hamiltonian

$$\hat{h}_i = -\frac{1}{2} \nabla_i^2 - \sum_{A=1}^{M_{\text{nucl}}} \frac{Z_A}{r_{iA}} \quad (2.9)$$

which is a one-electron operator describing the kinetic aspect of the motion of an electron i in the field of fixed nuclei and the attractive coulombic interaction with the latter.

The third term in the electronic Hamiltonian expression, the electron-electron coulombic repulsion operator, is a two-electron operator in the sense that it depends of the instantaneous

positions of two electrons, i and j .

The fact is that it is much easier to solve a set of N one-electron problems than a single N -electron problem. For that reason, one must find a way to rewrite the electronic Hamiltonian as a sum of one-electron operators. Unfortunately, because of the two-electron term mentioned previously, the exact electronic Hamiltonian is not “separable”

$$\hat{H}_{\text{elec}} = \sum_{i=1}^N \left(\hat{h}_i + \frac{1}{2} \sum_{\substack{j=1 \\ j \neq i}}^N \frac{1}{r_{ij}} \right). \quad (2.10)$$

That is the issue Hartree-Fock theory proposes to overcome. In order to simplify the above mentioned complexity of the electronic Hamiltonian, Hartree and Fock proposed to approximate the electron-electron repulsion in an average way.

Whereas in the exact electronic repulsion, the interaction between each pair of electrons have to be considered, Hartree and Fock chose to consider that each electron would rather interact with an averaged electrostatic field due to the charge distribution of all the remaining electrons. Therefore, each electron will experience an “effective one-electron potential” due to the presence of all the other electrons.

That is why Hartree-Fock theory is sometimes referred to as an “independent-particle model” or a “mean-field theory”.

2.2.2 The Hartree-Fock Energy

The Hartree-Fock ground state energy of the system is defined as the expectation value of the electronic Hamiltonian operator \hat{H}_{elec} for a ground state single Slater determinant wave function Φ_0 . It can be expressed in terms of the occupied spin orbitals from which the Slater determinant is built as follows

$$E^{\text{HF}} = \langle \Phi_0 | \hat{H}_{\text{elec}} | \Phi_0 \rangle = \sum_{i=1}^N h_i + \frac{1}{2} \sum_{i=1}^N \sum_{j=1}^N (J_{ij} - K_{ij}), \quad (2.11)$$

where

$$\begin{aligned} h_i &= \langle \Phi_0 | \hat{h}_1 | \Phi_0 \rangle = \langle \chi_i | \hat{h}_1 | \chi_i \rangle \\ &= \int \chi_i^*(\mathbf{x}_1) \hat{h}_1(\mathbf{r}_1) \chi_i(\mathbf{x}_1) d\mathbf{x}_1 \end{aligned} \quad (2.12)$$

is the one-electron integral which represents the core energy of an electron placed in a spin orbital χ_i . In this definition, the summation is over all occupied spin orbitals and the integration is over the space-spin coordinate of any electron placed in the spin orbital χ_i . It is a dummy variable so we choose to use \mathbf{x}_1 for one-electron integrals and \mathbf{x}_1 and \mathbf{x}_2 for

two-electron integrals.

The second part of the Hartree-Fock energy consists of a double summation of the term

$$J_{ij} - K_{ij} = \langle \Phi_0 | \frac{1}{r_{12}} | \Phi_0 \rangle \quad (2.13)$$

and constitutes the two-electron part of the Hartree-Fock energy. It can be divided into two distinct contributions

$$\begin{aligned} J_{ij} &= \langle \chi_i \chi_j | \frac{1}{r_{12}} | \chi_i \chi_j \rangle = \langle ij | ij \rangle \\ &= \int \chi_i^*(\mathbf{x}_1) \chi_j^*(\mathbf{x}_2) \frac{1}{r_{12}} \chi_i(\mathbf{x}_1) \chi_j(\mathbf{x}_2) d\mathbf{x}_1 d\mathbf{x}_2 \end{aligned} \quad (2.14)$$

is the ‘‘Coulomb’’ integral, where we have used the physicist’s notation for two-electron integrals over spin orbitals

$$\langle ij | kl \rangle \equiv \langle \chi_i \chi_j | \chi_k \chi_l \rangle = \int \chi_i^*(\mathbf{x}_1) \chi_j^*(\mathbf{x}_2) \frac{1}{r_{12}} \chi_k(\mathbf{x}_1) \chi_l(\mathbf{x}_2) d\mathbf{x}_1 d\mathbf{x}_2. \quad (2.15)$$

The Coulomb part of the Hartree-Fock energy is purely classical and emerges from the electrostatic interaction between two charge distributions, or charge densities, due to the occupation of the spin orbitals χ_i and χ_j . Note that, in that definition, an electron placed in a spin orbital χ_i can interact with itself leading to the corresponding ‘‘self-interaction’’ energy J_{ii} which does not possess any physical meaning.

The second contribution to the two-electron part of the Hartree-Fock energy

$$\begin{aligned} K_{ij} &= \langle \chi_i \chi_j | \frac{1}{r_{12}} | \chi_j \chi_i \rangle = \langle ij | ji \rangle \\ &= \int \chi_i^*(\mathbf{x}_1) \chi_j^*(\mathbf{x}_2) \frac{1}{r_{12}} \chi_j(\mathbf{x}_1) \chi_i(\mathbf{x}_2) d\mathbf{x}_1 d\mathbf{x}_2 \end{aligned} \quad (2.16)$$

is known as the ‘‘exchange’’ integral and is much more subtle than the classical Coulomb contribution. It encompasses all the quantum aspects of the electron-electron repulsion and arises directly from the antisymmetry exact constraint imposed to the Hartree-Fock wave function.

The coulomb and exchange integrals are very similar except that in the latter the spin orbitals of the electrons are swapped, thus the denomination ‘‘exchange’’.

Note that K_{ij} exactly cancels out J_{ij} when $i = j$ which is why the summation is no longer restricted by the constraint $i \neq j$ in equation (2.11). Consequently, Hartree-Fock exchange

is said to be “exact exchange” in the sense that it exactly cancels out the above mentioned “self-interaction” term J_{ii} and restores the physical requirement that dictates that an electron cannot interact with itself.

The Hartree-Fock energy can be rewritten in terms of one and two-electron integrals over occupied spin orbitals as follows

$$E^{\text{HF}} = \sum_{i=1}^N \langle i | \hat{h} | i \rangle + \frac{1}{2} \sum_{i=1}^N \sum_{j=1}^N \langle ij || ij \rangle, \quad (2.17)$$

where we used the following compact notation for the combined Coulomb-exchange integrals

$$\langle ij || ij \rangle \equiv \langle ij | ij \rangle - \langle ij | ji \rangle = \langle \chi_i \chi_j | \chi_i \chi_j \rangle - \langle \chi_i \chi_j | \chi_j \chi_i \rangle = J_{ij} - K_{ij}. \quad (2.18)$$

Hence, each occupied spin-orbital χ_i will add a one-electron contribution $\langle i | \hat{h} | i \rangle$ to the energy and each unique pair of occupied spin-orbitals $\{\chi_i, \chi_j\}$ will add a two-electron contribution $\langle ij || ij \rangle$.

2.2.3 The Hartree-Fock Equations

At this point, we would like to transform the unsolvable many-electron Schrödinger equation associated with a Slater determinant

$$\hat{H}_{\text{elec}} |\Phi_0\rangle = E |\Phi_0\rangle \quad (2.19)$$

into a set of eigenvalue equations where some operator \hat{O} would act on each single spin orbital χ_i with orbital energy ε_i

$$\hat{O} |\chi_i\rangle = \varepsilon_i |\chi_i\rangle. \quad (2.20)$$

For that purpose, we need to introduce several operators which arise directly from the previous definitions introduced in 2.2.2.

Coulomb and exchange operators

First, we define the Coulomb operator $\hat{\mathcal{J}}_j$

$$\hat{\mathcal{J}}_j(\mathbf{x}_1) = \int |\chi_j(\mathbf{x}_2)|^2 \frac{1}{r_{12}} d\mathbf{x}_2 \quad (2.21)$$

which acts on an arbitrary spin orbitals χ_i as follows

$$\hat{\mathcal{J}}_j(\mathbf{x}_1) \chi_i(\mathbf{x}_1) = \left[\int |\chi_j(\mathbf{x}_2)|^2 \frac{1}{r_{12}} d\mathbf{x}_2 \right] \chi_i(\mathbf{x}_1). \quad (2.22)$$

The Coulomb operator is simply the local electrostatic potential generated by an electron placed in the spin orbital χ_j that an electron placed in \mathbf{x}_1 would experience.

Note that the definition of the Coulomb operator is independent of the spin orbital on which it acts.

Similarly, we also define the exchange operator which acts on spin orbitals in a more complicated manner

$$\hat{\mathcal{K}}_j(\mathbf{x}_1)\chi_i(\mathbf{x}_1) = \left[\int \chi_j^*(\mathbf{x}_2) \frac{1}{r_{12}} \chi_i(\mathbf{x}_2) d\mathbf{x}_2 \right] \chi_j(\mathbf{x}_1). \quad (2.23)$$

The exchange operator $\hat{\mathcal{K}}_j$ is much more subtle than the Coulomb operator in the sense that its definition depends explicitly on the spin orbital on which it acts. Thus, it represents a non-local potential.

Fock operator

If we apply the variation theorem to the Hartree-Fock energy defined in (2.11) and minimize it, using Lagrange's method of undetermined multipliers for instance, with respect to a change in the spin orbitals under the constraint that the spin orbitals remain orthonormal through the optimization process, we obtain the following "Hartree-Fock equations"

$$\left[\hat{h}(\mathbf{x}_1) + \sum_{j=1}^N \left(\hat{\mathcal{J}}_j - \hat{\mathcal{K}}_j \right) \right] \chi_i(\mathbf{x}_1) = \sum_{j=1}^N \varepsilon_{ji} \chi_j(\mathbf{x}_1). \quad (2.24)$$

Based on this equation, we can define the "Fock operator"

$$\hat{f}(\mathbf{x}_1) = \hat{h}(\mathbf{x}_1) + \hat{v}_{\text{HF}}(\mathbf{x}_1) \quad (2.25)$$

which includes the effective one-electron Hartree-Fock potential

$$\hat{v}_{\text{HF}}(\mathbf{x}_1) = \sum_{j=1}^N \left(\hat{\mathcal{J}}_j - \hat{\mathcal{K}}_j \right) \quad (2.26)$$

and acts on each spin orbital as follows

$$\hat{f}(\mathbf{x}_1)\chi_i(\mathbf{x}_1) = \sum_{j=1}^N \varepsilon_{ji} \chi_j(\mathbf{x}_1). \quad (2.27)$$

Since the Fock operator only approximates the two-electron part of the electronic Hamiltonian, in the absence of two-electron interactions, the Fock operator must reproduce the exact Hamiltonian of the system. That is why Hartree-Fock theory is known to be exact for one-electron systems.

The last equation does not exactly take the form of the usual eigenvalue equation and is referred to as a pseudo-eigenvalue equation.

2.2.4 Solutions to the Hartree-Fock equations

Canonical equations and canonical orbitals

As we have seen, the Fock operator is defined itself in terms of the occupied spin orbitals through the one-electron effective potential, and especially the exchange operator, thus the Hartree-Fock equations are non-linear equations and must be solved iteratively as we will see in a subsequent section.

As a matter of fact, any set of non-linear equations admits many independent variational solutions and it is always possible to transform a specific set of solutions into another set of more convenient solutions using a unitary transformation \mathbf{U} , which must verify the following property

$$\mathbf{U}^\dagger = \mathbf{U}^{-1}. \quad (2.28)$$

That is because the expectation value of the electronic Hamiltonian is stationary with respect to unitary variations of the spin orbitals.

For an arbitrary set of solutions $\{\chi_i\}$, the matrix representation of the fock operator will not be diagonal and neither will be the matrix $\boldsymbol{\varepsilon}$ of the Lagrange multipliers $\{\varepsilon_{ji}\}$.

There exists a unique set of solutions which diagonalizes the Fock matrix and for which $\boldsymbol{\varepsilon}$ is diagonal. This particular set can be obtained using a unitary transformation as mentioned before and is known as the “canonical spin orbitals” $\{\chi'_i\}$.

The Hartree-Fock equations can be rewritten in terms of the canonical orbitals in order to retrieve the form of a usual eigenvalue equation whose solutions are the canonical spin orbitals $\{\chi'_i\}$ with canonical spin orbital energies $\{\varepsilon'_i\}$

$$\hat{f}(\mathbf{x}_1)\chi'_i(\mathbf{x}_1) = \varepsilon'_i\chi'_i(\mathbf{x}_1). \quad (2.29)$$

Hence, in the Hartree-Fock framework, by solving a set of one-electron effective eigenvalue equations, we can find the best spin orbitals from which we can build the best Slater determinant with the lowest Hartree-Fock energy.

From now on, we will only consider the canonical spin orbitals and will drop the prime notation.

Interpretation of spin orbital energies

We have shown that in order to obtain the best Hartree-Fock energy, one must solve a set of eigenvalue equations associated with the Fock operator \hat{f} . Since the Fock operator is an hermitian operator, it admits an infinite set of eigenfunctions, or spin orbitals, $\{\chi_i\}$ and eigenvalues, spin orbital energies, $\{\varepsilon_i\}$.

Among those solutions, the N spin orbitals with the lowest orbital energies will be referred to as “occupied” spin orbitals while for all the remaining spin orbitals the denomination “virtual” or “unoccupied” will be used.

There have been attempts to connect the spin orbitals to physical property of the system, like

the total energy for instance. Indeed, we can express the Hartree-Fock ground state energy in terms of the occupied spin orbital energies $\{\varepsilon_i\}$

$$E^{\text{HF}} = \sum_{i=1}^N \varepsilon_i - \frac{1}{2} \sum_{i=1}^N \sum_{j=1}^N (J_{ij} - K_{ij}), \quad (2.30)$$

with

$$\varepsilon_i = \langle \chi_i | \hat{f} | \chi_i \rangle = h_i + \sum_{j=1}^N (J_{ij} - K_{ij}). \quad (2.31)$$

Hence, we see that the Hartree-Fock energy of the system cannot be written as a simple sum of orbital energies of occupied spin orbitals. The reason is that, in the Hartree-Fock framework, the spin orbital energies double count the electronic repulsion energy because of the average treatment of the electron-electron interaction.

Koopmans' theorem

Koopmans tried to relate occupied and virtual spin orbital energies with total energy differences involved in processes of removal or addition of an electron from/to a neutral system [43, 84, 35].

For instance, let us remove an electron of a N -electron system from a specific spin orbital χ_k with orbital energy ε_k under the assumption that the spin orbitals will not relax during the process.

Based on equation (2.30), we can express the Hartree-Fock energy of the N - and $(N - 1)$ -electron systems and subtract them in order to obtain the ionization potential of the N -electron system introduced in the first chapter

$$I_0^N = E_{\text{HF}}^{N-1} - E_{\text{HF}}^N = -\varepsilon_k \quad (2.32)$$

Hence, we find that the Hartree-Fock ionization potential is equivalent to the opposite of the orbital energy of the occupied spin orbital from which we removed the electron.

We can apply the same reasoning to the case where we decide to add an electron in a virtual spin orbital of the N -electron system, still under the strong assumption that the spin orbitals do not relax during the process

$$A_0^N = E_{\text{HF}}^N - E_{\text{HF}}^{N+1} = -\varepsilon_k. \quad (2.33)$$

Again, we find that the Hartree-Fock electron affinity of the N -electron system is identical to the opposite of the orbital energy of the virtual spin orbital into which we added an electron.

Although the idea of extracting physical meaning from spin orbital energies can seem very appealing, the fact is that those conclusions were derived under a very strong approximation, the “frozen orbital approximation”, in which we consider that the spin orbitals of the neutral, cationic and anionic systems are identical which is not physically relevant.

Moreover, Koopmans' theorem was originally established for "closed-shell" systems, which are systems with no unpaired electrons, and, besides the lack of orbital relaxation, Hartree-Fock orbitals do not include any correlation effects either.

Furthermore, whereas occupied spin orbitals are well-defined and usually behave in a rather consistent way when one does calculations, virtual spin orbitals are much seen like the left-overs of a calculation and can get more and more numerous depending on the size of the basis set used to perform the calculation.

For all those reasons, the subject of equating orbital energies to physical properties like ionization potentials or electron affinities remains a controversial debate.

2.3 The Basis-Set Formulation

We have seen in the previous sections that Hartree-Fock equations are integro-differential equations and although they can, in principle, be solved numerically for atomic systems, for large molecules it can turn to be a very demanding task.

Fortunately, a very simple procedure has been developed which proposes to overcome numerical limitations by turning the integro-differential Hartree-Fock equations into a much easier to compute matrix formulation as we will see.

Furthermore, we will see that it is possible to enforce some restrictions on the Hartree-Fock wave function, like symmetry constraints, in order to target specific solutions.

2.3.1 Restricted Hartree-Fock

In this subsection, we will explain how Hartree-Fock theory can be applied to closed-shell systems^[84].

Restricted spin orbitals

In closed-shell systems, there are no unpaired electrons so that each molecular orbital will be doubly occupied with an electron with spin α and an electron with spin β .

For that reason, restricted Hartree-Fock formalism (RHF) enforces the restriction that the spin orbitals of both spins are built from the same set of molecular orbitals $\{\varphi_i\}$. Thus, for that particular class of molecular systems the total number of occupied molecular orbitals is $\frac{N}{2}$ while the total number of occupied spin orbitals is N , where N is the total number of electrons.

The restricted spin orbitals take the form

$$\chi_i(\mathbf{x}) \equiv \begin{cases} \varphi_i(\mathbf{r})\alpha(\sigma) \\ \varphi_i(\mathbf{r})\beta(\sigma) \end{cases}, \quad (2.34)$$

where we used the same notations introduced in 2.1.1.

Restricted Hartree-Fock equations

Originally, we have introduced the Hartree-Fock equations in terms of spin orbitals which include the spin component of the electrons but it is possible to eliminate the spin functions of the spin orbitals in order to rewrite the Hartree-Fock equations into a more convenient space-only representation.

The restricted Hartree-Fock equations in terms of the molecular orbitals are then

$$\hat{f}(\mathbf{r}_1)\varphi_i(\mathbf{r}_1) = \varepsilon_i\varphi_i(\mathbf{r}_1), \quad (2.35)$$

where the spatial Fock operator $\hat{f}(\mathbf{r}_1)$ acting on the occupied spatial orbitals is defined as follows

$$\hat{f}(\mathbf{r}_1) = \hat{h}(\mathbf{r}_1) + \sum_{j=1}^{\frac{N}{2}} \left[2\hat{\mathcal{J}}_j(\mathbf{r}_1) - \hat{\mathcal{K}}_j(\mathbf{r}_1) \right]. \quad (2.36)$$

In this definition, the summation is made over all $\frac{N}{2}$ occupied molecular orbitals $\varphi_i(\mathbf{r})$ and the Coulomb and exchange operators, $\hat{\mathcal{J}}_j(\mathbf{r}_1)$ and $\hat{\mathcal{K}}_j(\mathbf{r}_1)$, are the spatial analogs of the Coulomb and exchange operators defined in (2.22) and (2.23) for the spin orbitals.

Restricted Hartree-Fock energy

Similarly to what was done with the spin orbital formulation of the Hartree-Fock energy, we can derive an expression of the restricted Hartree-Fock energy of a closed-shell in terms of the occupied molecular orbitals

$$E^{\text{RHF}} = 2 \sum_{i=1}^{\frac{N}{2}} h_i + \sum_{i=1}^{\frac{N}{2}} \sum_{j=1}^{\frac{N}{2}} (2J_{ij} - K_{ij}). \quad (2.37)$$

The factor 2 in the Coulomb term comes from the fact that an electron will interact with electrons of both spins through the classical coulombic interaction while it will only interact with same-spin electrons through the exchange quantum interaction.

The Roothaan-Hall equations

As mentioned before, Hartree-Fock equations are integro-differential equations and can be very troublesome to solve, especially for large molecular systems.

Fortunately, Roothaan [72] and Hall [33] proposed, separately, a simple and elegant procedure to overcome the complexity of integro-differential problems by introducing a finite basis set of basis functions.

The idea is to linearly expand each unknown molecular orbital φ_i in a finite basis set of K known basis function, the atomic orbitals $\{\phi_\mu\}$

$$\varphi_i(\mathbf{r}) = \sum_{\mu=1}^K C_{\mu i} \phi_\mu(\mathbf{r}), \quad (2.38)$$

where $\{C_{\mu i}\}$ are the expansion coefficients of the molecular orbital φ_i in terms of the atomic orbitals $\{\phi_\mu\}$. Atomic orbitals usually do not form an orthonormal basis.

If we inject the previous linear expansion of the molecular orbitals into the restricted Hartree-Fock equations (2.35), we obtain a complete matrix reformulation of the problem, the ‘‘Roothaan-Hall equations’’

$$\boxed{\mathbf{FC} = \mathbf{SC}\boldsymbol{\varepsilon}}, \quad (2.39)$$

where \mathbf{F} is the matrix representation of the Fock operator \hat{f} in the atomic orbital basis $\{\phi_\mu\}$ and is known as the Fock matrix. Its elements are defined as follows

$$F_{\mu\nu} = \int \phi_\mu^*(\mathbf{r}_1) \hat{f}(\mathbf{r}_1) \phi_\nu(\mathbf{r}_1) d\mathbf{r}_1. \quad (2.40)$$

\mathbf{S} is the overlap matrix with elements

$$S_{\mu\nu} = \int \phi_\mu^*(\mathbf{r}_1) \phi_\nu(\mathbf{r}_1) d\mathbf{r}_1 \quad (2.41)$$

and represents the amount of overlap between two atomic orbitals.

Finally, $\boldsymbol{\varepsilon}$ is a diagonal matrix containing the orbital energies of the molecular orbitals.

If the atomic orbitals were orthonormal, the overlap matrix would simply be identical to the $K \times K$ identity matrix and would vanish from the Roothaan-Hall equations. In that case, solving Roothaan-Hall’s equations would not differ from solving the usual matrix eigenvalue problem. It would consist in diagonalizing the Fock matrix in order to find the corresponding eigenfunctions \mathbf{C} with eigenvalues $\boldsymbol{\varepsilon}$.

In the general case, where the AO basis is not orthonormal, the Roothaan-Hall equations are called a ‘‘generalized eigenvalue problem’’ and are still non-linear equations that one must solve iteratively.

The orthogonalization procedure

Since matrix eigenvalue problems are much easier to solve than generalized eigenvalue problems, it would be in our interest to find a procedure to orthogonalize the atomic orbitals. Fortunately for us, such a procedure exists. Indeed, it is possible to orthogonalize any non-orthogonal basis with the help of a transformation matrix \mathbf{X} which must verify the following property

$$\mathbf{X}^\dagger \mathbf{S} \mathbf{X} = \mathbf{1}, \quad (2.42)$$

where \mathbf{S} is the overlap matrix of the non-orthonormal basis.

If we apply such a transformation matrix to the old coefficient matrix \mathbf{C} and to the old Fock matrix \mathbf{F} , we can build a new coefficient matrix

$$\mathbf{C}' = \mathbf{X}^{-1} \mathbf{C} \iff \mathbf{C} = \mathbf{X} \mathbf{C}', \quad (2.43)$$

as well as a new Fock matrix

$$\mathbf{F}' = \mathbf{X}^\dagger \mathbf{F} \mathbf{X}, \quad (2.44)$$

and we obtain the “transformed Roothaan-Hall equations” [84]

$$\boxed{\mathbf{F}' \mathbf{C}' = \mathbf{C}' \boldsymbol{\varepsilon}}. \quad (2.45)$$

As you can see, transformed Roothaan-Hall equations are indeed a standard matrix eigenvalue problem.

Actually, there exist multiple choices for the transformation matrix but some of the most commonly used would probably be

- symmetrical (Löwdin) orthogonalization

$$\mathbf{X} \equiv \mathbf{S}^{-\frac{1}{2}}, \quad (2.46)$$

- canonical orthogonalization

$$\mathbf{X} \equiv \mathbf{U} \mathbf{s}^{-\frac{1}{2}}, \quad (2.47)$$

where \mathbf{U} is the unitary matrix that transforms the non-diagonal overlap matrix \mathbf{S} of the non-orthonormal atomic basis into a new diagonal overlap matrix \mathbf{s}

$$\mathbf{U}^\dagger \mathbf{S} \mathbf{U} = \mathbf{s}. \quad (2.48)$$

Restricted charge densities and density matrices

In a closed-shell molecule, each occupied molecular orbital (or spatial orbital) $\varphi_i(\mathbf{r})$ is doubly occupied and contains one electron with a spin α and one electron with a spin β . Hence, the charge density for electrons with spin α and the charge density for electrons with spin β will be identical and will be exactly half the total charge density $n(\mathbf{r})$

$$\begin{cases} n(\mathbf{r}) &= 2 \sum_{i=1}^{\frac{N}{2}} |\varphi_i(\mathbf{r})|^2 \\ n^\alpha(\mathbf{r}) &= n^\beta(\mathbf{r}) = \frac{1}{2} n(\mathbf{r}) \end{cases}. \quad (2.49)$$

If we expand the molecular orbitals in a finite basis of atomic orbitals $\{\phi_\mu\}$ and inject these expansions in the previous definition for the total charge density we can obtain a matrix formulation of the total density

$$n(\mathbf{r}) = \sum_{\mu=1}^K \sum_{\nu=1}^K P_{\mu\nu} \phi_\mu(\mathbf{r}) \phi_\nu^*(\mathbf{r}), \quad (2.50)$$

where $P_{\mu\nu}$ are the matrix elements of the matrix representation of the charge density $n(\mathbf{r})$ which is known as the “density matrix” \mathbf{P}

$$P_{\mu\nu} = 2 \sum_{i=1}^{\frac{N}{2}} C_{\mu i} C_{\nu i}^* . \quad (2.51)$$

The density matrix contains all the information about the expansion of the molecular orbitals and thus perfectly describes the Hartree-Fock wave function of the system. The density matrix formulation is particularly useful and important, especially for the numerical implementation of the Self-Consistent-Field (SCF) procedure used to iteratively solve the Roothaan-Hall equations and in which the Fock operator will itself be written in terms of the density matrix as we will see.

Density matrix formulation of the restricted Hartree-Fock energy

The restricted Hartree-Fock energy can be reformulated in terms of the density matrix as follows

$$E^{\text{RHF}} = \frac{1}{2} \sum_{\mu=1}^K \sum_{\nu=1}^K P_{\nu\mu} (H_{\mu\nu}^{\text{core}} + F_{\mu\nu}) \quad (2.52)$$

with

$$\begin{cases} H_{\mu\nu}^{\text{core}} &= \int \phi_{\mu}^*(\mathbf{r}_1) \hat{h}(\mathbf{r}_1) \phi_{\nu}(\mathbf{r}_1) d\mathbf{r}_1 \\ F_{\mu\nu} &= H_{\mu\nu}^{\text{core}} + \sum_{\lambda=1}^K \sum_{\sigma=1}^K P_{\lambda\sigma} [\langle \mu\sigma | \nu\lambda \rangle - \frac{1}{2} \langle \mu\sigma | \lambda\nu \rangle] \end{cases} \quad (2.53)$$

and where $\langle \mu\nu | \lambda\sigma \rangle$ are the two-electron integrals defined between atomic orbitals in the same manner that we did with molecular orbitals and spin orbitals

$$\langle \mu\nu | \lambda\sigma \rangle = \int \phi_{\mu}^*(\mathbf{r}_1) \phi_{\nu}^*(\mathbf{r}_2) \frac{1}{r_{12}} \phi_{\lambda}(\mathbf{r}_1) \phi_{\sigma}(\mathbf{r}_2) d\mathbf{r}_1 d\mathbf{r}_2 . \quad (2.54)$$

We see that the restricted Hartree-Fock energy of the system can be expressed with only three terms, the core Hamiltonian matrix \mathbf{H}^{core} , the density matrix \mathbf{P} and the Fock matrix \mathbf{F} .

The core Hamiltonian matrix does not depend on the expansion coefficients which means that, in the iterative process, it will not be necessary to compute it at each iteration, that is to say each time the expansion coefficients of the molecular orbitals are changed.

The Fock matrix depends on the expansion coefficients through the density matrix and for that reason, at each new iteration, a new Fock matrix must be built. It also depends on atomic two-electron integrals which also must be computed and stored only once.

At this point we have seen all the required concepts to apply Hartree-Fock theory to closed-shell systems.

2.3.2 Unrestricted Hartree-Fock

When the molecular system includes singly occupied orbitals, which means that there are unpaired electrons, a new Hartree-Fock formalism must be employed: Unrestricted Hartree-Fock (UHF)[84].

Unrestricted spin orbitals

Let us recall the Hartree-Fock eigenvalue equation in terms of spin orbitals

$$\hat{f}(\mathbf{x}_1)\chi_i(\mathbf{x}_1) = \varepsilon_i\chi_i(\mathbf{x}_1). \quad (2.55)$$

In unrestricted Hartree-Fock theory, the molecular orbitals are allowed to vary with much more flexibility than in restricted Hartree-Fock in order to lower the energy.

In that sense, the spin orbitals are not required to be built from the same set of molecular orbitals. Instead, two different sets of molecular orbitals will be considered depending on the nature of the spin orbital, one set of molecular orbitals $\{\varphi_i^\alpha\}$ with orbital energies $\{\varepsilon_i^\alpha\}$ to describe electrons with a spin α and another set $\{\varphi_i^\beta\}$ with energies $\{\varepsilon_i^\beta\}$ to describe electrons with a spin β .

Hence, the unrestricted spin orbitals are defined as follows

$$\chi_i(\mathbf{x}) \equiv \begin{cases} \varphi_i^\alpha(\mathbf{r})\alpha(\sigma) \\ \varphi_i^\beta(\mathbf{r})\beta(\sigma) \end{cases} \quad (2.56)$$

Note that, although we distinguish two different sets of molecular orbitals it is yet possible that the most energetically favorable Hartree-Fock solution corresponds to the restricted solution where the same molecular orbitals are used for both spins. There exist some situations where the unrestricted Hartree-Fock solution reduces to the restricted one.

The derivation of unrestricted Hartree-Fock formalism is identical to the one detailed in the restricted section 2.3.1 with the peculiarity that it must be done twice and applied separately to each spin.

Unrestricted Hartree-Fock equations

From now on, we will consider a molecular system with N^α electrons of spin α occupying the spatial orbitals $\{\varphi_i^\alpha\}$ and N^β electrons of spin β occupying the spatial orbitals $\{\varphi_i^\beta\}$ so that the total number of electrons is

$$N \equiv N^\alpha + N^\beta. \quad (2.57)$$

We start by injecting the two previous unrestricted expansions into the general Hartree-Fock equations (2.55). By doing so, we obtain two different sets of unrestricted Hartree-Fock equations in terms of the molecular orbitals

$$\hat{f}^\alpha(\mathbf{r}_1)\varphi_i^\alpha(\mathbf{r}_1) = \varepsilon_i^\alpha\varphi_i^\alpha(\mathbf{r}_1) \quad (2.58) \quad \Bigg| \quad \hat{f}^\beta(\mathbf{r}_1)\varphi_i^\beta(\mathbf{r}_1) = \varepsilon_i^\beta\varphi_i^\beta(\mathbf{r}_1) \quad (2.59)$$

where the two Fock operators $\hat{f}^\alpha(\mathbf{r}_1)$ and $\hat{f}^\beta(\mathbf{r}_1)$ are defined as follows

$$\begin{aligned} \hat{f}^\alpha(\mathbf{r}_1) &= \hat{h}(\mathbf{r}_1) + \sum_{j=1}^{N^\alpha} [\hat{\mathcal{J}}_j^\alpha(\mathbf{r}_1) - \hat{\mathcal{K}}_j^\alpha(\mathbf{r}_1)] \\ &+ \sum_{j=1}^{N^\beta} \hat{\mathcal{J}}_j^\beta(\mathbf{r}_1) \end{aligned} \quad (2.60)$$

$$\begin{aligned} \hat{f}^\beta(\mathbf{r}_1) &= \hat{h}(\mathbf{r}_1) + \sum_{j=1}^{N^\beta} [\hat{\mathcal{J}}_j^\beta(\mathbf{r}_1) - \hat{\mathcal{K}}_j^\beta(\mathbf{r}_1)] \\ &+ \sum_{j=1}^{N^\alpha} \hat{\mathcal{J}}_j^\alpha(\mathbf{r}_1) \end{aligned} \quad (2.61)$$

and where the summations are over the N^α and N^β occupied molecular orbitals of each spin.

The Fock operator expressions show that an α electron in a molecular orbital φ_i^α will have a spin-independent core energy and will interact with all α and β electrons, including itself, through the Coulomb operators $\hat{\mathcal{J}}_j^\alpha$ and $\hat{\mathcal{J}}_j^\beta$, respectively, and will also interact exclusively with all α electrons through the exchange operator $\hat{\mathcal{K}}_j^\alpha$. The same reasoning holds for the β electrons.

Unrestricted Hartree-Fock energy

We can derive as well a formulation of the unrestricted Hartree-Fock energy in terms of the occupied molecular orbitals of each spin

$$\begin{aligned} E^{\text{UHF}} &= \sum_{i=1}^{N^\alpha} h_i^\alpha + \sum_{i=1}^{N^\beta} h_i^\beta \\ &+ \frac{1}{2} \sum_{i=1}^{N^\alpha} \sum_{j=1}^{N^\alpha} (J_{ij}^{\alpha\alpha} - K_{ij}^{\alpha\alpha}) + \frac{1}{2} \sum_{i=1}^{N^\beta} \sum_{j=1}^{N^\beta} (J_{ij}^{\beta\beta} - K_{ij}^{\beta\beta}) + \sum_{i=1}^{N^\alpha} \sum_{j=1}^{N^\beta} J_{ij}^{\alpha\beta}. \end{aligned} \quad (2.62)$$

The unrestricted Hartree-Fock energy of the system includes summation of the core energy of the N^α electrons with spin α and N^β electrons with spin β along with the coulombic and exchange energies of all pairs of electrons with spin α and all pairs of electrons with spin β . The last contribution comes from the coulombic interaction between all pairs of electrons with different spins.

The Pople-Nesbet Equations

Analogue to the derivation of Roothaan-Hall equations, we will try to derive a matrix formulation of the unrestricted Hartree-Fock equations by introducing a basis set of atomic orbitals.

We start by expanding both sets of spatial orbitals $\{\varphi_i^\alpha(\mathbf{r})\}$ and $\{\varphi_i^\beta(\mathbf{r})\}$ in the same atomic

orbital basis set $\{\phi_\mu(\mathbf{r})\}$ of size K .

The unrestricted molecular orbitals are then

$$\varphi_i^\alpha(\mathbf{r}) = \sum_{\mu=1}^K C_{\mu i}^\alpha \phi_\mu(\mathbf{r}) \quad (2.63)$$

$$\varphi_i^\beta(\mathbf{r}) = \sum_{\mu=1}^K C_{\mu i}^\beta \phi_\mu(\mathbf{r}). \quad (2.64)$$

By injecting those two expansions, we can reformulate the two unrestricted Hartree-Fock equations, in equations (2.58) and (2.59), in their respective matrix representations

$$\mathbf{F}^\alpha \mathbf{C}^\alpha = \mathbf{S} \mathbf{C}^\alpha \boldsymbol{\varepsilon}^\alpha \quad (2.65) \quad \mathbf{F}^\beta \mathbf{C}^\beta = \mathbf{S} \mathbf{C}^\beta \boldsymbol{\varepsilon}^\beta \quad (2.66)$$

where \mathbf{F}^α and \mathbf{F}^β are the matrix representations of the two Fock operators defined in equations (2.60) and (2.61) in the atomic orbital basis $\{\phi_\mu\}$, with matrix elements

$$F_{\mu\nu}^\alpha = \int \phi_\mu^*(\mathbf{r}_1) f^\alpha(\mathbf{r}_1) \phi_\nu(\mathbf{r}_1) d\mathbf{r}_1 \quad (2.67)$$

$$F_{\mu\nu}^\beta = \int \phi_\mu^*(\mathbf{r}_1) f^\beta(\mathbf{r}_1) \phi_\nu(\mathbf{r}_1) d\mathbf{r}_1. \quad (2.68)$$

\mathbf{C}^α and \mathbf{C}^β are $K \times K$ square matrices whose columns contain the expansion coefficients of the corresponding spatial orbitals $\{\varphi_i^\alpha\}$ and $\{\varphi_i^\beta\}$, respectively.

$\boldsymbol{\varepsilon}^\alpha$ and $\boldsymbol{\varepsilon}^\beta$ are diagonal matrices whose elements are the orbital energies $\{\varepsilon_i^\alpha\}$ and $\{\varepsilon_i^\beta\}$ associated with the spatial orbitals $\{\varphi_i^\alpha\}$ and $\{\varphi_i^\beta\}$, respectively.

Hence, we see that by introducing a finite basis of atomic orbitals in the unrestricted Hartree-Fock framework, we obtain a set of two generalized eigenvalue problems. Those two matrix equations are known as the ‘‘Pople-Nesbet equations’’ [71] and are a generalization of the restricted Roothaan-Hall equations.

We stress that Pople-Nesbet equations consist of two coupled Roothaan-Hall equations in the sense that they cannot be solved separately. Indeed, each of the two Fock operators depends on the expansion coefficients of the molecular orbitals of all electrons, not only the ones of a specific spin. That is why they must be solved simultaneously in the iterative process.

Of course, since the atomic orbitals are usually not orthonormal, we can apply the same orthogonalization procedure introduced before in order to transform the Pople-Nesbet equations into standard matrix eigenvalue problems.

Unrestricted charge densities and density matrices

Let us define the total charge density for electrons with spin α and the total charge density for electrons with spin β

$$n^\alpha(\mathbf{r}) = \sum_{i=1}^{N^\alpha} |\varphi_i^\alpha(\mathbf{r})|^2 \quad (2.69) \quad \left| \quad n^\beta(\mathbf{r}) = \sum_{i=1}^{N^\beta} |\varphi_i^\beta(\mathbf{r})|^2 \quad (2.70)\right.$$

as well as the total charge density for all electrons

$$n(\mathbf{r}) = n^\alpha(\mathbf{r}) + n^\beta(\mathbf{r}). \quad (2.71)$$

If we inject the expansions of the unrestricted molecular orbitals into the above-mentioned definitions, we can obtain matrix representations for the charge densities of each spin

$$n^\alpha(\mathbf{r}) = \sum_{\mu=1}^K \sum_{\nu=1}^K P_{\mu\nu}^\alpha \phi_\mu(\mathbf{r}) \phi_\nu^*(\mathbf{r}) \quad (2.72) \quad \left| \quad n^\beta(\mathbf{r}) = \sum_{\mu=1}^K \sum_{\nu=1}^K P_{\mu\nu}^\beta \phi_\mu(\mathbf{r}) \phi_\nu^*(\mathbf{r}) \quad (2.73)\right.$$

with

$$P_{\mu\nu}^\alpha = \sum_{i=1}^{N^\alpha} C_{\mu i}^\alpha (C_{\nu i}^\alpha)^* \quad (2.74) \quad \left| \quad P_{\mu\nu}^\beta = \sum_{i=1}^{N^\beta} C_{\mu i}^\beta (C_{\nu i}^\beta)^*. \quad (2.75)\right.$$

$P_{\mu\nu}^\alpha$ are the matrix elements of the density matrix \mathbf{P}^α for electrons with spin α and $P_{\mu\nu}^\beta$ are the matrix elements of the density matrix \mathbf{P}^β for electrons with spin β .

Finally, the matrix representation of the total charge density will be the total density matrix which is simply the sum of the density matrices of both spins

$$\mathbf{P} = \mathbf{P}^\alpha + \mathbf{P}^\beta \quad (2.76)$$

Density matrix formulation of the unrestricted Hartree-Fock energy

Similarly to what was done for the restricted Hartree-Fock energy, the unrestricted Hartree-Fock energy can be reformulated in terms of the density matrices defined previously as follows

$$E^{\text{UHF}} = \frac{1}{2} \sum_{\mu} \sum_{\nu} \left[P_{\nu\mu} H_{\mu\nu}^{\text{core}} + P_{\nu\mu}^\alpha F_{\mu\nu}^\alpha + P_{\nu\mu}^\beta F_{\mu\nu}^\beta \right] \quad (2.77)$$

with

$$\begin{cases} H_{\mu\nu}^{\text{core}} &= \int \phi_\mu^*(\mathbf{r}_1) \hat{h}(\mathbf{r}_1) \phi_\nu(\mathbf{r}_1) d\mathbf{r}_1 \\ F_{\mu\nu}^\alpha &= H_{\mu\nu}^{\text{core}} + \sum_{\lambda} \sum_{\sigma} [P_{\lambda\sigma} \langle \mu\sigma | \nu\lambda \rangle - P_{\lambda\sigma}^\alpha \langle \mu\sigma | \lambda\nu \rangle] \\ F_{\mu\nu}^\beta &= H_{\mu\nu}^{\text{core}} + \sum_{\lambda} \sum_{\sigma} [P_{\lambda\sigma} \langle \mu\sigma | \nu\lambda \rangle - P_{\lambda\sigma}^\beta \langle \mu\sigma | \lambda\nu \rangle]. \end{cases} \quad (2.78)$$

Multiple Hartree-Fock solutions

For a closed-shell system, where there are as many spin-up electrons as spin-down electrons, $N^\alpha = N^\beta$, restricted Hartree-Fock is usually employed but is known to show deficiencies

when applied to dissociation processes for instance. Indeed, when a closed-shell system must dissociate into open-shell fragments, restricted Hartree-Fock fails to provide the correct answer and one must turn to unrestricted Hartree-Fock instead.

In the iterative process, if one enforces the constraint that the first guess for the density matrices verify the property $\mathbf{P}^\alpha = \mathbf{P}^\beta$, which means that the two initial Fock matrices will be identical, $\mathbf{F}^\alpha = \mathbf{F}^\beta$, then the resulting Hartree-Fock solution will be the restricted one. However, if one relaxes the above-mentioned constraint on the density matrices, the two initial Fock matrices will be distinct and it is possible to target a solution with a lower energy than the restricted one, if such a solution exists, the unrestricted Hartree-Fock solution.

2.3.3 Hartree-Fock Limit and Correlation Energy

When we introduced Hartree-Fock theory, we explained that it was an independent-particle theory that described the motion of “uncorrelated” electrons by approximating the electronic repulsion in an average manner. The fact is that any single-determinantal wave function, like the Hartree-Fock wave function, cannot properly describe the behaviour and properties of an interacting many-electron system, even when using a complete basis set, because it does not account for correlation effects.

The single-determinantal wave function used in Hartree-Fock theory cannot describe the detailed correlated motion of the electrons and, thus, cannot recover all of the exact ground state energy of the system even when computed in an infinite basis of orthonormal spin orbitals. The missing part is called “correlation energy” [84].

To be precise, Hartree-Fock theory does include some correlation due to the exchange term that only applies to same spin electron pairs and arises directly from the antisymmetry requirement of the Pauli exclusion principle. This type of correlation is often called “Fermi correlation” and has to be distinguished from the general definition of correlation used in quantum chemistry.

“Hartree-Fock limit” E_0^{HF} is the intrinsic limitation of this single-determinantal model. It is the lower energy that can be obtained by performing a Hartree-Fock calculation in the limit of a complete basis set and is an upper bound to the exact energy of the system.

The exact ground state energy of the system \mathcal{E}_0 can be obtained by minimizing the energy of a multi-determinantal wave function in a complete basis set of determinants (FCI).

Hence, the correlation energy is defined as the difference between the exact ground state energy and the Hartree-Fock limit and is negative

$$E_{\text{corr}} \equiv \mathcal{E}_0 - E_0^{\text{HF}}. \quad (2.79)$$

Although correlation was defined originally in the limit of a complete basis set, the definition has since been extended to finite basis set calculations for practical considerations.

The concept of correlation is particularly difficult to apprehend and numerous attempts have been made to unravel its origins [58]. Correlation effects are sometimes classified into two categories: “dynamical correlation” [39], arising from the instantaneous nature of the

exact coulombic repulsion between electrons, and “static correlation”, arising from near-degeneracies among configurations that strongly interact and involved in dissociation processes for instance.

Nevertheless, the frontier between those two concepts is not always well-defined and it is far from obvious to give a proper definition of what one calls correlation effects apart from the generic definition of equation (2.79).

2.4 The Self-Consistent-Field Scheme

As we have seen, Hartree-Fock theory is a self-consistent-field method which has to be solved iteratively. For sake of simplicity, we will only discuss the computational procedure applied for restricted Hartree-Fock calculations. As a matter of fact, the unrestricted procedure only differs from the restricted one in the fact that some of the steps have to be done twice, one for each of the spins.

The restricted SCF procedure [84] is as follows:

1. Specify informations about the system (nuclear coordinates, atomic numbers, number of electrons) and the AO basis set.
2. Compute all required integrals that do not change from one iteration to the other (overlap of the non-orthogonal AOs, core-Hamiltonian matrix elements and 2-electron integrals in the AO basis).
3. Diagonalize the AO overlap matrix in order to obtain a transformation matrix required in the orthogonalization procedure for the AO basis.
4. Form an initial guess at the density matrix
5. Calculate the set of two-electron integrals and the elements that depend on the density matrix, such as the two-electron part of the Fock matrix.
6. Form the Fock matrix by summation of the core-Hamiltonian part obtained in step 2 and the two-body part obtained in step 5.
7. Calculate the transformed Fock matrix by use of the transformation matrix obtained in step 3.
8. Diagonalize the transformed Fock matrix to obtain a set of expansion coefficients and eigenvalues in the orthogonalized basis.
9. By inversion of the orthogonalization procedure, deduce the solutions in the initial non-orthogonal basis.
10. Form the new density matrix obtained from the expansion coefficients obtained in step 9.

11. Check if the new density matrix is close enough to the previous iteration, in accordance with the predefined convergence treshold. If the new density matrix is not satisfactory enough, return to step 5 in order to proceed to a new iteration.
12. If convergence is achieved, use the quantities obtained from the last iteration to compute expectation values like the energy and properties of interest.

Chapter 3

Density-Functional Theory

Contents

3.1	Early Stages of Density-Functional Theory	48
3.1.1	Reduced Density Matrices	48
3.1.2	The Exact kinetic-energy functional	50
3.1.3	The Thomas-Fermi Model	50
3.2	Density-Functional Theory Fundamental Idea	51
3.2.1	The Hohenberg-Kohn Theorems	51
3.2.2	The Levy Constrained-Search Formulation	52
3.3	Kohn and Sham Approach	54
3.3.1	Kohn-Sham system	54
3.3.2	Kohn-Sham equations	55
3.3.3	Interpretation of the Kohn-Sham Orbital Energies	57
3.4	The Basis-Set Formulation of DFT	58
3.5	Spin Density-Functional Theory	60
3.5.1	Spin Densities	60
3.5.2	Spin Extension of the Universal Density Functional	61
3.5.3	Unrestricted Kohn-Sham Approach	61
3.6	Exchange-Correlation Energy	63
3.6.1	Building Approximations	63
3.6.2	Jacob's Ladder	64

3.1 Early Stages of Density-Functional Theory

We have seen that all the information about a N -electron system was contained into its wave function and that the knowledge of the wave function could unravel the path to any electronic properties of the system. Unfortunately, the wave function remains difficult to access and one must rely on other alternatives to obtain proper predictions to physical and chemical properties.

Fortunately, the wave function is not the only quantity containing information about the system that one can exploit. Density-Functional Theory [65] stemmed from the need to find new formalisms, other than wave function-based methods, where one could rely on simpler quantities than the elusive wave function in order to access accurate descriptions of atoms, molecules and condensed-matter properties.

3.1.1 Reduced Density Matrices

There exist quantities, reduced quantities [65, 39], that, although containing less information than the wave function, are much more convenient to exploit computationally. We will discuss some of them.

For a N -electron system in a state represented by a wave function Ψ , we define the first-order density matrix as follows

$$\gamma_1(\mathbf{x}'_1, \mathbf{x}_1) = N \int \cdots \int \Psi(\mathbf{x}'_1, \mathbf{x}_2, \dots, \mathbf{x}_N) \Psi^*(\mathbf{x}_1, \mathbf{x}_2, \dots, \mathbf{x}_N) d\mathbf{x}_2 \dots d\mathbf{x}_N, \quad (3.1)$$

which is normalized to the total number of electrons N such that

$$\text{Tr}\{\gamma_1(\mathbf{x}'_1, \mathbf{x}_1)\} = \int \gamma_1(\mathbf{x}_1, \mathbf{x}_1) d\mathbf{x}_1 = N, \quad (3.2)$$

and from which we can obtain the total electron density of the system

$$n(\mathbf{x}_1) = \gamma_1(\mathbf{x}_1, \mathbf{x}_1). \quad (3.3)$$

$\gamma_1(\mathbf{x}'_1, \mathbf{x}_1)$ is the coordinate-space representation of a hermitian one-electron operator $\hat{\gamma}_1$ which admits an infinite set of eigenfunctions $\{\chi_i\}$ with eigenvalues $\{n_i\}$.

The eigenfunctions of the first-order density matrix operator are called “natural spin orbitals” and the corresponding eigenvalues are the “occupation numbers” of the natural spin orbitals. Since $\hat{\gamma}_1$ is a hermitian operator, it can be expanded in the complete basis of its eigenstates

$$\hat{\gamma}_1 = \sum_{i=1}^{\infty} n_i |\chi_i\rangle \langle \chi_i|, \quad (3.4)$$

or in the space-spin representation

$$\gamma_1(\mathbf{x}'_1, \mathbf{x}_1) = \sum_{i=1}^{\infty} n_i \chi_i(\mathbf{x}'_1) \chi_i^*(\mathbf{x}_1). \quad (3.5)$$

Many operators are spin-independent so one can decide to eliminate the spin-dependency by summation over spin components. Hence, one can define a first-order spinless density matrix

$$\rho_1(\mathbf{r}'_1, \mathbf{r}_1) = \sum_{\sigma} \gamma_1(\mathbf{r}'_1, \sigma, \mathbf{r}_1, \sigma). \quad (3.6)$$

Additionally, one can also define the second-order reduced density matrix

$$\gamma_2(\mathbf{x}'_1, \mathbf{x}'_2, \mathbf{x}_1, \mathbf{x}_2) = \frac{N(N-1)}{2} \int \cdots \int \Psi(\mathbf{x}'_1, \mathbf{x}'_2, \mathbf{x}_3, \dots, \mathbf{x}_N) \Psi^*(\mathbf{x}_1, \mathbf{x}_2, \mathbf{x}_3, \dots, \mathbf{x}_N) d\mathbf{x}_3 \cdots d\mathbf{x}_N \quad (3.7)$$

which is normalized to the number of unique pairs of electrons such that

$$\text{Tr}\{\gamma_2(\mathbf{x}'_1, \mathbf{x}'_2, \mathbf{x}_1, \mathbf{x}_2)\} = \iint \gamma_2(\mathbf{x}_1, \mathbf{x}_2, \mathbf{x}_1, \mathbf{x}_2) d\mathbf{x}_1 d\mathbf{x}_2 = \frac{N(N-1)}{2}. \quad (3.8)$$

Finally, there exists a more “complete” density matrix, the N th-order density matrix

$$\gamma_N(\mathbf{x}'_1, \mathbf{x}'_2 \dots \mathbf{x}'_N, \mathbf{x}_1, \mathbf{x}_2 \dots \mathbf{x}_N) = \Psi(\mathbf{x}'_1, \mathbf{x}'_2 \dots \mathbf{x}'_N) \Psi^*(\mathbf{x}_1, \mathbf{x}_2 \dots \mathbf{x}_N), \quad (3.9)$$

which contains as much information about the system as the wave function itself such that it can be used to calculate the expectation value of any operator \hat{O}

$$\langle \hat{O} \rangle = \text{Tr}\{\gamma_N \hat{O}\}, \quad (3.10)$$

like the Hamiltonian operator, for instance,

$$E[\gamma_N] = \text{Tr}\{\gamma_N \hat{H}\}. \quad (3.11)$$

As a matter of fact, it has been proved that the exact total energy could be written as a functional of the electron density and the first- and second-order density matrices only

$$E[n, \gamma_1, \gamma_2] = T[\gamma_1] + V_{\text{en}}[n] + V_{\text{ee}}[\gamma_2], \quad (3.12)$$

where T , V_{en} and V_{ee} are the kinetic, nuclear attraction and electronic repulsion energy functionals, respectively.

Since the kinetic and nuclear attraction operators are one-electron operators, it seems logical that they can be defined as functionals of one-body quantities such as the first-order density matrix and the electron density. Conversely, since the electron-electron term arises from the simultaneous interaction between each pairs of electrons, it makes sense that it is associated with a functional of a two-body quantity such as the second-order density matrix.

Furthermore, the electron density and the first-order density matrix can be built from integration of the second-order density matrix. Thus, in theory, one only needs the second-order density matrix in order to obtain the total energy of the system

$$E[\gamma_N] = E[n, \gamma_1, \gamma_2] = E[\gamma_2], \quad (3.13)$$

but, because of N -representability limitations, the second-order density matrix is often difficult to work with. Hence, in principle, it is possible to compute electronic properties, like the total energy, directly from reduced quantities much simpler than the wave function.

3.1.2 The Exact kinetic-energy functional

From the above discussion, the exact kinetic energy functional of the system can be expressed as a functional of the first-order density matrix

$$\hat{T} = \int \left[-\frac{1}{2} \nabla_{\mathbf{r}}^2 \gamma_1(\mathbf{x}'_1, \mathbf{x}_1) \right]_{\mathbf{x}'_1 = \mathbf{x}_1} d\mathbf{x}_1, \quad (3.14)$$

which, at this point, is our main interest.

If we inject the expansion of the first-order density matrix defined in equation (3.4) in terms of its eigenstates, the spin orbitals, and eigenvalues, the occupation numbers, the exact kinetic energy functional takes the form of an orbital functional, not a density functional,

$$T = \sum_{i=1}^{\infty} n_i \langle \chi_i | -\frac{1}{2} \nabla^2 | \chi_i \rangle. \quad (3.15)$$

Since electrons are fermionic particles and, thus, must obey the Fermi exclusion principle, the occupation numbers of the natural spin orbitals must obey the following constraint

$$0 \leq n_i \leq 1, \quad (3.16)$$

and we must retrieve the total number of electrons of the system by summation upon all occupation numbers

$$\sum_{i=1}^{\infty} n_i = N. \quad (3.17)$$

In the case of an interacting system, the state of the system will consist of an infinite set of occupied natural spin orbitals with possibly fractional occupation numbers [65].

Therefore, the total electron density of such a system takes the following form

$$n(\mathbf{r}) = \sum_{\sigma} \sum_{i=1}^{\infty} n_i |\chi_i(\mathbf{r}, \sigma)|^2. \quad (3.18)$$

3.1.3 The Thomas-Fermi Model

Decades before the foundational theorems of density-functional theory were even formalized, Thomas and Fermi [86] proposed the very first “density-functional” approximation. Whereas the exact formulation of the kinetic-energy functional of an electronic system was based on the first-order density matrix, they proposed an approximation in terms of the electron density. Indeed, their work was based on the concept of the local density approximation (LDA) [65], which has since been applied to other quantities. The LDA consists in making the assumption that matter behaves locally like a homogeneous electronic system. Hence, the Thomas-Fermi (TF) approximation for the kinetic energy functional

$$T_{\text{TF}}[n] = C_{\text{F}} \int n(\mathbf{r})^{\frac{5}{3}} d\mathbf{r}, \quad (3.19)$$

with $C_F = \frac{3}{10}(3\pi^2)^{\frac{2}{3}}$.

The Thomas-Fermi model [39, 65] stemmed from the will to design a total-energy functional that would truly be a functional of the sole electron density. The total energy provided by such a simple model includes the TF kinetic energy functional and the classical nuclear attraction and Hartree functional for the Coulombic electronic repulsion only,

$$E_{\text{TF}}[n] = T_{\text{TF}}[n] + E_{\text{H}}[n] + V_{\text{en}}[n], \quad (3.20)$$

with the classical Hartree energy functional

$$E_{\text{H}}[n] = \frac{1}{2} \iint \frac{n(\mathbf{r}_1)n(\mathbf{r}_2)}{|\mathbf{r}_1 - \mathbf{r}_2|} d\mathbf{r}_1 d\mathbf{r}_2, \quad (3.21)$$

and the nuclear attraction energy functional (for molecules)

$$V_{\text{en}}[n] = - \sum_{A=1}^{M_{\text{nucl}}} \int \frac{Z_A n(\mathbf{r})}{|\mathbf{R}_A - \mathbf{r}|} d\mathbf{r}. \quad (3.22)$$

Thus, the Thomas-Fermi model does not account for exchange or correlation contributions. A few years later, The TF model was extended to include an additional exchange contribution, yielding the Thomas-Fermi-Dirac (TFD) model [39].

Unfortunately, both TF and TFD models were atomic models and were not consistent with the description of chemical bonds, making the two theories highly unsuitable for chemical applications. Nevertheless, Thomas and Fermi were the first to introduce (although implicitly) the concept of density functionals, and their work therefore became a cornerstone for the development of a promising exact theory, density-functional theory.

3.2 Density-Functional Theory Fundamental Idea

3.2.1 The Hohenberg-Kohn Theorems

The fundamental and conceptual idea of density-functional theory strongly relies on the work of Hohenberg and Kohn [37] whose theorems provided legitimacy to this appealing theory.

The first Hohenberg-Kohn theorem proved that the electron density of a N -electron system could serve as basic variable to access all electronic properties of the system [65], which was a very attractive idea because of the system-size independent low dimensionality of the electron density, compared to the wave function.

They proved a one-to-one correspondence between the ground-state density of an electronic system and the external potential experienced by the electrons of the system. As a matter of fact, they have shown, in an astonishingly simple manner, that two external potentials differing by more than a constant cannot be associated with the same ground state density. Hence, the electron density determines the external potential, within an additive constant,

as well as the total number of electrons of the system through the normalization constraint. The first Hohenberg-Kohn theorem can be summarized as follows

“The ground-state electron density of a system of interacting electrons uniquely determines the external potential in which the electrons move and thus the Hamiltonian and all physical properties of the system.” [49]

The second Hohenberg-Kohn theorem states that there exists a density-based analog of the variational principle defined upon wave functions for the total energy of the system. First, they state that the total energy of the system is a functional of the electron density only. Indeed, for a given external potential $v(\mathbf{r})$, the total energy can be written according to the following density-functional decomposition

$$\begin{aligned} E[n] &= T[n] + V_{\text{ee}}[n] + V_{\text{en}}[n] \\ &= F_{\text{HK}}[n] + V_{\text{en}}[n], \end{aligned} \quad (3.23)$$

with

$$V_{\text{en}}[n] = \int n(\mathbf{r})v(\mathbf{r})d\mathbf{r} \quad (3.24)$$

and the Hohenberg-Kohn universal functional

$$F_{\text{HK}}[n] = T[n] + V_{\text{ee}}[n] = \langle \Psi | \hat{T} + \hat{V}_{\text{ee}} | \Psi \rangle. \quad (3.25)$$

In the above-mentioned definition, Ψ is the ground-state wave function associated with the ground-state density n .

Then, the second HK theorem states that any trial density \tilde{n} will lead to an upper bound of the true energy of the system that can only be obtained with the true ground-state density n_0 ,

$$E_0 \equiv E[n_0] \leq E[\tilde{n}]. \quad (3.26)$$

In practice, the major difficulty arises from the fact that the closed-form of the exact energy functional is unknown, especially the form of the Hohenberg-Kohn universal functional, and because of that one must resort to approximate functionals instead.

$F_{\text{HK}}[n]$ is said to be “universal” in the sense that it does not depend on the external field experienced by the electrons. For that reason, the energy of any electronic system placed in the field associated with a given local external potential $v(\mathbf{r})$, will be determined by the same exact functionals $F_{\text{HK}}[n]$, and thus $E[n]$. Density-functional theory is therefore a reformulation of wave mechanics in which the electron density plays a key role (crucial).

3.2.2 The Levy Constrained-Search Formulation

v-representability and *N*-representability of electron densities

An electron density is said to be *v*-representable if it is generated by an antisymmetric wave function associated with an external potential v through an Hamiltonian operator.

As a matter of fact, electronic properties can only be associated with functionals of v -representable densities and the density-based variational principle can exclusively be applied upon v -representable densities [65]. Unfortunately, all “well-behaved” densities are not necessary v -representable, even for simple systems, and the exact constraints that guarantee v -representability of the density are not known.

Hopefully, there exists a similar but less-restrictive constraint upon electron densities that still ensures the variational principle, the N -representability constraint. In practice, N -representable densities are much easier to obtain than v -representable densities and most positive, normalized and continuous densities are N -representable.

Constrained-search reformulation

Any v -representable trial density \tilde{n} will yield a greater energy than the true ground-state energy, that is the energy provided by the true ground-state density n_0 of the system,

$$E[\tilde{n}] = F_{\text{HK}}[\tilde{n}] + \int \tilde{n}(\mathbf{r})v(\mathbf{r})d\mathbf{r} \geq E[n_0]. \quad (3.27)$$

originally, the Hohenberg-Kohn functional was defined exclusively for v -representable densities but it has been since reformulated into a constrained-search form [53, 52, 54],

$$\begin{aligned} F_{\text{HK}}[n_0] &= T[n_0] + V_{\text{ee}}[n_0] \\ &= \langle \Psi_0 | \hat{T} + \hat{V}_{\text{ee}} | \Psi_0 \rangle \\ &= \min_{\Psi \rightarrow n_0} \langle \Psi | \hat{T} + \hat{V}_{\text{ee}} | \Psi \rangle, \end{aligned} \quad (3.28)$$

where Ψ_0 is the ground-state wave function associated with the v -representable density n_0 , and where the search is upon all antisymmetric and normalized wave functions, not only ground-state wave functions, which generate the density n_0 .

Hence, the definition of the Hohenberg-Kohn universal functional has been extended to a less restrictive class of densities, N -representable densities, such that

$$F[n] = \min_{\Psi \rightarrow n} \langle \Psi | \hat{T} + \hat{V}_{\text{ee}} | \Psi \rangle. \quad (3.29)$$

The last definition stands for any N -representable density n and the minimization is made upon all antisymmetric wave functions that gives the density n . Note that this definition allows the degeneracy of the ground-state wave function.

The variational minimization of the total energy therefore becomes

$$\begin{aligned} E_0 &= \min_{\Psi} \langle \Psi | \hat{T} + \hat{V}_{\text{ee}} + \hat{V}_{\text{en}} | \Psi \rangle \\ &= \min_n \left\{ \min_{\Psi \rightarrow n} \langle \Psi | \hat{T} + \hat{V}_{\text{ee}} + \hat{V}_{\text{en}} | \Psi \rangle \right\} \\ &= \min_n \left\{ F[n] + \int n(\mathbf{r})v(\mathbf{r})d\mathbf{r} \right\} \\ &= \min_n E[n]. \end{aligned} \quad (3.30)$$

The above-mentioned constrained-search scheme allows one to define an energy functional which is applicable to any N -representable density instead of only v -representable ones,

$$E[n] = F[n] + \int n(\mathbf{r})v(\mathbf{r})d\mathbf{r}. \quad (3.31)$$

Still, F remains very difficult to approximate. Note that, since the density contains less information than the wave function, functionals of reduced quantities such as the density may take a much complicated form than wave function functionals, or have a simple explicit form while applying to a very restricted domain.

Finally, one may rewrite the universal functional as

$$\begin{aligned} F[n] &\equiv \min_{\Psi \rightarrow n} \langle \Psi | \hat{T} + \hat{V}_{ee} | \Psi \rangle \\ &= \langle \Psi[n] | \hat{T} + \hat{V}_{ee} | \Psi[n] \rangle \\ &= T[n] + V_{ee}[n], \end{aligned} \quad (3.32)$$

where $\Psi[n]$ is the wave function that yields the electron density n and minimizes the quantity $\langle \Psi | \hat{T} + \hat{V}_{ee} | \Psi \rangle$. Thus, $\Psi[n]$ is a functional of the density.

With that definition, one can define the exact kinetic energy functional

$$T[n] = \langle \Psi[n] | \hat{T} | \Psi[n] \rangle, \quad (3.33)$$

and the exact electronic repulsion functional

$$V_{ee}[n] = \langle \Psi[n] | \hat{V}_{ee} | \Psi[n] \rangle. \quad (3.34)$$

3.3 Kohn and Sham Approach

For coulombic systems, the kinetic energy is known to represent a very significant part of the total energy so the use of approximate kinetic energy functionals can have a major impact on the final accuracy and thus their elaboration requires peculiar attention and care. In that matter, Kohn and Sham approach has been a tremendous breakthrough and gave rise to modern density-functional theory because it enables to retrieve almost all the exact kinetic energy of the system [9].

3.3.1 Kohn-Sham system

Kohn and Sham [42] proposed to connect the real N -electron system to a fictitious auxiliary system, the “Kohn-Sham system”. The Kohn-Sham system is a fictitious non-interacting N -electron system which has the particularity of having the same density than the real interacting system.

Non-interacting systems are usually assumed to be described by a single Slater determinant

wave function Φ and since the Kohn-Sham system is, by definition, a non-interacting system, the universal functional for such a system will only consist of a kinetic contribution

$$\begin{aligned} F_s[n] &\equiv \min_{\Phi \rightarrow n} \langle \Phi | \hat{T} | \Phi \rangle \\ &= \langle \Phi[n] | \hat{T} | \Phi[n] \rangle \\ &= T_s[n], \end{aligned} \tag{3.35}$$

where the constrained-search is over all Slater determinants that yield the density n [65], and $\Phi[n]$ is the Slater determinant that minimizes the kinetic energy $\langle \Phi | \hat{T} | \Phi \rangle$ and yields the density n . The subscript “s” is used to point out that the system is a non-interacting system and, thus, is described by a single Slater determinant wave function.

Since the electron density of the Kohn-Sham system is forced to mimic the density of the real system, the Kohn-Sham system cannot experience the same external potential $v(\mathbf{r})$ than the real interacting system. Instead, it will experience a one-electron effective potential, the Kohn-Sham potential $v_s(\mathbf{r})$, which encompasses all the potential contributions of the real interacting system, arising from its “interacting” nature in addition to the external nuclear potential $v(\mathbf{r})$, such that

$$\begin{aligned} v_s(\mathbf{r}) &= v(\mathbf{r}) + v_{ee}(\mathbf{r}) \\ &= v(\mathbf{r}) + v_H(\mathbf{r}) + v_{xc}(\mathbf{r}). \end{aligned} \tag{3.36}$$

$v_{ee}(\mathbf{r})$ is the potential experienced by the real interacting system due to the interacting nature of the electrons. It is usually decomposed into a classical coulombic contribution, the Hartree potential,

$$v_H(\mathbf{r}) = \int \frac{n(\mathbf{r}')}{|\mathbf{r} - \mathbf{r}'|} d\mathbf{r}', \tag{3.37}$$

and an unknown quantum contribution, the exchange-correlation potential $v_{xc}(\mathbf{r})$.

By modifying the potential, one can influence the density, and vice-versa. Hence, the Kohn-Sham potential is here to make sure that the Kohn-Sham electron density remains identical to the real electron density during the variational-optimization process.

3.3.2 Kohn-Sham equations

The Kohn-Sham wave function is a Slater determinant built from a set of Kohn-Sham molecular orbitals $\{\varphi_i(\mathbf{r})\}$. The N Kohn-Sham orbitals with lowest energies will each be occupied by a single electron while the remaining orbitals will be unoccupied.

For such non-interacting systems, the exact kinetic energy functional takes the form

$$T_s[n] = \min_{\Phi(\{\varphi_i\}) \rightarrow n} \sum_{i=1}^N \langle \varphi_i | -\frac{1}{2} \nabla^2 | \varphi_i \rangle, \tag{3.38}$$

where the optimization process consists in finding the best set of orthonormal molecular orbitals which generates a single Slater determinant with the lowest kinetic energy, and yields the given electron density

$$\sum_{i=1}^N |\varphi_i(\mathbf{r})|^2 = n(\mathbf{r}). \quad (3.39)$$

Let us recall the generic expression of the exact total energy functional of the interacting system experiencing the external local potential $v(\mathbf{r})$,

$$E[n] = T[n] + V_{ee}[n] + \int n(\mathbf{r})v(\mathbf{r})d\mathbf{r}. \quad (3.40)$$

Remember that this functional stands for any density generated by an antisymmetric N -electron wave function.

When one works in the Kohn-Sham framework, one only consider single Slater-determinant wave functions. For that reason one can reformulate the energy functional such that

$$E[n] = T_s[n] + E_H[n] + E_{xc}[n] + \int n(\mathbf{r})v(\mathbf{r})d\mathbf{r}, \quad (3.41)$$

where the exact kinetic energy functional $T[n]$ of the interacting system is replaced with the exact kinetic energy functional $T_s[n]$ of the non-interacting Kohn-Sham system, and the exact electronic repulsion energy functional $V_{ee}[n]$ is replaced by the classical coulombic Hartree repulsion energy functional $E_H[n]$.

The third term in the previous decomposition is the exchange-correlation energy functional

$$E_{xc}[n] \equiv (T[n] - T_s[n]) + (V_{ee}[n] - E_H[n]), \quad (3.42)$$

and arises from the two previously-mentioned kinetic and electron-electron approximations. Hence, the task of the exchange-correlation energy term is to correct the resulting errors in order to recover the exact total energy of the real interacting system.

We have seen that the Kohn-Sham kinetic energy functional and the electron density could be explicitly formulated in terms of the occupied Kohn-Sham orbitals from which the single Slater determinantal wave function is formed. For that reason, we can recast the variational optimization of the total energy in terms of the Kohn-Sham orbitals under the constraint that they remain orthonormal during the variational procedure

$$\int \varphi_i^*(\mathbf{r})\varphi_j(\mathbf{r})d\mathbf{r} = \delta_{ij}, \quad (3.43)$$

where δ_{ij} is the Kronecker delta.

Such optimization problems with specific-constraint requirements are usually treated using Lagrange's multipliers method which will not be detailed in this work.

Minimization of the energy defined in equation (3.41), under the orthonormalization constraint defined in equation (3.43) yields the following Kohn-Sham equations (in their canonical form)

$$\left(-\frac{1}{2}\nabla^2 + v_s(\mathbf{r})\right)\varphi_i(\mathbf{r}) = \varepsilon_i\varphi_i(\mathbf{r}). \quad (3.44)$$

$v_s(\mathbf{r})$ is the Kohn-Sham one-electron effective potential experienced by the non-interacting Kohn-Sham system and defined in equation (3.36). Moreover, in the KS scheme, the exchange-correlation potential is defined as the functional derivative of the exchange-correlation energy functional with respect to the electron density, such that

$$v_{xc}(\mathbf{r}) = \frac{\delta E_{xc}[n]}{\delta n(\mathbf{r})}. \quad (3.45)$$

Departing from the Kohn-Sham one-electron Hamiltonian operator \hat{h}_s , in its space-representation

$$h_s(\mathbf{r}) \equiv -\frac{1}{2}\nabla^2 + v_s(\mathbf{r}), \quad (3.46)$$

acting on the Kohn-Sham molecular orbitals such that

$$h_s(\mathbf{r})\varphi_i(\mathbf{r}) = \varepsilon_i\varphi_i(\mathbf{r}), \quad (3.47)$$

it is straightforward to see that the Kohn-Sham equations form a set of one-electron eigenvalue equations whose eigenfunctions are the Kohn-Sham orbitals $\{\varphi_i\}$, with eigenvalues the Kohn-Sham orbital energies $\{\varepsilon_i\}$. Note that the Kohn-Sham equations are nonlinear equations and must be solved iteratively.

Hence, we see that the Hartree-Fock and Kohn-Sham density-functional frameworks are very similar. Though, we must point out some fundamental differences between these two formalisms. The Hartree-Fock formalism is not exact in the sense that it completely neglects correlation effects arising from the mutual influence between electrons, while Kohn-Sham DFT takes them into account through the exchange-correlation functional and, thus, is an exact theory.

Another fundamental difference comes from the nature of the electronic repulsion potential. In Hartree-Fock theory, the single Slater determinantal approximation gives rise to a non-local exchange potential, while in KS-DFT it is the choice of the exchange-correlation functional that will determine the nature of the potential, local, semi-local or non-local.

Finally, KS-DFT offers much more flexibility by allowing one to design approximations for the exchange-correlation energy functional in order to improve the results.

3.3.3 Interpretation of the Kohn-Sham Orbital Energies

Analogously to Koopmans' theorem in Hartree-Fock theory, there have been attempts to provide physical meaning [2] for the eigenvalues of the Kohn-Sham equations. As a matter

of fact, Janak proposed a generalization of the KS scheme to fractional occupation numbers that allows for the electron number of the system to vary continuously.

Janak’s theorem [38] establishes a direct connection between the slope of the total energy E of the system with respect to the fractional occupation number n_i of a specific KS orbital and the energy ε_i of this orbital

$$\frac{\partial E}{\partial n_i} = \varepsilon_i. \quad (3.48)$$

Departing from Janak’s theorem, a direct connection between the ionization potential, defined as the slope of the energy with respect to the number of electrons of the system, and the KS HOMO energy can be derived

$$I_0^N = -\varepsilon^{\text{HOMO}}. \quad (3.49)$$

Note that this result, known as the “IP theorem” can be established as well by considering the asymptotic decay of the exact electron density of the system.

As for the electron affinity of the N -electron system, although there exists no direct connection with the LUMO energy, an expression based on these two quantities can be derived through the infamous “derivative discontinuity” Δ , a spatial step experienced by the exact xc-potential as the number of electrons N crosses an integral value.

Hence, the following formulation of the fundamental gap in terms of the Kohn-Sham frontier orbital energies

$$\Omega_{\text{fun}}^N = \varepsilon^{\text{LUMO}} - \varepsilon^{\text{HOMO}} + \Delta. \quad (3.50)$$

In DFT, for finite-size systems, it is possible to obtain excitation energies by use of different sets of occupation numbers in order to mimic the neutral, cationic and anionic ground states and by performing total-energy differences provided by multiple self-consistent DFT calculations. As a matter of fact, despite requiring multiple calculations, the above-mentioned Δ SCF method is known to provide much better excitation energies than the KS eigenvalues because ground-state KS-DFT favors total energies over potential quantities such as orbital energies. Finally, the KS gap is usually too small and strongly depends on the functional used in the calculation.

The physical meaning of the Kohn-Sham orbital energies will be extensively discussed in the next chapter.

3.4 The Basis-Set Formulation of DFT

Hartree-Fock and Kohn-Sham DFT are very similar in both conceptual and computational aspects. Within the scope of KS-DFT, one has to solve the Kohn-Sham equations

$$h_s(\mathbf{r})\varphi_i(\mathbf{r}) = \varepsilon_i\varphi_i(\mathbf{r}), \quad (3.51)$$

in order to find the Kohn-Sham molecular orbitals with Kohn-Sham energies.

Practical calculations of KS-DFT starts with the expansion of the Kohn-Sham molecular

orbitals in a finite basis of K atomic orbitals, like in Hartree-Fock theory

$$\varphi_i(\mathbf{r}) = \sum_{\mu=1}^K C_{\mu i} \phi_{\mu}(\mathbf{r}). \quad (3.52)$$

Kohn-Sham generalized eigenvalue problem

The use of a finite basis set allows for a matrix formulation of the Kohn-Sham problem, which is a generalized eigenvalue problem

$$\mathbf{FC} = \mathbf{SC}\varepsilon, \quad (3.53)$$

or equivalently

$$\sum_{\mu=1}^K F_{\mu\nu} C_{\nu i} = \varepsilon_i \sum_{\mu=1}^K S_{\mu\nu} C_{\nu i}. \quad (3.54)$$

In the KS-DFT framework, the Fock matrix elements can be decomposed as follows

$$F_{\mu\nu} = h_{\mu\nu} + J_{\mu\nu} + V_{\mu\nu}^{\text{xc}}, \quad (3.55)$$

and include the one-electron core Hamiltonian integral

$$h_{\mu\nu} = \int \phi_{\mu}^*(\mathbf{r}) \left(-\frac{1}{2} \nabla^2 + v(\mathbf{r}) \right) \phi_{\nu}(\mathbf{r}) \mathbf{d}\mathbf{r}, \quad (3.56)$$

the classical coulombic integral

$$J_{\mu\nu} = \int \phi_{\mu}^*(\mathbf{r}) v_{\text{H}}(\mathbf{r}) \phi_{\nu}(\mathbf{r}) \mathbf{d}\mathbf{r}, \quad (3.57)$$

and the combined exchange-correlation integral

$$V_{\mu\nu}^{\text{xc}} = \int \phi_{\mu}^*(\mathbf{r}) v_{\text{xc}}(\mathbf{r}) \phi_{\nu}(\mathbf{r}) \mathbf{d}\mathbf{r}. \quad (3.58)$$

Note that, one can apply the orthogonalization procedure in order to transform the Kohn-Sham generalized eigenvalue problem into a standard matrix eigenvalue problem by orthogonalizing the initial non-orthogonal atomic basis, as discussed for the Hartree-Fock framework.

Density matrix formulation

It is possible to reformulate the Kohn-Sham scheme in terms of the Kohn-Sham density matrix of the system \mathbf{P} with

$$P_{\mu\nu} = \sum_{i=1}^N C_{\mu i} C_{\nu i}^*, \quad (3.59)$$

where the summation is upon all occupied Kohn-Sham molecular orbitals. With the density matrix, one can generate the electron density of the system

$$n(\mathbf{r}) = \sum_{\mu=1}^K \sum_{\nu=1}^K P_{\mu\nu} \phi_{\mu}(\mathbf{r}) \phi_{\nu}^*(\mathbf{r}), \quad (3.60)$$

and the two-electron Hartree integral

$$J_{\mu\nu} = \sum_{\lambda=1}^K \sum_{\sigma=1}^K P_{\lambda\sigma} \langle \mu\sigma | \nu\lambda \rangle, \quad (3.61)$$

where we used the physicist's notation for two-electron integrals, previously introduced in the Hartree-Fock chapter.

Hence, we can obtain a much easier-to-compute expression for the total energy of the system

$$E = \sum_{\mu=1}^K \sum_{\nu=1}^K P_{\nu\mu} h_{\mu\nu} + \frac{1}{2} \sum_{\mu=1}^K \sum_{\nu=1}^K P_{\nu\mu} J_{\mu\nu} + E_{\text{xc}}. \quad (3.62)$$

We stress that the (restricted) Kohn-Sham computational procedure is extremely similar to the restricted Hartree-Fock procedure but still differs in the way one must treat the exchange-correlation contribution E_{xc} . Indeed, while the Hartree-Fock exact-exchange energy can be expressed explicitly in terms of the two-electron integrals and the density matrix, the exchange-correlation functionals used in Kohn-Sham-DFT do not possess a simple linear dependence on the electron density, and thus cannot be evaluated analytically. For that reason, numerical integrations must be employed instead.

3.5 Spin Density-Functional Theory

Like we have seen when we discussed the restricted- and unrestricted formulations of Hartree-Fock theory, there are situations where one must take into account the spin distributions of the system. Although, in principle, the total electron density of the system is sufficient to obtain the electronic properties of any electronic system, closed-shell as well as open-shell systems, considering both spin densities have shown to provide better results and have led to the elaboration of many spin-dependent approximate functionals.

3.5.1 Spin Densities

First, let us recall the expressions of the spin densities of an N -electron system with N^{α} spin-up electrons, N^{β} spin-down electrons and total electron density $n(\mathbf{r})$.

The spin density for spin-up electrons is defined as follows

$$n^{\alpha}(\mathbf{r}) = N \int \cdots \int |\Psi(\mathbf{r}, \alpha, \mathbf{x}_2 \dots \mathbf{x}_N)|^2 d\mathbf{x}_2 \dots d\mathbf{x}_N, \quad (3.63)$$

and is normalized to the total number of spin-up electrons such that

$$\int n^\alpha(\mathbf{r})d\mathbf{r} = N^\alpha. \quad (3.64)$$

Similarly, the spin density for spin-down electrons is defined as

$$n^\beta(\mathbf{r}) = N \int \cdots \int |\Psi(\mathbf{r}, \beta, \mathbf{x}_2 \dots \mathbf{x}_N)|^2 d\mathbf{x}_2 \dots d\mathbf{x}_N, \quad (3.65)$$

and is normalized to the total number of spin-down electrons such that

$$\int n^\beta(\mathbf{r})d\mathbf{r} = N^\beta. \quad (3.66)$$

Of course, the sum of the two spin densities recovers the total electron density

$$n(\mathbf{r}) = n^\alpha(\mathbf{r}) + n^\beta(\mathbf{r}). \quad (3.67)$$

3.5.2 Spin Extension of the Universal Density Functional

The universal density functional $F[n]$ previously introduced was defined for any N -representable density and was formulated under the form of a constrained-search minimization upon all normalized antisymmetric wave functions which yield a specific density $n(\mathbf{r})$.

As a matter of fact, this definition can be extended to spin densities into the form of a spin-density functional. The constrained-search will then be performed upon a double constraint, that all considered normalized antisymmetric wave functions yield the two specific spin-densities defined in equations (3.63) and (3.65) such that

$$F[n^\alpha, n^\beta] = \min_{\Psi \rightarrow \{n^\alpha, n^\beta\}} \langle \Psi | \hat{T} + \hat{V}_{ee} | \Psi \rangle. \quad (3.68)$$

3.5.3 Unrestricted Kohn-Sham Approach

The Kohn-Sham approach can be extended as well to a more general spin-density formulation. The universal functional will then be decomposed into the same contributions than for the standard Kohn-Sham scheme, except for the fact that some of those contributions will now be functionals of the two spin densities in place of the total electron density

$$\begin{aligned} F[n^\alpha, n^\beta] &= T_s[n^\alpha, n^\beta] + V_{ee}[n^\alpha, n^\beta] \\ &= T_s[n^\alpha, n^\beta] + E_H[n] + E_{xc}[n^\alpha, n^\beta] \end{aligned} \quad (3.69)$$

with

$$T_s[n^\alpha, n^\beta] = \min_{\Phi \rightarrow \{n^\alpha, n^\beta\}} \langle \Phi | \hat{T} | \Phi \rangle. \quad (3.70)$$

In the above kinetic energy functional, the constrained-search is made upon all Slater determinants built from unrestricted molecular orbitals, that is to say from two different sets of

molecular orbitals depending on the spin nature of the electrons occupying these orbitals: φ^α for spin-up electrons and φ^β for spin-down electrons. Of course, the spin densities can be obtained from the occupied Kohn-Sham unrestricted molecular orbitals

$$n^\alpha(\mathbf{r}) = \sum_{i=1}^{N^\alpha} |\varphi_i^\alpha(\mathbf{r})|^2 \quad (3.71) \quad \left| \quad n^\beta(\mathbf{r}) = \sum_{i=1}^{N^\beta} |\varphi_i^\beta(\mathbf{r})|^2. \quad (3.72)\right.$$

Because the classical Hartree functional is spin-independent, it therefore remains a functional of the total electron density as opposed to the exchange-correlation term which is usually decomposed into exchange and correlation contributions, and treated separately

$$E_{\text{xc}}[n^\alpha, n^\beta] = E_{\text{x}}[n^\alpha, n^\beta] + E_{\text{c}}[n^\alpha, n^\beta]. \quad (3.73)$$

Note that the exchange term has the specificity of originating from an interaction between same-spin electrons only. For that reason, the two spin-densities are entirely decoupled into the exchange functional. As a matter of fact, there exists a simple procedure which allows to transform any standard exchange functional $E_{\text{x}}[n]$ into a spin-density functional $E_{\text{x}}[n^\alpha, n^\beta]$, the ‘‘spin-scaling relation’’ [87]

$$E_{\text{x}}[n^\alpha, n^\beta] = \frac{1}{2} (E_{\text{x}}[2n^\alpha] + E_{\text{x}}[2n^\beta]). \quad (3.74)$$

Since correlation effects stem from the correlated motions of all electrons, there exists no similar scaling relation to extend standard correlation functionals $E_{\text{c}}[n]$ and it is thus necessary to build new spin-unrestricted correlation functionals $E_{\text{c}}[n^\alpha, n^\beta]$.

In order to find the best sets of Kohn-Sham molecular orbitals with orbital energies, one must solve two sets of unrestricted Kohn-Sham equations

$$h_s^\alpha(\mathbf{r})\varphi_i^\alpha(\mathbf{r}) = \varepsilon_i^\alpha\varphi_i^\alpha(\mathbf{r}) \quad (3.75) \quad \left| \quad h_s^\beta(\mathbf{r})\varphi_i^\beta(\mathbf{r}) = \varepsilon_i^\beta\varphi_i^\beta(\mathbf{r}), \quad (3.76)\right.$$

where $h_s^\alpha(\mathbf{r})$ and $h_s^\beta(\mathbf{r})$ are the space representations of the Kohn-Sham one-electron Hamiltonian operators, \hat{h}^α and \hat{h}^β , acting on the unrestricted Kohn-Sham molecular orbitals $\{\varphi_i^\alpha\}$ and $\{\varphi_i^\beta\}$, respectively.

They are defined as follows

$$h_s^\alpha(\mathbf{r}) = -\frac{1}{2}\nabla_{\mathbf{r}}^2 + v_s^\alpha(\mathbf{r}) \quad (3.77) \quad \left| \quad h_s^\beta(\mathbf{r}) = -\frac{1}{2}\nabla_{\mathbf{r}}^2 + v_s^\beta(\mathbf{r}). \quad (3.78)\right.$$

$v_s^\alpha(\mathbf{r})$ and $v_s^\beta(\mathbf{r})$ are the unrestricted Kohn-Sham one-electron effective potentials

$$v_s^\alpha(\mathbf{r}) = v(\mathbf{r}) + v_{\text{H}}(\mathbf{r}) + v_{\text{xc}}^\alpha(\mathbf{r}) \quad (3.79) \quad \left| \quad v_s^\beta(\mathbf{r}) = v(\mathbf{r}) + v_{\text{H}}(\mathbf{r}) + v_{\text{xc}}^\beta(\mathbf{r}), \quad (3.80)\right.$$

which include the external local potential $v(\mathbf{r})$, the spin-independent classical Hartree potential

$$v_{\text{H}}(\mathbf{r}) = \int \frac{n(\mathbf{r}')}{|\mathbf{r} - \mathbf{r}'|} d\mathbf{r}', \quad (3.81)$$

and the spin-dependent exchange-correlation potentials, defined as follows

$$v_{\text{xc}}^{\alpha}(\mathbf{r}) = \frac{\delta E_{\text{xc}}[n^{\alpha}, n^{\beta}]}{\delta n^{\alpha}(\mathbf{r})} \quad (3.82) \quad \left| \quad v_{\text{xc}}^{\beta}(\mathbf{r}) = \frac{\delta E_{\text{xc}}[n^{\alpha}, n^{\beta}]}{\delta n^{\beta}(\mathbf{r})}. \quad (3.83)$$

$v_{\text{xc}}^{\alpha}(\mathbf{r})$ and $v_{\text{xc}}^{\beta}(\mathbf{r})$ are functional derivatives of the spin-dependent exchange-correlation functional with respect to the spin densities $n^{\alpha}(\mathbf{r})$ and $n^{\beta}(\mathbf{r})$, respectively.

We stress that since the two sets of unrestricted Kohn-Sham equations depend on all the occupied Kohn-Sham molecular orbitals, they must be solved simultaneously like in the unrestricted Hartree-Fock framework.

3.6 Exchange-Correlation Energy

3.6.1 Building Approximations

Density-functional theory is, in principle, an exact theory in the sense that one is assured that there exists a unique and exact energy functional, valid for all systems and completely defined by the electron density. Unfortunately, the explicit form of such a functional remains elusive, even now, and scientists had to compromise and focus on the design and the elaboration of sufficiently accurate approximate functionals instead.

To this end, Kohn and Sham approach has constituted a tremendous progress, despite the need to reintroduce auxiliary orbitals, Kohn-Sham orbitals, in an originally intended density-based model. Kohn-Sham theory proposed to split the kinetic energy functional into two parts, the first one and major part being the kinetic energy $T_{\text{s}}[n]$ of a fictitious non-interacting system sharing the same density than the real interacting system, plus a small correction term, the kinetic correlation energy $T_{\text{c}}[n]$, in order to recover the exact kinetic energy $T[n]$ of the interacting system. Hence, the Kohn-Sham decomposition of the total energy

$$\begin{aligned} E[n] &= T[n] + E_{\text{ee}}[n] + E_{\text{ne}}[n] \\ &= T_{\text{s}}[n] + E_{\text{H}}[n] + E_{\text{xc}}[n] + E_{\text{ne}}[n]. \end{aligned} \quad (3.84)$$

The strength of Kohn-Sham theory comes from the fact that not only the kinetic energy is treated exactly in this model and a significant amount of the real kinetic energy is recovered, but, since kinetic energy is known to be a much larger part of the total energy compared

to the elusive non-classical electronic repulsion, focus has since been on designing accurate exchange-correlation functionals

$$\begin{aligned} E_{\text{xc}}[n] &= (T[n] - T_{\text{s}}[n]) + (E_{\text{ee}}[n] - E_{\text{H}}[n]) \\ &= T_{\text{c}}[n] + E_{\text{x}}[n] + U_{\text{c}}[n] \\ &= E_{\text{x}}[n] + E_{\text{c}}[n]. \end{aligned} \tag{3.85}$$

Although we do not know either the explicit form of the exact exchange-correlation functional, a number of exact conditions and properties that this exact functional must verify and possess are well known [9]. Among these, we can cite specific scaling properties [65] and asymptotic behaviors for the exchange and correlation functionals, the self-interaction-free requirement which imposes that the exchange functional must exactly cancel the spurious coulombic self-interaction of the electrons and, of course, the obvious requirements coming from the simple observation that there shall be no correlation effects in one-electron systems, among other things.

The choice to separate the exchange-correlation functional into two distinct contributions stem not only from the practical observation that exchange and correlation energy functionals must obey specific constraints and properties but also from the hope to benefit from error cancellations between the exchange and correlation counterparts. Indeed, while the exchange and correlation functionals may perform very poorly when used separately, it has been observed that the results could be greatly improved when the two functionals were used together. Many of the most used exchange-correlation functionals were designed with that objective in mind.

3.6.2 Jacob's Ladder

To this day, hundreds of exchange-correlation functionals have been developed, some were elaborated based on specific systems, like the Helium atom or the uniform electron gas (UEG), some are known to provide promising results for specific properties or specific phenomena, some were built to fit specific experimental data or were based on interpolations in order to fulfill specific asymptotic behaviors. . . Despite the profusion of functionals developed over the past decades, it is still difficult to argue which functional is the most adequate to use independently of the system or property of interest.

Nevertheless, most of these functionals [87] are based on a certain number of parameters and a classification has been proposed based on the intuitive idea that the more parameters the functional needs the more accurate the results will be, but, on the other hand, the larger the computational cost will be.

Perdew [69] proposed a classification of the exchange-correlation functionals according to the number of basic quantities they exploit and the degree of accuracy they can provide: “Jacob’s ladder”.

The Local Density Approximation

The simplest functionals are based on the electron density $n(\mathbf{r})$ only and constitute what is known as the “Local Density Approximation” (LDA) class of functionals

$$E_{xc}^{\text{LDA}}[n] = \int n(\mathbf{r}) \varepsilon_{xc}^{\text{unif}}(n(\mathbf{r})) d\mathbf{r}, \quad (3.86)$$

where the exchange-correlation energy per particle can be decomposed as a sum of exchange and correlation contributions

$$\varepsilon_{xc}^{\text{unif}}(n) = \varepsilon_x^{\text{unif}}(n) + \varepsilon_c^{\text{unif}}(n). \quad (3.87)$$

The local density approximation is known to provide better results when it distinguishes the spin-down and spin-up electron densities. Hence, in practice, its spin-scaled generalization, the “Local Spin Density Approximation” (LSDA), is preferred to its original formulation

$$E_{xc}^{\text{LSDA}}[n^\alpha, n^\beta] = \int n(\mathbf{r}) \varepsilon_{xc}^{\text{unif}}(n^\alpha(\mathbf{r}), n^\beta(\mathbf{r})) d\mathbf{r}. \quad (3.88)$$

The LDA functionals were designed based on the approximation that any inhomogeneous system, with electron density $n(\mathbf{r})$, locally behaves like an infinite uniform electron gas with the same density. The exchange energy functional of such a system were derived analytically by Dirac and, then, Slater (with the $X\alpha$ method) and was used to build the LDA exchange functional, referred to as the Dirac (1930) [22], or Slater (1951) [79] functional

$$E_x^{S51}[n] \equiv E_x^{\text{LDA}}[n] = C_x \int n(\mathbf{r})^{\frac{4}{3}} d\mathbf{r}, \quad (3.89)$$

with

$$C_x = -\frac{3}{4} \left(\frac{3}{\pi} \right)^{\frac{1}{3}}. \quad (3.90)$$

The analytical form of the correlation energy of a uniform electron gas has only be derived in distinct asymptotic configurations, the high- and low-density limits, but thanks to highly accurate quantum Monte Carlo calculations (performed by Ceperley and Alder in 1980 [11]), many analytic interpolation formulas have been successfully established, among which the ones constructed by Vosko, Wilk and Nusair (VWN) [89]

$$E_c^{\text{VWN}}[n] \equiv E_c^{\text{LDA}}[n] = \int n(\mathbf{r}) \varepsilon_c^{\text{VWN}}(n(\mathbf{r})) d\mathbf{r}. \quad (3.91)$$

For the sake of simplicity, we will not detail the explicit form of these parametrizations. The LDA is known to provide very acceptable results for systems with slowly varying electron densities and have been used extensively by the solid state community to describe extended systems, such as metals. For finite systems, like atoms and molecules, where the slowly varying density approximation becomes less relevant, LDA has shown some failures and limitations when predicting certain properties such as binding energies or gap predictions. Nevertheless, LDA remains the cornerstone of all approximate functionals and have unravelled the path to many other more sophisticated approximations, as we shall see below.

The Generalized Gradient Approximation

If one needs to go beyond LDA, one can choose to use functionals that not only depend explicitly on the local value of the electron density $n(\mathbf{r})$ but also include a dependence on the gradient of the density $\nabla n(\mathbf{r})$. These functionals are “semi-local” functionals and constitute the class of “Generalized Gradient Approximations” (GGAs)

$$E_{\text{xc}}^{\text{GGA}}[n] = \int n(\mathbf{r}) \varepsilon_{\text{xc}}^{\text{GGA}}(n(\mathbf{r}), \nabla_{\mathbf{r}} n(\mathbf{r})) d\mathbf{r}. \quad (3.92)$$

In this work, we will use the “BLYP” exchange-correlation GGA-functional which consists of the “B88” LDA-based exchange functional [3], developed by Becke, and the “LYP” Helium-based correlation functional [51, 17], developed by Lee, Yang and Parr.

Meta Generalized Gradient Approximations

Other exchange-correlation functionals were based on more complicated quantities such as the square of the density gradient, the laplacian of the density or the kinetic energy density τ . These functionals are known as the “Meta-Generalized-Gradient-Approximations” (mGGAs)

$$E_{\text{xc}}^{\text{mGGA}}[n] = \int n(\mathbf{r}) \varepsilon_{\text{xc}}^{\text{mGGA}}(n(\mathbf{r}), \nabla n(\mathbf{r}), \tau) d\mathbf{r}. \quad (3.93)$$

Hybrid functionals

Ultimately, more sophisticated, and presumably more accurate, functionals were designed, some including an occupied and/or virtual Kohn-Sham orbital dependency by mixing a fraction of Hartree-Fock exact-exchange functional with GGA or LDA functionals: “Hybrid Approximations” [4]. For instance, a general three-parameter hybrid functional takes the form

$$E_{\text{xc}}^{\text{3H}}[n] = aE_{\text{x}}^{\text{HF}}[n] + bE_{\text{x}}^{\text{GGA}}[n] + (1 - a - b)E_{\text{x}}^{\text{LDA}}[n] + cE_{\text{c}}^{\text{GGA}}[n] + (1 - c)E_{\text{c}}^{\text{LDA}}[n]. \quad (3.94)$$

In this work, we will use the famous and widely used “B3LYP” functional [83, 41] which includes the “B88” exchange and “LYP” correlation GGA-functionals, with the parameters $a = 0.20$, $b = 0.72$ and $c = 0.81$.

Part II

**eDFT: an Alternative Approach to
Access Excitation Energies and to
Palliate Infamous Deficiencies of
Standard Methods**

Chapter 4

PPLB Ensembles to Target Charged Excitations

Contents

4.1 Introduction: DFT for Open Systems	70
4.1.1 Grand Canonical Ensemble and Chemical Potential	70
4.1.2 PPLB Ensemble, Ionization Potential and Electron Affinity	72
4.1.3 From DFT to PPLB-DFT	74
4.2 Perdew-Parr-Levy-Balduz Density-Functional Theory Formalism	83
4.2.1 Open systems and ensembles	83
4.2.2 PPLB Ensemble Energy and Ensemble density	84
4.2.3 Theoretical Extraction of Individual-State Properties and Excitation Energies	85
4.2.4 PPLB Variational Principle and Universal Functional	86
4.2.5 Kohn-Sham Formulation of PPLB-DFT	88
4.2.6 Practical Extraction of Individual-State Properties and Excitation Energies	91
4.3 Numerical Implementation of PPLB-DFT	95
4.3.1 Basic Principles	95
4.3.2 With Weight-Independent xc-Functionals	98
4.3.3 With Weight-Dependent xc-Functionals	119

4.1 Introduction: DFT for Open Systems

4.1.1 Grand Canonical Ensemble and Chemical Potential

In quantum chemistry, in order to describe a system who has reached an equilibrium state in a multiplicative scalar external potential field $v(\mathbf{r})$, at temperature θ , with a given chemical potential μ and an electron density $n(\mathbf{r})$ in a grand canonical ensemble, we define the grand potential [65] density functional $\Omega[n]$ (also known as the Landau free energy or Landau potential) as

$$\Omega[n] \equiv F[n] + \int n(\mathbf{r})(v(\mathbf{r}) - \mu) d\mathbf{r}, \quad (4.1)$$

where $F[n]$ is the universal density functional

$$\begin{aligned} F[n] &\equiv T[n] + U[n] - \theta S[n] \\ &= \text{Tr} \left[\hat{I}_n^{\min} \left(\hat{T} + \hat{U} + \frac{1}{\beta} \ln \hat{I}_n^{\min} \right) \right]. \end{aligned} \quad (4.2)$$

Let us recall that, in this context, T and U are the kinetic energy and electron-electron interaction potential energy of the system, and \hat{T} and \hat{U} are the corresponding operators. Furthermore, S is the entropy of the system and

$$\beta = \frac{1}{k_B \theta}, \quad (4.3)$$

is a constant based on the absolute temperature θ of the system and the Boltzmann constant k_B . As for \hat{I}_n^{\min} , it is the density matrix operator that obeys the following two constraints: it minimizes the quantity

$$\text{Tr} \left[\hat{I} \left(\hat{T} + \hat{U} + \frac{1}{\beta} \ln \hat{I} \right) \right], \quad (4.4)$$

and gives the density $n(\mathbf{r})$, with Tr the trace operation in matrix algebra.

We stress that, since we are using the grand-canonical ensemble formalism, $F[n]$ defined in equation (4.2) is a universal functional of an electron density $n(\mathbf{r})$ that may integrate to a non-integer number of electron, which could be seen as the time-average electron number \mathcal{N} of a system that can exchange electrons with its surroundings.

Such systems are referred to as “open systems” in opposition to “closed systems” which have a fixed integer number of electrons. Furthermore, electronic states associated with a fixed integer number of electrons N are referred to as “pure states”.

In a grand-canonical ensemble at a given temperature θ and chemical potential μ , the Hohenberg-Kohn theorems remain valid through their extensions to isolated open systems with a fractional number of electrons \mathcal{N} :

- At equilibrium, the electron density $n_0(\mathbf{r})$ uniquely determines the equilibrium density operator \hat{T}_0 and, hence, all the properties of the equilibrium state.
- There is a variational principle that dictates the minimization of the grand potential of the system, among all electron densities $n(\mathbf{r})$ integrating to \mathcal{N} ,

$$\Omega_0 \equiv \Omega[n_0] = \min_{n(\mathbf{r})} \Omega[n]. \quad (4.5)$$

In the zero-temperature limit ($\theta = 0$ or, equivalently, $\beta = \infty$), the equilibrium state of the grand-canonical system becomes the ground state, which is our main concern in this work. In this limit, the entropy contribution disappears from the universal-functional expression (see equation (4.2)), leading to a grand-canonical extension of the standard DFT universal functional proposed by Hohenberg and Kohn

$$F[n] = \min_{\hat{T} \rightarrow n(\mathbf{r})} \text{Tr} \left[\hat{T} \left(\hat{T} + \hat{V}_{\text{ee}} \right) \right], \quad (4.6)$$

where \hat{V}_{ee} is the electron-electron interaction potential energy operator.

This is the grand-canonical ground-state universal functional proposed by Perdew, Parr, Levy and Balduz (PPLB) [70]. In that definition, they extend Levy's constrained search, used in pure-state DFT, to density operators in Fock space which are operators associated with statistical mixtures (or ensembles) of states with different numbers of electrons, that is to say grand-canonical ensembles. From now on, we will refer to those ensembles as "PPLB ensembles".

We have seen that, in the zero-temperature limit, the grand potential reduces to

$$\begin{aligned} \Omega[n] &= F[n] + \int n(\mathbf{r})(v(\mathbf{r}) - \mu) d\mathbf{r} \\ &= E[n] - \mu \mathcal{N}, \end{aligned} \quad (4.7)$$

with the grand-canonical ensemble energy functional

$$E[n] = F[n] + \int n(\mathbf{r})v(\mathbf{r})d\mathbf{r}, \quad (4.8)$$

defined for any electron densities integrating to any number of electrons \mathcal{N} , either integral or fractional.

Like in pure-state DFT, there exists a variational principle for the grand potential, which states that

$$\begin{aligned} \Omega_0 \equiv \Omega[n_0] &= E_0^{\mathcal{N}} - \mu \mathcal{N} \\ &\leq \text{Tr} \left[\hat{T} \left(\hat{H} - \mu \mathcal{N} \right) \right] \\ &\leq E[n] - \mu \int n(\mathbf{r})d\mathbf{r}, \end{aligned} \quad (4.9)$$

where $E_0^{\mathcal{N}} \equiv E[n_0]$ is the ground-state ensemble energy associated with the minimizing ground-state ensemble electron density $n_0(\mathbf{r})$ which integrates to the possibly fractional number of electrons \mathcal{N} .

The above-mentioned variation principle is equivalent to the variation equation that one must solve in order to obtain the stationary states of the energy (or eigenstates of the Hamiltonian operator \hat{H}) of the grand-canonical system,

$$\delta \left\{ E[n] - \mu \int n(\mathbf{r}) d\mathbf{r} \right\} = 0. \quad (4.10)$$

Equation (4.10) can be reformulated such that one obtains the following Euler-Lagrange equation

$$\frac{\delta E[n]}{\delta n(\mathbf{r})} - \mu = 0, \quad (4.11)$$

leading to the well-known definition of the chemical potential

$$\mu \equiv \frac{\partial E_0(\mathcal{N})}{\partial \mathcal{N}}. \quad (4.12)$$

Hence, the chemical potential μ of an open system placed in an external field potential $v(\mathbf{r})$ is defined as the slope of its total energy with respect to its number of electrons \mathcal{N} and must be constant through space.

4.1.2 PPLB Ensemble, Ionization Potential and Electron Affinity

Let us now look more closely to what happens to the chemical potential in two distinct situations, the removal and the addition of an electron from/to a pure-state system with an initial integer number of electrons N .

PPLB Ensembles

When an electron is gradually removed/added from/to the ground state of a neutral N -electron system, the open system transits from its neutral form towards its cationic/anionic form, that is the ground states of the $(N - 1)$ - or $(N + 1)$ -electron systems, respectively. As a consequence, the exact ground-state energy $E_0^{\mathcal{N}}$ of such an open system will consist of a linear combination of both N - and $(N - 1)$ -electron (or N - and $(N + 1)$ -electron) ground-state energies, each ponderated by a set of normalized weights $\{w_1, w_2\}$ such that

$$E_0^{\mathcal{N}} = w_1 E_0^N + w_2 E_0^{N \pm 1}. \quad (4.13)$$

In practice, when one works with ensembles, it is not mandatory for the weights of the ensemble to possess physical meaning. Nevertheless, in the present work, one intuitive and practical choice consists in using the fractional charge-deviation α defined as

$$\mathcal{N} \equiv \mathcal{N}^{\pm} = N \pm \alpha, \quad (4.14)$$

with $0 \leq \alpha \leq 1$.

By doing so, one obtains the “left” (superscript “−”) and “right” (superscript “+”) PPLB two-state ensembles (or biensembles) describing the ground-state energy of the grand-canonical \mathcal{N} -electron system, while an electron is removed/added from/to the ground state of its neutral form

$$E_0^{\mathcal{N}^-} = (1 - \alpha)E_0^N + \alpha E_0^{N-1} \quad (4.15) \quad \left| \quad E_0^{\mathcal{N}^+} = (1 - \alpha)E_0^N + \alpha E_0^{N+1}. \quad (4.16)$$

Ionization Potential, Electron Affinity and Piecewise Linearity Condition

Thus far, we have seen that, for a given external potential $v(\mathbf{r})$, in the zero-temperature limit, the chemical potential of a \mathcal{N} -electron system in its ground state was defined as the slope of its ground-state energy, with respect to the variation of the number of electrons

$$\mu \equiv \frac{\partial E_0(\mathcal{N})}{\partial \mathcal{N}}. \quad (4.17)$$

Let us apply this definition to the two above-mentioned PPLB ensemble ground-state energies. Given that $\mathcal{N}^- = N - \alpha$ and $\mathcal{N}^+ = N + \alpha$, and that the exact energy of an open system must be linear with respect to the charge deviation α , between two successive integer numbers of electrons, we obtain that

$$\begin{aligned} \mu^- &= \frac{\partial E_0^{\mathcal{N}^-}}{\partial \mathcal{N}^-} = -\frac{\partial E_0^{\mathcal{N}^-}}{\partial \alpha} \\ &= E_0^N - E_0^{N-1} \\ &\equiv -I_0^N \end{aligned} \quad (4.18) \quad \left| \quad \begin{aligned} \mu^+ &= \frac{\partial E_0^{\mathcal{N}^+}}{\partial \mathcal{N}^+} = \frac{\partial E_0^{\mathcal{N}^+}}{\partial \alpha} \\ &= E_0^{N+1} - E_0^N \\ &\equiv -A_0^N. \end{aligned} \quad (4.19)$$

I_0^N and A_0^N are the first ionization potential and first electron affinity of the neutral N -electron system, respectively. They can be seen as the respective costs in energy that one must provide for removing or adding an electron from/to the ground state of the neutral system.

Since, for most systems (atoms, molecules, solids), the ionization potential and electron affinity are not equal quantities (see Appendix A), it is straightforward to see that the chemical potential of an open system must therefore experience a “jump”, as the number of electrons crosses an integral value. From the energy point of view, this means that the exact ground-state energy curve with respect to the number of electrons of the open system must be a series of straight line segments with different slopes, between two successive pure-state energies. This is known as the “piecewise linearity condition” that any exact ground-state energy must obey.

Furthermore, the discontinuity experienced by the chemical potential when crossing an integer

number of electrons is known to be of major importance regarding band gaps predictions of solids. In this study, we will restrict our work to small atomic and molecular systems and will aim to calculate charged excitation energies such as ionization potentials, electron affinities or fundamental gaps, defined as follows

$$\Omega_0^N \equiv I_0^N - A_0^N, \quad (4.20)$$

within the scope of PPLB-DFT.

4.1.3 From DFT to PPLB-DFT

Fundamentals of DFT

Let us consider a N -electron system under the influence of a multiplicative external potential $v(\mathbf{r})$. First, we recall the two fundamental ideas stated by the Hohenberg and Kohn theorems, which are the two pillars of DFT [65]:

- There is a one-to-one correspondence between the external potential $v(\mathbf{r})$ and the electron density $n(\mathbf{r})$ of the system. Hence, the electron density uniquely determines all the properties of the system through the knowledge of density functionals.
- There exists a variational principle which dictates the minimization of the total energy $E[n]$ of the system upon all electron densities $n(\mathbf{r})$ integrating to the number of electrons N .

Hence, the total energy of the system is a functional of the electron density and is defined as follows

$$E[n] = F[n] + \int n(\mathbf{r})v(\mathbf{r})d\mathbf{r}, \quad (4.21)$$

where $F[n]$ is the universal density functional, in the sense that it is the same functional for any system of electrons with the same electron density $n(\mathbf{r})$, independently of the external potential $v(\mathbf{r})$ into which the electronic system is moving,

$$F[n] = T[n] + V_{ee}[n]. \quad (4.22)$$

We recall that, in the above definition, $T[n]$ is the total kinetic-energy density functional, and $V_{ee}[n]$ is the electron-electron interaction potential-energy density functional.

Now that we have defined the expression of the total-energy density functional, the variational principle stated in the second Hohenberg-Kohn theorem tells us that the electron density that minimizes the energy of the system is the ground-state electron density $n_0(\mathbf{r})$, and any other N -electron densities would yield a larger energy than the true ground-state energy of the system

$$E_0 \equiv E[n_0] = \min_{n(\mathbf{r})} \{E[n]\}, \quad (4.23)$$

where the minimization is upon all N -electron densities $n(\mathbf{r})$, such that

$$\int n(\mathbf{r})d\mathbf{r} = N. \quad (4.24)$$

We have seen that this minimization could be reformulated into the Euler-Lagrange equation, which highlights how a change in the electron density can affect the energy of the system

$$\frac{\delta E[n]}{\delta n(\mathbf{r})} - \mu = 0. \quad (4.25)$$

In the above expression, μ is the Lagrange multiplier associated with the normalization constraint, defined in equation (4.24), and can be interpreted as the chemical potential of the N -electron system, as discussed previously.

DFT is a in-principle-exact theory but the quality of the calculated quantities highly depends on how one decides to express the different contributions to the total-energy density functional, and either resort to exact functionals or approximations.

Kohn-Sham System

Kohn and Sham proposed to reintroduce the concept of orbitals into the DFT scheme in order to ease the computation of the total kinetic energy of the system, with an acceptable lost of accuracy.

Indeed, initially, the formulation of the exact ground-state kinetic-energy functional

$$T[\{\chi_i\}] \equiv \sum_{i=1}^{\infty} n_i \langle \chi_i | -\frac{1}{2} \nabla_{\mathbf{r}}^2 | \chi_i \rangle, \quad (4.26)$$

was based on a summation over an infinite number of natural spin orbitals $\{\chi_i(\mathbf{x})\}$, that is orbitals that diagonalize the density matrix operator \hat{T} , with occupation numbers $\{n_i\}$ such that $0 \leq n_i \leq 1$, in order to obey the Fermi exclusion principle. In addition, the summation upon all occupation numbers must recover the total number of electrons of the system such that

$$\sum_{i=1}^{\infty} n_i = N. \quad (4.27)$$

Hence, the exact ground-state kinetic-energy functional of the system is an implicit functional of the electron density through the spin orbitals, and the exact ground-state electron density is defined as follows

$$n_0(\mathbf{r}) = \sum_{i=1}^{\infty} \sum_{\sigma} n_i |\chi_i(\mathbf{r}, \sigma)|^2. \quad (4.28)$$

To avoid having to work with a large number of spin orbitals with random fractional occupation numbers, Kohn and Sham proposed to restrict the DFT framework to sets of orthonormal spin orbitals, where only the N lowest orbitals would be occupied with occupation numbers

$n_i = 1$, whereas all the remaining orbitals would be unoccupied with occupation numbers $n_i = 0$.

It is important to note that the Kohn-Sham formalism is actually a special case of a more general framework depicted in the formulation of the exact kinetic energy functional. Therefore, within the Kohn-Sham framework, one no longer obtains an exact formulation for the ground-state kinetic-energy functional of the interacting N -electron system, but an approximation

$$T_s[n] \equiv \sum_{i=1}^N \langle \chi_i | -\frac{1}{2} \nabla_{\mathbf{r}}^2 | \chi_i \rangle . \quad (4.29)$$

Furthermore, in the KS formulation, the ground-state electron density takes the form

$$n_0(\mathbf{r}) = \sum_i^N \sum_{\sigma} |\chi_i(\mathbf{r}, \sigma)|^2 . \quad (4.30)$$

We stress that this approximated formulation for the ground-state kinetic-energy functional of the interacting system is only valid for a set of orthonormal spin orbitals, which have to obey the following constraint

$$\int \chi_i^*(\mathbf{x}) \chi_j(\mathbf{x}) d\mathbf{x} = \delta_{ij} , \quad (4.31)$$

where the integration is over both spin and space coordinates, and becomes exact for a noninteracting N -electron system with the same density $n_0(\mathbf{r})$. Indeed, such noninteracting systems can be described by a single Slater determinantal wave function built from the N lowest occupied orthonormal spin orbitals. This is known as the Kohn-Sham system.

The Kohn-Sham system is a fictitious noninteracting N -electron system which has the specificity of having the exact same ground-state electron density than the density of the real interacting N -electron system.

The role of the Kohn-Sham system is to mimic the true density of the interacting system by hiding all the electron-electron interaction effects into a Kohn-Sham effective potential

$$v_s(\mathbf{r}) = v(\mathbf{r}) + v_{ee}(\mathbf{r}) , \quad (4.32)$$

where $v(\mathbf{r})$ is the external potential of the real interacting system, and $v_{ee}(\mathbf{r})$ is the electron-electron interaction potential which contains the Hartree, exchange and correlation contributions. Note that the subscript "s" stands for Slater determinant.

Since the ground-state electron density $n_0(\mathbf{r})$ which minimizes the total energy of the Kohn-Sham system has to be the exact same ground-state electron density than the one of the true interacting system, it can be obtained by solving a much simpler problem than the interacting many-body picture.

To find the set of orthonormal Kohn-Sham spin orbitals that minimizes the Kohn-Sham energy, one must solve self-consistently and independently the N nonlinear Kohn-Sham one-electron equations

$$\left[-\frac{1}{2} \nabla_{\mathbf{r}}^2 + v_s(\mathbf{r}) \right] \chi_i(\mathbf{x}) = \varepsilon_i \chi_i(\mathbf{x}) , \quad (4.33)$$

in order to obtain a set of Kohn-Sham orbitals (or eigenstates) $\{\chi_i\}$ and Kohn-Sham orbital energies (or eigenvalues) $\{\varepsilon_i\}$.

Once one has obtained the optimal set of spin orbitals and occupation numbers, one can build the ground-state electron density by putting the N electrons in the N Kohn-Sham orbitals with lowest energy, such that

$$n_0(\mathbf{r}) = \sum_i^N \sum_{\sigma} |\chi_i(\mathbf{r}, \sigma)|^2. \quad (4.34)$$

Finally, one can compute the corresponding ground-state energy of the interacting system

$$E[n_0] = T_s[n_0] + E_H[n_0] + E_{xc}[n_0] + \int v(\mathbf{r})n_0(\mathbf{r})d\mathbf{r}, \quad (4.35)$$

where $E_H[n]$ and $E_{xc}[n]$ are the Hartree and exchange-correlation energy density functionals, respectively.

Extension of DFT to Fractional Occupation Numbers

We have seen that the Kohn-Sham method originated from the simple choice to put the N electrons of the system into the N lowest spin orbitals, in order to obtain a much easier-to-compute formulation for the kinetic-energy functional.

Actually, there exists a more general Kohn-Sham scheme where one can choose to occupy an arbitrary number M of spin orbitals, with $M \geq N$, with fractional occupation numbers [65, 87] $0 \leq n_i \leq 1$. This generalization has shown to be particularly interesting when one wants to extract physical meaning from the Kohn-Sham eigenvalues ε_i .

It was Slater, with his "transition state" concept (applied in the X_{α} method [79]), who first helped to set the stage for fractional occupation numbers, which Janak has then generalized and extended to Kohn-Sham theory. Similarly to $T_s[n]$ in Kohn-Sham theory, Janak proposed the following formulation for the generalized kinetic-energy functional, where "J" stands for "Janak",

$$\begin{aligned} T_J[n] &\equiv \sum_{i=1}^M n_i \langle \chi_i | -\frac{1}{2} \nabla_{\mathbf{r}}^2 | \chi_i \rangle \\ &= \sum_{i=1}^M n_i \int \chi_i^*(\mathbf{x}) \left(-\frac{1}{2} \nabla_{\mathbf{r}}^2\right) \chi_i(\mathbf{x}) d\mathbf{x}. \end{aligned} \quad (4.36)$$

We stress that this generalized kinetic-energy functional is now a functional of both sets of orthonormal spin orbitals and occupation numbers $\{\chi_i, n_i\}$, as opposed to standard KS-DFT. Within this new approximation for the kinetic energy, the total-energy density functional of the noninteracting generalized Kohn-Sham system becomes

$$E[n] = T_J[n] + \int v_{\text{eff}}(\mathbf{r})n(\mathbf{r})d\mathbf{r}, \quad (4.37)$$

where $v_{\text{eff}}(\mathbf{r}) = v(\mathbf{r}) + v_{\text{H}}(\mathbf{r}) + v_{\text{xc}}(\mathbf{r})$.

Note that this "generalized" Kohn-Sham potential is not exactly the same that the one defined for the "Slater" Kohn-Sham system because the exchange-correlation potential $v_{\text{xc}}(\mathbf{r})$ has changed due to the change of approximation for the kinetic part of the energy.

In order to find the ground-state common electron density of both noninteracting and interacting systems, one has to minimize the above-mentioned total energy upon all sets of orthonormal spin orbitals and occupation numbers, obeying the following constraints

$$N = \sum_{i=1}^M n_i \quad (4.38) \quad \left| \quad n(\mathbf{r}) = \sum_{i=1}^M \sum_{\sigma} n_i |\chi_i(\mathbf{r}, \sigma)|^2. \quad (4.39)$$

The minimization of the energy will lead to a set of one-electron equations, very similar to the Kohn-Sham equations

$$\left[-\frac{1}{2} n_i \nabla_{\mathbf{r}}^2 + n_i v_{\text{eff}}(\mathbf{r}) \right] \chi_i(\mathbf{x}) = \varepsilon'_i \chi_i(\mathbf{x}). \quad (4.40)$$

For a given set of non-zero occupation numbers $\{n_i\}$, one can reformulate the previous equation by applying a change of variable

$$\varepsilon_i = \frac{\varepsilon'_i}{n_i}, \quad (4.41)$$

in order to recover the usual form of Kohn-Sham equations with new potential $v_{\text{eff}}(\mathbf{r})$

$$\left[-\frac{1}{2} \nabla_{\mathbf{r}}^2 + v_{\text{eff}}(\mathbf{r}) \right] \chi_i(\mathbf{x}) = \varepsilon_i \chi_i(\mathbf{x}). \quad (4.42)$$

Hence, the Kohn-sham scheme can be extended to an arbitrary set of orthonormal spin orbitals with fractional occupation numbers, under the condition that the total number of electrons, which can either be fractional or integer, is recovered as well as the ground-state electron density.

Finally, once one have obtained the ground-state electron density $n_0(\mathbf{r})$ of the interacting system, one can compute the corresponding ground-state energy

$$E[n_0] = T_{\text{J}}[n_0] + E_{\text{H}}[n_0] + E_{\text{xc}}[n_0] + \int v(\mathbf{r}) n_0(\mathbf{r}) d\mathbf{r}, \quad (4.43)$$

where the exchange-correlation functional $E_{\text{xc}}[n]$ includes an additional correction due to the change of approximation for the kinetic energy (as opposed to standard KS-DFT), for which we choose to use $T_{\text{J}}[n]$ instead of the usual Kohn-Sham kinetic energy functional $T_{\text{s}}[n]$.

Physical Interpretation of the Kohn-Sham Orbital Energies

In both Hartree-Fock and Kohn-Sham theories, one has to solve an eigenvalue equation (Hartree-Fock equation and Kohn-Sham equation) in order to obtain the ground-state electron density of a N -electron system and the minimization of the energy of the system will result in an infinite number of spin orbitals $\{\chi_i\}$ with spin orbital energies $\{\varepsilon_i\}$.

The N spin orbitals with lowest energy are referred to as “occupied” spin orbitals while the remaining infinite number of spin orbitals with higher energy are unoccupied and referred to as “virtual” spin orbitals.

We have seen that the ground-state density of a system can be obtained by summation over all occupied spin orbitals, and that the ground-state energy can be determined through the use of density functionals. But, what about the spin orbital energies? It is well-known that the energy of the system is not the sum of the occupied spin-orbital energies, but it would be very convenient if one could extract physical meaning from the spin-orbital energies.

As a matter of fact, Koopmans [43, 39] has shown that, for a closed-shell system, that is a system with no unpaired electrons, the ionization potential and the electron affinity of a N -electron system are exactly the opposite of the energy of the occupied/virtual spin orbital from which/into which we remove/add an electron

$$I_0^N = -\varepsilon_N^N \quad (4.44) \quad \Bigg| \quad A_0^N = -\varepsilon_{N+1}^N. \quad (4.45)$$

Hence, in this context, the ionization potential is the opposite of the HOMO (highest occupied molecular orbital) energy and the electron affinity is the opposite of the LUMO (lowest unoccupied molecular orbital) energy of the neutral N -electron system.

Nevertheless, Koopmans’ theorem was derived under the strong assumption that the spin orbitals of the neutral, cationic and anionic species were identical, which is not true in practice. This is known as the “frozen orbital” approximation, which completely neglects orbital relaxation. Moreover, Koopmans’ theorem was first derived in the restricted Hartree-Fock (RHF) framework and then generalized to Kohn-Sham DFT where correlation effects are incorporated, despite of the above-mentioned considerations.

Therefore, Koopmans’ theorem is merely a first approximation [84] for the ionization potential and electron affinity of a system but has the undeniable advantage of only requiring a single HF or DFT calculation where it usually takes three calculations to get the N -, $(N - 1)$ - and $(N + 1)$ -electron ground-state energies, to compute ionization potentials and electron affinities.

The idea of connecting physical properties to fictitious spin orbitals and, in particular, to virtual orbitals, is regularly subject to controversy. Indeed, in Koopmans’ theorem, ionization potentials are directly connected to occupied spin-orbital energies (often known as the “IP theorem”) while electron affinities are obtained from virtual spin-orbital energies, which are usually seen like the mathematical leftovers of the self-consistent calculation.

In practice, Hartree-Fock and DFT calculations are performed in a specific basis set whose size determines the amount of spin orbitals that one will obtain at the end of the calculation. The amount of occupied orbitals does not depend on the size of the basis set, but the number of virtual orbitals has shown to quickly increase as one uses larger basis.

In fact, when one increases the size of the basis set, the occupied orbital energies tend to converge towards specific values but the virtual ones do not exhibit such a nice physical behaviour and get more and more numerous. This is why equating physical properties with orbital energies is reasonable enough for ionization potentials but becomes highly questionable for electron affinities.

For instance, in Hartree-Fock theory, virtual orbitals are usually positive, leading to negative Koopmans' electron affinities, but many neutral systems are known to form stable anions when adding an electron to the neutral ground state, which implies having a lower energy for the $(N + 1)$ -electron system and, thus, a positive electron affinity.

Hartree-Fock orbital energies are acceptable approximations for the ionization potential and electron affinity of atomic systems and finite solids, but Kohn-Sham orbitals are known to be poorer orbitals and to yield smaller HOMO-LUMO gaps than in Hartree-Fock calculations. Nevertheless, Kohn-Sham DFT orbitals have the advantage to incorporate correlation effects, which Hartree-Fock orbitals lack of, and benefit from the possibility of improving the exchange-correlation energy functional to get better approximations, through the Kohn-Sham gap.

Note that, even with the exact functional, the KS-DFT LUMO energy is not equal to the opposite of the electron affinity of the neutral system, because there must be a “jump” in the potential as the number of electrons of the open system crosses an integer value. This discontinuity Δ has shown to be exactly the missing part that must be taken into account in order to connect the electron affinity with the LUMO energy

$$I_0^N = -\varepsilon^{\text{HOMO}} \quad (4.46) \quad \Bigg| \quad A_0^N = -\varepsilon^{\text{LUMO}} + \Delta. \quad (4.47)$$

As for the fundamental gap, one sees that the Kohn-Sham HOMO-LUMO gap, defined as

$$\Omega_0^{\text{KS}} = \varepsilon^{\text{LUMO}} - \varepsilon^{\text{HOMO}}, \quad (4.48)$$

can be used as a first approximation for the fundamental gap of the neutral N -electron system

$$\begin{aligned} \Omega_0^N &\equiv I_0^N - A_0^N \\ &= \Omega_0^{\text{KS}} - \Delta. \end{aligned} \quad (4.49)$$

The missing term Δ is known as the “derivative discontinuity” and will be discussed further throughout this work

$$\Delta = \Omega_0^{\text{KS}} - \Omega_0^N = (\varepsilon^{\text{LUMO}} + A_0^N) - (\varepsilon^{\text{HOMO}} + I_0^N). \quad (4.50)$$

In order to have a qualitative idea of the level of accuracy than one would obtain using orbital energies to approximate physical properties, HOMO and LUMO energies of the Li atom are depicted in Figure 4.1 for various unrestricted methods and levels of xc-approximations, in the cc-pVDZ basis set, compared to the experimental references for the opposites of the ionization potential and electron affinity of Li.

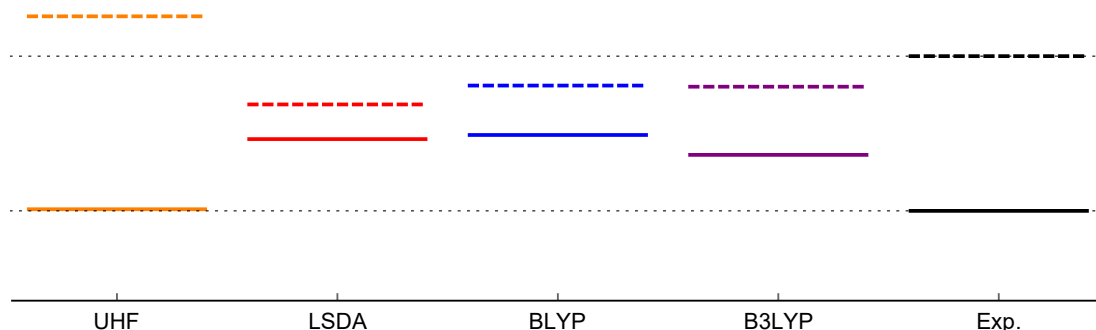


Figure 4.1: HOMO-LUMO gap (solid line-dashed line gap) of Li obtained from a single ground-state DFT calculation within different levels of approximations in the cc-pVDZ basis, compared to its experimental fundamental gap (black) (see Appendix A).

We see that the UHF orbital energies give quite a good approximation for the opposite of the ionization potential of Li but are too high for the opposite of the electron affinity. As for the DFT xc-functionals, it is straightforward to see that the KS HOMO-LUMO gaps are much smaller than the UHF gap, with the HOMO energy being too high and the LUMO energy being too low, compared to the experimental references.

All the previous discussion was made within the scope of integer number of electrons but what we would like to know is how does this work when we study a system with a fractional number of electrons, or an ensemble.

Fortunately, Slater, and then Janak, have shown that for a set of spin orbitals with fractional occupation numbers, which have been discussed previously, the spin-orbital energies ε_i can be interpreted as the variation of the total energy of the system, with respect to the variation of the fractional occupation number of the same spin orbital

$$\frac{\partial E}{\partial n_i} = \varepsilon_i. \quad (4.51)$$

We stress that, in the above definition, which is known as “Janak’s theorem” [38], the occupation numbers are allowed to vary continuously and the relaxation of the orbitals is taken into account.

Hence, we see that the spin orbital energies can be interpreted as the slope of the total energy with respect to the variation of the occupation numbers, and thus the number of electrons of the system. In that sense, orbital energies are very similar to chemical potentials, as discussed in the beginning of this chapter, which are identical to either the opposite of ionization

potentials or the opposite of electron affinities, depending on the situation we are describing, that is the removal or the addition of an electron to the neutral system.

As a matter of fact, Perdew and Levy [67] have proved that, when $|\mathbf{r}| \rightarrow \infty$ (that is far from the system), the asymptotic decay of the exact electron density of an interacting N -electron system evolving in a vanishing external potential $v(\mathbf{r})$, with a highest fully, or partly, occupied Kohn-Sham orbital, was entirely dictated by its ionization potential

$$n(\mathbf{r}) \sim \exp \left[-2\sqrt{2I_0^N} |\mathbf{r}| \right]. \quad (4.52)$$

Furthermore, they derived the asymptotic behavior of the exact Kohn-Sham non-interacting ensemble density, which includes an explicit dependence on the HOMO energy of the system

$$n^{\text{KS}}(\mathbf{r}) \sim \exp \left[-2\sqrt{2[-\varepsilon_N^N + v_s(\infty)]} |\mathbf{r}| \right]. \quad (4.53)$$

Since the interacting system and the non-interacting Kohn-Sham system must, by definition of the Kohn-Sham system, share the same exact electron density, and since the exact Kohn-Sham effective potential $v_s(\mathbf{r})$ has also been proved to vanish far from the system, they managed to prove the validity of the ionization potential (IP) theorem with no use of Janak's theorem,

$$\varepsilon_N^N = -I_0^N. \quad (4.54)$$

Ensemble Formalism versus DFT with Fractional Occupation Numbers

We would like to point out the subtle difference between DFT with fractional occupation numbers and PPLB (ensemble) DFT. Let us say that one's interest is to know the ground-state energy of a N -electron system from which a fraction $0 \leq \alpha \leq 1$ of the electron occupying the highest spin orbital is removed. The electronic configuration of such a system would consist of a set of orthonormal spin orbitals in which only the $N - 1$ lowest orbitals would be occupied with occupation numbers $n_i = 1$ and the N th orbital would be fractionally occupied with $n_N = 1 - \alpha$.

Hence, the quantum state of this system can be described by an electron density integrating to a fractional electron number \mathcal{N} , such that

$$\sum_{i=1}^M n_i = \sum_{i=1}^{N-1} (1) + 1 - \alpha = N - \alpha = \mathcal{N}, \quad (4.55)$$

and

$$\begin{aligned} n(\mathbf{r}) &= \sum_{i=1}^M \sum_{\sigma} n_i |\chi_i(\mathbf{r}, \sigma)|^2 \\ &= \sum_{i=1}^{N-1} \sum_{\sigma} |\chi_i(\mathbf{r}, \sigma)|^2 + (1 - \alpha) |\chi_N(\mathbf{r}, \sigma)|^2. \end{aligned} \quad (4.56)$$

We have seen that the Kohn-Sham DFT framework was still valid for electron densities with fractional electron numbers, thus one can apply total-energy density functionals to such a density, for a given set of occupation numbers, and then minimize it in order to find the best set of spin orbitals from which one can build the minimizing ground-state electron density and compute the corresponding ground-state energy of the system. To do so, the only requirement would be to have a DFT computational code capable of handling fractional occupation numbers.

Actually, there exists another possible framework that one could resort to to study a system with a fractional number of electrons within the scope of DFT, the ensemble formalism. The ensemble formalism has the advantage to allow one to extract individual properties, like excitation energies, through the calculation of simple derivatives of the ensemble energy as we shall see.

For instance, in order to describe the removal of an electron from a N -electron system, as discussed previously, the first step would be to build the corresponding left PPLB ensemble density

$$n_0^\alpha(\mathbf{r}) = (1 - \alpha)n_0^N(\mathbf{r}) + \alpha n_0^{N-1}(\mathbf{r}), \quad (4.57)$$

a linear mixture of the two ground-state densities of the N - and $(N - 1)$ -electron systems built from the same set of molecular orbitals, such that

$$n_0^N(\mathbf{r}) = \sum_{i=1}^N |\varphi_i^\alpha(\mathbf{r})|^2 \quad (4.58) \quad \left| \quad n_0^{N-1}(\mathbf{r}) = \sum_{i=1}^{N-1} |\varphi_i^\alpha(\mathbf{r})|^2. \quad (4.59)$$

We stress that, in the ensemble formalism, all the individual densities included in the ensemble are built from the same set of weight-dependent molecular orbitals $\{\varphi_i^\alpha\}$ with integral occupation numbers. In that sense, for a given ensemble weight α , the variationally optimized set of ensemble molecular orbitals will not necessarily be the same as the set of orbitals optimized for the ground-state of the neutral system, nor the same set of orbitals optimized for the cationic system.

Therefore, in an ensemble DFT calculation, the molecular orbitals are not truly fractionally occupied but it is the ensemble weight instead that will mimic the open system with overall fractional number of electrons.

4.2 Perdew-Parr-Levy-Balduz Density-Functional Theory Formalism

4.2.1 Open systems and ensembles

In quantum mechanics, a system which can exchange electrons with other systems is referred to as an “open system” and is associated with a fluctuating and possibly fractional total number of electrons \mathcal{N} . A fractional number of electrons can be interpreted as a time average

in an open system which exchanges electrons with its surroundings.

As a matter of fact, the quantum ground state of an open system cannot be described by a single wave function Ψ_o , but will instead take the form of a statistical mixture, or ensemble, associated with an ensemble density matrix

$$\Gamma_0^{\mathbf{w}} \equiv \sum_I w_I |\Psi_0^{N_I}\rangle \langle \Psi_0^{N_I}|, \quad (4.60)$$

where $\{\Psi_0^{N_I}\}$ is the set of allowed “pure” ground states for the open system, and $\{N_I\}$ are the corresponding integer number of electrons associated with these ground states.

The ensemble weights, $\mathbf{w} \equiv \{w_I\}$, can be interpreted as the probabilities associated with the respective pure states, from which the ensemble is built. Hence, the weights must be positive and normalized such that the total number of electrons the system is recovered

$$\sum_I w_I = 1 \quad (4.61) \quad \left| \quad \sum_I w_I N_I = \mathcal{N}. \quad (4.62)$$

In that context, the expectation value of any observable \mathcal{O} associated with an Hermitian operator $\hat{\mathcal{O}}$ is defined as follows

$$\langle \hat{\mathcal{O}} \rangle_{\Gamma_0^{\mathbf{w}}} \equiv \sum_I w_I \langle \Psi_0^{N_I} | \hat{\mathcal{O}} | \Psi_0^{N_I} \rangle. \quad (4.63)$$

Hence, the ground-state ensemble energy of an open system is given as

$$\begin{aligned} E_0^{\mathbf{w}} &\equiv \sum_I w_I \langle \Psi_0^{N_I} | \hat{H} | \Psi_0^{N_I} \rangle \\ &= \sum_I w_I E_0^{N_I}, \end{aligned} \quad (4.64)$$

where $E_0^{N_I}$ and $\Psi_0^{N_I}$ are the ground-state energy and ground state wave function, respectively, of the N_I -electron system.

4.2.2 PPLB Ensemble Energy and Ensemble density

From now on, as an illustrative concrete example, we will consider the ionization of a N -electron system, that is to say an open system whose total number of electrons \mathcal{N} continuously varies from the integer number N to $(N - 1)$, while an electron is gradually removed from it. Of course, the current explanation can similarly be extended to the description of the addition of a new electron to a N -electron system. For practical reasons, we choose to use the physical charge deviation α

$$\alpha \equiv |\mathcal{N} - N|, \quad (4.65)$$

as single-weight variable for the left PPLB ensemble, so that $\alpha = 0$ corresponds to $\mathcal{N} = N$ and $\alpha = 1$ corresponds to the situation where the electron has been fully ionized, such that

$\mathcal{N} = N - 1$.

The ground state of such an open system is described by a ground-state ensemble density matrix [12], built from the ground-states density matrices of the N - and $(N - 1)$ -electron systems,

$$\Gamma_0^{\mathcal{N}} \equiv \Gamma_0^\alpha = (1 - \alpha) |\Psi_0^N\rangle \langle \Psi_0^N| + \alpha |\Psi_0^{N-1}\rangle \langle \Psi_0^{N-1}|. \quad (4.66)$$

With this exact ground-state ensemble density matrix, one can generate the exact ground-state ensemble density

$$\begin{aligned} n_0^\alpha(\mathbf{r}) &\equiv \text{Tr}[\Gamma_0^\alpha \hat{n}(\mathbf{r})] \\ &= (1 - \alpha)n_0^N(\mathbf{r}) + \alpha n_0^{N-1}(\mathbf{r}), \end{aligned} \quad (4.67)$$

where Tr is the trace operator, and $\hat{n}(\mathbf{r})$ is the density operator.

In this definition,

$$n_0^N(\mathbf{r}) \equiv n_{\Psi_0^N}(\mathbf{r}) \quad (4.68) \quad \left| \quad n_0^{N-1}(\mathbf{r}) \equiv n_{\Psi_0^{N-1}}(\mathbf{r}) \quad (4.69)$$

are the exact individual ground-state densities of the N - and $(N - 1)$ -electron systems.

Similarly, one can obtain the exact ground-state ensemble energy of the open system, defined as

$$\begin{aligned} E_0^\alpha &\equiv \text{Tr}[\Gamma_0^\alpha \hat{H}] \\ &= (1 - \alpha)E_0^N + \alpha E_0^{N-1}. \end{aligned} \quad (4.70)$$

4.2.3 Theoretical Extraction of Individual-State Properties and Excitation Energies

In the exact theory, the exact ground-state ensemble energy and density must be linear with respect to the weight of the ensemble, α , which in the present situation has been chosen to represent the fractional deviation of the number of electrons of the open system from its initial integer value N . As a matter of fact, one can exploit this linear feature of the energy in order to extract physical properties of the individual states included in the ensemble, as well as the corresponding charged excitation energies, by taking simple derivatives of the ensemble energy with respect to the ensemble weight

$$\begin{cases} E_0^N &= E_0^\alpha - \alpha \frac{dE_0^\alpha}{d\alpha} \\ E_0^{N-1} &= E_0^\alpha + (1 - \alpha) \frac{dE_0^\alpha}{d\alpha} \\ I_0^N &\equiv E_0^{N-1} - E_0^N = \frac{dE_0^\alpha}{d\alpha}. \end{cases} \quad (4.71)$$

4.2.4 PPLB Variational Principle and Universal Functional

Canonical formalism

The Hohenberg-Kohn theorems of standard ground-state density-functional theory state that for a N -electron system, with electron density $n(\mathbf{r})$, experiencing an external potential $v(\mathbf{r})$, there exists a functional

$$E_v[n] = F[n] + \int n(\mathbf{r})v(\mathbf{r})d\mathbf{r}, \quad (4.72)$$

whose minimization with respect to number-conserving variations of the density

$$\int n(\mathbf{r})d\mathbf{r} = N, \quad (4.73)$$

yields the exact ground-state density $n_0(\mathbf{r})$ with exact ground-state energy

$$E_0^N \equiv E_v[n_0] = \min_n E_v[n], \quad (4.74)$$

where the minimization is over all N -electron trial densities.

Furthermore, let us recall the constrained-search formulation for the universal functional

$$\begin{aligned} F[n] &\equiv \min_{\Psi \rightarrow n} \langle \hat{T} + \hat{V}_{ee} \rangle_{\Psi} \\ &= \langle \Psi[n] | \hat{T} + \hat{V}_{ee} | \Psi[n] \rangle \\ &= T[n] + V_{ee}[n], \end{aligned} \quad (4.75)$$

where the search is over all antisymmetric trial wave functions which yield the given electron density $n(\mathbf{r})$, and where $\Psi[n]$ is the particular antisymmetric wave function that yields the density $n(\mathbf{r})$ and minimizes the quantity $\langle \hat{T} + \hat{V}_{ee} \rangle$.

Grand canonical formalism

The Hohenberg-Kohn theorems and the constrained-search formulation of the universal functional, first, have been applied to pure states and ensembles with fixed integer number of electrons N . They have then been extended to trial densities which integrate to fractional numbers of electrons \mathcal{N} .

Indeed, for an open system with a fractional number of electrons $\mathcal{N} = N - \alpha$, described by an ensemble density matrix Γ^α and ensemble density $n^\alpha(\mathbf{r})$, subject to an external potential $v(\mathbf{r})$, there exists a functional

$$E_v[n^\alpha] = F[n^\alpha] + \int n^\alpha(\mathbf{r})v(\mathbf{r})d\mathbf{r}, \quad (4.76)$$

whose minimization with respect to number-conserving variations of the ensemble density,

$$\int n^\alpha(\mathbf{r})d\mathbf{r} = \mathcal{N}, \quad (4.77)$$

yields the lowest average energy, or ensemble energy,

$$E_0^N \equiv E_v[n_0^\alpha] = \min_{n^\alpha} E_v[n^\alpha], \quad (4.78)$$

for a \mathcal{N} -electron open system in a statistical mixture of a specific type.

Indeed, the left PPLB universal ensemble density functional [12] is defined as follows

$$\begin{aligned} F[n^\alpha] &\equiv \min_{\Gamma^\alpha \rightarrow n^\alpha} \langle \hat{T} + \hat{V}_{ee} \rangle_{\Gamma^\alpha} \\ &= (1 - \alpha) \langle \Psi_0^{N,\alpha}[n^\alpha] | \hat{T} + \hat{V}_{ee} | \Psi_0^{N,\alpha}[n^\alpha] \rangle + \alpha \langle \Psi_0^{N-1,\alpha}[n^\alpha] | \hat{T} + \hat{V}_{ee} | \Psi_0^{N-1,\alpha}[n^\alpha] \rangle, \end{aligned} \quad (4.79)$$

where the search is over all \mathcal{N} -electron ensemble density matrix operators $\hat{\Gamma}^\alpha$ of the type

$$\Gamma^\alpha = (1 - \alpha) |\Psi_0^{N,\alpha}\rangle \langle \Psi_0^{N,\alpha}| + \alpha |\Psi_0^{N-1,\alpha}\rangle \langle \Psi_0^{N-1,\alpha}|, \quad (4.80)$$

built from an arbitrary set of weight-dependent N - and $(N - 1)$ -electron ground states $\{\Psi_0^{N,\alpha}, \Psi_0^{N-1,\alpha}\}$ that yields the ensemble density

$$n_{\hat{\Gamma}^\alpha}(\mathbf{r}) = \text{Tr}[\hat{\Gamma}^\alpha \hat{n}(\mathbf{r})] = (1 - \alpha)n_{\Psi_0^{N,\alpha}}(\mathbf{r}) + \alpha n_{\Psi_0^{N-1,\alpha}}(\mathbf{r}) = n^\alpha(\mathbf{r}). \quad (4.81)$$

$\Psi_0^{N,\alpha}[n^\alpha]$ and $\Psi_0^{N-1,\alpha}[n^\alpha]$ are the particular ground states that minimize the quantity

$$\langle \hat{T} + \hat{V}_{ee} \rangle_{\Gamma^\alpha} = \text{Tr}[\hat{\Gamma}^\alpha (\hat{T} + \hat{V}_{ee})], \quad (4.82)$$

for a given weight α , and yield the ensemble density $n^\alpha(\mathbf{r})$ such that

$$(1 - \alpha)n_{\Psi_0^{N,\alpha}[n^\alpha]}(\mathbf{r}) + \alpha n_{\Psi_0^{N-1,\alpha}[n^\alpha]}(\mathbf{r}) = n^\alpha(\mathbf{r}). \quad (4.83)$$

Hence, the minimization of the ensemble energy $E_v[n^\alpha]$ yields the exact ground-state ensemble energy which is the lowest energy for a $(N - \alpha)$ -electron system in a statistical mixture of the type

$$E_0^\alpha = (1 - \alpha)E_0^N + \alpha E_0^{N-1}, \quad (4.84)$$

where E_0^N and E_0^{N-1} are the ground-state energies of a N - and $(N - 1)$ -electron systems experiencing the external potential $v(\mathbf{r})$.

As a matter of fact, the constrained-search can conveniently be extended to any type of statistical mixtures yielding the given density $n^\alpha(\mathbf{r})$, under the ‘‘concave-upward condition’’ which requires that the plot of the ground-state ensemble energy, E_0^N , with respect to the number of electrons, \mathcal{N} , must verify the following condition

$$E_0^N < \frac{(E_0^{N+1} + E_0^{N-1})}{2}. \quad (4.85)$$

In practice, this condition is always true for coulombic electronic systems, allowing for a less restrictive minimization.

4.2.5 Kohn-Sham Formulation of PPLB-DFT

Kohn-Sham system

Analogous to standard Kohn-Sham DFT formalism, one can choose to decompose the universal PPLB functional into two contributions

$$F[n^\alpha] = T_s[n^\alpha] + E_{\text{Hxc}}[n^\alpha], \quad (4.86)$$

where $T_s[n^\alpha]$ is the non-interacting ensemble kinetic-energy functional, and $E_{\text{Hxc}}[n^\alpha]$ is the combined Hartree-exchange-correlation ensemble energy functional.

By doing so, one assumes that there exists an auxiliary non-interacting system, the Kohn-Sham system, which will have the same ensemble density than the interacting system associated with the ensemble density $n^\alpha(\mathbf{r})$.

One important feature of the PPLB framework is that the weight of the ensemble, α , and the ensemble density, $n^\alpha(\mathbf{r})$, are not independent quantities. Indeed, since the ensemble density has to integrate to the fractional number of electrons $\mathcal{N} = N - \alpha$, a change of the weight α will automatically result in a variation of the density. Therefore, all the information that defines the ensemble will already be encompassed within the ensemble density. This means that the exact functional, that is to say the one that shall guarantee the piecewise linearity of the ensemble energy, as mentioned in the chemical potential section, is not required to possess a weight-dependency to properly describe the energy of the open system. Of course, since the exact functional is not known, one is not compelled to restrict his work to the sole domain of standard weight-independent functionals and always has the possibility to explore the feasibility and the relevance of building better approximations based on an explicit weight-dependency, as will be further discussed through this work.

From now on, for sake of simplicity, we will use the generic notation $n(\mathbf{r})$ instead of $n^\alpha(\mathbf{r})$ when referring to any ensemble density which integrates to the fractional number of electrons \mathcal{N} , especially when defining functionals.

Non-interacting ensemble kinetic energy

The PPLB Kohn-Sham non-interacting ensemble kinetic-energy functional can be expressed in a constrained-search formulation [12] defined as follows

$$\begin{aligned} T_s[n] &= \min_{\hat{\gamma}^\alpha \rightarrow n} \left\{ \text{Tr}[\hat{\gamma}^\alpha \hat{T}] \right\} \\ &= (1 - \alpha) \left\langle \Phi_0^{N,\alpha}[n] \left| \hat{T} \right| \Phi_0^{N,\alpha}[n] \right\rangle + \alpha \left\langle \Phi_0^{N-1,\alpha}[n] \left| \hat{T} \right| \Phi_0^{N-1,\alpha}[n] \right\rangle, \end{aligned} \quad (4.87)$$

where the constrained-search is over all non-interacting ensemble density matrix operators $\hat{\gamma}^\alpha$, built from an arbitrary set of weight-dependent single Slater determinantal ground states $\{\Phi_0^{N,\alpha}, \Phi_0^{N-1,\alpha}\}$, such that

$$\hat{\gamma}^\alpha = (1 - \alpha) \left| \Phi_0^{N,\alpha} \right\rangle \left\langle \Phi_0^{N,\alpha} \right| + \alpha \left| \Phi_0^{N-1,\alpha} \right\rangle \left\langle \Phi_0^{N-1,\alpha} \right|, \quad (4.88)$$

recovers the interacting ensemble density

$$\begin{aligned}
 n_{\hat{\gamma}^\alpha}(\mathbf{r}) &= \text{Tr}[\hat{\gamma}^\alpha \hat{n}(\mathbf{r})] \\
 &= (1 - \alpha)n_{\Phi_0^{N,\alpha}}(\mathbf{r}) + \alpha n_{\Phi_0^{N-1,\alpha}}(\mathbf{r}) \\
 &= n(\mathbf{r}).
 \end{aligned} \tag{4.89}$$

$\{\Phi_0^{N,\alpha}[n], \Phi_0^{N-1,\alpha}[n]\}$ are the particular Slater determinants from which is built the non-interacting ensemble density-matrix operator that minimizes the ensemble kinetic energy

$$\text{Tr}[\hat{\gamma}^\alpha \hat{T}], \tag{4.90}$$

that is the Kohn-Sham ensemble density matrix operator

$$\hat{\gamma}_{\text{KS}}^\alpha = (1 - \alpha) \left| \Phi_0^{N,\alpha}[n] \right\rangle \left\langle \Phi_0^{N,\alpha}[n] \right| + \alpha \left| \Phi_0^{N-1,\alpha}[n] \right\rangle \left\langle \Phi_0^{N-1,\alpha}[n] \right|, \tag{4.91}$$

and yields the interacting ensemble density, for a fixed given weight α , such that

$$\begin{aligned}
 n_{\text{KS}}^\alpha(\mathbf{r}) &= \text{Tr}[\hat{\gamma}_{\text{KS}}^\alpha \hat{n}(\mathbf{r})] \\
 &= (1 - \alpha)n_{\Phi_0^{N,\alpha}[n]}(\mathbf{r}) + \alpha n_{\Phi_0^{N-1,\alpha}[n]}(\mathbf{r}) \\
 &= n(\mathbf{r}).
 \end{aligned} \tag{4.92}$$

PPLB-DFT Kohn-Sham molecular orbitals

One can express the variational principle for the PPLB ensemble energy in terms of the weight-dependent molecular orbitals $\{\varphi_p^\alpha(\mathbf{r})\}$ from which the Kohn-Sham single Slater determinants $\{\Phi_0^{N,\alpha}, \Phi_0^{N-1,\alpha}\}$ are built

$$\begin{aligned}
 E_0^\alpha &= \min_{\{\varphi_p^\alpha\}} \left\{ \text{Tr} \left[\hat{\gamma}^\alpha \left(\hat{T} + \hat{V}_{\text{en}} \right) \right] + E_{\text{Hxc}}[n_{\hat{\gamma}^\alpha}] \right\} \\
 &= \text{Tr} \left[\hat{\gamma}_{\text{KS}}^\alpha \left(\hat{T} + \hat{V}_{\text{en}} \right) \right] + E_{\text{Hxc}}[n_{\text{KS}}^\alpha].
 \end{aligned} \tag{4.93}$$

From now on, we will use the notation $\{\varphi_p^\alpha\}$ to refer to the specific set of minimizing weight-dependent Kohn-Sham orbitals, that is to say the orbitals from which is built the set of single Slater determinantal Kohn-Sham wave functions $\{\Phi_0^{N,\alpha}[n^\alpha], \Phi_0^{N-1,\alpha}[n^\alpha]\} \equiv \{\Phi_0^{N,\alpha}, \Phi_0^{N-1,\alpha}\}$, that minimize the PPLB ensemble energy and mimic the true PPLB ensemble density $n(\mathbf{r})$. For that reason, in the exact theory, one must have

$$\begin{aligned}
 n_{\text{KS}}^\alpha(\mathbf{r}) &= (1 - \alpha)n_{\Phi_0^{N,\alpha}}(\mathbf{r}) + \alpha n_{\Phi_0^{N-1,\alpha}}(\mathbf{r}) \\
 &= (1 - \alpha)n_{\Psi_0^N}(\mathbf{r}) + \alpha n_{\Psi_0^0}(\mathbf{r}) \\
 &= n(\mathbf{r})
 \end{aligned} \tag{4.94}$$

$\{n_{\Psi_0^N}(\mathbf{r}) \equiv n_0^N(\mathbf{r}), n_{\Psi_0^{N-1}}(\mathbf{r}) \equiv n_0^{N-1}(\mathbf{r})\}$ are the exact individual ground-state electron densities generated by the exact eigenstates $\{\Psi_0^N, \Psi_0^{N-1}\}$ of the interacting system.

We stress that in an eDFT calculation, all the individual states of the ensemble are built from the same set of weight-dependent Kohn-Sham orbitals, as opposed to the standard KS-DFT framework where these states would be built from different sets of optimized orbitals obtained from distinct calculations.

The individual Kohn-Sham densities can be obtained by summation over all occupied weight-dependent Kohn-Sham orbitals for the given state

$$n_{\Phi_0^{N,\alpha}}(\mathbf{r}) = \sum_{p=1}^N |\varphi_p^\alpha(\mathbf{r})|^2 \quad (4.95) \quad \left| \quad n_{\Phi_0^{N-1,\alpha}}(\mathbf{r}) = \sum_{p=1}^{N-1} |\varphi_p^\alpha(\mathbf{r})|^2. \quad (4.96)$$

Based on these definitions, one can reformulate the non-interacting Kohn-Sham ensemble density in terms of the occupied weight-dependent Kohn-Sham molecular orbitals, such that

$$\begin{aligned} n_{\text{KS}}^\alpha(\mathbf{r}) &= (1 - \alpha) \sum_{p=1}^N |\varphi_p^\alpha(\mathbf{r})|^2 + \alpha \sum_{p=1}^{N-1} |\varphi_p^\alpha(\mathbf{r})|^2 \\ &= \sum_{p=1}^{N-1} |\varphi_p^\alpha(\mathbf{r})|^2 + (1 - \alpha) |\varphi_N^\alpha(\mathbf{r})|^2 \\ &= n(\mathbf{r}). \end{aligned} \quad (4.97)$$

Hence, it is straightforward to see that the ensemble density of the \mathcal{N} -electron open system corresponds to having the $(N - 1)$ lowest Kohn-Sham molecular orbitals occupied by one electron while the N th Kohn-Sham molecular orbital, the ‘‘HOMO’’ of the open system, is fractionally occupied by a fraction of $(1 - \alpha)$ electron.

Note that, although the Kohn-Sham molecular orbitals must mimic the true ensemble density of the interacting open system, that does not mean that the individual Kohn-Sham densities will mimic the true interacting individual densities as well. Indeed, apart from the $\alpha = 0$ and $\alpha = 1$ cases, the Kohn-Sham molecular orbitals will be optimized with respect to the ensemble, that is to say for a specific weight-configuration and not for a specific state included in the ensemble.

PPLB-DFT Kohn-Sham equations

The weight-dependent minimizing Kohn-Sham orbitals are the solutions of a set of non-linear equations, the self-consistent PPLB-DFT Kohn-Sham equations [12]

$$\left(-\frac{1}{2}\nabla^2 + v(\mathbf{r}) + v_{\text{Hxc}}(\mathbf{r}) \right) \varphi_p^\alpha(\mathbf{r}) = \varepsilon_p^\alpha \varphi_p^\alpha(\mathbf{r}), \quad (4.98)$$

where $v(\mathbf{r})$ is the weight-independent local external nuclear potential, and $v_{\text{Hxc}}(\mathbf{r})$ is the weight-independent Hartree-exchange-correlation potential

$$v_{\text{Hxc}}(\mathbf{r}) = \frac{\delta E_{\text{Hxc}}[n]}{\delta n(\mathbf{r})}, \quad (4.99)$$

defined as the functional derivative of the Hartree-exchange-correlation energy functional $E_{\text{Hxc}}[n]$, with respect to the ensemble density $n(\mathbf{r})$.

Hence, we see that PPLB-DFT is very similar to the standard ground-state formulation of Kohn-Sham DFT, with the difference that the Kohn-Sham solutions are now a set of weight-dependent molecular orbitals $\{\varphi_p^{\mathbf{w}}(\mathbf{r})\}$ with weight-dependent orbital energies $\{\varepsilon_p^{\mathbf{w}}\}$. As previously mentioned, in PPLB-DFT, the exact Hartree-exchange-correlation functional is not weight-dependent since all the information about the ensemble, that is to say the weight configuration, is already encompassed within the ensemble density.

Of course, like in standard DFT, the exact functional remains out of reach and, for that reason, one is free to resort to standard weight-independent exchange-correlation approximate functionals, or to design new functionals [30, 29, 24, 45], with or without explicit weight-dependency [55, 59], in order to improve the quality and accuracy of the self-consistent results.

4.2.6 Practical Extraction of Individual-State Properties and Excitation Energies

Removal of an electron

From now on, we will consider the possibility to use a weight-dependent Hartree-exchange-correlation density functional $E_{\text{Hxc}}^\alpha[n]$ so that the PPLB ensemble density takes the form

$$\begin{aligned} E_0^\alpha &= \text{Tr} \left[\hat{\gamma}_{\text{KS}}^\alpha \left(\hat{T} + \hat{V}_{\text{en}} \right) \right] + E_{\text{Hxc}}^\alpha[n_{\text{KS}}^\alpha] \\ &= (1 - \alpha) \langle \Phi_0^{N, \alpha} | \hat{T} + \hat{V}_{\text{en}} | \Phi_0^{N, \alpha} \rangle + \alpha \langle \Phi_0^{N-1, \alpha} | \hat{T} + \hat{V}_{\text{en}} | \Phi_0^{N-1, \alpha} \rangle + E_{\text{Hxc}}^\alpha[n_{\text{KS}}^\alpha], \end{aligned} \quad (4.100)$$

with the non-interacting single Slater determinantal Kohn-Sham wave functions, $\{\Phi_0^{N, \alpha}, \Phi_0^{N-1, \alpha}\}$, and Kohn-Sham ensemble density

$$n_{\text{KS}}^\alpha(\mathbf{r}) = (1 - \alpha)n_{\Phi_0^{N, \alpha}}(\mathbf{r}) + \alpha n_{\Phi_0^{N-1, \alpha}}(\mathbf{r}). \quad (4.101)$$

According to the Hellmann-Feynman theorem, we can express the derivative of the PPLB ensemble energy with respect to the weight α in terms of the occupied Kohn-Sham orbital energies and the derivative of the possibly weight-dependent Hartree-exchange-correlation func-

tional, with respect to the weight,

$$\begin{aligned}
 \frac{dE_0^\alpha}{d\alpha} &= \langle \Phi_0^{N-1,\alpha} | \hat{T} + \hat{V}_{\text{en}} | \Phi_0^{N-1,\alpha} \rangle - \langle \Phi_0^{N,\alpha} | \hat{T} + \hat{V}_{\text{en}} | \Phi_0^{N,\alpha} \rangle \\
 &+ \int \frac{\delta E_{\text{Hxc}}^\alpha[n_{\text{KS}}^\alpha]}{\delta n(\mathbf{r})} \left(n_{\Phi_0^{N-1,\alpha}}(\mathbf{r}) - n_{\Phi_0^{N,\alpha}}(\mathbf{r}) \right) d\mathbf{r} + \frac{\partial E_{\text{Hxc}}^\alpha[n_{\text{KS}}^\alpha]}{\partial \alpha} \\
 &= \sum_{p=1}^{N-1} \varepsilon_p^\alpha - \sum_{p=1}^N \varepsilon_p^\alpha + \frac{\partial E_{\text{Hxc}}^\alpha[n_{\text{KS}}^\alpha]}{\partial \alpha} \\
 &= \mathcal{E}_0^{N-1,\alpha} - \mathcal{E}_0^{N,\alpha} + \frac{\partial E_{\text{Hxc}}^\alpha[n_{\text{KS}}^\alpha]}{\partial \alpha}
 \end{aligned} \tag{4.102}$$

where $\mathcal{E}_0^{N,\alpha}$ and $\mathcal{E}_0^{N-1,\alpha}$ are the Kohn-Sham auxiliary energies of the individual states of the PPLB ensemble.

We obtain the following left-PPLB key-formulation for the ionization potential of the neutral N -electron system, defined as the slope of the energy of the open system,

$$I_0^N = -\varepsilon_N^\alpha + \frac{\partial E_{\text{Hxc}}^\alpha[n_{\text{KS}}^\alpha]}{\partial \alpha}. \tag{4.103}$$

We stress that, in the exact theory [12], since the exact Hxc functional is known to be weight-independent, the additional weight derivative in equations (4.102) and (4.103) would reduce to zero.

Hence we see that $-\varepsilon_N^\alpha$, which corresponds to the opposite of the HOMO energy of the N -electron system, is a first approximation for the ionization potential I_0^N of the neutral N -electron system, which is consistent with Janak's theorem.

Indeed, since $(1 - \alpha)$ is the occupation number of the N th Kohn-Sham orbital, by applying Janak's theorem one obtains

$$\varepsilon_N^\alpha = \frac{dE_0^\alpha}{d(1 - \alpha)} = -\frac{dE_0^\alpha}{d\alpha} = -I_0^N. \tag{4.104}$$

Thus, with the exact functional, which must be weight-independent, the prediction for the ionization potential of the neutral system must reduce to the opposite of the weight-dependent HOMO energy of the neutral system.

As a matter of fact, when approximate functionals are used, this first Kohn-Sham prediction is usually poor but can be improved by means of an explicit weight-dependent Hartree-exchange-correlation approximate functional, through the additional contribution stemming from its derivative with respect to the ensemble weight.

In the same manner, one can obtain an analog formulation for the ground-state energies

of the individual states included in the left PPLB ensemble

$$\begin{aligned}
 E_0^N &= E_0^\alpha - \alpha \frac{dE_0^\alpha}{d\alpha} \\
 &= \mathcal{E}_0^{N,\alpha} + E_{\text{Hxc}}^\alpha[n_{\text{KS}}^\alpha] - \int \frac{\delta E_{\text{Hxc}}^\alpha[n_{\text{KS}}^\alpha]}{\delta n(\mathbf{r})} n_{\text{KS}}^\alpha(\mathbf{r}) d\mathbf{r} - \alpha \frac{\partial E_{\text{Hxc}}^\alpha[n_{\text{KS}}^\alpha]}{\partial \alpha},
 \end{aligned} \tag{4.105}$$

and

$$\begin{aligned}
 E_0^{N-1} &= E_0^\alpha + (1 - \alpha) \frac{dE_0^\alpha}{d\alpha} \\
 &= \mathcal{E}_0^{N-1,\alpha} + E_{\text{Hxc}}^\alpha[n_{\text{KS}}^\alpha] - \int \frac{\delta E_{\text{Hxc}}^\alpha[n_{\text{KS}}^\alpha]}{\delta n(\mathbf{r})} n_{\text{KS}}^\alpha(\mathbf{r}) d\mathbf{r} + (1 - \alpha) \frac{\partial E_{\text{Hxc}}^\alpha[n_{\text{KS}}^\alpha]}{\partial \alpha}.
 \end{aligned} \tag{4.106}$$

Addition of an electron

At this point, we have thoroughly studied how to apply the PPLB-DFT formalism to describe an open system from which an electron was continuously removed. We will now briefly depict the main differences and key-results that one would obtain when applying this formalism to describe the addition of an electron to a \mathcal{N} -electron open system, such that

$$\mathcal{N} = N + \alpha. \tag{4.107}$$

The quantum state of such an open system would then be described by an ensemble density matrix operator built from the N - and $(N + 1)$ -electron ground-state wave functions

$$\Gamma_0^{\mathcal{N}} \equiv \Gamma_0^\alpha = (1 - \alpha) |\Psi_0^N\rangle \langle \Psi_0^N| + \alpha |\Psi_0^{N+1}\rangle \langle \Psi_0^{N+1}|, \tag{4.108}$$

which yield the exact right PPLB ensemble density

$$n_0^\alpha(\mathbf{r}) = (1 - \alpha)n_0^N(\mathbf{r}) + \alpha n_0^{N+1}(\mathbf{r}), \tag{4.109}$$

with exact right PPLB ensemble energy

$$E_0^\alpha = (1 - \alpha)E_0^N + \alpha E_0^{N+1}. \tag{4.110}$$

Once the minimizing weight-dependent Kohn-Sham molecular orbitals and energies are self-consistently obtained, the derivative of the right PPLB ensemble energy can be expressed in terms of Kohn-Sham quantities, as follows

$$\begin{aligned}
 \frac{dE_0^\alpha}{d\alpha} &= \langle \Phi_0^{N+1,\alpha} | \hat{T} + \hat{V}_{\text{en}} | \Phi_0^{N+1,\alpha} \rangle - \langle \Phi_0^{N,\alpha} | \hat{T} + \hat{V}_{\text{en}} | \Phi_0^{N,\alpha} \rangle \\
 &+ \int \frac{\delta E_{\text{Hxc}}^\alpha[n_{\text{KS}}^\alpha]}{\delta n(\mathbf{r})} \left(n_{\Phi_0^{N+1,\alpha}}(\mathbf{r}) - n_{\Phi_0^{N,\alpha}}(\mathbf{r}) \right) d\mathbf{r} + \frac{\partial E_{\text{Hxc}}^\alpha[n_{\text{KS}}^\alpha]}{\partial \alpha} \\
 &= \sum_{p=1}^{N+1} \varepsilon_p^\alpha - \sum_{p=1}^N \varepsilon_p^\alpha + \frac{\partial E_{\text{Hxc}}^\alpha[n_{\text{KS}}^\alpha]}{\partial \alpha} \\
 &= \mathcal{E}_0^{N+1,\alpha} - \mathcal{E}_0^{N,\alpha} + \frac{\partial E_{\text{Hxc}}^\alpha[n_{\text{KS}}^\alpha]}{\partial \alpha}.
 \end{aligned} \tag{4.111}$$

Hence, one can derive the following key-formulation for the electronic affinity of the neutral N -electron system

$$-A_0^N = \varepsilon_{N+1}^\alpha + \frac{\partial E_{\text{Hxc}}^\alpha[n_{\text{KS}}^\alpha]}{\partial \alpha}. \tag{4.112}$$

Again, we stress that the additional weight-derivative of the (approximate) Hxc functional must reduce to zero for the exact Hxc functional.

Indeed, if one were to use the exact functional, the $(N + 1)$ th Kohn-Sham orbital energy, which by definition is the HOMO energy of the anionic $(N + 1)$ -electron system, would equal the opposite of the electron affinity of the neutral system. The last result is consistent with Janak's theorem which states that, since the occupation number of the $(N + 1)$ th Kohn-Sham orbital is precisely α , one must have

$$\varepsilon_{N+1}^\alpha = \frac{dE_0^\alpha}{d\alpha} = -A_0^N. \tag{4.113}$$

Again, since most weight-independent approximate functionals give poor predictions for ionization potentials and electron affinities, the ensemble-DFT framework enables one to improve these predictions by designing weight-dependent approximate functionals.

Finally, predictions for the individual states included in the right PPLB ensemble can be obtained as well from the right PPLB-DFT self-consistent calculation, such that

$$\begin{aligned}
 E_0^N &= E_0^\alpha - \alpha \frac{dE_0^\alpha}{d\alpha} \\
 &= \mathcal{E}_0^{N,\alpha} + E_{\text{Hxc}}^\alpha[n_{\text{KS}}^\alpha] - \int \frac{\delta E_{\text{Hxc}}^\alpha[n_{\text{KS}}^\alpha]}{\delta n(\mathbf{r})} n_{\text{KS}}^\alpha(\mathbf{r}) d\mathbf{r} - \alpha \frac{\partial E_{\text{Hxc}}^\alpha[n_{\text{KS}}^\alpha]}{\partial \alpha}
 \end{aligned} \tag{4.114}$$

and

$$\begin{aligned}
 E_0^{N+1} &= E_0^\alpha + (1 - \alpha) \frac{dE_0^\alpha}{d\alpha} \\
 &= \mathcal{E}_0^{N+1,\alpha} + E_{\text{Hxc}}^\alpha[n_{\text{KS}}^\alpha] - \int \frac{\delta E_{\text{Hxc}}^\alpha[n_{\text{KS}}^\alpha]}{\delta n(\mathbf{r})} n_{\text{KS}}^\alpha(\mathbf{r}) d\mathbf{r} + (1 - \alpha) \frac{\partial E_{\text{Hxc}}^\alpha[n_{\text{KS}}^\alpha]}{\partial \alpha}.
 \end{aligned} \tag{4.115}$$

4.3 Numerical Implementation of PPLB-DFT

From now on, our aim is to extract charged excitation energies, more precisely ionization potentials and electron affinities, from self-consistent PPLB-DFT calculations applied to real systems. To do so, we will use the ensemble formalism to mimic open systems from/to which a single electron is removed/added from/to the HOMO/LUMO of the neutral N -electron system, in its ground-state electronic configuration.

Such left and right PPLB-DFT calculations have been performed for a small range of small atomic systems, within various levels of approximation, in order to present a more consistent overview of the performance of commonly used methods and xc-functionals within the scope of the PPLB-DFT ensemble framework.

Furthermore, we will study as well to what extent designing explicitly weight-dependent xc-functionals can overtake standard ground-state approximations in improving and restoring the quality of the physical properties extracted from the self-consistent PPLB-DFT ensemble calculations.

4.3.1 Basic Principles

As introduced previously, we will apply the PPLB ensemble formalism to study the removal and the addition of an electron from/to the ground-state of some small atomic systems. In this work, the lithium atom Li will serve as an illustrative model-system and, for all considered systems, unrestricted calculations have been performed at both Hartree-Fock and density-functional theory levels. Hence, the spin-unrestricted Hartree-Fock (UHF) formalism has been used as well as some of the standard weight-independent exchange-correlation functionals of standard ground-state DFT: the Local Spin Density Approximation (LSDA), the Generalized Gradient Approximation (GGA) BLYP functional and the hybrid GGA B3LYP functional, which includes specific amounts of UHF, LSDA and GGA contributions, as mentioned in Chapter 3.

When an electron is continuously removed or added from/to a N -electron system, the latter behaves like an open system with a fractional number of electrons $\mathcal{N} = N \pm \alpha$, with α the fractional charge deviation from the central integer value N

$$\alpha \equiv |\mathcal{N} - N|. \quad (4.116)$$

Moreover, the exact ground-state electron densities and energies of such open systems consist of linear mixtures of the pure-state ground-state densities and energies, respectively, upon which the corresponding charged excitations are defined, that is the N - and $(N \pm 1)$ -electron quantities.

To avoid the use of too heavy notations, and since the present work's only concern is ground-state energies, we choose to loose the subscript "0" and use instead the generic notations $\{E^\alpha, n^\alpha(\mathbf{r})\}$ to refer to the ground-state energies and densities associated with either the removal or the addition processes, and described by left and right PPLB ensembles, respectively.

We recall the compact expressions of the exact ground-state ensemble densities and energies associated with PPLB ensembles

$$n^\alpha(\mathbf{r}) = (1 - \alpha)n_0^N(\mathbf{r}) + \alpha n_0^{N\pm 1}(\mathbf{r}) \quad (4.117) \quad \left| \quad E^\alpha = (1 - \alpha)E_0^N + \alpha E_0^{N\pm 1}, \quad (4.118)\right.$$

where $0 \leq \alpha \leq 1$ is the PPLB ensemble weight which describes, in those two processes, the physical charge deviation from the central integer number of electron N .

In that context, the $\alpha = 0$ weight-configuration corresponds to the initial neutral N -electron system, while the case $\alpha = 1$ corresponds to the cationic/anionic system, depending on the left or right nature of the PPLB ensemble. In these three scenarios, the PPLB-DFT ensemble calculations reduce to standard ground-state DFT calculations.

One important feature of the PPLB framework is that the weight of the ensemble and the ensemble density are not independent quantities. Indeed, since the ensemble density has to integrate to the fractional number of electrons $\mathcal{N} = N \pm \alpha$, a change in the weight α will automatically result in a change in the density. All the information that defines the ensemble is therefore already encompassed in the ensemble density, which means that the exact functional, that is the functional that must guarantee the piecewise linearity of the ensemble energy, is not required to possess an additional weight-dependency to properly describe the energy of the open system. Of course, since the exact functional is not known, one is not compelled to restrict his work to the sole domain of standard weight-independent functionals, and always has the possibility to explore the feasibility and the relevance of building better approximations based on an explicit weight-dependency, as will be further discussed through this work.

Since the exact ground-state ensemble energy of the \mathcal{N} -electron system is supposed to be linear with respect to the ensemble weight α , one can easily extract the individual ground-state energies $\{E_0^N; E_0^{N\pm 1}\}$ and excitation energies, such as the ionization potential I_0^N and the electron affinity A_0^N of the N -electron system, directly from the left and right PPLB ensemble energies E^α and their derivatives with respect to the weight α , such that

$$\left. \begin{aligned} E_0^N &= E^\alpha - \alpha \frac{\partial E^\alpha}{\partial \alpha} \\ E_0^{N-1} &= E^\alpha + (1 - \alpha) \frac{\partial E^\alpha}{\partial \alpha} \\ I_0^N &= E_0^{N-1} - E_0^N = \frac{\partial E^\alpha}{\partial \alpha} \end{aligned} \right| \quad (4.119) \quad \left. \begin{aligned} E_0^N &= E^\alpha - \alpha \frac{\partial E^\alpha}{\partial \alpha} \\ E_0^{N+1} &= E^\alpha + (1 - \alpha) \frac{\partial E^\alpha}{\partial \alpha} \\ A_0^N &= E_0^N - E_0^{N+1} = -\frac{\partial E^\alpha}{\partial \alpha}. \end{aligned} \right. \quad (4.120)$$

In practice, when one performs DFT or eDFT calculations, some of the primal pieces to which one has access once the convergence is achieved, are the Kohn-Sham orbital energies $\{\varepsilon_i\}$. Hence, it would be very convenient to extract the above-mentioned individual energies and excitation energies, directly from the ensemble Kohn-Sham quantities. Again, we insist that, for an ensemble DFT calculation, the set of Kohn-Sham orbitals will be weight-dependent and optimized relative to the whole ensemble, and not for one specific state included in the ensemble. For that reason, the individual and excitation energy predictions will all be obtained from the same ensemble Kohn-Sham system. Let us recall the key formulas that will be used to predict individual-state properties and excitation energies from PPLB-DFT practical calculations

$$\begin{aligned}
 E_0^N &= \mathcal{E}_0^{N,\alpha} \\
 &+ E_{\text{Hxc}}^\alpha[n_{\text{KS}}^\alpha] - \int \frac{\delta E_{\text{Hxc}}^\alpha[n_{\text{KS}}^\alpha]}{\delta n(\mathbf{r})} n_{\text{KS}}^\alpha(\mathbf{r}) d\mathbf{r} \\
 &- \alpha \frac{\partial E_{\text{Hxc}}^\alpha[n_{\text{KS}}^\alpha]}{\partial \alpha} \\
 E_0^{N-1} &= \mathcal{E}_0^{N-1,\alpha} \\
 &+ E_{\text{Hxc}}^\alpha[n_{\text{KS}}^\alpha] - \int \frac{\delta E_{\text{Hxc}}^\alpha[n_{\text{KS}}^\alpha]}{\delta n(\mathbf{r})} n_{\text{KS}}^\alpha(\mathbf{r}) d\mathbf{r} \\
 &+ (1 - \alpha) \frac{\partial E_{\text{Hxc}}^\alpha[n_{\text{KS}}^\alpha]}{\partial \alpha} \\
 I_0^N &= -\varepsilon_N^\alpha + \frac{\partial E_{\text{Hxc}}^\alpha[n_{\text{KS}}^\alpha]}{\partial \alpha}
 \end{aligned} \tag{4.121}$$

$$\begin{aligned}
 E_0^N &= \mathcal{E}_0^{N,\alpha} \\
 &+ E_{\text{Hxc}}^\alpha[n_{\text{KS}}^\alpha] - \int \frac{\delta E_{\text{Hxc}}^\alpha[n_{\text{KS}}^\alpha]}{\delta n(\mathbf{r})} n_{\text{KS}}^\alpha(\mathbf{r}) d\mathbf{r} \\
 &- \alpha \frac{\partial E_{\text{Hxc}}^\alpha[n_{\text{KS}}^\alpha]}{\partial \alpha} \\
 E_0^{N+1} &= \mathcal{E}_0^{N+1,\alpha} \\
 &+ E_{\text{Hxc}}^\alpha[n_{\text{KS}}^\alpha] - \int \frac{\delta E_{\text{Hxc}}^\alpha[n_{\text{KS}}^\alpha]}{\delta n(\mathbf{r})} n_{\text{KS}}^\alpha(\mathbf{r}) d\mathbf{r} \\
 &+ (1 - \alpha) \frac{\partial E_{\text{Hxc}}^\alpha[n_{\text{KS}}^\alpha]}{\partial \alpha} \\
 A_0^N &= -\varepsilon_{N+1}^\alpha - \frac{\partial E_{\text{Hxc}}^\alpha[n_{\text{KS}}^\alpha]}{\partial \alpha}.
 \end{aligned} \tag{4.122}$$

To perform an ensemble DFT calculation, the first step is to define the characteristics of the ensemble for which one aims to variationally optimize the Kohn-Sham orbitals, in order to minimize the ensemble energy of the system.

Indeed, to define a given ensemble, one must specify the number and nature of the individual states included in this ensemble, along with the weights associated with these states. To do so, one must indicate how to populate the unique set of ensemble Kohn-Sham orbitals by specifying the distinct sets of occupation numbers to use for all molecular orbitals of both spin channels and, this, for each individual state of the ensemble.

To illustrate these practical considerations, the characteristics of both left and right PPLB

ensembles applied to the lithium atom, for mimicking the removal and addition of an electron from/to its ground state, are reported in Tables 4.1 and 4.2. Note that, all occupation numbers must be specified, that is occupation numbers for both occupied and virtual sets of molecular orbitals built from a specific atomic orbital basis set. For all considered atomic systems, the electronic configurations of the individual states included in the PPLB ensembles were chosen in accordance with the Aufbau principle and the known spin multiplicity of the states [1, 40].

Table 4.1: Electronic configurations of the individual states of the left PPLB biensemble mimicking the removal of a spin-up electron from the electronic configuration of the lithium ground state. Only the occupation numbers of the six lowest molecular orbitals of each spin channel are depicted.

State of the ensemble	Weight	Spin	Occupation numbers					
1	$1 - \alpha$	\uparrow	1	1	0	0	0	0
		\downarrow	1	0	0	0	0	0
2	α	\uparrow	1	0	0	0	0	0
		\downarrow	1	0	0	0	0	0

Table 4.2: Electronic configurations of the individual states of the right PPLB biensemble mimicking the addition of a spin-down electron to the electronic configuration of the lithium ground state. Only the occupation numbers of the six lowest molecular orbitals of each spin channel are depicted.

State of the ensemble	Weight	Spin	Occupation numbers					
1	$1 - \alpha$	\uparrow	1	1	0	0	0	0
		\downarrow	1	0	0	0	0	0
2	α	\uparrow	1	1	0	0	0	0
		\downarrow	1	1	0	0	0	0

4.3.2 With Weight-Independent xc-Functionals

We have performed PPLB ensemble density-functional theory calculations to study the behavior of a simple open system, the lithium atom, when we continuously vary its total number of electrons within the range $\mathcal{N} \in [0; 4]$. We did these calculations using both unrestricted Hartree-Fock and spin density-functional theory methods, within different range of standard weight-independent exchange-correlation functionals, in order to present a global overview of how standard ab initio methods, originally designed and widely used for pure-state (ground-state) applications, perform when extended to ensemble frameworks.

We have successively removed/added an electron from/to the lithium atom and its cationic and anionic counterparts in their ground-state configurations in order to plot the variation of the total energy $E^{\mathcal{N}} \equiv E^{\alpha}$ of such an open system with respect to the fractional number of electrons $\mathcal{N} \equiv N \pm \alpha$, with $N \in \llbracket 0, 4 \rrbracket$.

In the exact theory, for a fixed integral number N , the plot of the exact ensemble energy, depicted in the range $\mathcal{N} \in]N - 1, N]$, must be linear and its slope must be identical to the ionization potential of the N -electron system, I_0^N , or equivalently the electron affinity of the $(N - 1)$ -electron system, such that

$$I_0^N \equiv A_0^{N-1}. \quad (4.123)$$

Similarly, in the range $\mathcal{N} \in]N, N + 1]$, the exact ensemble energy must also be linear but with a different slope which must be identical to the electron affinity of the N -electron system, A_0^N , also equivalent to the ionization potential of the $(N + 1)$ -electron system,

$$A_0^N \equiv I_0^{N+1}. \quad (4.124)$$

As discussed in the introduction, the costs in energy for the removal and the addition of an electron from/to the ground state of a neutral system are different. Hence, the exact ensemble energy $E^{\mathcal{N}}$ of an open system must be piecewise linear with respect to the variation of the number of electrons \mathcal{N} .

Perdew, Parr, Levy and Balduz have derived two fundamental exact properties that an in-principle-exact theory, such as Kohn-Sham DFT, must obey when applied to an open system

- The exact total-energy curve with respect to the number of electrons of the open system, $E^{\mathcal{N}}(\mathcal{N})$, must consist of a series of straight lines between integral electron numbers N .
- When crossing an integral number of electrons, the exact exchange-correlation potential must experience a “jump”, known as the “derivative discontinuity”, Δ_{xc} .

These two exact constraints are in fact intrinsically connected and violation of one shall cause immediate consequences on the other, as we shall see in this work.

Indeed, using an approximate exchange-correlation functional that lacks a derivative discontinuity will result in deviation from the piecewise linearity exact condition for the total energy. For that reason, designing functionals that possess a derivative discontinuity property can help to restore the piecewise linear behavior of the total energy.

It is interesting to note that these considerations are not specific to the PPLB-DFT framework, but are rather general observations that remain valid within the scope of many quantum-chemistry methods, such as Hartree-Fock theory, standard Kohn-Sham DFT and generalized Kohn-Sham (GKS) DFT, among others.

As a consequence, if an approximate functional does not possess a derivative discontinuity, it may yield erroneous predictions when describing real phenomena such as dissociation or charge-transfer processes, and result in significant errors, like the infamous localization and delocalization errors, for instance.

Piecewise linearity of the energy

First, let us verify the capability of standard methods and functionals to behave in accordance with the “piecewise linearity” exact requirement for the energy, as depicted in Figure E.1.

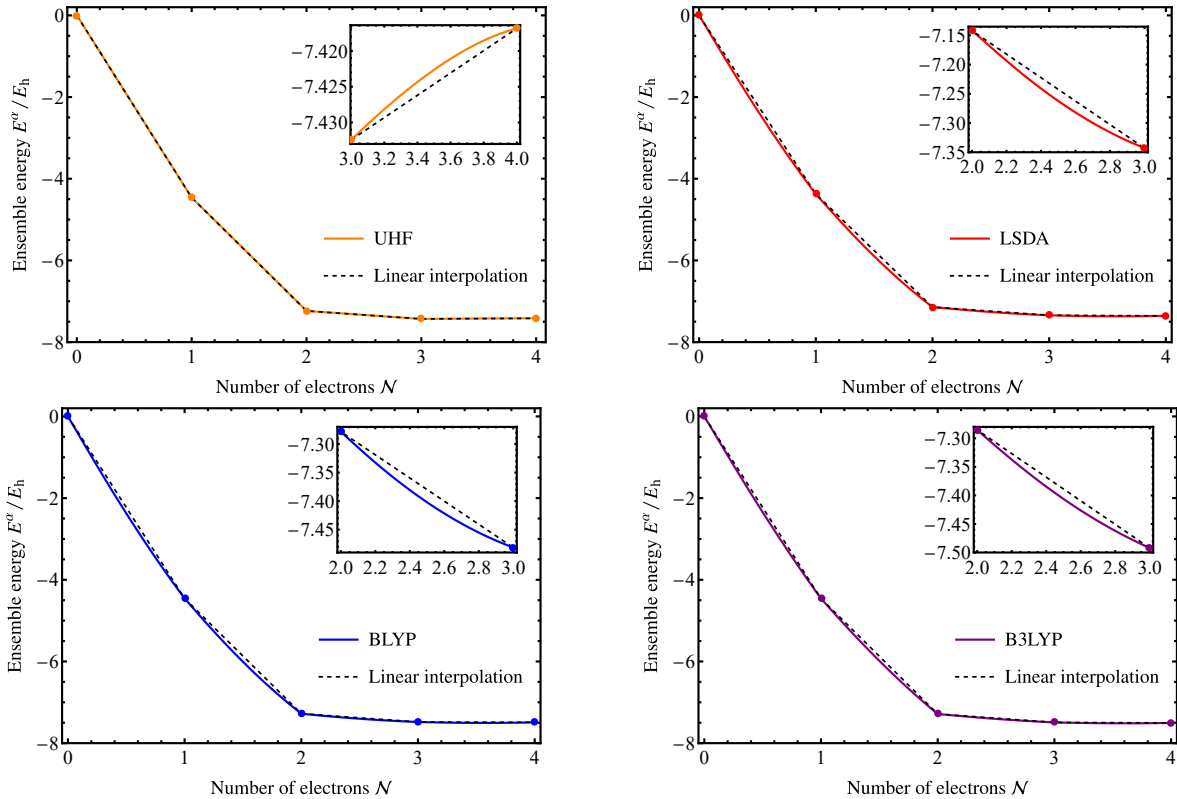


Figure 4.2: Violation of the piecewise-linearity criterion of the PPLB ensemble energy of Li with respect to the number of electrons of the open system with various methods and xc-functionals, in the cc-pVDZ basis. PPLB ensemble energies are compared to the corresponding linear-interpolation energies defined with the same methods and functionals, between the corresponding pure-state energies (dots).

Hartree-Fock energy is known to depict a concave behaviour, that is to say a positive curvature (see Table 4.3), which means that fractional configurations of the open system will be given a greater energy than integral configurations and, thus, will be less energetically favourable. To illustrate this point, let us consider a simple dimer with a total number of electrons $(2N+1)$, where N is an integer. We would like to know which electronic distribution of such a system would be favored by a concave energy function, such as Hartree-Fock energy. To do so, let us recall the following mathematical property that any midpoint-concave function f must obey

$$f\left(\frac{x_1 + x_2}{2}\right) \geq \frac{f(x_1) + f(x_2)}{2}, \quad (4.125)$$

where x_1 and x_2 are basic variables of the function f .

In the present work, the function of interest depicts the variation of the total energy of an open system with respect to the variation of its number of electrons \mathcal{N} . Therefore, if one applies the previous concave property to $E(\mathcal{N})$, with $x_1 = N$ and $x_2 = N + 1$, one obtains

the following condition for the energy of the open system

$$2E\left(N + \frac{1}{2}\right) \geq E(N) + E(N + 1). \quad (4.126)$$

This means that, in the Hartree-Fock formalism, the dimer that we have considered to illustrate our point would be less energetically stable if the two sites were open systems with fractional number of electrons ($N + \frac{1}{2}$), than if they were closed systems with respective integral number of electrons N and $N + 1$.

Hence, in an Hartree-Fock calculation, the delocalization of the charge will raise the energy of the system. Such functionals that tend to favor too localized charge distributions over much delocalized ones are associated with “localization errors”.

Conversely, commonly-used DFA functionals are known to deviate from the piecewise linearity exact condition with negative curvatures, thus, yielding convex energy curves. If one applies the previous reasoning to a convex energy, one obtains the following property

$$2E\left(N + \frac{1}{2}\right) \leq E(N) + E(N + 1), \quad (4.127)$$

which states that, in that case, fractional configurations, that is to say delocalized charge distributions, will be given a lower, and thus more stable, energy than integral configurations, or pure states. These observations have led to the concept of “fractional-charge error” or “delocalization error” which is a direct consequence of the negative deviation of the approximate energy of an open system from the piecewise-linear exact energy.

Fractional charges are not, at first, real phenomena but can arise from dissociation processes of real systems [14], such as stretched molecules where the electron density will delocalize over all dissociated fragments and may cause significant errors throughout binding curves in their dissociation limits, exhibiting too low or too high predictions for binding energies. Fractional charge is not specific to atoms and molecules but is a more general problem that may arise from any delocalized charge distribution. Indeed, the inability of commonly-used approximate functionals to properly predict the energy for fractional charges in small finite systems will lead to significant systematic errors in the prediction of properties of larger systems, like larger molecules or solid state materials [61]. For instance, poor description of fractional charges may have major implications on band-gap predictions. Evaluating the performance and limitations of approximate functionals when applied to fictitious systems, such as fractionally charged systems, can help to better apprehend their physical consequences on real systems.

To confirm these general observations regarding Hartree-Fock’s and Kohn-Sham DFT standard functionals’ performances, we have applied the PPLB ensemble DFT framework to a small benchmark of small simple atomic systems, mainly composed of the atoms of the first two rows of the periodic table, in addition to the first three noble gas (see Table 4.3). For these systems, we have estimated the curvature of the PPLB ensemble energy in two situations, the “left” PPLB framework depicting the response of the neutral N -electron system in

its ground-state configuration when we remove an electron from its highest occupied orbital, and the “right” PPLB framework depicting the response of the neutral N -electron system in its ground-state configuration when we add a new electron in its lowest unoccupied orbital. The curvature of the PPLB ensemble energies were estimated by applying the trapezoidal rule in order to estimate the area between the non-linear PPLB ensemble-energy curves and their linear interpolations.

As you can see in Table 4.3, Hartree-Fock method provides a positive curvature, and thus a concave ensemble energy, for all considered systems and for both removal and addition processes, whereas the local, semi-local and hybrid density-functional approximations (DFAs) provide a negative curvature, and thus a convex ensemble energy, in all cases. It seems that the curvature of the ensemble energy of the open system tends to diminish when the number of electrons increases, and the results seem to show that of all considered DFAs, the hybrid B3LYP functional appears to be the one that depicts a total energy with the less deviation from the piecewise linearity exact criterion, confirming somehow its recognized supremacy over other DFAs, just like in standard ground-state DFT.

Table 4.3: Estimation of the curvature of the “left” and “right” PPLB ensemble energies obtained by computing the area, using the trapezoidal rule, between the curves of the ensemble energy and the corresponding linear interpolation between the individual pure state energies of the $(N - 1)$ -, N - and $(N + 1)$ -electron systems. The calculations were performed in Dunning’s correlation-consistent cc-pVDZ basis set, using different range of exchange-correlation approximations. The blanks correspond to calculations that did not converge throughout the whole removal/addition process.

	Removal: $N \rightarrow N - 1$				Addition: $N \rightarrow N + 1$			
	UHF	LSDA	BLYP	B3LYP	UHF	LSDA	BLYP	B3LYP
H	0.000	-13.611	-14.480	-11.235	0.897	-5.606	-5.490	-4.242
He	0.323	-2.208	-2.211	-1.727	0.296	-2.152	-2.041	-1.560
Li	0.000	-0.179	-0.199	-0.155	0.017	-0.157	-0.159	-0.126
Be	0.012	-0.145	-0.147	-0.118	0.013	-0.120	-0.119	-0.092
B	0.012	-0.120	-0.119	-0.092	0.017	-	-0.093	-0.071
C	0.015	-0.093	-0.093	-0.071	0.017	-	-0.077	-0.059
N	0.015	-	-0.076	-0.058	0.015	-0.063	-0.063	-0.047
O	0.014	-0.059	-0.058	-0.032	0.015	-	-0.053	-0.039
F	0.014	-	-0.049	-0.037	0.014	-	-0.045	-
Ne	0.013	-	-0.043	-0.032	-	-	-0.032	-0.024
Ar	0.001	-	-	-0.005	0.000	-	-0.004	-0.003
Mean	0.038	-2.345	-1.747	-1.232	0.130	-1.619	-0.743	-0.626

The curvature of the PPLB ensemble energy can be explained by the intrinsic nature of the functional used to predict the total energy of the open system. Indeed, many approximate functionals have been designed to compensate the practical void stemming from the elusive nature of the exact functional, and, although those functionals can have various analytical forms, can be functionals of different quantities (orbitals, electron density, Green’s function,

...) or have different characteristics (non-local, local, semi-local, ...), the large majority of those functionals happens to be non-linear with respect to the quantity they are applied to. Indeed, if one considers the Slater (or Dirac) exchange functional already mentioned in Chapter 3, one can see that this particular functional of the electron density is highly non-linear with respect to the electron density to which it must be applied.

Let us briefly recall the definition of a linear density functional. A linear functional, when applied to a linear combination of electron densities, must yield the exact same result that it would have yielded if one had first applied it to individual electron densities, and then built a linear combination of these results as follows

$$E[an_1 + bn_2] = aE[n_1] + bE[n_2], \quad (4.128)$$

where a and b are real coefficients, and $n_1(\mathbf{r})$ and $n_2(\mathbf{r})$ are individual electron densities. When one performs ensemble DFT (eDFT), the primary quantity required to compute the ensemble energy is the corresponding ensemble density and is, by construction, a linear combination of individual electron densities. Explicit functionals of ensemble densities have not been elaborated to this day, but one can still benefit from decades of development that have been devoted to the design and the elaboration of many density functionals within the scope of standard Kohn-Sham DFT. For that reason, one can choose to apply standard density functionals directly to ensemble densities instead.

However, because of the non-linear nature of most approximate functionals, such a procedure will result in significant errors as we shall see. Indeed, if one considers the left PPLB ensemble density, defined previously, and applies a non-linear functional to it according to the following equation, one obtains the following ensemble energy

$$E[n^\alpha] \equiv E\left[(1 - \alpha)n_0^N(\mathbf{r}) + \alpha n_0^{N-1}(\mathbf{r})\right] = E^\alpha. \quad (4.129)$$

On the other hand, if one chooses to perform multiple standard ground-state DFT calculations by applying this same functional to the individual densities, included in the PPLB ensemble density, in order to build in a second step a linear combination of these individual energies, one would obtain the following energy

$$(1 - \alpha)E[n_0^N] + \alpha E[n_0^{N-1}] = (1 - \alpha)E_0^N + \alpha E_0^{N-1} = E_0^\alpha. \quad (4.130)$$

Note that, while equation (4.129) depicts the result of an ensemble DFT calculation, equation (4.130) is provided exclusively by multiple standard ground-state DFT calculations and therefore should be perfectly linear with respect to the weight of the linear combination, α . The fact is that, because of the non-linearity of the approximate density functional, these two procedures will not yield the same energy [14] and will be responsible for the deviation of the PPLB ensemble energy from the piecewise-linearity exact requirement.

We would like to draw attention on the particular weight configurations, $\alpha = 0$ and $\alpha = 1$, for which the corresponding PPLB ensemble densities simply reduce to the ground-state electron densities of the N - and $(N - 1)$ -electron systems, respectively. In these two situations, the non-linearity of the approximate functional is no longer a problem and the two

above-mentioned procedures become identical and reduce to standard ground-state DFT calculations.

Furthermore, we would like to point out that these considerations about the non-linearity of approximate functionals are not specific to DFT, nor to PPLB (ensemble) DFT, but remain valid and have shown to have significant impact for many quantum chemistry methods, and other ensemble formalisms, as we shall see in upcoming chapters.

Another way to understand the origin of the wrong description of fractional charges by approximate functionals is to make an analogy with the concept of “self-interaction error” that occurs in standard Kohn-Sham DFT and Hartree-Fock theory. Recall that for one-electron systems, the Fock exchange functional is referred to as “exact exchange” because it exactly cancels out the unphysical spurious interaction resulting from the fact that the classical Hartree functional allows a given electron to interact with itself. For that reason, one of the exact criteria to enforce on any approximate exchange functionals should be its ability to compensate the additional contribution to the total energy of a one-electron system, stemming from the self-interaction error inherent to the classical Hartree functional. Unfortunately, in practice, it is far from trivial to design such approximate exchange functionals. As a matter of fact, the concept of self-interaction error has been generalized to many-electron systems, under the name “many-electron self-interaction error” [62], in order to point out the fact that approximate exchange functionals could still be exact for one-electron systems but yet fail to cancel out the self-interaction error additional terms for many-electron systems. In ensemble DFT, an intuitive way to proceed would be to apply standard DFT functionals to the ensemble density built as a linear combination of several individual electron densities. To illustrate this point, we apply the Hartree functional to the previously-defined left PPLB ensemble density, and it is straightforward to see that such a construction will inexorably result in additional artificial terms resulting from the unphysical interaction between the individual densities of the ensemble.

$$\begin{aligned}
 E_{\text{H}}[n^\alpha] &= \frac{1}{2} \iint \frac{n^\alpha(\mathbf{r}_1)n^\alpha(\mathbf{r}_2)}{|\mathbf{r}_1 - \mathbf{r}_2|} d\mathbf{r}_1 d\mathbf{r}_2 \\
 &= \frac{1}{2} \iint \frac{\left[(1 - \alpha)n_0^N(\mathbf{r}_1) + \alpha n_0^{N-1}(\mathbf{r}_1) \right] \left[(1 - \alpha)n_0^N(\mathbf{r}_2) + \alpha n_0^{N-1}(\mathbf{r}_2) \right]}{|\mathbf{r}_1 - \mathbf{r}_2|} d\mathbf{r}_1 d\mathbf{r}_2 \quad (4.131) \\
 &= (1 - \alpha)^2 E_{\text{H}}[n_0^N] + \alpha^2 E_{\text{H}}[n_0^{N-1}] + \alpha(1 - \alpha) \iint \frac{n_0^N(\mathbf{r}_1)n_0^{N-1}(\mathbf{r}_2)}{|\mathbf{r}_1 - \mathbf{r}_2|} d\mathbf{r}_1 d\mathbf{r}_2 .
 \end{aligned}$$

Hence, we see that applying standard-DFT approximate functionals to an ensemble density not only results in a non-linear combination of the contribution of each individual densities included in the ensemble density (first two terms of equation (4.131)), but also yields additional terms which correspond to spurious unphysical interactions between these individual

densities. Note that, in addition to the explicit quadratic weight-dependency of the ensemble Hartree energy, there is also an implicit weight-dependency of the individual densities due to the weight-dependency of the orbitals from which they are built.

As a consequence, standard-DFT approximate functionals may give rise to additional sources of errors when used in an ensemble framework compared to their behaviour within the scope of standard Kohn-Sham DFT and Hartree-Fock theory. Furthermore, these additional erroneous features may have significant impact on the relevance of using ensemble quantities to extract physical properties as we shall see.

Derivative discontinuity and physical meaning of the frontier orbital energies

We will now analyse the impact that a non-piecewise-linear energy may have on the behaviour and physical relevance of Kohn-Sham and Hartree-Fock orbitals, and more especially on the frontier orbitals, that is to say the HOMO and LUMO, of the neutral N -electron system [46].

In our attempt to study and understand the impact that the curvature of the energy of an open system may have on the prediction of ionization potentials, electron affinities and, by extension, fundamental gaps, we must go back to the definition of the chemical potential expressed in terms of the slope of the total energy with respect to the number of electrons of the system. From this definition, one obtains that the ionization potential I_0^N is the constant slope of the energy curve $E^{\mathcal{N}}(\mathcal{N})$ in the range $\mathcal{N} \in [N - 1; N]$, whereas the electron affinity A_0^N is the constant slope of the energy curve in the range $\mathcal{N} \in [N; N + 1]$. Note that the electron affinity of the N -electron system is identical to the ionization potential of the $(N + 1)$ -electron system

$$A_0^N \equiv I_0^{N+1} . \quad (4.132)$$

Since ionization potentials and electron affinities have distinct values, the slope of $E^{\mathcal{N}}(\mathcal{N})$ must change discontinuously when \mathcal{N} crosses an integral value N from left to right.

On the left side of the energy curve, that is to say, for $\mathcal{N} \in]N - 1; N]$, the highest occupied molecular orbital of the open system is the N th Kohn-Sham orbital with a fractional occupation number $(1 - \alpha)$, and the HOMO energy is then $\varepsilon_N^{\mathcal{N}}$ and must be constant and equal to the opposite of the ionization potential of the N -electron system, in accordance with both the IP theorem and Janak's theorem

$$\varepsilon_N^{\mathcal{N}} = \frac{dE^{\mathcal{N}}}{d(1 - \alpha)} = -\frac{dE^{\mathcal{N}}}{d\alpha} = \frac{dE^{\mathcal{N}}}{d\mathcal{N}} = E_0^N - E_0^{N+1} \equiv -I_0^N . \quad (4.133)$$

Note that, when $\mathcal{N} = N - 1$, the HOMO of the open system is no longer the N th orbital, but becomes the $(N - 1)$ th orbital instead and does not approximate I_0^N anymore, but I_0^{N-1} instead. Nevertheless, in that particular case, it is still the N th orbital energy that must be interpreted as I_0^N .

Similarly, on the right side of the energy curve, that is, for $\mathcal{N} \in]N; N + 1]$, the HOMO of the open system is the $(N + 1)$ th Kohn-Sham orbital with fractional occupation number

α and energy $\varepsilon_{N+1}^{\mathcal{N}}$, which must as well be constant and equal to the opposite of the electron affinity of the N -electron system, A_0^N , such that

$$\varepsilon_{N+1}^{\mathcal{N}} = \frac{dE^{\mathcal{N}}}{d\alpha} = \frac{dE^{\mathcal{N}}}{d\mathcal{N}} = E_0^{N+1} - E_0^N \equiv -A_0^N. \quad (4.134)$$

Note that, when $\mathcal{N} = N$, the HOMO of the open system changes and becomes the N th orbital and is no longer an approximation for $-A_0^N$, instead it is still ε_{N+1}^N , which becomes the LUMO energy, that must approximate $-A_0^N$.

Thus, we see that the variation of the exact HOMO of a \mathcal{N} -electron system with respect to \mathcal{N} must be a piecewise-constant function, and each step must match the successive ionization potentials and electron affinities defined for each integral number of electrons N .

We would like to add that, in ensemble DFT, one must be cautious when using ‘‘HOMO’’ and ‘‘LUMO’’ terminologies in the context of using ensemble quantities to approximate real properties, like ionization potentials and electron affinities, of a given real pure-state system. Indeed, in ensemble DFT, the orbitals are optimized with respect to the whole ensemble, with fractional number of electrons \mathcal{N} , and not to the real N -electron system of whom we want to predict real physical properties, such as ionization potentials and electron affinities.

The fact is that, even in the exact theory [12], the LUMO of the N -electron system, ε_{N+1}^N , is not the HOMO of the $(N + 1)$ -electron system, ε_{N+1}^{N+1} ,

$$\lim_{\mathcal{N} \rightarrow N^-} \left(\varepsilon_{N+1}^{\mathcal{N}} \right) \neq \lim_{\mathcal{N} \rightarrow N^+} \left(\varepsilon_{N+1}^{\mathcal{N}} \right). \quad (4.135)$$

As a matter of fact, when crossing an integral number of electrons N , the exact Kohn-Sham potential must experience a discontinuity, known as the ‘‘derivative discontinuity’’ [81], Δ_{xc} , and this ‘‘jump’’ must be passed on to the frontier orbitals of the N -electron system, that is, the HOMO and LUMO, thus affecting the physical interpretation of the Kohn-Sham frontier orbital energies.

Indeed, when crossing an integral number of electrons N from the left to the right, because of the multiplicative nature of the exact Kohn-Sham potential, applying a constant shift to the exact Kohn-Sham potential will result for all the Kohn-Sham eigenvalues to jump by the same quantity. Note that, conversely, the Kohn-Sham orbitals will remain unchanged by this jump-in-potential. Hence, in the exact theory, an exact Kohn-Sham DFT calculation, at fixed integral number N , must yield HOMO and LUMO energies that verify

$$\begin{cases} \varepsilon_{\text{HOMO}}^N & \equiv \varepsilon_N^N = -I_0^N \\ \varepsilon_{\text{LUMO}}^N + \Delta_{xc} & \equiv \varepsilon_{N+1}^N + \Delta_{xc} = -A_0^N. \end{cases} \quad (4.136)$$

Consequently, the exact Kohn-Sham HOMO-LUMO gap of the N -electron system can be connected to its fundamental gap as follows

$$\varepsilon_{\text{LUMO}}^N - \varepsilon_{\text{HOMO}}^N + \Delta_{xc} \equiv \varepsilon_{N+1}^N - \varepsilon_N^N + \Delta_{xc} = I_0^N - A_0^N, \quad (4.137)$$

where I_0^N , and A_0^N are obtained by total-energy differences from exact Kohn-Sham DFT individual self-consistent calculations for the N -, $(N - 1)$ - and $(N + 1)$ -electron ground-state energies (Δ SCF method).

Hence, due to the derivative discontinuity, the HOMO and LUMO energies of a single, even exact, Kohn-Sham DFT calculation cannot be simultaneously interpreted as the opposite of the ionization potential and electron affinity of a N -electron system, respectively. This is known as the “fundamental gap problem”.

As a matter of fact, most of commonly used approximate exchange-correlation functionals are known to lack a derivative discontinuity, and it has been proved that local and semi-local functionals, such as LSDA and GGAs functionals, simply do not allow for such a derivative discontinuity because of their intrinsic analytical nature [81].

Indeed, since the Kohn-Sham electron density is continuous across an integral number of electrons N , and since most of standard local and semi-local approximate exchange-correlation potentials are continuous functions of the electron density and its gradient, it is straightforward that such approximate Kohn-Sham potentials are unable to exhibit such a discontinuity [45]. Nevertheless, standard DFAS can still be used as starting point in the design and the elaboration of new functionals, which could naturally inherit a derivative discontinuity through additional corrections, or ensemble generalizations [50].

In the present discussion, we would like to take the opportunity to highlight a substantial distinction between a characteristic of the exact Kohn-Sham potential defined for a system with a fractional number of electrons \mathcal{N} and its alter-ego for integral number N . Early studies have proved that, for an open system, the exact Kohn-Sham potential was well-defined whereas, for a system with integral number of electrons N , it was only defined up to a constant [68, 64]. The latter point can be understood by considering that reaching the integer point N from the left and from the right would correspond to different calculations, describing different open systems, $\mathcal{N} \in [N - 1, N]$ and $\mathcal{N} \in [N, N + 1]$, and then associated with different exact Kohn-Sham potentials.

In practice, Hartree-Fock’s HOMO and LUMO are known to have too low and too high energies, respectively, yielding overestimated and underestimated ionization potential and electron affinity predictions, compared to the Δ SCF results (see Table 4.4).

Conversely, standard exchange-correlation density-functional approximations (DFAs) are known to yield HOMO and LUMO energies that underestimate and overestimate the ionization potential and the electron affinity of the neutral N -electron system, respectively. One can see in Table 4.4, that standard DFAs yield LUMO energies that give very poor predictions for the electron affinity and fail to reproduce the corresponding Δ SCF references.

Note that all these methods yield frontier orbital energies with different-sign errors such that they can still benefit from error cancellation, and manage to yield “acceptable” predictions

for fundamental gaps. Nevertheless, DFAs are known to yield very small Kohn-Sham gaps.

Table 4.4: Comparison between the unrestricted Hartree-Fock and Kohn-Sham HOMO and LUMO energies obtained from a single ground-state DFT calculation for Li, using various range of exchange-correlation functionals in the cc-pVDZ basis set. The Δ notations refer to relative errors between the quantity in the line above and the corresponding Δ SCF property.

	UHF	LSDA	BLYP	B3LYP	Experiment ¹
Δ SCF I_0	0.196 31	0.200 87	0.202 95	0.206 61	0.198 14
$-\varepsilon_N$	0.196 32	0.116 78	0.112 10	0.134 66	-
Δ (%)	0.005	-41.862	-44.759	-34.824	-
Δ SCF A_0	-0.015 58	0.013 79	0.008 70	0.013 11	0.022 71
$-\varepsilon_{N+1}$	-0.022 45	0.077 49	0.056 06	0.057 35	-
Δ (%)	-44.094	461.856	544.367	337.452	-
Δ SCF $I_0 - A_0$	0.211 89	0.187 07	0.194 25	0.193 49	0.175 43
$\varepsilon_{N+1} - \varepsilon_N$	0.218 77	0.039 28	0.056 04	0.077 30	-
Δ (%)	3.246	-79.002	-71.150	-60.049	-

¹ Ref. [19]

If one performs PPLB ensemble DFT calculations and continuously varies the ensemble weight α , or charge deviation, one will observe that the weight-dependent Kohn-Sham orbital energies and more especially, the frontier orbital energies of the N -electron system, will significantly deviate from the piecewise-constant feature dictated by the exact theory. As a consequence, the variation of the HOMO energy of the N -electron system with respect to the variation of the number of electrons \mathcal{N} , will not depict a “piecewise-constant” behaviour as depicted in Figure E.2.

The positive curvature of the unrestricted Hartree-Fock energy (see Table 4.3 and Figure 4.4) will cause a negative deviation of the HOMO energy, that is to say that the HOMO energy will be lower than the opposite of the Δ SCF ionization potential that it is supposed to mimic, whereas the negative curvature of DFA functionals will cause a positive deviation of the HOMO energy, yielding too low ionization potentials. Therefore, to what extent the HOMO and LUMO energies of a N -electron system approximate ionization potentials and electron affinities depends on how well the functional respects the piecewise-linearity exact constraint for the total ensemble energy of the open system [46].

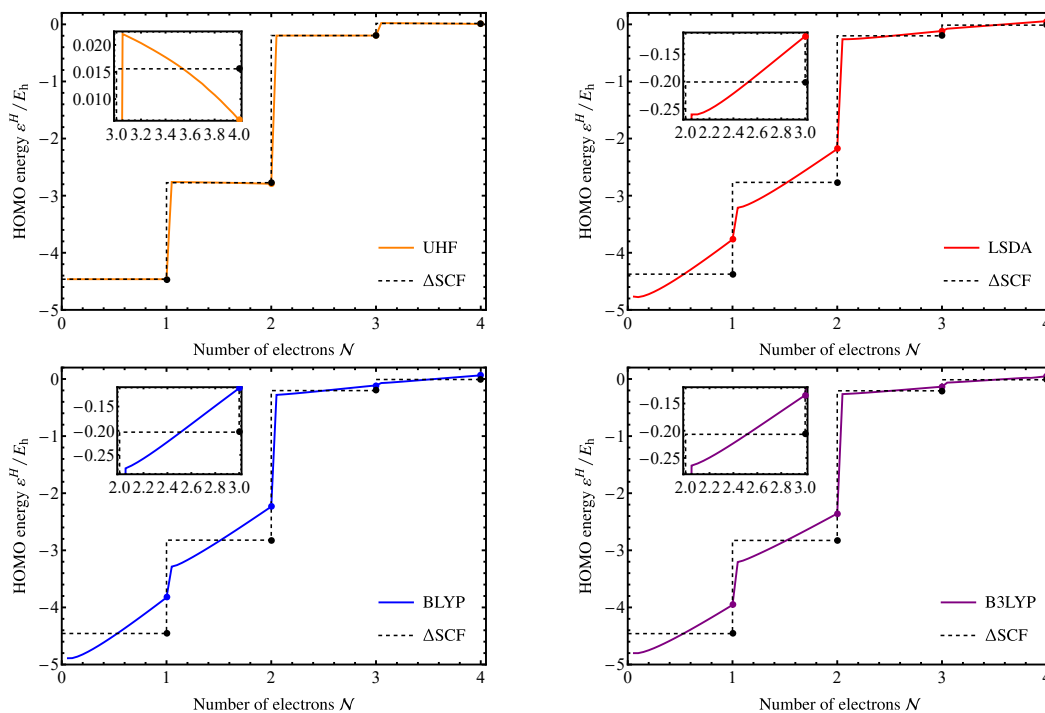


Figure 4.3: Violation of the piecewise-constant feature of the HOMO energy of Li with respect to the number of electrons N , using various methods and levels of xc-approximation, in the cc-pVDZ basis. The weight-dependent HF/KS orbital energies are compared to the opposite of the corresponding ionization potentials and electron affinities obtained by total energy differences (Δ SCF) between successive pure-state energies.

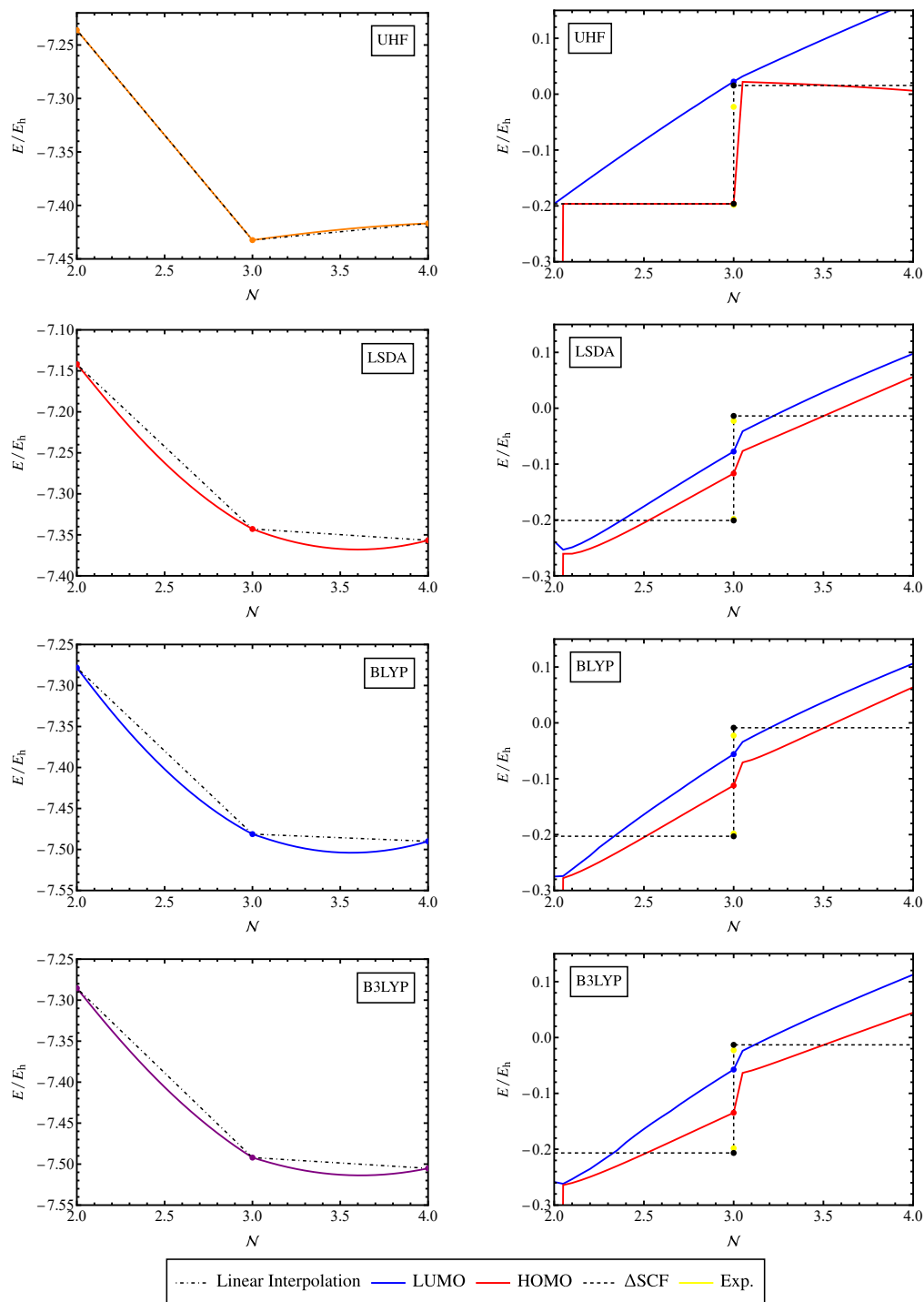


Figure 4.4: Impact of the violation of the piecewise-linearity exact condition of the total energy of an open system on the physical relevance of the Hartree-Fock/Kohn-Sham gap. Calculations were performed on Li in the cc-pVDZ basis within different levels of approximation. A parallel is drawn between the curvature of the total energy of the open system (left panel) and the inability of the HF/KS HOMO-LUMO gap (right panel) to reproduce the fundamental gap of the system, obtained by total-energy differences within the same level of approximation (ΔSCF method). The experimental fundamental gap of Li is also reported for comparison (see Appendix A).

Weight-dependent orbitals

One practical advantage of ensemble DFT is to allow for the extraction of physical properties of an electronic system, like excitation energies for instance, from a single calculation, as opposed to the standard scheme that would normally require multiple DFT calculations.

Until now, we have only considered two-state ensembles to illustrate the theory, since such ensembles can be seen like transient states between the two physical states included in the ensemble. If one was to consider a larger ensemble, including many more physical excited states, or ensembles with different weights, it would probably be less obvious to retain physical meaning within the total ensemble energy.

When performing ensemble DFT calculations, one has to keep in mind that, unlike in standard ground-state DFT where the set of orbitals, that will be used to build the ground-state electron density of the system and compute its total ground-state energy, is optimized with respect to a single physical state (the ground state), in ensemble DFT, the set of weight-dependent orbitals will be optimized with respect to the whole ensemble. This means that, for any given weight-configuration, the optimal set of ensemble orbitals that minimizes the total ensemble energy is not expected to match the minimizing set of orbitals of one specific individual state of the ensemble.

When variationally optimized, the set of ensemble orbitals will be associated with specific sets of integral occupation-numbers in order to rebuild each individual state of the ensemble. Then, these individual states will be linearly combined, by use of the fixed set of ensemble weights, such that the ensemble density is recovered

$$n^\alpha(\mathbf{r}) = (1 - \alpha)n_0^{N,\alpha}(\mathbf{r}) + \alpha n_0^{N\pm 1,\alpha}(\mathbf{r}), \quad (4.138)$$

where the superscript “ α ” is used to highlight the fact that the individual densities included in the ensemble density are both built from the same weight-dependent set of variationally optimized orbitals. Hence, the individual states obtained from a single PPLB ensemble DFT calculation will not necessarily correspond to the true physical individual states that the ensemble is expected to be built on.

If one considers the so-called left and right PPLB ensembles defined in this chapter,

$$E^\alpha = E[n^\alpha(\mathbf{r})] = (1 - \alpha)E_0^{N,\alpha} + \alpha E_0^{N\pm 1,\alpha}, \quad (4.139)$$

only the two weight-configurations, $\alpha = 0$ and $\alpha = 1$, correspond to standard ground-state DFT calculations and must yield the exact set of weight-independent orbitals optimized relatively to the ground state of the neutral N -electron system (for $\alpha = 0$) and its anionic or cationic counterparts (for $\alpha = 1$), as illustrated in Figure 4.5. Any other weight-configuration will yield a set of weight-dependent orbitals, comprised between these two physical configurations. Note that, for two-state ensembles (or biensembles), the weight-configuration $\alpha = \frac{1}{2}$, referred to as “equi(bi)ensemble”, is of particular interest since, by construction, it doesn’t favor one individual state of the ensemble over the other and treats both equally, as well as the physical properties associated to these states,

$$E^{\alpha=\frac{1}{2}} = \frac{1}{2}E_0^{N,\alpha=\frac{1}{2}} + \frac{1}{2}E_0^{N\pm 1,\alpha=\frac{1}{2}}. \quad (4.140)$$

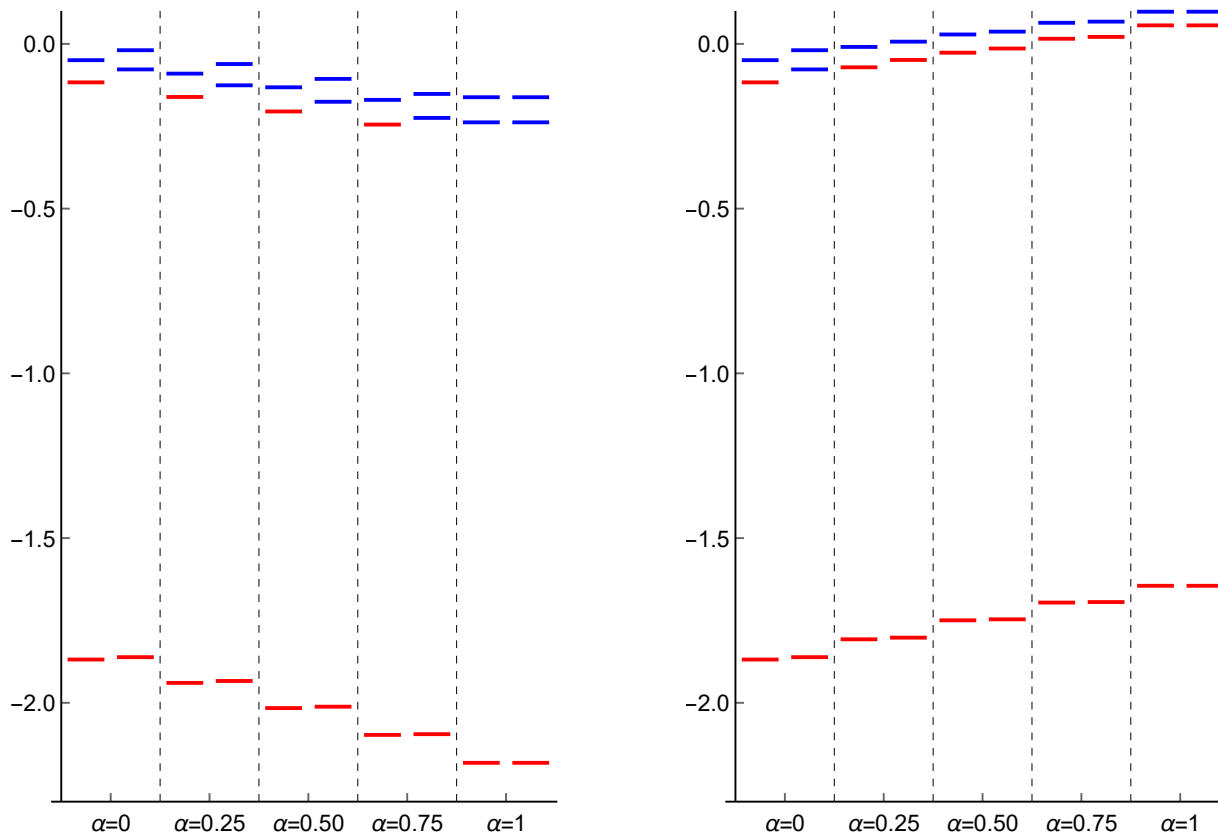


Figure 4.5: Variations of the three lowest occupied (red) and virtual (blue) spin-up (left channel) and spin-down (right channel) Kohn-Sham orbital energies with respect to the PPLB weight α when removing (left panel) a fraction α of the highest spin-up electron of Li and when adding (right panel) a fraction α of a spin-down electron to Li, using the LSDA xc-functional and cc-pVDZ basis.

In order to study the impact of the weight-dependency of the ensemble Kohn-Sham orbitals on the quality of the Kohn-Sham predictions for the ionization potential and the electron affinity of a system, we have performed left and right PPLB calculations for various atomic systems, in their ground-state configurations, and tried to quantify this impact by computing percent errors between the ensemble Kohn-Sham predictions and the corresponding Δ SCF results, within the same level of approximation. To do so, the ground-state electronic configurations of the neutral, anionic and cationic systems were defined in accordance with the Aufbau principle and the spin multiplicity available in the NIST Atomic Spectra Database [1]. Hence, left PPLB calculations were performed in order to extract ionization potentials (see equations (E.6)) whereas right PPLB calculations were performed to extract electron affinities (see equations (E.7)).

For a small charge deviation, the left and right PPLB eDFT predictions for the ionization potential and the electron affinity of the neutral systems considered do not match what one would obtain by performing total-energy differences with the Δ SCF method, as depicted in Table 4.5. Indeed, one can see that, for all systems considered in this work, unrestricted

Hartree-Fock left PPLB calculations yield predictions that overestimate the ionization potential of the system compared to the Δ SCF reference that one would obtain with the same level of approximation. Conversely, UHF right PPLB calculations yield underestimated predictions for the electron affinity. Note that the magnitude of the percent errors for the ionization potential and the electron affinity are significantly different in the same way as it is in standard ground-state Hartree-Fock calculations (see Table 4.4).

For standard weight-independent DFAs, the results are also in accordance with standard ground-state DFT observations and one can see that left PPLB calculations yield underestimated ionization potentials and considerably-overestimated electron affinities. Moreover, one can see that the hybrid xc-functional B3LYP is the DFA that exhibits the lesser deviation from its Δ SCF predictions.

Table 4.5: Percent errors of the weight-dependent Hartree-Fock/Kohn-Sham predictions for the ionization potential and electron affinity of simple atomic systems obtained from left and right PPLB biensemble calculations, respectively, compared to the Δ SCF references. The calculations were performed for a small charge deviation $\alpha = 0.05$ in both unrestricted Hartree-Fock and DFT frameworks with standard weight-independent xc-functionals in the cc-pVDZ basis set. The blanks correspond to calculations that did not converge.

	$\Delta(\%)$ Removal and addition at $\alpha = 0.05$							
	UHF		LSDA		BLYP		B3LYP	
	$-\varepsilon_N$	$-\varepsilon_{N+1}$	$-\varepsilon_N$	$-\varepsilon_{N+1}$	$-\varepsilon_N$	$-\varepsilon_{N+1}$	$-\varepsilon_N$	$-\varepsilon_{N+1}$
H	0.000	-41.765	-39.918	794.219	-41.434	691.558	-32.501	859.715
He	5.372	-2.636	-33.583	17.787	-33.445	17.996	-25.886	13.904
Li	0.005	-41.399	-37.476	455.329	-40.251	713.793	-31.242	382.837
Be	3.638	-21.529	-34.188	324.181	-35.161	267.414	-27.614	241.083
B	6.034	-71.016	-48.875	-	-49.257	738.726	-37.901	883.215
C	8.369	-535.667	-	-	-45.465	2755.613	-34.481	896.918
N	9.319	-34.870	-	275.905	-42.669	276.013	-32.053	219.715
O	14.616	-80.478	-33.286	-	-46.562	1055.969	-34.793	1086.863
F	14.099	-818.481	-	-	-42.252	664.854	-31.269	410.378
Ne	13.429	13.613	-	-	-39.114	14.163	-28.775	10.714
Mean	7.488	-163.422	-37.887	373.484	-41.561	719.609	-31.651	500.534

Similarly, Table 4.6 shows percent errors obtained for the “equibiensemble” weight-configuration, $\alpha = 0.5$, which equally mixes both ground states of the neutral system and its cationic or anionic form (see equation (4.140)).

It is worth noting that the equibiensemble calculations considerably improve the HF/KS predictions for the ionization potentials and electron affinities, compared to the predictions obtained for a small charge deviation in Table 4.5. Although the sign of the percent errors appears to be more erratic for that weight-configuration, we note that B3LYP remains the standard weight-independent DFA that exhibits the smallest deviation from its Δ SCF references.

Table 4.6: Percent errors of the weight-dependent Hartree-Fock/Kohn-Sham predictions for the ionization potential and electron affinity of simple atomic systems obtained from left and right PPLB biensemble calculations, respectively, compared to the Δ SCF references. The calculations were performed for the “equibiensemble” configuration, $\alpha = 0.5$, in both unrestricted Hartree-Fock and DFT frameworks with standard weight-independent xc-functionals in the cc-pVDZ basis set. The blanks correspond to calculations that did not converge.

	$\Delta(\%)$ Removal and addition at $\alpha = 0.5$							
	UHF		LSDA		BLYP		B3LYP	
	$-\varepsilon_N$	$-\varepsilon_{N+1}$	$-\varepsilon_N$	$-\varepsilon_{N+1}$	$-\varepsilon_N$	$-\varepsilon_{N+1}$	$-\varepsilon_N$	$-\varepsilon_{N+1}$
H	0.000	-2.951	2.594	27.967	1.943	20.360	1.757	19.367
He	-0.306	0.049	1.327	0.522	0.932	0.508	0.602	0.330
Li	0.000	-4.314	2.143	1.744	0.973	8.110	1.003	2.701
Be	-0.224	-0.512	0.396	1.545	0.251	-0.539	0.061	0.817
B	-0.001	-2.542	-0.578	-	-0.271	-0.176	-0.061	3.595
C	-0.288	-18.762	-	-	-0.080	3.437	0.029	3.956
N	-0.288	-2.123	-	1.259	-0.018	1.109	0.057	1.108
O	-0.726	-4.327	24.502	-	0.065	5.324	0.070	6.616
F	-0.590	-37.766	-	-	0.139	3.317	0.126	2.539
Ne	-0.478	16.129	-	-	0.145	0.183	0.133	0.108
Mean	-0.290	-5.711	5.064	6.607	0.407	4.163	0.377	4.113

Extraction of individual-state energies

In order to understand why PPLB equibiensembles seem to be the “optimal” weight-configuration which yields ionization potentials and electronic affinities most in line with those that one would obtain with standard ground-state DFT calculations, we will look more closely at the behaviour of the weight-dependent individual-state energies that one would obtain from left and right PPLB calculations (see equations (E.6) and (E.7)) and, more specifically, how they behave when we vary the PPLB weight α in the full range $[0; 1]$.

As one can see in Figure 4.6, in the zero-weight limit, $\alpha = 0$, the left PPLB calculation reduces to a standard ground-state DFT calculation for the ground-state of the neutral system, Li. Hence, the ensemble prediction for the ground-state energy of Li perfectly matches its standard ground-state DFT reference (black, dashed lines).

Conversely, this zero-weight configuration will result in the worst prediction for the ground-state energy of the cationic system, yielding an underestimated ground-state energy for Li^+ with maximum error, for all density-functional approximations. For this particular system, only unrestricted Hartree-Fock formalism seems to be able to yield both neutral and cationic ground-state energies with negligible errors, which was expected since we have seen that, for this system and level of approximation, the left PPLB ensemble energy has exhibited near-zero curvature.

As the PPLB weight increases, and thus the physical charge deviation, the left PPLB biensemble includes more and more of the cationic ground state, increasing the error for the

prediction of the ground-state energy of Li, and diminishing the error for the ground-state energy of Li^+ . Finally, when $\alpha = 1$, the left PPLB ensemble reduces to a standard ground-state DFT calculation but, this time, optimized for the description of the ground state of the cationic system Li^+ , thus yielding a prediction for its ground-state energy in total adequation with standard ground-state DFT calculations, and an underestimated ground-state energy of Li, with maximum error.

Note that the maximum errors of the ground-state energies of Li, obtained when $\alpha = 1$, and Li^+ , obtained when $\alpha = 0$, exhibit similar magnitudes, for all DFAs considered. Finally, we see that for the equibiensemble configuration, $\alpha = 0.5$, as expected, both individual states of the left PPLB ensemble are equally deteriorated and underestimated with respect to their standard DFT references.

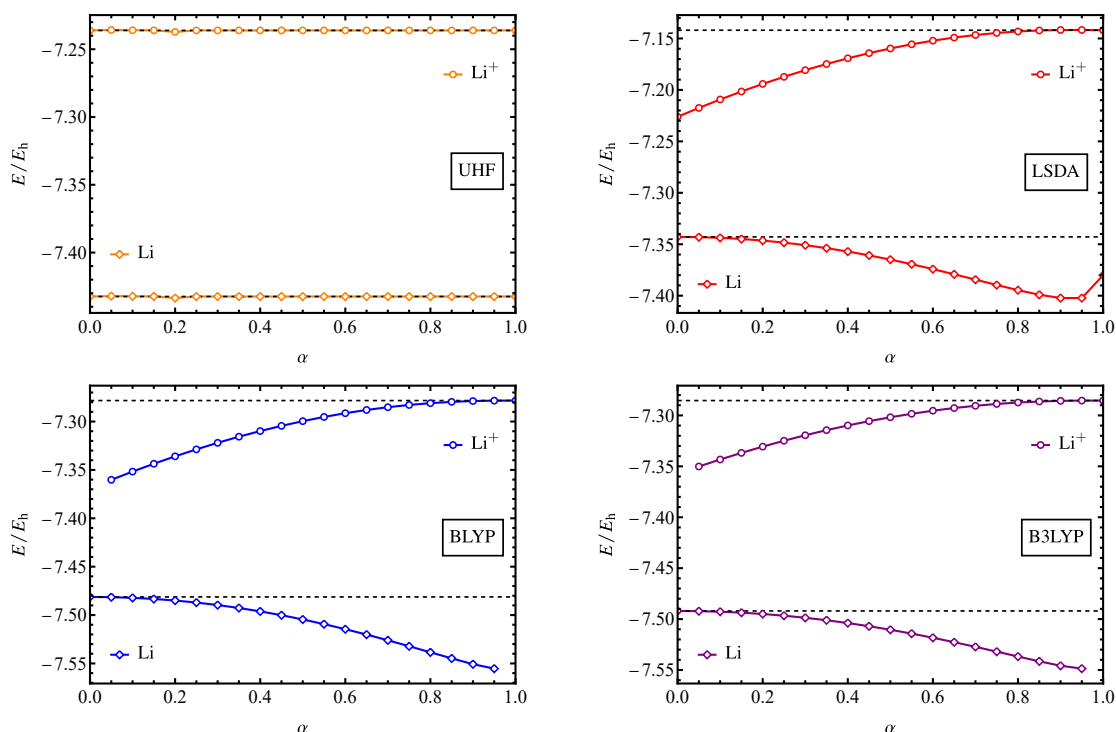


Figure 4.6: Variations of the weight-dependent individual states extracted from the left PPLB biensemble with respect to the physical charge deviation α . The weight-dependent ground-state energies of the neutral and cationic forms of the lithium atom are recovered by use of the variationally optimized ensemble orbitals as described in 4.3.2. Left PPLB calculations were performed with various xc-approximations, in the cc-pVDZ basis set. The black dashed lines correspond to the same individual states obtained from standard ground-state DFT calculations with the same level of approximation.

As a matter of fact, most of these observations remain applicable to right PPLB results, apart from a few subtleties. Indeed, one can see in Figure 4.7 that, similarly to left PPLB results, the maximum errors for the weight-dependent ground-state energies of Li and Li^- are of a similar magnitude. When increasing the weight, that is to say when adding a larger fraction of a new electron to the neutral system, the ensemble prediction for the ground-state

energy of Li starts to gradually deteriorate, whereas the prediction for the ground-state energy of Li^- is improved. Again, the equibiensemble configuration appears to be an acceptable compromise that equally takes into account both neutral and anionic ground states, yielding similar amount of errors for both ground-state energies.

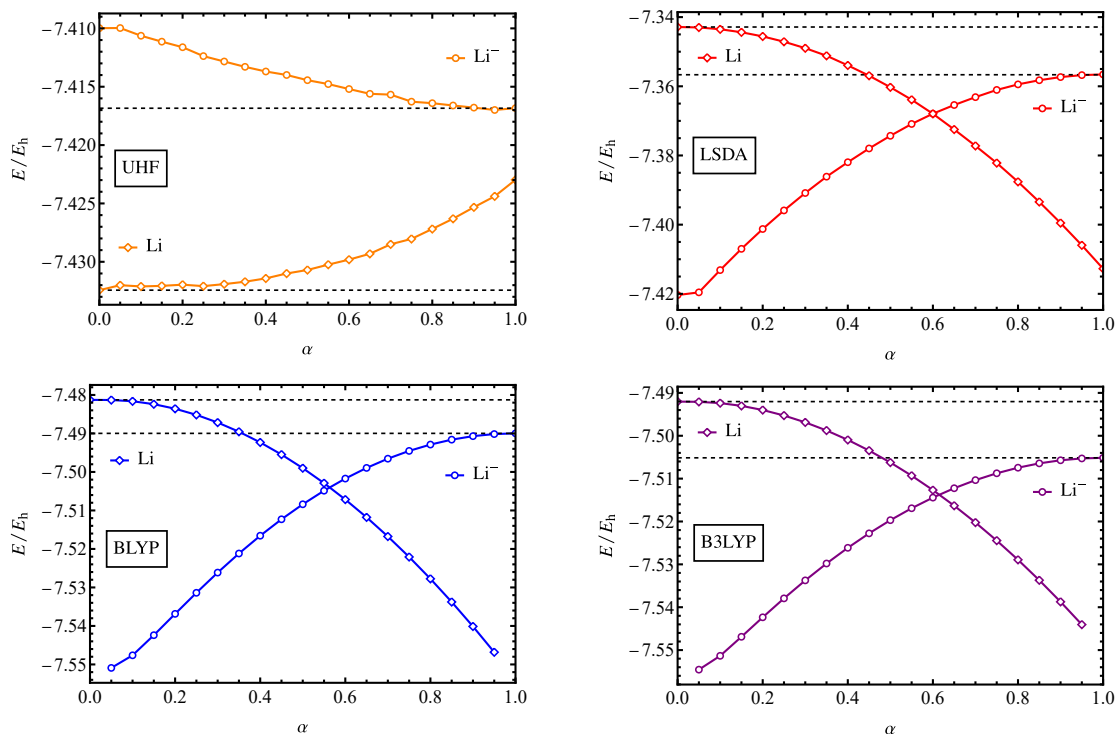


Figure 4.7: Variations of the weight-dependent individual states extracted from the right PPLB biensemble with respect to the physical charge deviation α . The weight-dependent ground-state energies of the neutral and anionic forms of the lithium atom are recovered by use of the variationally optimized ensemble orbitals as described in 4.3.2. Right PPLB calculations were performed with various xc-approximations, in the cc-pVDZ basis set. The black dashed lines correspond to the same individual states obtained from standard ground-state DFT calculations with the same level of approximation.

Note that, in the PPLB-DFT framework, unrestricted Hartree-Fock tends to overestimate both ground-state energies included in the ensemble, whereas density-functional approximations tend to underestimate them. Moreover, for any weight-configurations, UHF yields an unstable anionic form, that is to say with a higher ground-state energy than the one of the neutral form, in accordance with standard ground-state UHF results (black dashed lines). As opposed to DFAs which start to yield stable anionic ground-state energies, yet significantly underestimated, as one starts increasing the weight, until an inversion happens and the ensemble prediction for the neutral form becomes more energetically stable than the ensemble prediction for the anionic ground-state energy.

Extraction of excitation energies

Considering the previous observations relative to the extraction of individual ground-state energies from PPLB biensembles and the definitions of the ionization potential and electron affinity, expressed as total-energy differences of these individual ground-state energies (see equations 1.21 and 1.22), it is straightforward to understand that a variation of the PPLB weight, or fractional-charge deviation, will have a direct impact on the quality of the predictions of these excitation energies.

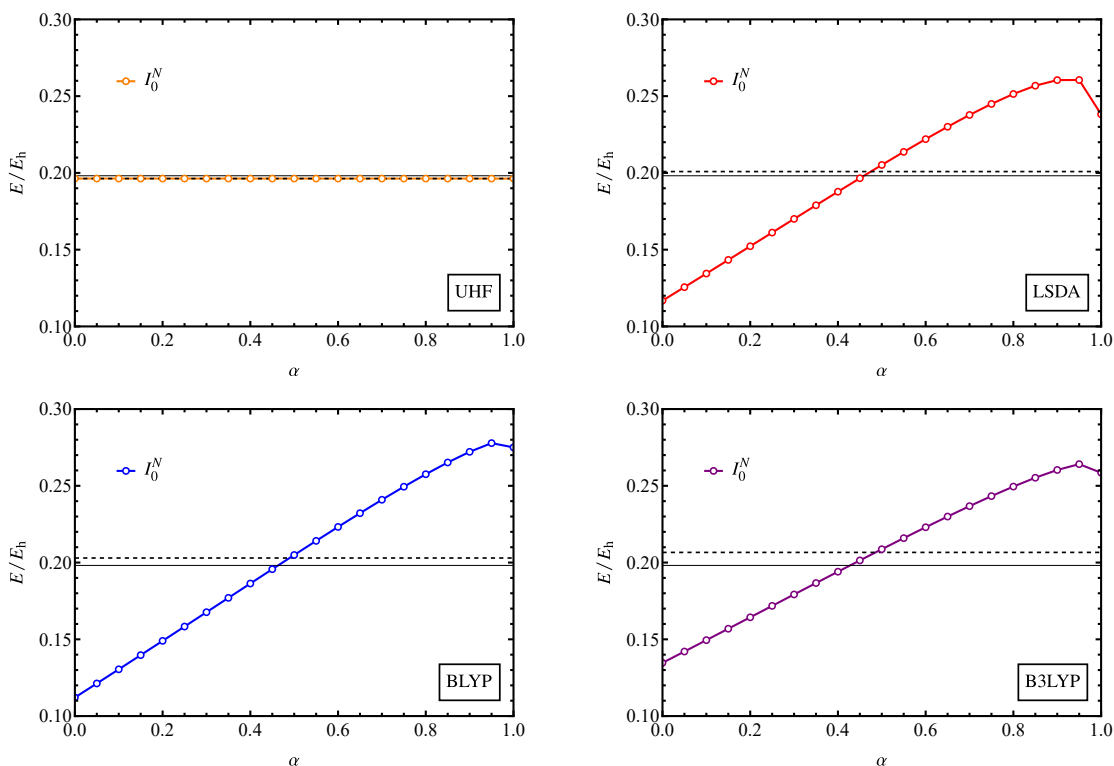


Figure 4.8: Variations of the weight-dependent ionization potential of Li extracted from left PPLB biensembles with respect to the physical charge deviation α . The left PPLB calculations were performed with various xc-approximations, in the cc-pVDZ basis set. The black dashed lines correspond to ionization potentials obtained by total-energy differences (Δ SCF) from standard ground-state HF and DFT calculations with the same level of approximation. The experimental (black solid line) ionization potential of Li (see Appendix A) is also reported for sake of completeness.

As depicted in Figure 4.8, the left PPLB prediction for the ionization potential of the neutral system Li nearly linearly varies as the weight increases, going from an underestimated to an overestimated prediction, with similar magnitudes, for all DFAs considered. As expected, the equibiensemble configurations, $\alpha = 0.5$, yield ionization-potential predictions that are almost identical to the ones that one would have obtained with the Δ SCF method, under the same level of approximation (black dashed lines). Note that, because of the almost perfectly linear UHF left PPLB ensemble energy, for this particular system, unrestricted Hartree-Fock

yields an almost perfectly constant and correct prediction for the ionization potential.

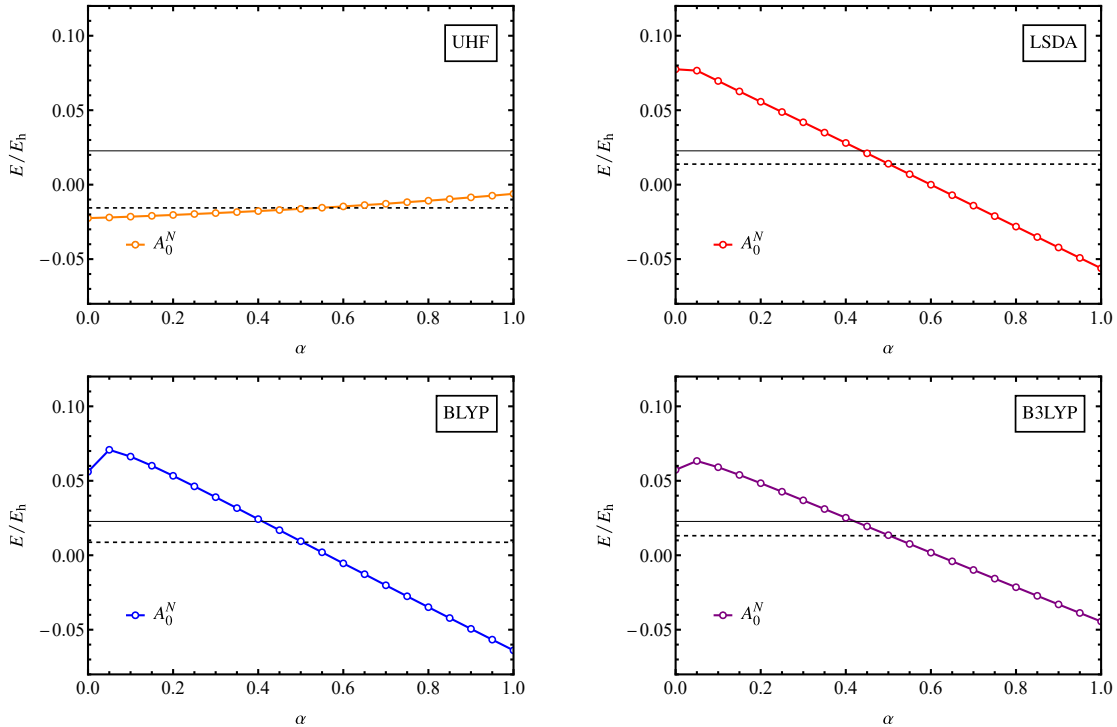


Figure 4.9: Variations of the weight-dependent electron affinity of Li extracted from right PPLB biensembles with respect to the physical charge deviation α . The right PPLB calculations were performed with various xc-approximations, in the cc-pVDZ basis set. The black dashed lines correspond to electron affinities obtained by total-energy differences (Δ SCF) from standard ground-state HF and DFT calculations with the same level of approximation. The experimental (black solid line) electron affinity of Li (see Appendix A) is also reported for sake of completeness.

Similarly, if one applies the same considerations to right PPLB biensembles (see Figure 4.9), one sees that the ensemble prediction for the electron affinity of the neutral system, Li, also depicts an almost perfectly linear variation with respect to the ensemble weight and will, in all cases, match the Δ SCF references, for calculations that are performed in the equibiensemble configuration, $\alpha = 0.5$. Moreover, one can see that UHF right PPLB biensemble calculations yield, at first, underestimated electron affinities and, as the weight increases, overestimated electron affinities, with respect to the Δ SCF references. Conversely, right PPLB electron affinities obtained from DFAs depict an opposite behaviour.

In conclusion, the results discussed in the present work confirm that the violation of the piecewise-linearity exact criteria for the total energy of an open system, due to the inability of standard approximations to restore such exact feature, may have significant consequences on the quality of the physical properties that the ensemble was intentionally designed to predict. Indeed, the weight-dependency of the predictions of the individual states included in the PPLB ensembles has shown to be non-negligible. Such a consideration has to be taken

into account in order to motivate which weight-configuration would be the most relevant to consider, depending on the quantity or property of interest that one would like to extract from a single ensemble DFT calculation. Of course, in the case of simple biensembles like the ones presented in this work, the answer remains quite intuitive and the equibiensemble configuration has proved to be the “best” option, but if one were to consider larger ensembles, with various weights for instance, the adequate answer, if such exists, would probably be less obvious.

4.3.3 With Weight-Dependent xc-Functionals

Building weight-dependent exchange functionals

From now on, we explore the feasibility of designing an explicitly weight-dependent xc-functional which would be capable of correcting the spurious curvature of PPLB-DFT ensemble energies provided by standard weight-independent functionals.

Since exchange energies are much significant than correlation energies, we assume that injecting an explicit weight-dependency into the exchange part of the total ensemble energy could correct most of the curvature of the energy.

To do so, we start from the assumption that replacing the weight-independent exchange energy with a weight-dependent one will not affect much the remaining ensemble energy, which may be a very crude approximation since the orbitals are optimized for a given potential that will inexorably be affected by the change of the exchange functional.

To proceed, we start by removing the standard “DFA” exchange energy from the total ensemble energy, and replacing it by a weight-dependent “eDFA” exchange energy such that

$$E^{\alpha, \text{eDFA}}[n] = E^{\alpha, \text{DFA}}[n] - E_{\text{x}}^{\alpha, \text{DFA}}[n] + E_{\text{x}}^{\alpha, \text{eDFA}}[n], \quad (4.141)$$

with the weight-dependent ensemble density-functional approximation (eDFA) for the exchange energy

$$E_{\text{x}}^{\alpha, \text{eDFA}}[n] \equiv F_{\text{x}}^{\alpha} E_{\text{x}}^{\alpha, \text{DFA}}[n], \quad (4.142)$$

in which F_{x}^{α} is an explicitly weight-dependent multiplicative exchange scaling factor.

The eDFA exchange approximation must correct the curvature of the ensemble energy stemming from the use of standard ground-state density-functional approximations (DFAs), with ensemble densities instead of pure-state densities. Moreover, the eDFA must recover as well the pure-state individual ground-state energies obtained with the standard DFAs in ground-state DFT, that is, when $\alpha = 0$ and $\alpha = 1$, in addition to yielding a perfectly linear ensemble energy between these two limits. The weight-dependent eDFA total-energy functional must therefore obey the following property

$$E^{\alpha, \text{eDFA}} = E^{\alpha=0, \text{DFA}} + \alpha(E^{\alpha=1, \text{DFA}} - E^{\alpha=0, \text{DFA}}). \quad (4.143)$$

Hence, we reverse engineer the analytical expression of the weight-dependent “curvature-corrected” (CC) exchange scaling factor, in terms of the DFA ensemble total and exchange

energy contributions at various weights

$$F_x^\alpha = \frac{E^{\alpha=0, \text{DFA}} + \alpha(E^{\alpha=1, \text{DFA}} - E^{\alpha=0, \text{DFA}}) - (E^{\alpha, \text{DFA}} - E_x^{\alpha, \text{DFA}})}{E_x^{\alpha, \text{DFA}}}. \quad (4.144)$$

Since there must be no curvature at weight $\alpha = 0$ and $\alpha = 1$, and since we have observed that for standard weight-independent functionals, the curvature of the ensemble energy seems to be maximal for $\alpha = \frac{1}{2}$, we choose to approximate the exchange scaling factor with a 4th order polynomial expression

$$F_x^\alpha \approx 1 - \alpha(1 - \alpha) \left[a + b \left(\alpha - \frac{1}{2} \right) + c \left(\alpha - \frac{1}{2} \right)^2 \right], \quad (4.145)$$

centered on $\alpha = \frac{1}{2}$, and which reduces to 1 when $\alpha = 0$ and $\alpha = 1$, as depicted in Figure 4.10.

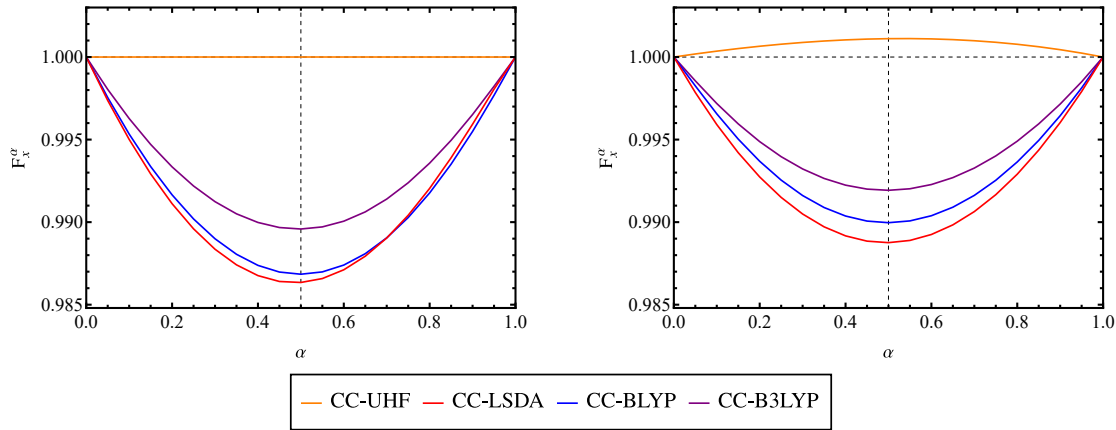


Figure 4.10: Comparison between the weight-dependent left and right PPLB exchange scaling factors F_x^α associated with the removal of an electron (left panel) and the addition of an electron (right panel) from/to Li, using different methods and xc-functionals in the cc-pVDZ basis set.

The “eDFA” total ensemble energy functional is therefore given as

$$E^{\alpha, \text{eDFA}}[n] = T_s[n] + E_H[n] + E_x^{\alpha, \text{eDFA}}[n] + E_c^{\text{DFA}}[n] + E_{\text{en}}[n], \quad (4.146)$$

where we choose to put all the explicit weight-dependency of the ensemble Hartree-exchange-correlation functional into the exchange part, and to resort to the classical weight-independent Hartree functional $E_H[n]$, and a standard weight-independent DFA correlation functional $E_c^{\text{DFA}}[n]$. Of course, the explicit weight-dependency will be included as well in the Hartree-exchange-correlation potential

$$v_{\text{Hxc}}^{\alpha, \text{eDFA}}(\mathbf{r}) = v_H(\mathbf{r}) + v_x^{\alpha, \text{eDFA}}(\mathbf{r}) + v_c^{\text{DFA}}(\mathbf{r}), \quad (4.147)$$

where $v_H(\mathbf{r})$ and $v_c^{\text{DFA}}(\mathbf{r})$ are the weight-independent Hartree and correlation potentials, respectively, and

$$\begin{aligned} v_x^{\alpha, \text{eDFA}}(\mathbf{r}) &= \frac{\delta E^{\alpha, \text{eDFA}}[n]}{\delta n(\mathbf{r})} \\ &= F_x^\alpha v_x^{\text{DFA}}(\mathbf{r}), \end{aligned} \quad (4.148)$$

is the weight-dependent exchange potential.

The use of a weight-dependent exchange functional may allow for the extraction of more stable individual-state properties and excitation energies, that is to say more constant with respect to the variation of the ensemble weight. This is due to its additional contribution through its derivative with respect to the ensemble weight, as discussed in 4.2.6,

$$\frac{\partial E_{\text{Hxc}}^{\alpha, \text{eDFA}}[n]}{\partial \alpha} = \frac{\partial E_x^{\alpha, \text{eDFA}}[n]}{\partial \alpha} = \frac{\partial F_x^\alpha}{\partial \alpha} E_x^{\text{DFA}}[n]. \quad (4.149)$$

Henceforth, such eDFA exchange functionals will be referred to as ‘‘Curvature-Corrected’’ (CC) functionals and will be designed based on standard DFAs, such as the LSDA functional, the BLYP GGA-functional, the B3LYP hybrid-functional, and Unrestricted Hartree-Fock exact-exchange functional (UHF). From now on, these weight-dependent exchange-correlation functionals will be referred to as ‘‘CC-LSDA’’, ‘‘CC-BLYP’’, ‘‘CC-B3LYP’’ and ‘‘CC-UHF’’, respectively (see Figure 4.10).

Weight-dependent CC-exchange multiplicative scaling factors have been computed within the scope of both left and right PPLB-DFT biensembles applied to a small set of atomic systems, and for various levels of xc-approximation, as depicted in Figures 4.11 and 4.12.

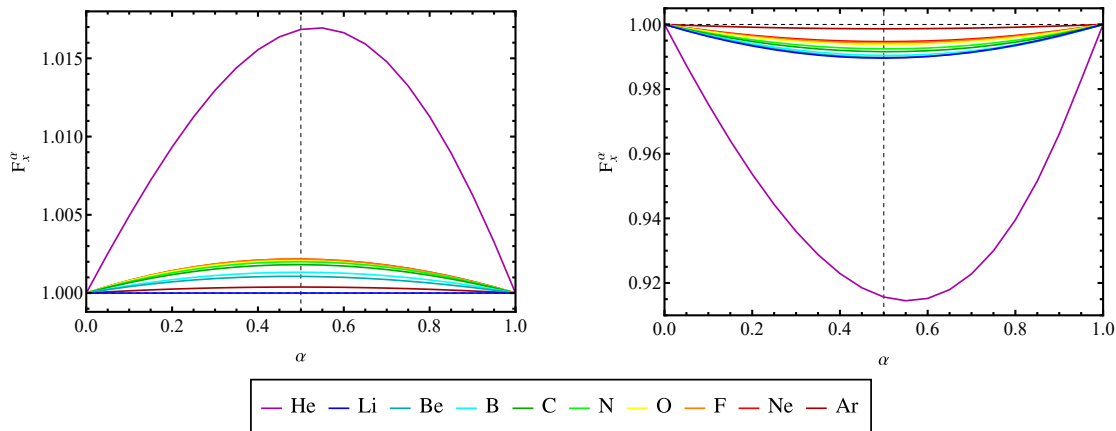


Figure 4.11: Comparison between the weight-dependent left PPLB exchange scaling factors F_x^α associated with the removal of an electron from simple atomic systems using the spin unrestricted Hartree-Fock (UHF) method (left panel) and the hybrid-GGA xc-functional B3LYP (right panel), in the cc-pVDZ basis set. Elements from the second row of the periodic table plus the first three noble gases are considered.

Note that, apart from the noble gases, the atomic systems considered in this work exhibit well-ordered weight-dependent exchange scaling factors in both left and right PPLB-DFT frameworks, and for all levels of xc-approximation considered.

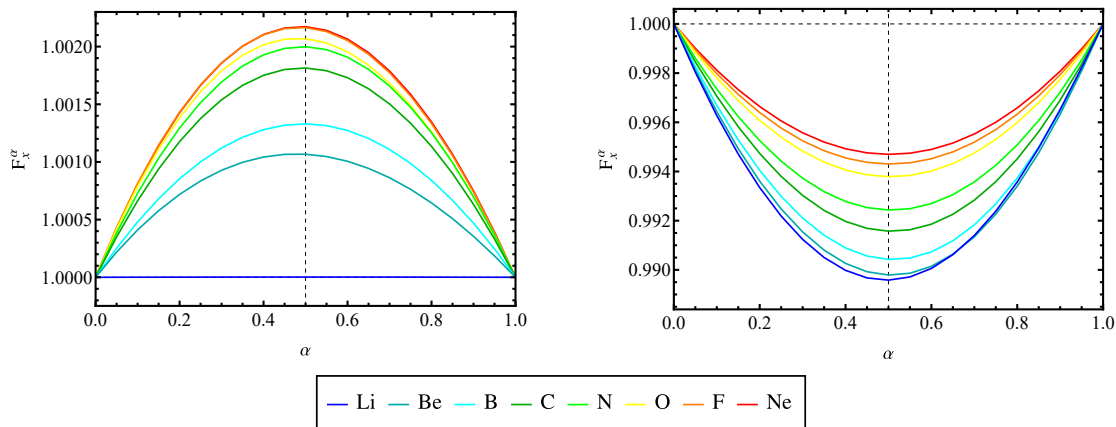


Figure 4.12: Comparison between the weight-dependent left PPLB exchange scaling factors F_x^α associated with the removal of an electron from simple atomic systems using the spin unrestricted Hartree-Fock (UHF) method (left panel) and the hybrid-GGA xc-functional B3LYP (right panel) in the cc-pVDZ basis set. Elements from the second row of the periodic table are considered.

Numerical results

We have performed self-consistent left PPLB calculations with the above-mentioned weight-dependent “CC” xc-functionals in order to assess to what extent the curvature of PPLB ensemble energies obtained with standard DFAs would affect the quality of the ensemble predictions of physical properties such as ionization potentials and electron affinities.

Regarding the PPLB ensemble energies obtained with weight-dependent CC-functionals (see Figure 4.13), one can see that such functionals managed to recover ensemble energies with near-zero curvatures, for all considered levels of approximation, as they were intended to.

Turning now to the ensemble predictions of ionization potentials and electron affinities of open systems obtained with CC-functionals. One can see that by enforcing the piecewise-linearity exact condition on PPLB ensemble energies, the weight-dependent CC-functionals managed to restore a much satisfactory piecewise-constant feature for the IP/EA diagram (see Figure 4.14), as opposed to the performance of the weight-independent DFAs.

As a matter of fact, the weight-dependent orbital energies obtained with a given weight-independent DFA are very similar to the ones provided by its weight-dependent CC alter-ego. As a consequence, most of the improvement of the results is due to the additional contribution of the weight derivative of the CC-functionals, due to their explicit weight-dependency, and illustrated by the “DD” term (see Tables 4.7 and 4.8 for more details).

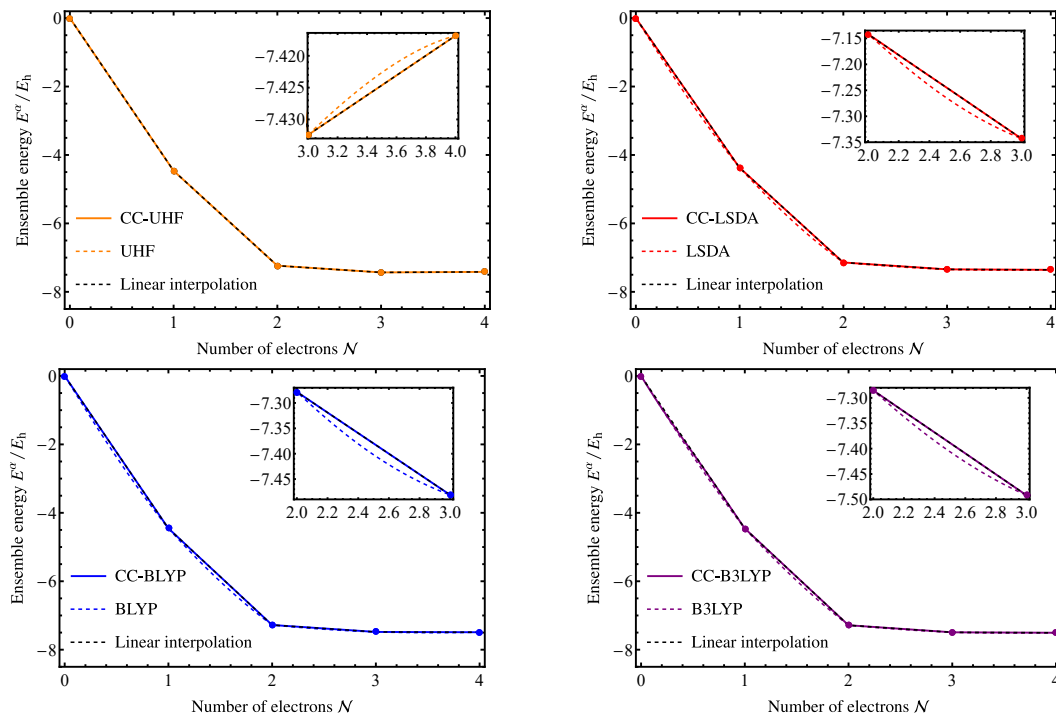


Figure 4.13: Restoring the piecewise-linearity criterion of the PPLB ensemble energy of Li with respect to the number of electrons of the open system using the weight-dependent (CC) analogs (colored solid lines) of standard weight-independent approximations (colored dashed lines) in the cc-pVDZ basis set.

As for predicting individual-state energies and excitation energies from PPLB ensembles, one can see in Figures 4.15 and 4.16 that the CC-functionals succeed in providing more stable and accurate PPLB predictions for the ground-state energies of the neutral, cationic and anionic forms of Li, as well as for ionization potentials and electronic affinities. By accurate, we mean more in accordance with the ground-state energies obtained with multiple self-consistent calculations within the scope of standard ground-state DFT, for individual-state energies, or by total-energy differences (Δ SCF method) for excitation energies, with the same level of approximations.

Indeed, the present work has shown that the well-known performance of standard weight-independent xc-functionals in ground-state DFT is not necessarily recovered within the scope of ensemble DFT. This is due to the fact that, in their original conception, such functionals were not intended to be applied to ensemble densities, that is, to linear mixtures of electron densities. As a result, this “misuse” of commonly used functionals reveals erroneous features that are responsible for unphysical and inaccurate descriptions of physical systems, such as predicting weight-dependent ground-state energies or excitation energies.

Nevertheless, in the PPLB-DFT framework, although the exact xc-functional is known to be weight-independent, designing weight-dependent approximate xc-functionals may provide a promising alternative to overcome the limitations of standard ground-state approximations that seem to suffer from additional deficiencies when extended to ensemble applications.

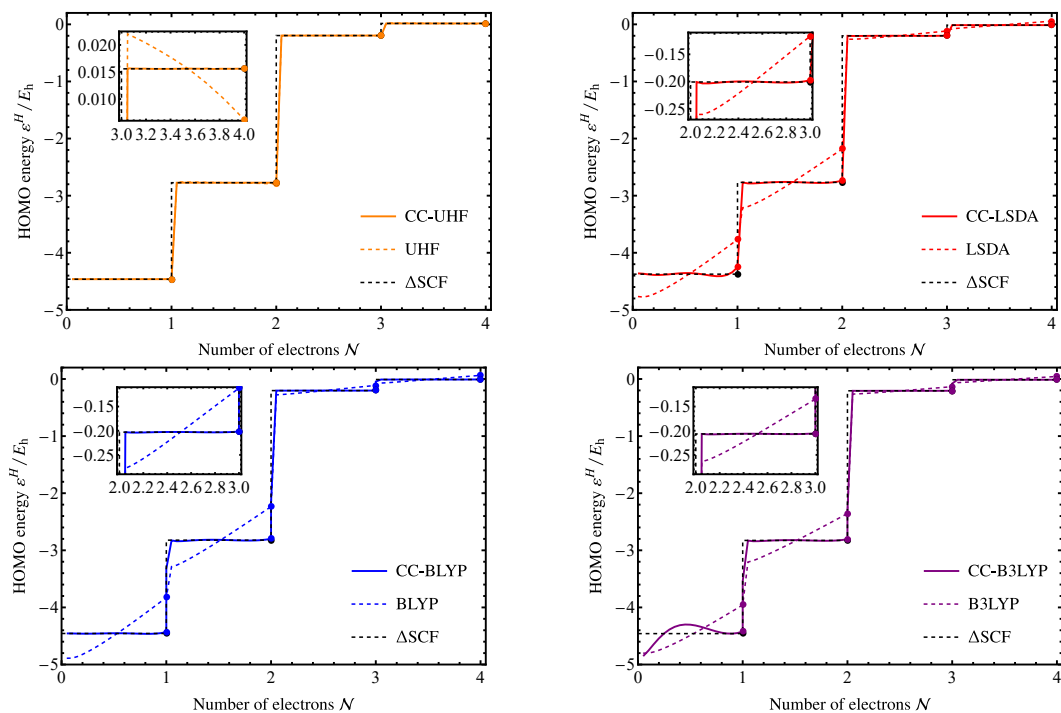


Figure 4.14: Restoring the step-diagram feature of the HOMO energy of Li with respect to the number of electrons of the open system using the weight-dependent (CC) analogs (colored solid lines) of standard weight-independent approximations (colored dashed lines) in the cc-pVDZ basis set. The corresponding ionization potentials and electron affinities obtained by total energy differences (Δ SCF) between successive pure-state energies are also reported for comparison.

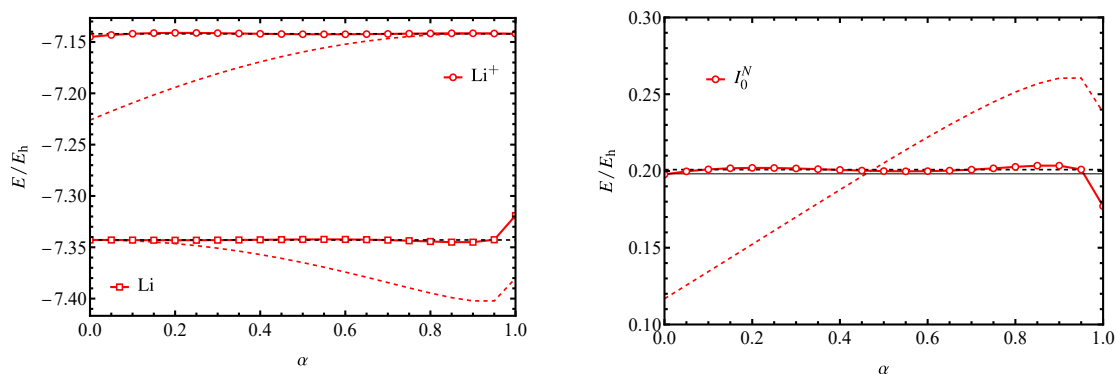


Figure 4.15: Comparison between left PPLB-DFT individual-state energies (left panel) and ionization potentials of Li (right panel), obtained with the weight-independent LSDA xc-functional (red dashed lines) and its weight-dependent CC-counterpart (red solid lines), as functions of the fractional-charge deviation α , in the cc-pVDZ basis set. SCF individual-state energies and Δ ionization potential (black dashed line) are reported for comparison as well as the experimental ionization potential (black solid line) of Li (see Appendix A).

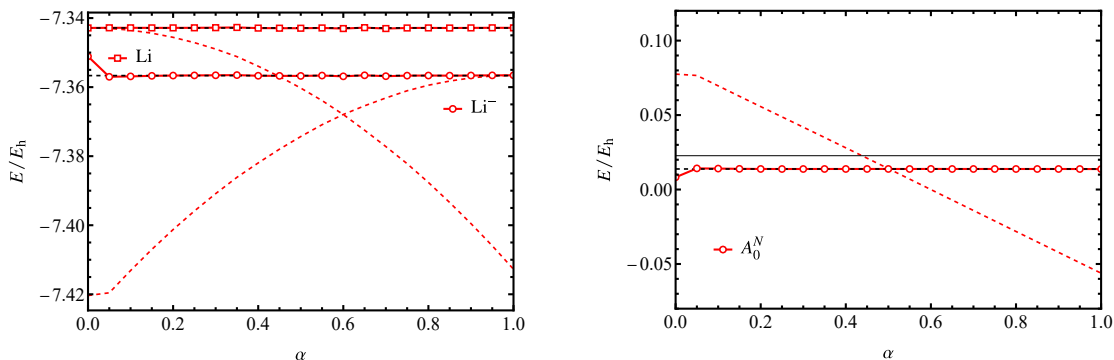


Figure 4.16: Comparison between right PPLB-DFT individual-state energies (left panel) and electron affinities of Li (right panel), obtained with the weight-independent LSDA xc-functional (red dashed lines) and its weight-dependent CC-counterpart (red solid lines), as functions of the fractional-charge deviation α , in the cc-pVDZ basis set. SCF individual-state energies and Δ electron affinity (black dashed line) are reported for comparison as well as the experimental electron affinity (black solid line) of Li (see Appendix A).

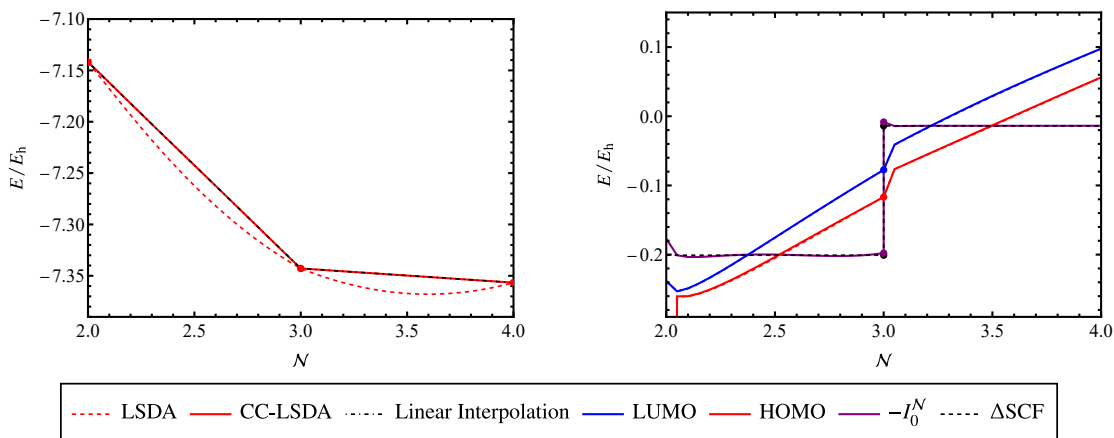


Figure 4.17: Impact of the ability of CC-functionals to restore the piecewise-linearity exact condition of the total energy of an open system on the physical relevance of the ensemble prediction for the fundamental gap. Calculations were performed on Li in the cc-pVDZ basis set with the LSDA xc-functional and its weight-dependent CC counterpart. A parallel is drawn between the re-establishment of the piecewise-linearity condition of the total energy of the open system (left panel) and the improvement of the ensemble fundamental gap (right panel). The corresponding fundamental gap obtained by total energy differences (ΔSCF method) between successive pure-state energies within the same level of approximation is also reported for comparison.

In conclusion, the inability of commonly used weight-independent approximations to provide piecewise-linear energies for open systems has shown to have critical implications of the quality and physical relevance of using ensemble quantities to approximate real physical properties. For instance, the capability of a given approximate functional to yield accurate

band-gap predictions is inextricably linked to its ability to obey the piecewise-linearity requirement for the energy, as depicted in Figure E.3.

For the sake of completeness, Tables 4.7 and 4.8 provide more detailed overviews of the performance of weight-dependent CC-approximations within the scope of PPLB ensemble DFT, compared to the performance of their weight-independent alter-egos.

Table 4.7: Comparison between the left PPLB biensemble predictions for the ionization potential of Li and the Δ SCF references obtained with standard weight-independent and weight-dependent (CC) xc-functionals in the cc-pVDZ basis set, for various weight-configurations. The “DD” notation refers to the additional weight-derivative contributions of the CC-functionals to the ionization potential predictions. The blanks are left to highlight the fact that, unlike CC-functionals, standard weight-independent functionals do not benefit from the additional “DD” term. Percent errors ($\Delta(\%)$ notations) of the quantity shown in the line above, with respect to the Δ SCF ionization potentials, are reported. All energies are in hartree and experimental references are available in Appendix A.

Removal: $N \rightarrow N - 1$									
	UHF	CC-UHF	LSDA	CC-LSDA	BLYP	CC-BLYP	B3LYP	CC-B3LYP	
Δ SCF I_0	0.19631	0.19631	0.20087	0.20087	0.20295	0.20295	0.20661	0.20661	0.20661
$\alpha = 0.00$									
$-\varepsilon_N$	0.19632	0.19632	0.11678	0.11678	0.11210	0.11210	0.13466	0.13466	0.13466
$\Delta(\%)$	0.005	0.005	-41.862	-41.862	-44.759	-44.759	-34.824	-34.824	-34.824
$-\varepsilon_N + \text{DD}$	-	0.19631	-	0.19777	-	0.20169	-	0.205413	0.205413
$\Delta(\%)$	-	0.000	-	-1.538	-	-0.615	-	-0.575	-0.575
$\alpha = 0.05$									
$-\varepsilon_N$	0.19632	0.19632	0.12558	0.12525	0.12125	0.12091	0.142054	0.14174	0.14174
$\Delta(\%)$	0.005	0.005	-37.476	-37.641	-40.251	-40.423	-31.242	-31.392	-31.392
$-\varepsilon_N + \text{DD}$	-	0.19631	-	0.19975	-	0.20250	-	0.20618	0.20618
$\Delta(\%)$	-	0.000	-	-0.552	-	-0.216	-	-0.203	-0.203
$\alpha = 0.50$									
$-\varepsilon_N$	0.19631	0.19631	0.20517	0.20346	0.20492	0.20309	0.20869	0.20725	0.20725
$\Delta(\%)$	0.000	0.000	2.140	1.289	0.970	0.068	1.006	0.309	0.309
$-\varepsilon_N + \text{DD}$	-	0.19631	-	0.19992	-	0.20257	-	0.20625	0.20625
$\Delta(\%)$	-	0.000	-	-0.467	-	-0.182	-	-0.169	-0.169

Table 4.8: Comparison between the right PPLB biensemble predictions for the electron affinity of Li and the Δ SCF references obtained with standard weight-independent and weight-dependent (CC) xc-functionals in the cc-pVDZ basis set, for various weight-configurations. The "DD" notation refers to the additional weight-derivative contributions of the CC-functionals to the electron affinity predictions. The blanks are left to highlight the fact that, unlike CC-functionals, standard weight-independent functionals do not benefit from the additional "DD" term. Percent errors ($\Delta(\%)$ notations) of the quantity shown in the line above, with respect to the Δ SCF electron affinities, are reported. All energies are in hartree and experimental references are available in Appendix A.

Addition: $N \rightarrow N + 1$									
	UHF	CC-UHF	LSDA	CC-LSDA	BLYP	CC-BLYP	B3LYP	CC-B3LYP	
Δ SCF A_0	-0.01558	-0.01558	0.01379	0.01379	0.00870	0.00870	0.01311	0.01311	
$\alpha = 0.00$									
$-\epsilon_{N+1}$	-0.02245	-0.02245	0.07749	0.07749	0.05606	0.05606	0.05735	0.05735	
$\Delta(\%)$	-44.094	-44.094	461.928	461.928	544.367	544.367	337.452	337.452	
$-\epsilon_{N+1} + \text{DD}$	-	-0.01560	-	0.00823	-	-0.01115	-	0.00267	
$\Delta(\%)$	-	-0.128	-	-40.319	-	-228.160	-	-79.633	
$\alpha = 0.05$									
$-\epsilon_{N+1}$	-0.02203	-0.02203	0.07658	0.07649	0.07080	0.07071	0.06330	0.06324	
$\Delta(\%)$	-41.399	-41.399	455.329	454.677	713.793	712.758	382.837	382.379	
$-\epsilon_{N+1} + \text{DD}$	-	-0.01567	-	0.01419	-	0.00894	-	0.01332	
$\Delta(\%)$	-	-0.057	-	2.900	-	2.758	-	1.601	
$\alpha = 0.50$									
$-\epsilon_{N+1}$	-0.01626	-0.01617	0.01403	0.01314	0.00938	0.00852	0.01347	0.01276	
$\Delta(\%)$	-4.364	-3.786	1.740	-4.713	7.816	-2.068	2.745	-2.669	
$-\epsilon_{N+1} + \text{DD}$	-	-0.01561	-	0.01381	-	0.00831	-	0.01287	
$\Delta(\%)$	-	-0.192	-	0.145	-	-4.482	-	-1.830	

Chapter 5

GOK Ensembles to Target Neutral Excitations

Contents

5.1	Introduction: Excited States in Quantum Chemistry	129
5.2	Gross-Oliveira-Kohn Density-Functional Theory Formalism . . .	131
5.2.1	GOK Ensemble Energy and Ensemble Density	131
5.2.2	Theoretical Extraction of Individual-State Properties and Excitation Energies	132
5.2.3	GOK Variational Principle	133
5.2.4	Universal GOK Ensemble Density-Functional	134
5.2.5	Kohn-Sham Formulation of GOK-DFT	135
5.2.6	Decomposition of the Ensemble Hxc-Functional	137
5.2.7	Practical Extraction of Individual-State Properties and Excitation Energies	139
5.3	Numerical Implementation of GOK-DFT	141
5.3.1	With Standard Weight-Independent Exchange-Correlation Functionals	141
5.3.2	With Weight-Dependent Exchange-Correlation Functionals	156

5.1 Introduction: Excited States in Quantum Chemistry

As we have seen in Chapter 3, DFT is a ground state theory originally designed to describe static (time-independent) systems associated with a time-independent external potential $v(\mathbf{r})$. Nevertheless, similarly to the Hohenberg-Kohn theorem, the Runge-Gross theorem

[73] proved the existence of a unique one-to-one correspondence between a time-dependent external potential $v(\mathbf{r}, t)$ and the electron density of a system evolving in such a potential $n(\mathbf{r}, t)$.

Hence, DFT has been extended to include time-dependent external potentials which allow the description of excited states and give access to excitations associated with the conservation of the number of electrons of the system, such as optical excitations with excitonic effects. Note that, in a similar spirit, there also exists a time-dependent extension of Hartree-Fock theory, TD-HF.

In practice, the most common application of TD-DFT is in the linear response regime which avoid solving the full time-dependent Schrödinger equation. TD-DFT is very similar to standard ground state DFT and consists in solving self-consistently a set of time-dependent Kohn-Sham equations with an additional difficulty arising from the observation that the exchange-correlation potential is much more subtle than in ground state DFT due to the fact that it must encompass a “time-memory” effect [57] through its dependency on the density. In general, a way to avoid this difficulty is to use TD-DFT in the scope of the adiabatic approximation which consist in neglecting this time-memory characteristic of the xc-potential by using instead its time-independent ground state analog used in standard ground state DFT.

Unfortunately, the adiabatic approximation, which implies the use of a static xc-kernel, restricts the domain of application of TD-DFT to the sole description of singly excited states and, as a consequence, completely misses multiple excitations which description would require a frequency-dependent xc-kernel.

TD-DFT, in its linear response and adiabatic formulation, has emerged as one of the most promising alternative in the context of neutral excitations.

Despite the fact that it can predict excitation energies quite accurately, it yet suffers of numerous qualitative deficiencies [56] which still need to be overcome.

TD-DFT has been widely and successfully employed over the last decades but fails to provide a proper description of a number of phenomena [9] and properties of interest such as the description of Rydberg states, charge transfer excitations [27] or conical intersections which play a key role in photochemical mechanisms. Moreover, multiple excitations are completely absent from the spectra provided by TD-DFT.

Hence, the need to develop a more general approach applicable to arbitrary excited states and able to access the whole spectrum of a system within a time-independent formalism and with a low computational cost.

Gross-Oliveira-Kohn ensemble-DFT formalism may provide such an appealing alternative. As we will see in this chapter, GOK-DFT is an in-principle exact and time-independent theory which can not only access all kind of excitation energies but also excited state energies and densities in a single DFT-like calculation through the use of the ensemble formalism. Nevertheless, such a formalism will raise a number of questions which remain to be answered in order to fully exploit this method. For instance, the choice of optimal weight values and the necessity to design new weight-dependent approximate xc-functionals [28] will be of

primary interest in this work. Moreover, we will highlight the necessity to go beyond standard weight-independent xc-functionals and the possibility to use the Linear Interpolation Method (LIM) as an alternative to obtain accurate predictions of excitation energies for atomic and molecular systems.

5.2 Gross-Oliveira-Kohn Density-Functional Theory Formalism

5.2.1 GOK Ensemble Energy and Ensemble Density

To give insight to the fundamental idea of GOK-DFT, let us consider a non-degenerate energy spectrum of a N -electron system $\{E_I^N\}$ where E_0^N is the energy of the ground state, E_1^N is the energy of the first excited state ...

We recall that the energy spectrum is the set of eigenvalues of the time-independent Schrödinger equation

$$\hat{H} |\Psi_I^N\rangle = E_I^N |\Psi_I^N\rangle \quad (5.1)$$

where the Hamiltonian operator takes the form

$$\hat{H} = \hat{T} + \hat{V}_{ee} + \hat{V}_{en}. \quad (5.2)$$

We admit that those eigenstates are numbered so that

$$E_0 \leq E_1 \leq E_2 \leq \dots \leq E_\infty. \quad (5.3)$$

While DFT is a ground state theory, GOK-DFT allows the description of both ground and excited states of an electronic system with a fixed integer number of electrons N , thus paving the way to neutral excitation energies. GOK-DFT was developed in the 1980s by Gross, Oliveira and Kohn (see [31]), as a generalization of the equiensemble DFT developed by Theophilou [85].

GOK-DFT formalism is very similar to standard DFT except that the primary variable will be an ensemble density instead of the usual electron density. Although we only consider non-degenerate cases in this work, the theory still holds in case of degeneracy where multiplet degeneracy can be handled by assigning the same weight to the degenerate states of the ensemble.

The GOK ensemble energy takes the following form

$$E^{\mathbf{w}} = \sum_{I=0}^{M-1} w_I E_I \quad (5.4)$$

and consists of a linear statistical mixture, an ensemble, of the M lowest energy levels of the system $\{E_I^N \equiv E_I\}$. In the ensemble formulation of the energy, each energy level is ponderated by a weight w_I so that the set of weights $\mathbf{w} = \{w_I\}$ which defines the ensemble

is normalised and monotonically decreasing so that the lowest energy gets the larger weights and so on

$$w_0 = 1 - \sum_{I=1}^{M-1} w_I \quad (5.5) \quad \left| \quad 0 \leq w_{M-1} \leq \dots \leq w_1 \leq w_0. \quad (5.6)\right.$$

Hence, the GOK ensemble energy takes the form

$$E^{\mathbf{w}} = \left(1 - \sum_{I=1}^{M-1} w_I\right) E_0 + \sum_{I=1}^{M-1} w_I E_I. \quad (5.7)$$

Along with the GOK ensemble energy, a GOK ensemble density $n^{\mathbf{w}}(\mathbf{r})$ is similarly defined as the corresponding linear mixture, with the same fixed set of weights, of the individual densities $n_I(\mathbf{r})$ of each states included in the GOK ensemble.

$$n^{\mathbf{w}}(\mathbf{r}) = \left(1 - \sum_{I=1}^{M-1} w_I\right) n_0(\mathbf{r}) + \sum_{I=1}^{M-1} w_I n_I(\mathbf{r}) \quad (5.8)$$

Hence, in GOK-DFT, the system of interest will be jointly defined by its ensemble density and ensemble energy, the latter being expressed as a functional of the former, in complete analogy with ground state DFT.

We stress that, in the exact theory, each individual density $n_I(\mathbf{r})$ is generated by a specific wave function Ψ_I which is an eigenstate of the Hamiltonian operator of the N -electron system. Conversely, the exact GOK ensemble density is not generated by a wave function which would consist of a linear mixture of the individual states $\{\Psi_I\}$.

5.2.2 Theoretical Extraction of Individual-State Properties and Excitation Energies

At this point, we would like to emphasize the fact that the GOK ensemble energy $E^{\mathbf{w}}$ is an auxiliary quantity in the sense that it does not possess any physical meaning but can rather be exploited to extract individual-state properties of interest, like excitation energies for instance [20]. Indeed, because the exact individual energies of the GOK ensemble are real energies and therefore must be weight-independent, it is straightforward to see that the exact ensemble energy must be linear with respect to the weights. For that reason, the energy levels of the individual states included in the ensemble can be extracted by taking simple derivatives of the GOK ensemble energy with respect to the weights.

Hence, the extraction of the i th excitation energy of the N -electron system

$$\frac{\partial E^{\mathbf{w}}}{\partial w_I} = E_I - E_0. \quad (5.9)$$

Based on that simple observation, a general expression of the individual states of the ensemble can be derived by combining the ensemble energy and its derivatives with respect to the ensemble weights

$$E_I = E^{\mathbf{w}} + \sum_{J=1}^M (\delta_{JI} - w_J) \frac{\partial E^{\mathbf{w}}}{\partial w_J}, \quad (5.10)$$

where $0 \leq I \leq M - 1$.

Although we will focus on the extraction of individual energies and excitation energies, it is yet possible to access the individual densities of the states of the ensemble through a similar formulation

$$n_I(\mathbf{r}) = n^{\mathbf{w}}(\mathbf{r}) + \sum_{J=1}^M (\delta_{JI} - w_J) \frac{\partial n^{\mathbf{w}}(\mathbf{r})}{\partial w_J}. \quad (5.11)$$

5.2.3 GOK Variational Principle

Whereas in standard ground state DFT, the state of interest is associated with a density generated by a wave function, in GOK-DFT, the basic variable will be a statistical mixture of densities and will be generated by a density matrix.

First, let us define the exact GOK density matrix

$$\hat{\Gamma}_0^{\mathbf{w}} = \left(1 - \sum_{I=1}^{M-1} w_I\right) |\Psi_0\rangle \langle \Psi_0| + \sum_{I=1}^{M-1} w_I |\Psi_I\rangle \langle \Psi_I|, \quad (5.12)$$

with exact GOK ensemble energy

$$E_0^{\mathbf{w}} = \text{Tr}\{\hat{\Gamma}_0^{\mathbf{w}} \hat{H}\}, \quad (5.13)$$

built from the exact eigenstates $\{\Psi_I\}$ of the Hamiltonian operator of the N -electron system. Similarly, if the true eigenstates were unknown and we were to use a set of trial wave functions $\{\tilde{\Psi}_I\}$ instead, we would therefore obtain a trial GOK density matrix

$$\hat{\Gamma}^{\mathbf{w}} = \left(1 - \sum_{I=1}^{M-1} w_I\right) |\tilde{\Psi}_0\rangle \langle \tilde{\Psi}_0| + \sum_{I=1}^{M-1} w_I |\tilde{\Psi}_I\rangle \langle \tilde{\Psi}_I|, \quad (5.14)$$

with trial GOK ensemble energy

$$E^{\mathbf{w}} = \text{Tr}\{\hat{\Gamma}^{\mathbf{w}} \hat{H}\}. \quad (5.15)$$

In complete analogy with ground state DFT, GOK-DFT is a variational formalism and is based on the GOK variational principle [32] for the ensemble energy which takes the following form

$$E_0^{\mathbf{w}} \leq E^{\mathbf{w}} = \sum_{I=0}^M w_I \langle \tilde{\Psi}_I | \hat{H} | \tilde{\Psi}_I \rangle. \quad (5.16)$$

The GOK variational principle states that if we use a set of orthonormal and normalized trial wave functions $\{\tilde{\Psi}_I\}$ instead of the true eigenstates $\{\Psi_I\}$ of the Hamiltonian of the system

to build the individual states of the ensemble, we will inevitably obtain an approximate GOK ensemble energy instead of the exact GOK ensemble energy. Nevertheless, we are assured by the variational principle that this approximate ensemble energy will be an upper bound to the exact GOK ensemble energy. It is worth noting that the GOK variational principle remains valid even for infinite ensembles $M = \infty$.

In standard DFT, Rayleigh and Ritz variational principle is mostly applied to ground states because for excited states, the trial wave functions must be orthogonal to all the lower eigenstates of the Hamiltonian and this orthogonality constraint is extremely complicated to ensure in practice.

Originally, Theophilou's density-functional formalism for excited states was an extension of Rayleigh-Ritz variational principle to equiensembles which are ensembles of equally weighted states. Following this work, Gross, Oliveira and Kohn proposed a generalization to ensembles of unequally weighted states. Although GOK-DFT allows one to use distinct weights for each state of the ensemble, in practice, it may seem convenient to express all the weights of the ensemble in terms of a single real parameter, w , or to use a set of well-defined and more physical weights such as Boltzmann's weights, among other possibilities. There have been many attempts to find an "optimal" weight configuration which would be able to yield satisfactory predictions for the properties of interest on a relatively steady basis.

5.2.4 Universal GOK Ensemble Density-Functional

Similarly to standard DFT, it is possible to extend the Hohenberg-Kohn theorems to GOK ensembles and to establish a one-to-one mapping between a local external potential and an ensemble density for a given set of fixed weights \mathbf{w} . Moreover, the GOK ensemble energy and all the electronic properties of the ensemble can be expressed as functionals of the ensemble energy. Furthermore, the GOK ensemble energy can be obtained variationally and can take the form of a constrained-search minimization over all N -electron densities generated by an antisymmetric wave function instead of the originally ensemble v -representability restriction. Let us define the universal GOK ensemble density-functional

$$\begin{aligned} F^{\mathbf{w}}[n] &= \min_{\hat{I}^{\mathbf{w}} \rightarrow n} \text{Tr} \left\{ \hat{I}^{\mathbf{w}} \left(\hat{T} + \hat{V}_{\text{ee}} \right) \right\} \\ &= \sum_{I=0}^M w_I \langle \Psi_I^{\mathbf{w}}[n] | \hat{T} + \hat{V}_{\text{ee}} | \Psi_I^{\mathbf{w}}[n] \rangle \end{aligned} \quad (5.17)$$

where the search is over all N -electron ensemble density matrices $\hat{I}^{\mathbf{w}}$, built from an arbitrary set of weight-dependent orthonormal wave functions $\{\Psi_I^{\mathbf{w}}\}$, that yield the density

$$n_{I^{\mathbf{w}}}(\mathbf{r}) = \text{Tr} \{ \hat{I}^{\mathbf{w}} \hat{n}(\mathbf{r}) \} = \sum_{I=0}^{M-1} w_I n_{\Psi_I^{\mathbf{w}}}(\mathbf{r}) = n(\mathbf{r}), \quad (5.18)$$

and where $\{\Psi_I^{\mathbf{w}}[n]\}$ are the weight-dependent wave functions that minimize the quantity

$$\text{Tr} \left\{ \hat{I}^{\mathbf{w}} \left(\hat{T} + \hat{V}_{\text{ee}} \right) \right\} \quad (5.19)$$

for a given set of fixed weights $\mathbf{w} = \{w_I\}$ and yield the density

$$\sum_{I=0}^{M-1} w_I n_{\Psi_I^{\mathbf{w}}}[n](\mathbf{r}) = n(\mathbf{r}). \quad (5.20)$$

Hence, the variational principle for the ensemble energy takes the form

$$E^{\mathbf{w}} = \min_n \{F^{\mathbf{w}}[n] + \int n(\mathbf{r})v(\mathbf{r})d\mathbf{r}\} \quad (5.21)$$

and is valid for any N -electron density.

Note that while the GOK universal functional is indeed “universal” in the sense that it does not depend on the external potential $v(\mathbf{r})$, it is not ensemble-independent and may depend on the excited states included in the ensemble. For that reason, designing approximate functionals for ensemble applications appears to be a very challenging task.

5.2.5 Kohn-Sham Formulation of GOK-DFT

Kohn-Sham system

The standard Kohn-Sham DFT formalism can be extended to GOK-DFT in order to decompose the universal GOK functional into two contributions

$$F^{\mathbf{w}}[n] = T_s^{\mathbf{w}}[n] + E_{\text{Hxc}}^{\mathbf{w}}[n], \quad (5.22)$$

where $T_s^{\mathbf{w}}[n]$ is the non-interacting ensemble kinetic energy functional and $E_{\text{Hxc}}^{\mathbf{w}}[n]$ is the combined Hartree-exchange-correlation ensemble energy functional.

Hence, Kohn and Sham ensemble extension assumes that there exists an auxiliary non-interacting system, the Kohn-Sham system, which will have the same ensemble density $n(\mathbf{r})$ than the interacting system.

Non-interacting ensemble kinetic energy

The non-interacting ensemble kinetic energy functional can be expressed in a constrained-search formulation

$$\begin{aligned} T_s^{\mathbf{w}}[n] &= \min_{\hat{\gamma}^{\mathbf{w}} \rightarrow n} \text{Tr}\{\hat{\gamma}^{\mathbf{w}}\hat{T}\} \\ &= \sum_{I=0}^{M-1} w_I \langle \Phi_I^{\mathbf{w}}[n] | \hat{T} | \Phi_I^{\mathbf{w}}[n] \rangle, \end{aligned} \quad (5.23)$$

where the constrained-search is over all non-interacting ensemble density matrix operator $\hat{\gamma}^{\mathbf{w}}$ built from an arbitrary set of weight-dependent single Slater determinant $\{\Phi_I^{\mathbf{w}}\}$,

$$\hat{\gamma}^{\mathbf{w}} = \sum_{I=0}^{M-1} w_I |\Phi_I^{\mathbf{w}}\rangle \langle \Phi_I^{\mathbf{w}}|, \quad (5.24)$$

that yields the interacting ensemble density $n(\mathbf{r})$,

$$n_{\hat{\gamma}^{\mathbf{w}}}(\mathbf{r}) = \text{Tr}\{\hat{\gamma}^{\mathbf{w}}\hat{n}(\mathbf{r})\} = \sum_{I=0}^{M-1} w_I n_{\Phi_I^{\mathbf{w}}}(\mathbf{r}) = n(\mathbf{r}), \quad (5.25)$$

and where $\{\Phi_I^{\mathbf{w}}[n]\}$ are the Slater determinants from which is built the non-interacting ensemble density operator that minimizes the ensemble kinetic energy $\text{Tr}\{\hat{\gamma}^{\mathbf{w}}\hat{T}\}$,

$$\hat{\gamma}_{\text{KS}}^{\mathbf{w}} = \sum_{I=0}^{M-1} w_I |\Phi_I^{\mathbf{w}}[n]\rangle \langle \Phi_I^{\mathbf{w}}[n]|, \quad (5.26)$$

and yield the interacting ensemble density for a given set of fixed weights $\mathbf{w} = \{w_I\}$,

$$n_{\text{KS}}^{\mathbf{w}}(\mathbf{r}) = \sum_{I=0}^{M-1} w_I n_{\Phi_I^{\mathbf{w}}[n]}(\mathbf{r}) = n(\mathbf{r}). \quad (5.27)$$

GOK-DFT variational ensemble energy

The variational principle for the GOK ensemble energy can be formulated in terms of the weight-dependent molecular orbitals $\{\varphi_p^{\mathbf{w}}(\mathbf{r})\}$ from which the single Slater determinants $\{\Phi_I^{\mathbf{w}}\}$ are built

$$\begin{aligned} E^{\mathbf{w}} &= \min_{\{\varphi_p\}} \left\{ \text{Tr} \left[\hat{\gamma}^{\mathbf{w}} \left(\hat{T} + \hat{V}_{en} \right) \right] + E_{\text{Hxc}}^{\mathbf{w}}[n_{\hat{\gamma}^{\mathbf{w}}}] \right\} \\ &= \text{Tr} \left[\hat{\gamma}_{\text{KS}}^{\mathbf{w}} \left(\hat{T} + \hat{V}_{en} \right) \right] + E_{\text{Hxc}}^{\mathbf{w}}[n_{\text{KS}}^{\mathbf{w}}]. \end{aligned} \quad (5.28)$$

From now on, we will use the notation $\{\varphi_p^{\mathbf{w}}\}$ to refer to the minimizing Kohn-Sham weight-dependent orbitals, that is to say the orbitals from which is built the set of single Slater determinantal Kohn-Sham wave functions, $\{\Phi_I^{\mathbf{w}}\} \equiv \{\Phi_I^{\mathbf{w}}[n^{\mathbf{w}}]\}$, that minimize the GOK ensemble energy $E^{\mathbf{w}}$ and mimic the true GOK ensemble density $n^{\mathbf{w}}(\mathbf{r})$.

Hence, in the exact theory, we must have

$$n_{\text{KS}}^{\mathbf{w}}(\mathbf{r}) = \sum_{I=0}^{M-1} w_I n_{\Phi_I^{\mathbf{w}}}(\mathbf{r}) = \sum_{I=0}^{M-1} w_I n_{\Psi_I}(\mathbf{r}) = n^{\mathbf{w}}(\mathbf{r}) \quad (5.29)$$

where $\{n_{\Psi_I}(\mathbf{r}) \equiv n_I(\mathbf{r})\}$ are the exact individual electron densities generated by the exact eigenstates $\{\Psi_I\}$ of the interacting system.

We stress that all the individual states of the ensemble are built from the same set of weight-dependent Kohn-Sham orbitals but will be associated with specific occupation numbers in order to reproduce the different excited configurations.

The individual Kohn-Sham densities can be obtained by summation over all occupied Kohn-Sham squared orbitals for the given state

$$n_{\Phi_I^{\mathbf{w}}}(\mathbf{r}) = \sum_p n_p^I |\varphi_p^{\mathbf{w}}(\mathbf{r})|^2, \quad (5.30)$$

where $\{n_p^I\}$ is the set of occupation numbers of the weight-dependent Kohn-Sham orbitals for the individual single-determinantal Kohn-Sham wave function $\Phi_I^{\mathbf{w}}$ of the I th state of the ensemble. Recall that, for a single determinantal wave function, the occupied and virtual molecular orbitals must verify

$$n_p^{I,\text{occ}} = 1 \quad (5.31) \quad \Bigg| \quad n_p^{I,\text{virt}} = 0. \quad (5.32)$$

Finally, the occupation numbers are inherent to the nature of the states included in the ensemble and, therefore, are fixed and do not depend on the ensemble weights.

GOK-DFT Kohn-Sham equations

The minimizing Kohn-Sham orbitals are the solutions of a set of non-linear equations, the self-consistent GOK-DFT Kohn-Sham equations

$$\left(-\frac{1}{2}\nabla^2 + v(\mathbf{r}) + v_{\text{Hxc}}^{\mathbf{w}}(\mathbf{r}) \right) \varphi_p^{\mathbf{w}}(\mathbf{r}) = \varepsilon_p^{\mathbf{w}} \varphi_p^{\mathbf{w}}(\mathbf{r}) \quad (5.33)$$

where $v(\mathbf{r})$ is the weight-independent local external nuclear potential and $v_{\text{Hxc}}^{\mathbf{w}}(\mathbf{r})$ is the weight-dependent Hartree-exchange-correlation potential

$$v_{\text{Hxc}}^{\mathbf{w}}(\mathbf{r}) = \frac{\delta E_{\text{Hxc}}^{\mathbf{w}}[n]}{\delta n(\mathbf{r})} \quad (5.34)$$

which is the functional derivative of the weight-dependent Hartree-exchange-correlation energy functional $E_{\text{Hxc}}^{\mathbf{w}}[n]$ with respect to the ensemble density $n(\mathbf{r})$.

Hence, we see that GOK-DFT is very similar to the standard ground-state formulation of Kohn-Sham DFT with the substantial difference that the Kohn-Sham solutions are now a set of weight-dependent molecular orbitals $\{\varphi_p^{\mathbf{w}}(\mathbf{r})\}$ with weight-dependent orbital energies $\{\varepsilon_p^{\mathbf{w}}\}$ and that the Hartree-exchange-correlation energy functional must be weight-dependent.

Indeed, since any variation of the ensemble weights will not affect the total number of electron of the system, which will always be N , by construction of the ensemble,

$$\int n^{\mathbf{w}}(\mathbf{r}) d\mathbf{r} = N, \quad \forall \mathbf{w} \quad (5.35)$$

any change in the ensemble weights must be encompassed into the energy functional, and more precisely into the Hartree-exchange-correlation functional through an explicit weight-dependence.

5.2.6 Decomposition of the Ensemble Hxc-Functional

Like in standard Kohn-Sham density-functional theory, a common choice is to decompose $E_{\text{Hxc}}^{\mathbf{w}}[n]$ into three parts, the Hartree, exchange and correlation contributions

$$E_{\text{Hxc}}^{\mathbf{w}}[n] = E_{\text{H}}^{\mathbf{w}}[n] + E_{\text{x}}^{\mathbf{w}}[n] + E_{\text{c}}^{\mathbf{w}}[n] \quad (5.36)$$

with, for each term, the possibility to use standard weight-independent ground-state functionals or to design new weight-dependent functionals.

For instance, for the classical electronic repulsion functional, it is possible to use the standard Hartree functional which does not contain an explicit dependence on the ensemble weights but still possesses an implicit weight-dependence when applied to the ensemble density

$$E_{\text{H}}[n^{\mathbf{w}}] = \frac{1}{2} \iint \frac{n^{\mathbf{w}}(\mathbf{r})n^{\mathbf{w}}(\mathbf{r}')}{|\mathbf{r} - \mathbf{r}'|} d\mathbf{r}d\mathbf{r}'. \quad (5.37)$$

Another intuitive possibility would be to consider that each individual state of the ensemble would contribute commensurately with its respective weight so that the total weight-dependent ensemble Hartree functional would take the form of a linear statistical mixture of the Hartree energies of the individual states built from the ensemble Kohn-Sham orbitals

$$E_{\text{H}}^{\mathbf{w}}[n^{\mathbf{w}}] = \sum_{I=0}^{M-1} w_I E_{\text{H}}[n_{\Phi_I^{\mathbf{w}}}(\mathbf{r})]. \quad (5.38)$$

The exact GOK ensemble exchange energy functional is defined as follows

$$E_{\text{x}}^{\mathbf{w}}[n] = \sum_{I=0}^{M-1} w_I \langle \Phi_I^{\mathbf{w}}[n] | \hat{V}_{\text{ee}} | \Phi_I^{\mathbf{w}}[n] \rangle - E_{\text{H}}[n], \quad (5.39)$$

where \hat{V}_{ee} is the electronic repulsion potential energy operator.

In complete analogy with standard KS-DFT, we define the GOK ensemble correlation energy functional, which stems from the use of non-interacting single Slater determinantal Kohn-Sham wave functions $\{\Phi_I^{\mathbf{w}}\}$ instead of the true interacting eigenstates $\{\Psi_I^{\mathbf{w}}\}$, and which includes the kinetic and potential missing parts of the energy as discussed in Chapter 3

$$\begin{aligned} E_{\text{c}}^{\mathbf{w}}[n] &= \sum_{I=0}^{M-1} w_I \left(\langle \Psi_I^{\mathbf{w}}[n] | \hat{T} + \hat{V}_{\text{ee}} | \Psi_I^{\mathbf{w}}[n] \rangle - \langle \Phi_I^{\mathbf{w}}[n] | \hat{T} + \hat{V}_{\text{ee}} | \Phi_I^{\mathbf{w}}[n] \rangle \right) \\ &= \left(T^{\mathbf{w}}[n] - T_{\text{s}}^{\mathbf{w}}[n] \right) + \left(V_{\text{ee}}^{\mathbf{w}}[n] - E_{\text{H}}^{\mathbf{w}}[n] - E_{\text{x}}^{\mathbf{w}}[n] \right) \\ &= T_{\text{c}}^{\mathbf{w}}[n] + U_{\text{c}}^{\mathbf{w}}[n]. \end{aligned} \quad (5.40)$$

Similarly to standard DFT, the choice of the Hartree, exchange and correlation functionals will be crucial for the accurate prediction of physical properties of interest within the GOK-DFT framework, with an additional challenge stemming from the lack of explicitly weight-dependent approximate functionals specifically designed for ensemble applications on real atomic and molecular systems [28]. Many attempts to go beyond conventional ground state approximate functionals have been explored so far [30, 24, 29, 74], like the Optimized Effective Potential method (OEP) [48] or the use of orbital-dependent Exact-Exchange energy (EXX), to name a few.

The OEP method consists in variationally minimizing an orbital-dependent energy functional

with respect to a local effective potential associated with the orbitals through a set of one-particle Kohn-Sham equations. In OEP, for a given trial local potential, the Kohn-Sham orbitals are determined as solutions of the Kohn-Sham equations associated with this local potential and then the energy is variationally minimized with respect to this local potential instead of the orbitals, as opposed to conventional KS-DFT. Unfortunately, OEP requires a higher computational cost than standard KS-DFT.

Another possibility would be to use orbital-dependent exact-exchange energy (EXX) which consists in using Fock exchange energy functional calculated from the Kohn-Sham orbitals, that is to say orbitals optimized with respect to a local multiplicative potential instead of the non-local Hartree-Fock potential. In the ensemble framework, the construction of an orbital-dependent ensemble exact-exchange functional (EEXX) [27, 21] could be a way to include weight-dependencies into the exchange functional but would remain computationally demanding since the OEP procedure should, in principle, be used.

Recently, accurate ensemble DFT calculations have been performed for very simple systems, such as the helium atom [90] and the hydrogen molecule [6], in order to provide more insight into the weight-dependence of ensemble xc-energies and potentials. In those works, an inversion method as well as Lieb maximisation were used in order to extract and evaluate accurate xc potentials and energies from accurate densities. Still, the need to substantial additional work in order to model the unknown and elusive weight dependence of the ensemble exchange-correlation functional.

5.2.7 Practical Extraction of Individual-State Properties and Excitation Energies

Based on the definition of the GOK ensemble energy and the application of the Hellmann-Feynman theorem, excitations energies can be expressed, in principle exactly, in terms of Kohn-Sham energies and weight derivatives of the exchange-correlation functional

$$\frac{\partial E^{\mathbf{w}}}{\partial w_I} = E_I - E_0 = \mathcal{E}_I^{\mathbf{w}} - \mathcal{E}_0^{\mathbf{w}} + \left. \frac{\partial E_{\text{Hxc}}^{\mathbf{w}}[n]}{\partial w_I} \right|_{n=n_{\text{KS}}^{\mathbf{w}}}. \quad (5.41)$$

In this definition, $\mathcal{E}_I^{\mathbf{w}}$ is the I th weight-dependent Kohn-Sham auxiliary total energy, obtained by summation of the energy of the Kohn-Sham orbitals which are occupied in the I th state of the ensemble

$$\mathcal{E}_I^{\mathbf{w}} = \sum_p n_p^I \varepsilon_p^{\mathbf{w}}. \quad (5.42)$$

We stress that, even in the exact theory, that is to say with the exact functional, $\mathcal{E}_I^{\mathbf{w}}$ is not equal to the exact energy associated with the true eigenstates Ψ_I . As it was pointed out in the density-functional theory chapter, the exact total energy of the system is not the sum of the occupied Kohn-Sham orbital energies.

Hence, for each excited state included in the ensemble, there will be an additional shift in the

Hartree-exchange-correlation potential which will result in a weight derivative of the Hxc-energy functional with respect to the weight of the additional excited state. Although the physics encompassed within GOK-DFT is different from the scope of PPLB DFT, derivative discontinuities also exist in GOK-DFT and are directly connected to the weight-derivatives of the Hxc-functional. Moreover, note that, as opposed to PPLB DFT, in GOK-DFT the Kohn-Sham potential is not uniquely defined but only up to a constant.

In conventional ground state DFT, Levy and Zahariev proposed to inject a shift in the Hartree-exchange-correlation potential in order to reformulate the exact total ground state energy of the system in terms of the above-mentioned Kohn-Sham auxiliary energy only. The Levy-Zahariev shifting procedure has since been extended to GOK ensembles where the weight-dependent Levy-Zahariev shift for the potential is defined as follows

$$\bar{v}_{\text{Hxc}}^{\mathbf{w}}(\mathbf{r}) = v_{\text{Hxc}}^{\mathbf{w}}(\mathbf{r}) + \frac{E_{\text{Hxc}}^{\mathbf{w}}[n] - \int v_{\text{Hxc}}^{\mathbf{w}}(\mathbf{r})n(\mathbf{r})d\mathbf{r}}{\int n(\mathbf{r})d\mathbf{r}}, \quad (5.43)$$

where $\bar{v}_{\text{Hxc}}^{\mathbf{w}}(\mathbf{r})$ is the LZ-shifted Hartree-exchange-correlation potential and $v_{\text{Hxc}}^{\mathbf{w}}(\mathbf{r})$ is the originally unshifted potential

$$v_{\text{Hxc}}^{\mathbf{w}}(\mathbf{r}) = \frac{\delta E_{\text{Hxc}}^{\mathbf{w}}[n]}{\delta n(\mathbf{r})}. \quad (5.44)$$

Once the LZ-shifting procedure is applied to the potential, the GOK ensemble energy reduces to a more convenient expression and will be reformulated as a weighted sum of the LZ-shifted Kohn-Sham auxiliary total energies

$$E^{\mathbf{w}} = \left(1 - \sum_{I=1}^{M-1} w_I\right) \bar{\mathcal{E}}_0^{\mathbf{w}} + \sum_{I=1}^{M-1} w_I \bar{\mathcal{E}}_I^{\mathbf{w}}. \quad (5.45)$$

Since the GOK ensemble density must always integrate to the fixed number of electrons N and since all the states of the ensemble are associated with that same fixed number of electrons, the Kohn-Sham auxiliary energies of the individual states of the ensemble will all be obtained from distinct sets of N occupied Kohn-Sham orbital energies and will be equally shifted as follows

$$\bar{\mathcal{E}}_I^{\mathbf{w}} = \mathcal{E}_I^{\mathbf{w}} + E_{\text{Hxc}}^{\mathbf{w}}[n_{\text{KS}}^{\mathbf{w}}] - \int \frac{\delta E_{\text{Hxc}}^{\mathbf{w}}[n_{\text{KS}}^{\mathbf{w}}]}{\delta n(\mathbf{r})} n_{\text{KS}}^{\mathbf{w}}(\mathbf{r})d\mathbf{r}. \quad (5.46)$$

Note that the Kohn-Sham excitation energies are not affected by the LZ-shift

$$\bar{\mathcal{E}}_I^{\mathbf{w}} - \bar{\mathcal{E}}_0^{\mathbf{w}} = \mathcal{E}_I^{\mathbf{w}} - \mathcal{E}_0^{\mathbf{w}}. \quad (5.47)$$

Excitation energies are not the only properties that can be extracted from a single GOK-DFT ensemble calculation. Individual properties such as ground and excited state energies

$$E_I = \bar{\mathcal{E}}_I^{\mathbf{w}} + \sum_{J=1}^M (\delta_{JI} - w_J) \frac{\partial E_{\text{Hxc}}^{\mathbf{w}}}{\partial w_J}, \quad (5.48)$$

and densities

$$n_I(\mathbf{r}) = n_{\Psi_I}(\mathbf{r}) = n_{\Phi_I^w}(\mathbf{r}) + \sum_{J=1}^M \sum_{K=0}^M (\delta_{JI} - w_J) w_K \frac{\partial n_{\Phi_K^w}(\mathbf{r})}{\partial w_J}, \quad (5.49)$$

can be recovered as well from the ensemble.

The following work focus on the extraction of excitation energies from GOK-DFT ensemble calculations.

5.3 Numerical Implementation of GOK-DFT

5.3.1 With Standard Weight-Independent Exchange-Correlation Functionals

Biensembles

As a first concrete application of GOK-DFT, we will consider two specific GOK biensembles applied to a set of two-electron atomic and molecular systems, the helium atom He, the hydrogen molecule H_2 in its equilibrium geometry ($R_{\text{H-H}} = 1.40$ bohr) and the helium hydride cation HeH^+ also in its equilibrium geometry ($R_{\text{He-H}} = 1.46$ bohr). Calculations will be performed by the QuAcK eDFT Fortran code especially implemented during this PhD thesis to perform ensemble DFT calculations. Various basis sets and levels of approximations will be used in order to give a more complete overview of the practical application of the theory.

In that spirit, we will first consider the two-state ensemble including the ground state energy $E_0^N \equiv E_0$ of the N -electron system (with $N = 2$) and its first singly-excited singlet state energy $E_1^N \equiv E_1$ which we will admit to be the lower excited state energy of the system. This biensemble will be referred to as the “single” GOK biensemble and takes the following form

$$E^{w_1} = (1 - w_1)E_0 + w_1E_1. \quad (5.50)$$

Table 5.1: Electronic configurations of the individual states of the “single” GOK biensemble applied to a system with $N = 2$ electrons.

State of the ensemble	Weight	Spin	Occupation numbers					
1	$1 - w_1$	↑	1	0	0	0	0	0
		↓	1	0	0	0	0	0
2	w_1	↑	0	1	0	0	0	0
		↓	1	0	0	0	0	0

Similarly, we will also consider a second biensemble by including only the ground state energy of the system and its lower doubly-excited singlet state energy $E_2^N \equiv E_2$ which we

will admit to be the lower excited state energy of the system. This biensemble will then be referred to as the “double” GOK biensemble and is expressed as

$$E^{w_2} = (1 - w_2)E_0 + w_2E_2. \quad (5.51)$$

Tables 5.1 and 5.2 summarize the main characteristics of the “single” and “double” GOK biensembles that will serve as inputs for the eDFT Fortran code.

Table 5.2: Electronic configurations of the individual states of the “double” GOK biensemble applied to a system with $N = 2$ electrons.

State of the ensemble	Weight	Spin	Occupation numbers					
1	$1 - w_2$	↑	1	0	0	0	0	0
		↓	1	0	0	0	0	0
2	w_2	↑	0	1	0	0	0	0
		↓	0	1	0	0	0	0

Although GOK theory enforces GOK ensembles to arrange ground and excited state energies in increasing order, we will exceptionnally ignore this requirement in order to study separately the impact of each excited state in the ensemble. Moreover, the domain of validity of the GOK variational principle requires both weights of the above-mentioned biensembles to be restricted to the range $0 \leq w_i \leq \frac{1}{2}$, with $i \in \{1; 2\}$, but we will intentionally extend the study by exploring the full range of weights $0 \leq w_1 \leq 1$ and $0 \leq w_2 \leq 1$ in order to build weight-dependent exchange-correlation functionals afterwards.

Hence, we see that for such GOK biensembles, despite the fact that the GOK variational principle requires the weights w_1 and w_2 to be restricted to the domain $[0, \frac{1}{2}]$, for the zero-weight limits $w_i = 0$ and for the particular weight configurations $w_1 = 1$ and $w_2 = 1$, the GOK biensemble calculations reduce to standard DFT calculations and must yield standard DFT references for the ground state energy

$$E^{w_1=0} = E^{w_2=0} = E_0, \quad (5.52)$$

the singly-excited state energy

$$E^{w_1=1} = E_1, \quad (5.53)$$

and the doubly-excited state energy

$$E^{w_2=1} = E_2, \quad (5.54)$$

respectively. We would like to stress out that these individual energies will not necessarily match the exact ground and excited states of the system unless in the scope of the exact theory. In practice, since the exact universal functional defined by Hohenberg and Kohn is not known, one must rely on approximations instead and will obtain approximated ground and excited state energies.

Our interest will be to extract the corresponding single and double excitation energies of the

system, defined as total energy differences between the singly-excited state energy and the ground state energy,

$$\Omega_1 = E_1 - E_0, \quad (5.55)$$

and between the doubly-excited state energy and the ground state energy of the system

$$\Omega_2 = E_2 - E_0. \quad (5.56)$$

Note that, in standard DFT, predictions of these quantities would require to perform two standard DFT calculations for each excitation energy while in the GOK biensemble frameworks defined previously, a single biensemble calculation can allow one to extract one of these excitation energies according to equation (E.15).

If one uses conventional weight-independent approximate functionals, there will be no contribution from the weight-derivative term in equation (E.15) and the ensemble predictions of the excitation energies will be solely determined by the corresponding weight-dependent Kohn-Sham auxiliary excitation energies. In accordance with the electronic configurations of the individual states of the “single” and “double” GOK biensembles, depicted in Tables 5.1 and 5.2, it is straightforward to see that the ensemble Kohn-Sham auxiliary excitation energies reduces to

$$\Omega_1^{\text{KS}} = \varepsilon_2^\uparrow - \varepsilon_1^\uparrow, \quad (5.57)$$

for the lowest single excitation energy, also known as the optical gap, and

$$\Omega_2^{\text{KS}} = (\varepsilon_2^\uparrow + \varepsilon_2^\downarrow) - (\varepsilon_1^\uparrow + \varepsilon_1^\downarrow), \quad (5.58)$$

for the lowest double excitation energy.

In order to study the performance of a given approximate functionals in GOK ensemble DFT compared to its performance in standard ground state DFT, we will compare the GOK ensemble predictions of the above-mentioned excitation energies to the ΔSCF references that one would obtain by performing total energy differences between multiple standard DFT calculations. To avoid confusion, we recall the definition of the ΔSCF excitation energies, which will be used as references in this work

$$\Omega_1^{\Delta\text{SCF}} = E^{w_1=1} - E^{w_1=0}, \quad (5.59)$$

$$\Omega_2^{\Delta\text{SCF}} = E^{w_2=1} - E^{w_2=0}. \quad (5.60)$$

For comparison, we will also report the excitation energy predictions obtained with the Linear Interpolation Method (LIM) [78] which consists in extracting weight-independent (by construction) excitation energies from equiensembles energies. By applying the LIM method to the two above-mentioned GOK biensembles, we obtain the following compact notation

$$\Omega_i^{\text{biLIM}} = 2 \left[E^{w_i=\frac{1}{2}} - E^{w_i=0} \right], \quad (5.61)$$

where $i \in \{1; 2\}$.

In GOK-DFT, the exact weight-dependent xc-functional would yield a perfectly linear ensemble energy and, hence, a constant value of the excitation energies independently of the ensemble weights. In practice, because conventional density-functional approximations (DFAs) do not depend on the ensemble weights, the resulting ensemble energy will be far from being linear and there will be no contribution to the excitation energies from the weight-derivative term in equation (E.15). The deviation from linearity of the “single” and “double” GOK biensemble energies of He is depicted in Figure E.4 for various approximate xc-functionals.

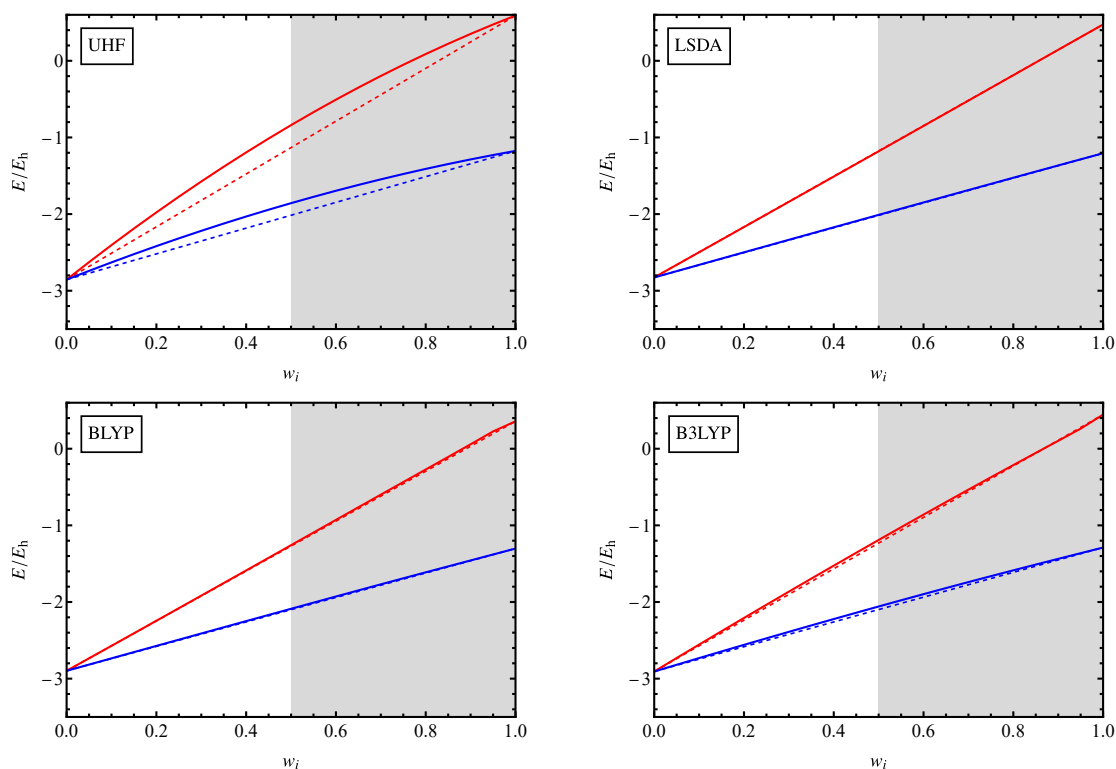


Figure 5.1: Violation of the linearity exact-criteria of the GOK ensemble energy of He obtained for the single (blue) and double (red) GOK biensembles for various methods and levels of xc-approximation in the cc-pVDZ basis set. The SCF GOK ensemble energies (solid line) are compared to the corresponding linear interpolations (dashed line). The shaded areas highlight the GOK variational principle restricted-domain of validity.

In order to quantify the deviation from linearity of the “single” and “double” GOK-biensembles, the curvature of both ensemble energies was evaluated by computing the area between the ensemble energy curves and the linear interpolations in between the two weight limits $w_i = 0$ and $w_i = 1$, with $i \in \{1; 2\}$. To do so, the trapezoidal rule was used and percent errors of the curvature were computed. We report in Table 5.3 the curvature percent errors of the GOK biensemble energies applied to He, H_2 and HeH^+ , with various methods, xc-functionals and basis sets. Whereas this work is focused on two-electron systems, it appears that even for such “simple” systems, the curvature of GOK biensemble energies can be highly dependent on the system of interest, the nature of the ensemble, the choice of method and

approximation or the basis set used to perform the calculations. Despite the observation that unrestricted Hartree-Fock (UHF) seems to yield positive curvatures while density-functional approximations (DFAs) show a tendency to yield negative curvatures and that “double” GOK biensemble energies seem to have larger curvature than the “single” GOK biensemble energies, it seems to be no clear “rule of thumb” that may be used to classify somehow the curvature of GOK ensemble energies. Hence revealing the subtleties that a potential accurate “ensemble” functional may have to overcome in order to yield an overall efficiency for a wide range of systems, applications . . .

Table 5.3: Estimation of the curvature of the GOK ensemble energies of the “single” and “double” biensemble energies. The curvature errors are expressed in terms of percent errors compared to the linear interpolation of the ensemble energies in between the two limits of the weight, $w_i = 0$ and $w_i = 1$, with $i \in \{1; 2\}$. Calculations were performed in both cc-pVDZ and cc-pVQZ basis sets, with unrestricted Hartree-Fock (UHF) and standard weight-independent density-functional approximations (DFAs), LSDA, BLYP and B3LYP.

	UHF		LSDA		BLYP		B3LYP	
	cc-pVDZ	cc-pVQZ	cc-pVDZ	cc-pVQZ	cc-pVDZ	cc-pVQZ	cc-pVDZ	cc-pVQZ
“Single” GOK biensemble curvature (%)								
He	5.212	2.969	0.208	-0.327	0.365	-0.213	1.257	0.390
H ₂	6.373	5.733	-0.094	-0.242	0.141	-0.038	1.301	1.056
HeH ⁺	3.398	3.387	-0.291	-0.269	-0.206	-0.181	0.503	0.517
“Double” GOK biensemble curvature (%)								
He	17.198	3.426	-0.209	-5.899	0.923	-6.214	1.830	-4.242
H ₂	15.468	13.780	-3.967	-4.547	-3.761	-4.353	-0.103	-0.834
HeH ⁺	4.671	4.985	-5.740	-5.153	-5.914	-5.311	-3.739	-3.214

Since weight-dependent approximate xc-functionals fail to provide perfectly linear GOK ensemble energies, excitation energies associated with the singly- and doubly-excited states obtained via the derivatives of the biensemble energies with respect to the weights w_1 and w_2 , respectively, vary significantly with the weights, which is highly unphysical, compared to the Δ SCF references obtained within standard DFT with the same level of approximations, as depicted in Figures 5.2 and 5.3 in the case of the helium atom.

As expected, equiensemble weight-configurations, $w_i = 0.5$, tend to yield predictions of the single and double excitation energies that are in good accordance with what one would obtain in the scope of standard DFT with the Δ SCF method. Interestingly, when the ensemble Kohn-Sham excitation energies are nearly linear in the range $w_i \in [0, 0.5]$, the particular weight configurations $w_i = 0.25$ tend to match the linear interpolation method (LIM) weight-independent predictions obtained from equiensemble energies. In the case of the single excitation energy, we see that in the zero-weight limit, which corresponds to a standard ground-state DFT calculation, the ensemble Kohn-Sham prediction overestimates the excitation energy for all methods and functionals considered compared to the Δ SCF predictions.

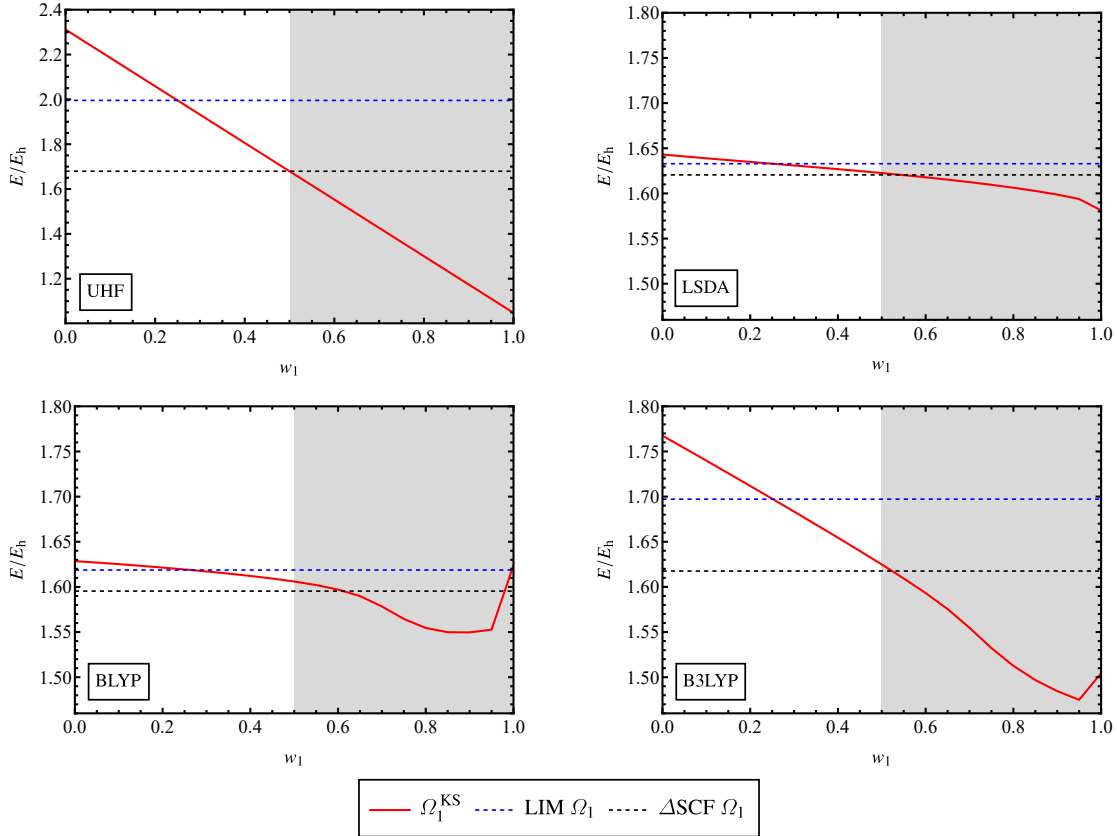


Figure 5.2: Weight-dependence of the lowest single excitation energy of He obtained from the “single” GOK biensemble for various methods and xc-approximations in the cc-pVDZ basis set. The weight-dependent ensemble Kohn-Sham excitation energies (equation (5.57)) are compared to the corresponding weight-independent Linear Interpolation Method (LIM) predictions (equation (5.61)) and the ΔSCF predictions (equation (5.66)) obtained by total energy differences within the same level of approximation. The shaded areas highlight the GOK variational principle restricted-domain of validity.

The LIM predictions tend as well to yield overestimated predictions for the single and double excitations but with an amount up to twice smaller than the zero-weight ensemble Kohn-Sham predictions. For the double excitations depicted in Figure 5.3, only the LSDA functional yield an underestimated LIM prediction relative to the ΔSCF compared to the other approximations considered. Moreover, the LSDA and BLYP ensemble Kohn-Sham double excitation energies are increasing functions of the weight while all the other ensemble Kohn-Sham predictions of both single and double excitation energies of He are decreasing functions of the weights.

Note that, although convergence of the SCF ensemble DFT calculation have been achieved, the BLYP GGA xc-functional has shown some difficulties to yield perfectly smooth ensemble Kohn-Sham prediction for both single and double excitation energies of He in the range $w_i \in [0.5, 1]$ which one may consider without consequence since it is out of the GOK variational principle validity domain.

Tables 5.4, 5.5 and 5.6 provide a more detailed overview of the weight-dependence of the

ensemble Kohn-Sham predictions of the single and double excitation energies of He, H₂ and HeH⁺ for various weight-configurations, methods, xc-functionals and basis sets.

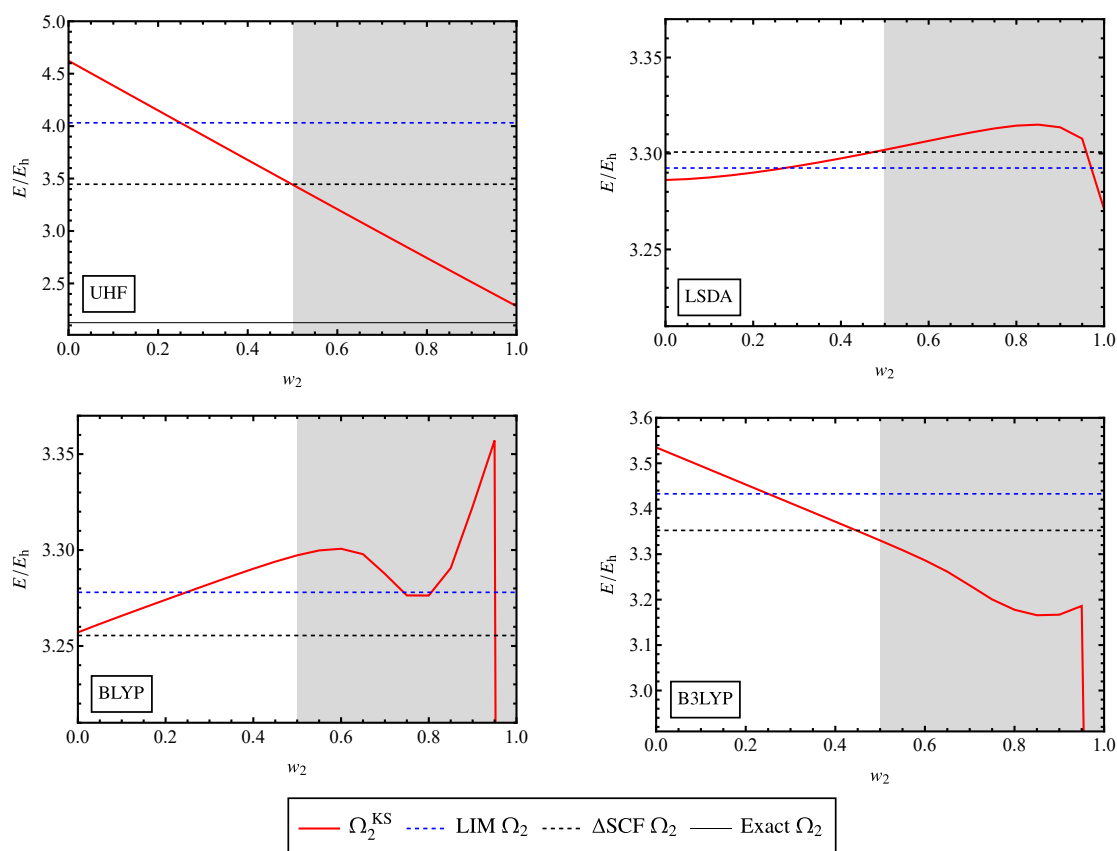


Figure 5.3: Weight-dependence of the lowest double excitation energy of He obtained from the “double” GOK biensemble for various methods and xc-approximations in the cc-pVDZ basis set. The weight-dependent ensemble Kohn-Sham excitation energies (5.58) are compared to the corresponding weight-independent Linear Interpolation Method (LIM) predictions (equation (5.61)) and the Δ SCF predictions (5.67) obtained by total energy differences within the same level of approximation. The exact lowest double excitation of He (from [8]) is reported as well for comparison. The shaded areas highlight the GOK variational principle restricted-domain of validity.

Table 5.4: Single and double GOK biensemble predictions for the lowest single and double excitation energies of He compared to the linear interpolation method (LIM) and ASCF predictions. The ensemble Kohn-Sham excitation energies are expressed in terms of percent errors compared to the ASCF references (in hartree). Calculations have been performed in the cc-pVDZ and cc-pVQZ basis sets and within various levels of approximation.

	UHF		LSDA		BLYP		B3LYP	
	cc-pVDZ	cc-pVQZ	cc-pVDZ	cc-pVQZ	cc-pVDZ	cc-pVQZ	cc-pVDZ	cc-pVQZ
ASCF Ω_1	1.679 51	0.920 00	1.620 50	0.910 54	1.595 35	0.905 55	1.617 58	0.915 73
LIM Ω_1	1.995 46	1.134 32	1.632 88	0.886 307	1.618 69	0.889 78	1.697 18	0.944 71
Δ (%) LIM Ω_1	18.811	23.294	0.763	-2.661	1.464	-1.742	4.920	3.166
	Δ (%) Kohn-Sham gap $\epsilon_2^\downarrow - \epsilon_1^\uparrow$							
$w_1 = 0.05$	33.869	42.159	1.262	-4.167	1.981	-3.366	8.415	5.534
$w_1 = 0.25$	18.809	23.232	0.765	-2.915	1.503	-1.639	4.949	3.233
$w_1 = 0.50$	-0.005	-0.0104	0.126	-0.080	0.666	-0.114	0.446	-0.071
ASCF Ω_2	3.445 89	2.338 25	3.300 73	2.253 11	3.255 47	2.311 45	3.352 33	2.319 25
LIM Ω_2	4.031 68	2.512 05	3.292 41	1.944 84	3.277 97	1.982 58	3.432 80	2.094 04
Δ (%) LIM Ω_2	16.999	7.433	-0.251	-13.682	0.691	-14.227	2.400	-9.710
	Δ (%) Kohn-Sham gap $(\epsilon_2^\uparrow + \epsilon_2^\downarrow) - (\epsilon_1^\uparrow + \epsilon_1^\downarrow)$							
$w_2 = 0.05$	30.722	13.899	-0.426	-21.507	0.185	-22.919	4.840	-15.271
$w_2 = 0.25$	16.983	7.308	-0.275	-14.473	0.698	-14.728	2.401	-10.141
$w_2 = 0.50$	-0.102	-0.272	0.035	-1.527	1.284	-1.790	-0.661	-1.426

Table 5.5: Single and double GOK biensemble predictions for the lowest single and double excitation energies of H_2 compared to the linear interpolation method (LIM) and ΔSCF predictions. The ensemble Kohn-Sham excitation energies are expressed in terms of percent errors compared to the ΔSCF references (in hartree). Calculations have been performed in the cc-pVDZ and cc-pVQZ basis sets and within various levels of approximation.

	UHF			LSDA			BLYP			B3LYP		
	cc-pVDZ	cc-pVQZ	cc-pVQZ									
$\Delta\text{SCF } \Omega_1$	0.43458	0.42039	0.43285	0.43285	0.42287	0.42726	0.41930	0.41930	0.43441	0.42571		
LIM Ω_1	0.60920	0.57958	0.42986	0.41559	0.43066	0.41732	0.47143	0.45586				
Δ (%) LIM Ω_1	40.180	37.865	-0.691	-1.722	0.795	-0.472	8.521	7.083				
Δ (%) Kohn-Sham gap $\epsilon_2^\uparrow - \epsilon_1^\uparrow$												
$w_1 = 0.05$	73.211	68.055	-1.165	-2.945	0.591	-1.626	14.719	12.020				
$w_1 = 0.25$	40.010	37.866	-0.842	-1.959	0.789	-0.558	8.529	7.049				
$w_1 = 0.50$	-0.561	0.100	0.293	0.404	1.010	1.136	0.705	0.936				
$\Delta\text{SCF } \Omega_2$	1.06418	1.05647	1.00643	1.00191	1.01267	1.01114	1.02634	1.02362				
LIM Ω_2	1.34148	1.30762	0.92927	0.91259	0.93869	0.92398	1.02439	1.00686				
Δ (%) LIM Ω_2	26.057	23.773	-7.666	-8.915	-7.305	-8.619	-0.189	-1.637				
Δ (%) Kohn-Sham gap $(\epsilon_2^\uparrow + \epsilon_2^\downarrow) - (\epsilon_1^\uparrow + \epsilon_1^\downarrow)$												
$w_2 = 0.05$	44.139	37.137	-13.838	-16.770	-13.752	-16.881	-1.419	-5.157				
$w_2 = 0.25$	26.481	24.737	-7.933	-9.124	-7.384	-8.625	-0.158	-1.453				
$w_2 = 0.50$	2.072	3.977	0.733	1.327	0.863	1.525	1.127	1.995				

Table 5.6: Single and double GOK biensemble predictions for the lowest single and double excitation energies of HeH^+ compared to the linear interpolation method (LIM) and ASCF predictions. The ensemble Kohn-Sham excitation energies are expressed in terms of percent errors compared to the ASCF references (in hartree). Calculations have been performed in the cc-pVDZ and cc-pVQZ basis sets and within various levels of approximation.

	UHF		LSDA		BLYP		B3LYP	
	cc-pVDZ	cc-pVQZ	cc-pVDZ	cc-pVQZ	cc-pVDZ	cc-pVQZ	cc-pVDZ	cc-pVQZ
ASCF Ω_1	0.87274	0.86062	0.87350	0.86300	0.86196	0.85352	0.87025	0.86107
LIM Ω_1	1.12695	1.11575	0.85110	0.84198	0.84538	0.83859	0.90831	0.90034
Δ (%) LIM Ω_1	29.126	29.643	-2.564	-2.435	-1.924	-1.749	4.374	4.561
	Δ (%) Kohn-Sham gap $\epsilon_2^\downarrow - \epsilon_1^\uparrow$							
$w_1 = 0.05$	52.061	52.941	-3.873	-3.786	-2.662	-2.646	8.359	8.480
$w_1 = 0.25$	29.193	29.751	-2.848	-2.707	-2.216	-1.997	4.187	4.405
$w_1 = 0.50$	0.245	0.204	-0.151	-0.006	-0.184	0.054	-0.095	0.077
ASCF Ω_2	2.26081	2.21731	2.20155	2.15496	2.23116	2.18747	2.23844	2.19496
LIM Ω_2	2.51283	2.49124	1.88570	1.86511	1.89891	1.88253	2.02784	2.00977
Δ (%) LIM Ω_2	11.147	12.354	-14.346	-13.450	-14.891	-13.940	-9.408	-8.437
	Δ (%) Kohn-Sham gap $(\epsilon_2^\uparrow + \epsilon_2^\downarrow) - (\epsilon_1^\uparrow + \epsilon_1^\downarrow)$							
$w_2 = 0.05$	19.743	21.218	-22.515	-21.686	-23.218	-22.409	-14.156	-13.237
$w_2 = 0.25$	11.225	12.586	-15.144	-14.159	-15.680	-14.617	-10.018	-8.937
$w_2 = 0.50$	0.178	0.588	-1.722	-1.043	-2.059	-1.297	-1.607	-0.928

Triensembles

Let us define the GOK “triensemble” which includes the three lowest electronic states of the N -electron system, which we will assume to be the ground state, the lowest singly-excited state and the lowest doubly-excited state. Thus, this triensemble will contain the ground state of configuration $1s^2$, the lowest singly-excited state of configuration $1s2s$ and the first doubly-excited state of configuration $2s^2$. We assume that the singly-excited state is lower in energy than the doubly-excited state and that there are no additional lower-in-energy single excitations between the ground state and the doubly-excited state which can be a rather crude assumption for some systems.

For instance, in the particular case of the hydrogen molecule in a stretched geometry, with $R_{\text{H-H}} = 3.7$ bohr, the doubly-excited state becomes the lowest excited state with the same symmetry as the ground state and, therefore, should be included in the GOK ensemble accordingly. Moreover, in practice, there may be a large number of singly-excited states lying in between the ground state and the lowest doubly-excited state. Although it may not be consistent with the GOK theory to ignore those additional low-lying excited states, from a practical point of view, it is impossible to take into account a complete finite spectrum of a system in order to access a specific excitation energy. Therefore, in this work, we take the liberty to study a more practical type of GOK ensemble.

We will first distinguish the two-weight triensemble

$$E^{\mathbf{w}} = (1 - w_1 - w_2)E_0 + w_1E_1 + w_2E_2, \quad (5.62)$$

where $\mathbf{w} = \{w_1; w_2\}$, and the single-weight triensemble which is a variant of the former triensemble where $w_1 = w_2 = w$

$$E^w = (1 - 2w)E_0 + wE_1 + wE_2. \quad (5.63)$$

Note that, to ensure the validity of the GOK variational principle, one should have

$$0 \leq w_2 \leq \frac{1}{3} \quad (5.64) \quad \left| \quad w_2 \leq w_1 \leq \frac{1}{2}(1 - w_2). \quad (5.65)$$

Table 5.7 summarizes the characteristics of the GOK triensemble that will serve as inputs for the eDFT Fortran code.

Table 5.7: Electronic configurations of the individual states of the GOK triensemble applied to two-electron systems.

State of the ensemble	Weight	Spin	Occupation numbers					
1	$1 - w_1 - w_2$	↑	1	0	0	0	0	0
		↓	1	0	0	0	0	0
2	w_1	↑	0	1	0	0	0	0
		↓	1	0	0	0	0	0
3	w_2	↑	0	1	0	0	0	0
		↓	0	1	0	0	0	0

Based on that definition of the GOK triensemble, we straightforwardly retrieve the Δ SCF predictions of the single and double excitation energies that one would obtain by total energy differences

$$\Omega_1^{\Delta\text{SCF}} = E^{w_1=1;w_2=0} - E^{w_1=0;w_2=0}, \quad (5.66)$$

and

$$\Omega_2^{\Delta\text{SCF}} = E^{w_1=0;w_2=1} - E^{w_1=0;w_2=0}. \quad (5.67)$$

The “equitriensemble” corresponds to the particular weight configuration $\{w_1 = w_2 = w = \frac{1}{3}\}$ where the three individual states contribute equally to the GOK ensemble

$$E^{w=\frac{1}{3}} = \frac{1}{3}E_0 + \frac{1}{3}E_1 + \frac{1}{3}E_2. \quad (5.68)$$

The “single” and “double” excitation energies extracted from this particular ensemble will be referred to as “equitri Ω_1 ” and “equitri Ω_2 ”, respectively.

Moreover, in order to extract multiple excitation energies from the GOK triensemble defined previously, we will apply the Linear Interpolation Method which can be easily extended to higher excitations [77]. These excitations will be referred to as “triLIM Ω_1 ” and “triLIM Ω_2 ”. In the case of an ensemble of three non-degenerate states, the first LIM excitation energy is identical to the one obtained from the “single” GOK biensemble

$$\Omega_1^{\text{triLIM}} = 2 \left[E^{w_1=\frac{1}{2};w_2=0} - E^{w_1=0;w_2=0} \right]. \quad (5.69)$$

while the second LIM excitation energy takes the form

$$\Omega_2^{\text{triLIM}} = 3 \left[E^{w_1=\frac{1}{3};w_2=\frac{1}{3}} - E^{w_1=\frac{1}{2};w_2=0} \right] + \frac{1}{2} \Omega_1^{\text{triLIM}}. \quad (5.70)$$

We have computed the various above-mentioned predictions of the single and double excitation energies in order to highlight to what extent one given excited state of the GOK triensemble may influence the accuracy of each ensemble excitation energies. The results obtained for the helium atom within the LSDA approximation and the cc-pVDZ basis set are depicted in Figures E.5 and 5.5 for both excitation energies.

In the case of the single excitation energy, we see that the addition of the doubly-excited state to the GOK triensemble, by increase of the weight w_2 , has only very small impact on the prediction of the single excitation energy, slightly increasing the ensemble prediction of the latter. Similarly, the variation of the weight w_1 of the singly-excited state will not have a significant impact on the quality of the ensemble double excitation energy, as depicted in Figure 5.5. Conversely the equiensemble limit, $w_1 = w_2 = \frac{1}{3}$, yield significantly overestimated single and double excitation energies by around 0.1 hartree and 0.2 hartree, respectively, compared to the Δ SCF predictions.

The LIM single excitation energy is as well higher than the Δ SCF prediction, but with a smaller increase, around 0.01 hartree. Interestingly, for the double excitation energy, the presence of the singly-excited state in the GOK triensemble yields a surprisingly and significantly lower LIM double excitation energy, by around 1.5 hartree compared to the Δ SCF

prediction, which is actually much closer to the exact double excitation energy of He (see Table 5.8). Finally, note that the single-weight GOK triensemble doesn't seem to be a pertinent choice to obtain accurate predictions of the single and double excitation energies, yielding drastically too high excitation energies as the ensemble weight increases.

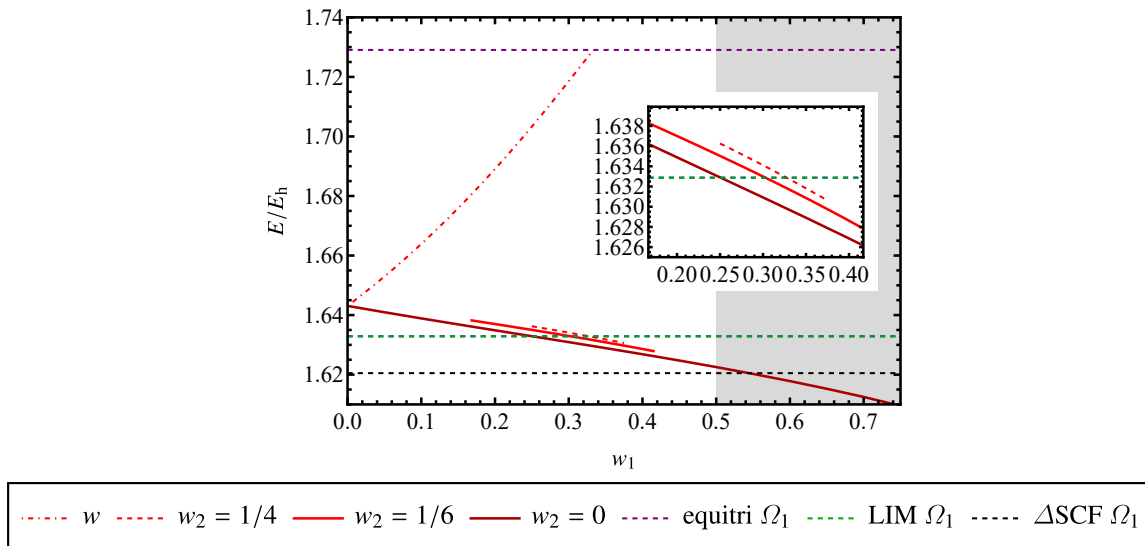


Figure 5.4: Weight-dependence of the lowest single excitation energy of He obtained from GOK triensembles. The ensemble Kohn-Sham single excitation energies obtained from GOK triensembles are reported for the single-weight configuration ($w_1 = w_2 = w$, see equation (E.12)), for various weight-configurations of the two-weight triensemble (equation (E.11)) as well as for the equiensemble configuration ($w_1 = w_2 = \frac{1}{3}$, see equation (5.68)) and are compared to single excitations obtained from the “single” GOK biensemble ($w_2 = 0$), the Linear Interpolation Method (LIM) prediction obtained from the biensemble or triensemble, equivalently, (equations (5.61) and (5.69)) as well as the Δ SCF prediction (equation (5.66)) obtained with the same level of approximation. Calculations were performed within the LSDA approximation and in the cc-pVDZ basis set.

For a more quantitative overview, Table 5.8 reports excitation energies of He, H₂ and HeH⁺, for various methods and exchange-correlation functionals in the cc-pVDZ basis set. In particular, we report the excitation energies obtained with GOK-DFT for the equiensemble configurations of the biensembles and triensemble considered in this work. For comparison, we also report results obtained with the Linear Interpolation Method (LIM) applied to both biensembles (biLIM) and triensemble (triLIM) defined in equations (5.61), (5.69) and (5.70). Note that two calculations are needed to get the first triLIM excitation energy with an additional equiensemble calculation for each higher excitation energy. Additionally, Δ SCF excitation energies, defined in equations (5.66) and (5.67), which also require three separate calculations at specific set of ensemble weights, have been computed to highlight the “poor” performance of conventional weight-independent ground state xc-functionals when used in the scope of GOK ensemble DFT calculations. Finally, we report accurate predictions of the double excitation energy of He and H₂ at equilibrium bond length,

obtained from [59].

It is worth mention that in the case of the helium atom, the lowest doubly-excited state is extremely high in energy and lies in the continuum. For that reason, its description requires the use of a basis set containing enough diffuse functions. In this work we used the same basis sets for all two-electron systems considered, independently of such consideration. Based on the poor results obtained for the double excitation energy of He, compared to the accurate reference reported in Table 5.8, the choice of the basis set may be held responsible for that particular system (see Table C.1 for additional results regarding this point). Nevertheless, despite the possibly inappropriate basis set, the linear interpolation method (LIM) still manages to yield a more accurate prediction of the double excitation energy compared to all other predictions.

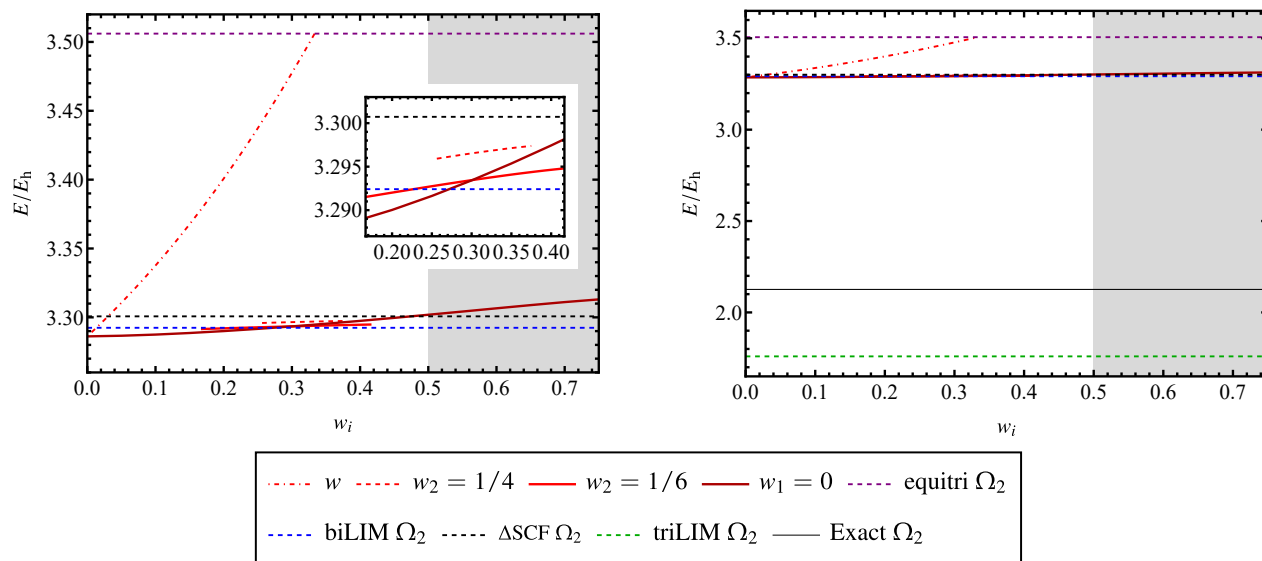


Figure 5.5: Weight-dependence of the lowest double excitation energy of He obtained from GOK triensembles. The ensemble Kohn-Sham double excitations obtained from GOK triensembles are reported for the single-weight configuration ($w_1 = w_2 = w$, see equation (E.12)), for various weight-configurations of the two-weight triensemble (equation (E.11)) as well as for the equiensemble configuration ($w_1 = w_2 = \frac{1}{3}$, see equation (5.68)) and are compared to double excitations obtained from the “double” GOK biensemble ($w_1 = 0$), the Linear Interpolation Method (LIM) predictions obtained from the biensemble (equation (5.61)) and triensemble (equation (5.70)) as well as the Δ SCF prediction (equation (5.67)) obtained with the same level of approximation and the exact double excitation (from [8]). Calculations were performed within the LSDA approximation and in the cc-pVDZ basis set.

Table 5.8: Excitation energies (in hartree) associated with the lowest single and double excitations of He, H₂ with $R_{\text{H-H}} = 1.40$ bohr and HeH⁺ with $R_{\text{He-H}} = 1.46$ bohr, for various methods and exchange-correlation functionals in the cc-pVDZ basis set. Accurate predictions of the single and double excitation energies of He and H₂ are also reported for comparison.

	UHF	LSDA	BLYP	B3LYP		
He	$\Delta\text{SCF } \Omega_1$	1.679 51	1.620 50	1.595 35	1.617 58	
	biLIM Ω_1	1.995 46	1.632 88	1.618 69	1.697 18	
	equibi Ω_1	1.679 42	1.622 55	1.605 98	1.624 80	
	triLIM Ω_1	1.995 46	1.632 88	1.618 69	1.697 18	
	equitri Ω_1	1.741 72	1.729 06	1.721 80	1.728 68	
	Accurate ^a				0.757 75	
	$\Delta\text{SCF } \Omega_2$	3.445 89	3.300 73	3.255 47	3.352 33	
	biLIM Ω_2	4.031 68	3.292 41	3.277 97	3.432 80	
	equibi Ω_2	3.442 36	3.301 89	3.297 26	3.330 17	
	triLIM Ω_2	2.105 19	1.759 43	1.805 39	1.888 48	
	equitri Ω_2	3.943 31	3.506 04	3.508 29	3.597 37	
	Accurate ^a				2.125 85	
	H ₂	$\Delta\text{SCF } \Omega_1$	0.434 58	0.432 85	0.427 26	0.434 41
		biLIM Ω_1	0.609 20	0.429 86	0.430 66	0.471 43
equibi Ω_1		0.432 14	0.434 12	0.431 58	0.437 48	
triLIM Ω_1		0.609 20	0.429 86	0.430 66	0.471 43	
equitri Ω_1		0.385 94	0.485 17	0.481 16	0.465 55	
$\Delta\text{SCF } \Omega_2$		1.064 18	1.006 43	1.012 67	1.026 34	
biLIM Ω_2		1.341 48	0.929 27	0.938 69	1.024 39	
equibi Ω_2		1.086 23	1.013 81	1.021 42	1.037 90	
triLIM Ω_2		1.323 51	0.953 69	0.963 51	1.039 08	
equitri Ω_2		1.089 48	1.011 95	1.017 59	1.035 16	
Accurate ^b					1.056 54	
HeH ⁺	$\Delta\text{SCF } \Omega_1$	0.872 74	0.873 50	0.861 96	0.870 25	
	biLIM Ω_1	1.126 95	0.851 10	0.845 38	0.908 31	
	equibi Ω_1	0.874 88	0.872 17	0.860 38	0.869 42	
	triLIM Ω_1	1.126 95	0.851 10	0.845 38	0.908 31	
	equitri Ω_1	0.867 92	1.033 02	1.028 03	0.998 38	
	$\Delta\text{SCF } \Omega_2$	2.260 81	2.201 55	2.231 16	2.238 44	
	biLIM Ω_2	2.512 83	1.885 70	1.898 91	2.027 84	
	equibi Ω_2	2.264 85	2.163 64	2.185 21	2.202 46	
	triLIM Ω_2	2.511 05	1.954 65	1.972 45	2.083 65	
	equitri Ω_2	2.259 05	2.157 48	2.176 91	2.194 54	

^a obtained from [8].

^b obtained from [59].

5.3.2 With Weight-Dependent Exchange-Correlation Functionals

In complete analogy with what has been done for PPLB ensembles (see 4.3.3), we designed weight-dependent exchange functionals based on standard ground state DFT density-functional approximations (DFAs) in order to correct curvature errors of GOK ensemble energies of the “single” and “double” biensembles

$$E_x^{w_i, \text{eDFA}}[n] \equiv F_x^{w_i} E_x^{w_i, \text{DFA}}[n], \quad (5.71)$$

in which $F_x^{w_i}$ is an explicit weight-dependent scaling factor.

To do so, we reverse-engineered the weight-dependent exchange multiplicative scaling factor $F_x^{w_i}$ of the “single” and “double” GOK biensembles for all considered two-electron systems, xc-approximations, and basis sets.

As expected, such weight-dependent scaling factors are highly dependent on the nature of the ensemble, the xc-functional, the basis set and the system of interest, as depicted in Figures 5.6 and 5.7. We would like to stress that such curvature-corrected (CC) exchange functionals are obviously not transposable to routine applications but are rather intended to highlight the necessity to design explicit weight-dependent xc-functionals which could be used to palliate the limitations and deficiencies of standard weight-independent xc-functionals which fail to yield acceptable results when transposed to the scope of ensemble DFT, not even with the same accuracy that they provide in standard DFT.

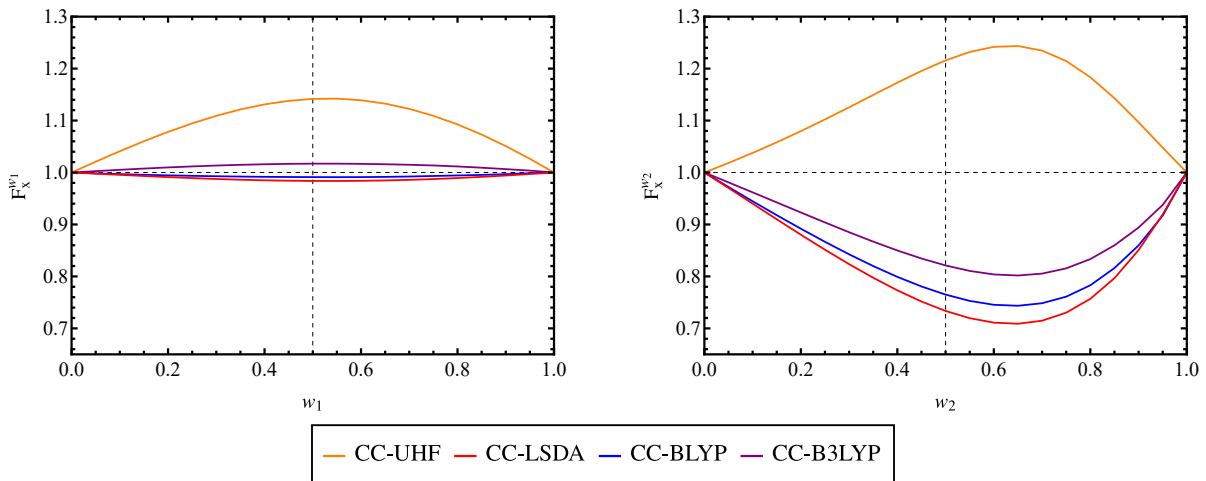


Figure 5.6: Comparison between the weight-dependent exchange scaling factors of He for the “single” (left panel) and “double” (right panel) GOK biensembles in the cc-pVQZ basis set for various methods and weight-dependent xc-functionals.

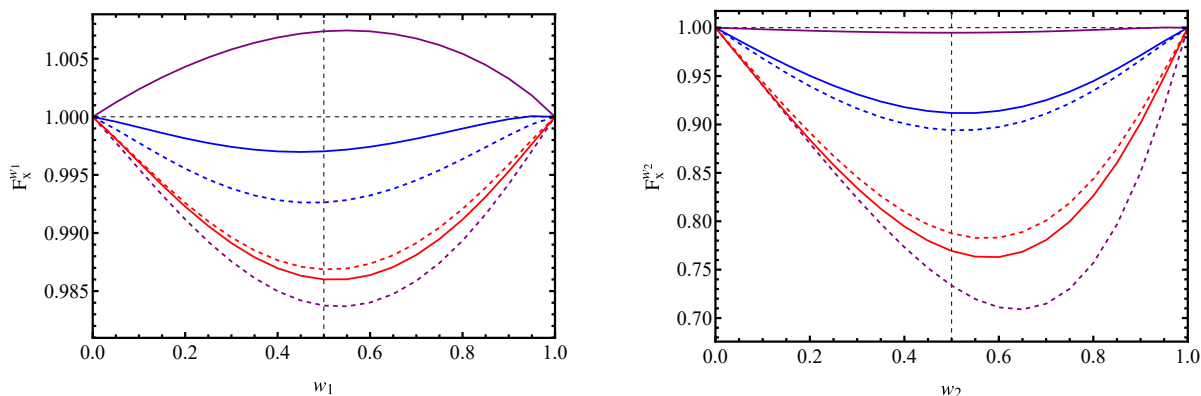


Figure 5.7: Comparison between the weight-dependent LSDA exchange scaling factors of He (purple), H₂ (blue) and HeH⁺ (red) for the “single” (left panel) and “double” (right panel) GOK biensembles in the cc-pVDZ (solid line) and cc-pVQZ (dashed line) basis sets.

Nevertheless, recently, there have been attempts to design more general weight-dependent xc-functionals, especially designed to access single and double excitation energies of two-electron systems by use of a GOK triensemble such as the one studied in this work. The exchange part of this functional was also based on an optimized weight-dependent multiplicative scaling factor while the correlation part was designed as a linear combination of two functionals designed to access single and double excitation energies of a two-electron finite uniform electron gas (FUEG) [55, 59].

For a given level of approximation, the weight-dependent CC-functional will rely on its explicit weight-dependence to restore the linearity of the GOK biensemble energy obtained from its weight-independent analog. We stress that since the weight-dependent exchange scaling factors are enforced to reduce to unity in the weight limits $w_i = 0$ and $w_i = 1$, so that the CC-functionals reduce to their standard weight-independent analogs in those two specific weight configurations, only the curvature of the ensemble energy will be affected by the new weight-dependent functionals. In no case will they yield more accurate energies than the weight-independent approximations they were built from in the particular weight-configurations $w_i = 0$ and $w_i = 1$, which we recall must reduce to standard DFT calculations. Hence, if one were to use the Δ SCF method to extract excitation energies from the ensemble energy, by performing total energy differences from multiple DFT calculations, the results obtained with a given weight-dependent CC-functional would be identical to the ones obtained with the corresponding weight-independent functional.

For that reason, the weight-dependent ensemble Kohn-Sham orbitals obtained with the CC-functionals reduce to the standard Kohn-Sham orbitals obtained with the weight-independent functionals, as depicted in Figure E.6. Nevertheless, for any other weight-configuration, we see that the weight-dependent CC-functionals will slightly change the Kohn-Sham orbitals in order to yield a perfectly linear ensemble energy.

In the case of the “single” GOK biensemble, we note that the unrestricted Hartree-Fock orbitals will be slightly increased by the weight-dependent CC-UHF functional while the

LSDA and BLYP density-functional approximations (DFAs) Kohn-Sham orbitals will be slightly lowered by the CC-functionals. Note that the change induced by the CC-procedure is much significant in unrestricted Hartree-Foch than in the LSDA and BLYP cases, which was expected since the UHF GOK biensemble energy had the most significant amount of curvature to correct. As a matter of fact, because the hybrid functional B3LYP includes, by construction, a specific amount of Hartree-Fock exchange energy, the resulting Kohn-Sham orbitals are slightly increased by the weight-dependent CC-functional.

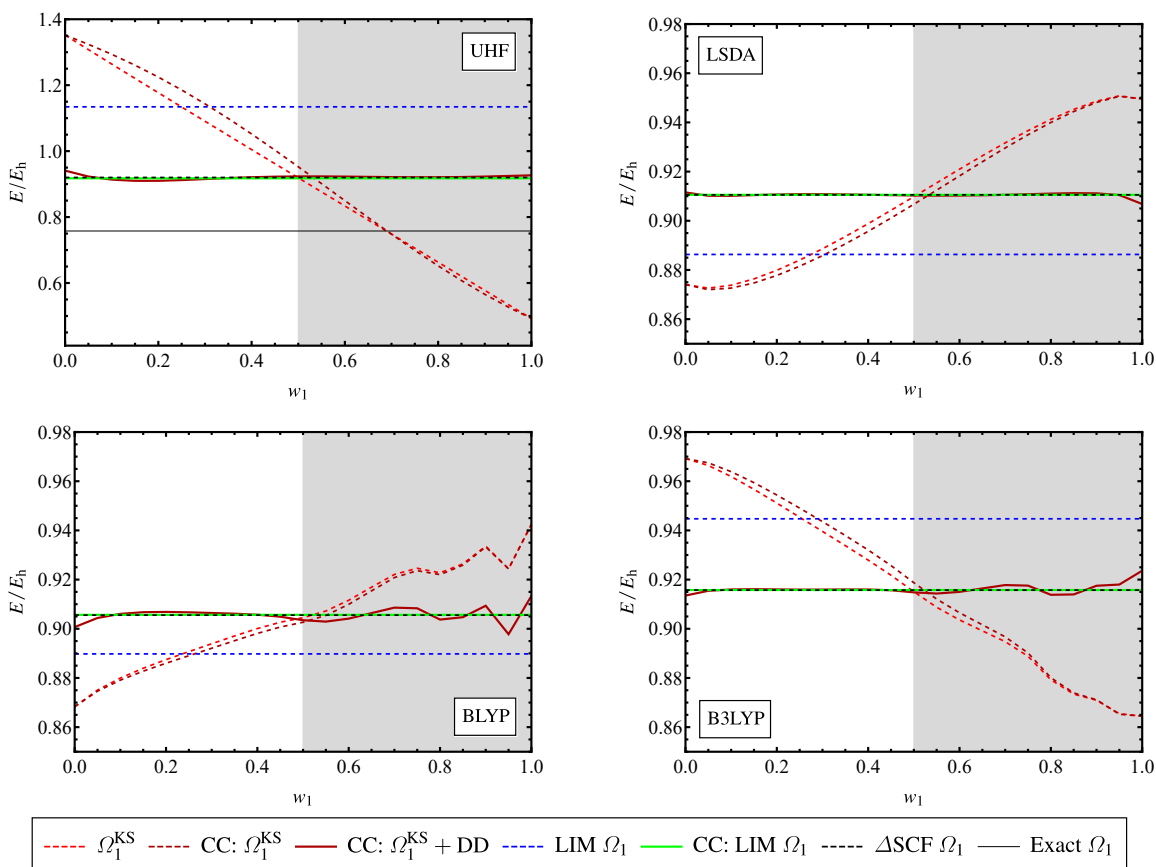


Figure 5.8: Weight-dependence of the lowest single excitation energy of He obtained from the “single” GOK biensemble. The ensemble Kohn-Sham excitation energies of the weight-independent standard functionals and their weight-dependent CC-analogs are reported. The complete ensemble single excitation energies, which include the additional weight-derivative “DD” contributions of the CC-functionals, are reported. For comparison, the LIM predictions of the weight-independent and weight-dependent approximations are also reported. Finally, the Δ SCF single excitation energies obtained within the same level of approximation are reported as well as the exact single excitation energy (from [8]). Calculations were performed in the cc-pVQZ basis set with various methods and levels of approximations.

By restoring the linearity of the GOK biensemble energy and, thus, the weight-independence of its constant slope, the CC-functionals yield much more stabilised and accurate predictions of the single excitation energy, compared to the corresponding Δ SCF references, through

the additional weight-derivatives of the CC-exchange-correlation functionals. Note that, by construction, the linearity of the ensemble energy will yield as well a more accurate LIM prediction of the excitation energy, as depicted in Figure E.6. Indeed, with the exact functional, the linear interpolation method would yield exact excitation energies. We report in Table 5.9 a more detailed overview of the performance of the CC-functionals, compared to their weight-independent standard analogs, to extract single and double excitation energy predictions from the “single” and “double” GOK biensembles studied in this work.

Table 5.9: Single and double GOK biensemble predictions for the lowest single and double excitation energies of He for various weight-configurations, compared to the linear interpolation method (LIM) and ASCF predictions obtained with standard weight-independent and weight-dependent (CC) xc-functionals in the cc-pVQZ basis set. The "DD" notation refers to the additional weight-derivative contributions of the CC-functionals to the excitation energy predictions. The blanks are left to highlight the fact that, unlike CC-functionals, standard weight-independent functionals do not provide an additional "DD" term. The results are expressed in terms of percent errors compared to the ASCF excitation energies (in hartree).

	UHF	CC-UHF	LSDA	CC-LSDA	BLYP	CC-BLYP	B3LYP	CC-B3LYP
ASCF Ω_1	0.920 00	0.920 00	0.910 54	0.910 54	0.905 55	0.905 55	0.915 73	0.915 73
LIM Ω_1	1.134 32	0.917 55	0.886 307	0.910 54	0.889 78	0.905 66	0.944 71	0.915 75
Δ (%) LIM Ω_1	23.294	-0.266	-2.661	0.000	-1.742	0.011	3.166	0.002
	Δ (%) Kohn-Sham gap $\epsilon_2^\downarrow - \epsilon_1^\uparrow$							
$w_1 = 0.05$	42.159	43.903	-4.167	-4.233	-3.366	-3.416	5.534	5.650
$w_1 = 0.25$	23.232	28.852	-2.915	-3.187	-1.639	-1.824	3.233	3.639
$w_1 = 0.50$	-0.0104	3.546	-0.080	-0.420	-0.114	-0.321	-0.071	0.329
	Δ (%) Kohn-Sham gap $\epsilon_2^\downarrow - \epsilon_1^\uparrow + \text{DD}$							
$w_1 = 0.05$	-	0.326	-	-0.041	-	-0.129	-	-0.032
$w_1 = 0.25$	-	-0.854	-	0.031	-	0.124	-	0.020
$w_1 = 0.50$	-	0.361	-	-0.028	-	-0.229	-	-0.100
ASCF Ω_2	2.338 25	2.338 25	2.253 11	2.253 11	2.311 45	2.311 45	2.319 25	2.319 25
LIM Ω_2	2.512 05	2.335 19	1.944 84	2.251 26	1.982 58	2.307 81	2.094 04	2.317 68
Δ (%) LIM Ω_2	7.433	-0.130	-13.682	-0.081	-14.227	-0.109	-9.710	-0.067
	Δ (%) Kohn-Sham gap $(\epsilon_2^\uparrow + \epsilon_2^\downarrow) - (\epsilon_1^\uparrow + \epsilon_1^\downarrow)$							
$w_2 = 0.05$	13.899	14.690	-21.507	-22.241	-22.919	-23.641	-15.271	-15.933
$w_2 = 0.25$	7.308	12.983	-14.473	-18.091	-14.728	-18.277	-10.141	-13.246
$w_2 = 0.50$	-0.272	6.617	-1.527	-8.083	-1.790	-8.169	-1.426	-6.421
	Δ (%) Kohn-Sham gap $(\epsilon_2^\uparrow + \epsilon_2^\downarrow) - (\epsilon_1^\uparrow + \epsilon_1^\downarrow) + \text{DD}$							
$w_2 = 0.05$	-	2.768	-	-0.276	-	0.320	-	-0.109
$w_2 = 0.25$	-	-2.486	-	-0.041	-	-0.525	-	-0.044
$w_2 = 0.50$	-	1.728	-	-0.022	-	0.295	-	-0.101

Chapter 6

N-centered Ensembles: a Canonical Formalism for Charged Excitations

Contents

6.1	Introduction: Charged Excitations	161
6.2	<i>N</i>-centered Ensemble Density-Functional Theory	163
6.2.1	<i>N</i> -centered eDFT Fundamental Idea	163
6.2.2	Left and Right <i>N</i> -centered Formalisms	164
6.2.3	Theoretical Extraction of Individual-State Properties and Excitation Energies	167
6.2.4	Kohn-Sham Formulation of <i>N</i> -centered Ensemble DFT	168
6.2.5	Practical Extraction of Individual-State Properties and Excitation Energies	172
6.3	Numerical Implementation of <i>N</i>-centered Density-Functional Theory	174
6.3.1	With Standard Weight-Independent Exchange-Correlation Functionals	174
6.3.2	With Weight-dependent Exchange-Correlation Functionals	191
6.4	Extended <i>N</i>-centered Ensembles: Combining Charged and Neutral Excitation Energies	200
6.4.1	Left Extended <i>N</i> -centered Triensemble	200
6.4.2	Right Extended <i>N</i> -centered Triensemble	205

6.1 Introduction: Charged Excitations

Although DFT has been made widely applicable to a large variety of many-electron systems, mainly due to the fact that major efforts have been dedicated to the design of a large panel

of approximations, and became over the last decades a reliable and practical method with a reasonably low computational cost in many scientific fields such as physics, chemistry and material science, it still suffers from some serious discrepancies.

Indeed, there are still some specific quantities whose direct extraction from the Kohn-Sham (KS) eigenvalues provided by a DFT calculation fails to provide satisfactory accuracy compared to experimental references. For instance, ionization potentials, electron affinities and, by construction, fundamental gaps are some examples of elusive properties that are poorly predicted by Kohn-Sham quantities resulting from a DFT calculation, like we have seen in the PPLB chapter. However, those quantities can still be evaluated by mean of the Δ SCF method as ground-state total energy differences between neutral, anionic and cationic species [13].

In fact, such properties arising from processes which involve alteration of the total number of electrons of the system of interest can be quite challenging in some situations. For instance, in the case of periodic systems, such as crystalline solids, varying the total number of electrons constitutes an additional difficulty to overcome because of the periodic nature of such systems. Indeed, because of the periodic boundary conditions, an infinitesimal change of the charge of a unit cell would imply an identical change in each replica of the unit cell which would therefore result in an infinitely large change of the total number of electrons of the whole system.

Hence, the need to overcome this difficulty and to find a way to extract charged excitations such as fundamental gaps based on quantities arising from calculations of the neutral system only, without the imperative to vary the total charge of the system. Of course, many successful attempts have been made so far to improve the accuracy of fundamental gap predictions provided by conventional semi-local functionals in the KS-DFT framework. For instance, the use of the exact-exchange (EXX) functional combined with the optimized effective potential (OEP) method [48] to restore the missing derivative discontinuity of approximate functionals, as discussed in the PPLB chapter, or the possibility to go beyond the KS framework and to rely on the generalized Kohn-Sham scheme (GKS) instead [82], where the interacting-electron system is mapped into an interacting fictitious system that can still be described by a single Slater determinant but associated with a non-local orbital-dependent operator.

Although the GKS framework, combined with the screened-exchange approach or the hybrid functional approach, has led to significant improvement in the prediction of fundamental gaps of solids compared to the standard KS scheme, for finite-sized systems, like atoms and molecules, it remains unsuccessful because of its inability to take into account sufficient long-range exchange term.

Another alternative, suggested by Kraisler and Kronik, would consist in the ensemble generalization of the Hartree and exchange-correlation terms [45, 47, 50].

Nevertheless, a very appealing idea would be to be able to extract charged excitation energies from a first-principles approach which would only require a DFT-like low computational cost and the sole use of quantities associated with the neutral system, thus avoiding any alteration of the number of electrons, which would make it broadly-applicable to either finite or periodic systems.

In this chapter, we will present an in-principle-exact canonical reformulation of the fun-

damental gap problem in DFT and will explore its practical application to simple atomic systems.

6.2 *N*-centered Ensemble Density-Functional Theory

6.2.1 *N*-centered eDFT Fundamental Idea

Quite recently, Senjean and Fromager have introduced the concept of *N*-centered ensembles [76] to yield accurate descriptions of charged excitation processes through a canonical formalism which artificially maintains the total number of electrons of the system fixed and equal to a specific integer value within the ensemble DFT (eDFT) framework. Conversely to the standard PPLB grand canonical approach where the number of electrons of the physical open system is expected to vary continuously, resulting in a discontinuous shift in the exact exchange-correlation potential, known as the derivative discontinuity, everytime that an integral number of electrons is crossed, in the *N*-centered canonical framework, the exact xc-potential does not have to exhibit such a discontinuous shift.

Hence, while the absence of derivative discontinuity in commonly used approximations to the xc-energy is highly detrimental to the accurate prediction of charged excitations such as the fundamental gap in standard PPLB-DFT and often results in substantial errors, in *N*-centered ensemble DFT, it is inconsequential and the ability of approximate functionals to yield accurate predictions for charged excitations will rather be determined by the ensemble-weight dependence of such functionals [36].

In this chapter, we explore different choices of *N*-centered ensembles for the purpose of describing properties resulting from charge fluctuations around the so-called central integral number of electrons *N* of a neutral atomic system.

Originally, the concept of *N*-centered ensemble was introduced for the purpose of calculating fundamental gaps in a single in principle exactly DFT-like calculation, in complete analogy with GOK-DFT ensembles [12]. Formally, an *N*-centered ensemble consists of a linear mixture of the ground states of the neutral, cationic and/or anionic forms of a given species and a set of ensemble weights scaled so that the total number of electrons associated with the corresponding auxiliary *N*-centered ensemble density is fixed and equal to the central integral number of electrons *N* of the neutral system for any variation of the ensemble weights, hence the name *N*-centered.

Note that, in the original formulation of the theory, the ensemble weights have no physical meaning and are just auxiliary variables on which any true physical property extracted from the ensemble should not depend.

So far, various definitions of *N*-centered ensembles have been proposed, among which the single-weight *N*-centered ensemble, which allows a direct extraction of the fundamental gap of the neutral *N*-electron system

$$E^\xi = (1 - 2\xi)E_0^N + \xi E_0^{N-1} + \xi E_0^{N+1}, \quad (6.1)$$

with $0 \leq \xi \leq \frac{1}{2}$, and its two-weight generalization

$$E^{\xi} = \left(1 - \frac{(N-1)}{N}\xi^- - \frac{(N+1)}{N}\xi^+ \right) E_0^N + \xi^- E_0^{N-1} + \xi^+ E_0^{N+1} \quad (6.2)$$

which enables direct extraction of both ionization potential and electron affinity of the neutral system in a single calculation and whose ensemble weights $\xi \equiv \{\xi^-, \xi^+\}$ must obey the following convexity conditions

$$\xi^{\pm} \geq 0 \quad (6.3) \quad \left| \quad \xi^-(N-1) + \xi^+(N+1) \leq N. \quad (6.4)$$

Note that the single-weight *N*-centered ensemble defined in expression (6.1) is simply recovered when $\xi^- = \xi^+ = \xi$.

In addition to the above-mentioned *N*-centered reformulation of the fundamental gap problem, two additional variants of *N*-centered ensembles were proposed for the purpose of describing an open *N*-electron system resulting from both addition and removal of an electron [75]. For such canonical ensembles, a convenient and physical choice for the ensemble weight value is to use the physical charge deviation α of the fractional electron number of the open system, $\mathcal{N} = N \pm \alpha$, associated with the ensemble relative to the central integer value *N* of the neutral system, thus drawing a parallel with PPLB grand canonical ensembles. The so-called left (subscript “-”) and right (subscript “+”) *N*-centered ensembles, which correspond to the special weight configurations

$$\left\{ \xi^- = \frac{N\alpha}{N-1}, \xi^+ = 0 \right\} \quad (6.5) \quad \left| \quad \left\{ \xi^- = 0, \xi^+ = \frac{N\alpha}{N+1} \right\}, \quad (6.6)$$

respectively, with $0 \leq \alpha \leq 1$, allow to treat both scenarios separately and to obtain an in-principle-exact reformulation of the ionization potential and electron affinity theorems. From now on, we will focus on the concept of left and right *N*-centered ensemble DFT and compare it with conventional left and right PPLB-DFT for open systems, as discussed in the PPLB chapter.

6.2.2 Left and Right *N*-centered Formalisms

Auxiliary ensembles

First, let us introduce the so-called left and right *N*-centered ensemble density matrix operators, respectively,

$$\hat{I}^{\xi^-} = (1 - \alpha)\hat{I}^N + \frac{N\alpha}{N-1}\hat{I}^{N-1} \quad (6.7) \quad \left| \quad \hat{I}^{\xi^+} = (1 - \alpha)\hat{I}^N + \frac{N\alpha}{N+1}\hat{I}^{N+1} \quad (6.8)$$

based upon the $(N - 1)$ -, N - and $(N + 1)$ -electron ground-state density matrix operators

$$\begin{cases} \hat{I}^{N-1} &= |\Psi_0^{N-1}\rangle \langle \Psi_0^{N-1}| \\ \hat{I}^N &= |\Psi_0^N\rangle \langle \Psi_0^N| \\ \hat{I}^{N+1} &= |\Psi_0^{N+1}\rangle \langle \Psi_0^{N+1}|. \end{cases} \quad (6.9)$$

Furthermore, we define the left and right N -centered ensemble weights

$$\xi^- = \frac{N}{N-1}\alpha \quad (6.10) \quad \left| \quad \xi^+ = \frac{N}{N+1}\alpha \quad (6.11)$$

whose expressions depend on the physical charge deviation α , from the central integral number of electrons N , of the left and right physical open systems with fractional number of electrons

$$\mathcal{N}^- = N - \alpha \quad (6.12) \quad \left| \quad \mathcal{N}^+ = N + \alpha, \quad (6.13)$$

respectively.

Consequently, based on the individual ground-state energies and densities of the $(N - 1)$ -, N - and $(N + 1)$ -electron systems, we can derive the following left and right N -centered ensemble energies

$$\begin{aligned} E^{\xi^-} &= (1 - \alpha)E_0^N + \frac{N\alpha}{N-1}E_0^{N-1} & (6.14) \\ &= \text{Tr}[\hat{I}^{\xi^-} \hat{H}] \end{aligned} \quad \left| \quad \begin{aligned} E^{\xi^+} &= (1 - \alpha)E_0^N + \frac{N\alpha}{N+1}E_0^{N+1} & (6.15) \\ &= \text{Tr}[\hat{I}^{\xi^+} \hat{H}] \end{aligned}$$

as well as the corresponding left and right N -centered ensemble densities

$$\begin{aligned} n^{\xi^-}(\mathbf{r}) &= (1 - \alpha)n_0^N(\mathbf{r}) + \frac{N\alpha}{N-1}n_0^{N-1}(\mathbf{r}) & (6.16) \\ &= \text{Tr}[\hat{I}^{\xi^-} \hat{n}(\mathbf{r})] \end{aligned} \quad \left| \quad \begin{aligned} n^{\xi^+}(\mathbf{r}) &= (1 - \alpha)n_0^N(\mathbf{r}) + \frac{N\alpha}{N+1}n_0^{N+1}(\mathbf{r}) \\ &= \text{Tr}[\hat{I}^{\xi^+} \hat{n}(\mathbf{r})] \end{aligned} \quad (6.17)$$

which always integrate to the central integral number of electrons N , independently of the physical charge deviation α of the true physical open systems. Hence, the left and right

N-centered normalization constraints

$$\int n^{\xi^-}(\mathbf{r})d\mathbf{r} = N \quad (6.18) \quad \left| \quad \int n^{\xi^+}(\mathbf{r})d\mathbf{r} = N. \quad (6.19)$$

True physical ensembles

We stress that the left and right *N*-centered ensembles are not the true physical ensembles describing the open systems from/to which we remove/add an electron, they are auxiliary quantities and thus do not possess any physical meaning. Let us recall the definitions of the true physical ensembles associated with the open systems, the PPLB ensembles, which are generated by ensemble density matrix operators of the form

$$\hat{I}^{\mathcal{N}^-} \equiv \hat{I}^{\alpha^-} = (1 - \alpha)\hat{I}^N + \alpha\hat{I}^{N-1} \quad (6.20) \quad \left| \quad \hat{I}^{\mathcal{N}^+} \equiv \hat{I}^{\alpha^+} = (1 - \alpha)\hat{I}^N + \alpha\hat{I}^{N+1} \quad (6.21)$$

with PPLB ensemble energies

$$\begin{aligned} E^{\mathcal{N}^-} \equiv E^{\alpha^-} &= (1 - \alpha)E_0^N + \alpha E_0^{N-1} \\ &= \text{Tr}[\hat{I}^{\mathcal{N}^-} \hat{H}] \end{aligned} \quad (6.22) \quad \left| \quad \begin{aligned} E^{\mathcal{N}^+} \equiv E^{\alpha^+} &= (1 - \alpha)E_0^N + \alpha E_0^{N+1} \\ &= \text{Tr}[\hat{I}^{\mathcal{N}^+} \hat{H}] \end{aligned} \quad (6.23)$$

and PPLB ensemble densities

$$\begin{aligned} n^{\mathcal{N}^-}(\mathbf{r}) \equiv n^{\alpha^-}(\mathbf{r}) &= (1 - \alpha)n_0^N(\mathbf{r}) + \alpha n_0^{N-1}(\mathbf{r}) \\ &= \text{Tr}[\hat{I}^{\mathcal{N}^-} \hat{n}(\mathbf{r})] \end{aligned} \quad (6.24) \quad \left| \quad \begin{aligned} n^{\mathcal{N}^+}(\mathbf{r}) \equiv n^{\alpha^+}(\mathbf{r}) &= (1 - \alpha)n_0^N(\mathbf{r}) + \alpha n_0^{N+1}(\mathbf{r}) \\ &= \text{Tr}[\hat{I}^{\mathcal{N}^+} \hat{n}(\mathbf{r})] \end{aligned} \quad (6.25)$$

which integrate to the true physical fractional numbers of electrons of the open systems relative to the charge deviation α

$$\int n^{\mathcal{N}^-}(\mathbf{r})d\mathbf{r} = N - \alpha = \mathcal{N}^- \quad (6.26) \quad \left| \quad \int n^{\mathcal{N}^+}(\mathbf{r})d\mathbf{r} = N + \alpha = \mathcal{N}^+. \quad (6.27)$$

Connection between *N*-centered ensembles and PPLB ensembles

Nevertheless, a direct connection between the true physical PPLB ensemble density matrix operators of the open systems and their canonical auxiliary *N*-centered counterparts can be

derived

$$\hat{I}^{\alpha^-} = \left(1 - \frac{\alpha}{N}\right) \hat{I}^{\xi^-} - \frac{\alpha(1-\alpha)}{N} \frac{d\hat{I}^{\xi^-}}{d\alpha} \quad (6.28) \quad \left| \quad \hat{I}^{\alpha^+} = \left(1 + \frac{\alpha}{N}\right) \hat{I}^{\xi^+} + \frac{\alpha(1-\alpha)}{N} \frac{d\hat{I}^{\xi^+}}{d\alpha}, \quad (6.29)$$

as well as for the true physical PPLB ensemble energies

$$E^{\alpha^-} = \left(1 - \frac{\alpha}{N}\right) E^{\xi^-} - \frac{\alpha(1-\alpha)}{N} \frac{dE^{\xi^-}}{d\alpha} \quad (6.30) \quad \left| \quad E^{\alpha^+} = \left(1 + \frac{\alpha}{N}\right) E^{\xi^+} + \frac{\alpha(1-\alpha)}{N} \frac{dE^{\xi^+}}{d\alpha} \quad (6.31)$$

and PPLB ensemble densities

$$n^{\alpha^-}(\mathbf{r}) = \left(1 - \frac{\alpha}{N}\right) n^{\xi^-}(\mathbf{r}) - \frac{\alpha(1-\alpha)}{N} \frac{dn^{\xi^-}(\mathbf{r})}{d\alpha} \quad (6.32) \quad \left| \quad n^{\alpha^+}(\mathbf{r}) = \left(1 + \frac{\alpha}{N}\right) n^{\xi^+}(\mathbf{r}) + \frac{\alpha(1-\alpha)}{N} \frac{dn^{\xi^+}(\mathbf{r})}{d\alpha}. \quad (6.33)$$

6.2.3 Theoretical Extraction of Individual-State Properties and Excitation Energies

As already discussed in the PPLB and GOK chapters, the practical advantage of the ensemble formalism is to enable extraction of physical properties such as individual-state energies and excitation energies from a given ensemble by taking simple derivatives of the ensemble energy with respect to the ensemble weights.

First, let us recall the key expressions derived from the left and right PPLB ensembles for the prediction of the ionization potential and electron affinity of the neutral N -electron system, respectively

$$\begin{aligned} E_0^N &= E^{\alpha^-} - \alpha \frac{dE^{\alpha^-}}{d\alpha} & E_0^N &= E^{\alpha^+} - \alpha \frac{dE^{\alpha^+}}{d\alpha} \\ E_0^{N-1} &= E^{\alpha^-} + (1-\alpha) \frac{dE^{\alpha^-}}{d\alpha} & E_0^{N+1} &= E^{\alpha^+} + (1-\alpha) \frac{dE^{\alpha^+}}{d\alpha} \\ I_0^N &= E_0^{N-1} - E_0^N = \frac{dE^{\alpha^-}}{d\alpha} & A_0^N &= E_0^N - E_0^{N+1} = -\frac{dE^{\alpha^+}}{d\alpha}. \end{aligned} \quad (6.34) \quad (6.35)$$

Turning now to the left and right N -centered canonical auxiliary ensembles, we derive similar results for the extraction of the same set of exact properties of the true physical systems

$$\begin{array}{l|l}
 E_0^N = E^{\xi^-} - \alpha \frac{dE^{\xi^-}}{d\alpha} & E_0^N = E^{\xi^+} - \alpha \frac{dE^{\xi^+}}{d\alpha} \\
 E_0^{N-1} = \frac{N-1}{N} \left[E^{\xi^-} + (1-\alpha) \frac{dE^{\xi^-}}{d\alpha} \right] & E_0^{N+1} = \frac{N+1}{N} \left[E^{\xi^+} + (1-\alpha) \frac{dE^{\xi^+}}{d\alpha} \right] \\
 I_0^N = -\frac{1}{N} \left[E^{\xi^-} + (1-\alpha-N) \frac{dE^{\xi^-}}{d\alpha} \right] & A_0^N = -\frac{1}{N} \left[E^{\xi^+} + (1-\alpha+N) \frac{dE^{\xi^+}}{d\alpha} \right].
 \end{array}
 \tag{6.36} \qquad \tag{6.37}$$

6.2.4 Kohn-Sham Formulation of *N*-centered Ensemble DFT

From now on, for the sake of clarity, we will only detail the Kohn-Sham formulation of left *N*-centered ensemble density-functional theory which can easily be adapted for right *N*-centered ensembles.

N-centered variational principle and universal functional

In complete analogy with the GOK-DFT variational principle, the left *N*-centered ensemble energy is variationally determined as follows

$$E^{\xi^-} = \min_n \left\{ F^{\xi^-}[n] + \int n(\mathbf{r})v(\mathbf{r})d\mathbf{r} \right\}, \tag{6.38}$$

where the minimization is over all left *N*-centered trial ensemble densities of the type

$$n(\mathbf{r}) \equiv n^{\xi^-}(\mathbf{r}), \tag{6.39}$$

and where the left *N*-centered universal ensemble density functional can be decomposed as follows

$$F^{\xi^-}[n] = T_s^{\xi^-}[n] + E_{\text{Hxc}}^{\xi^-}[n], \tag{6.40}$$

where the superscript “ ξ^- ” emphasizes the fact that, unlike standard KS-DFT functionals, the hereby ensemble functionals are weight-dependent. Naturally, since ensemble DFT is a generalization of standard DFT to ensembles, when the ensemble density reduces to a standard electron density, that is to say associated with a single electronic state, the ensemble functionals must reduce as well to their standard weight-independent analogs.

N-centered non-interacting kinetic functional

Following the decomposition of the left *N*-centered universal functional, we define the left *N*-centered non-interacting ensemble kinetic energy functional which can be expressed within

the following constrained-search formulation

$$\begin{aligned}
 T_s^{\xi^-}[n] &= \min_{\hat{\gamma}^{\xi^-} \rightarrow n} \left\{ \text{Tr}[\hat{\gamma}^{\xi^-} \hat{T}] \right\} \\
 &= (1 - \alpha) \left\langle \Phi_0^{N, \xi^-}[n] \left| \hat{T} \right| \Phi_0^{N, \xi^-}[n] \right\rangle + \frac{N\alpha}{N-1} \left\langle \Phi_0^{N-1, \xi^-}[n] \left| \hat{T} \right| \Phi_0^{N-1, \xi^-}[n] \right\rangle,
 \end{aligned} \tag{6.41}$$

where the constrained-search is over all non-interacting left *N*-centered ensemble density matrix operators $\hat{\gamma}^{\xi^-}$, built from an arbitrary set of weight-dependent single Slater determinants $\{\Phi_0^{N, \xi^-}, \Phi_0^{N-1, \xi^-}\}$

$$\hat{\gamma}^{\xi^-} = (1 - \alpha) \left| \Phi_0^{N, \xi^-} \right\rangle \left\langle \Phi_0^{N, \xi^-} \right| + \frac{N\alpha}{N-1} \left| \Phi_0^{N-1, \xi^-} \right\rangle \left\langle \Phi_0^{N-1, \xi^-} \right|, \tag{6.42}$$

that yield the interacting left *N*-centered ensemble density $n(\mathbf{r})$

$$\begin{aligned}
 n_{\hat{\gamma}^{\xi^-}}(\mathbf{r}) &= \text{Tr}[\hat{\gamma}^{\xi^-} \hat{n}(\mathbf{r})] \\
 &= (1 - \alpha) n_{\Phi_0^{N, \xi^-}}(\mathbf{r}) + \frac{N\alpha}{N-1} n_{\Phi_0^{N-1, \xi^-}}(\mathbf{r}) \\
 &= n(\mathbf{r}).
 \end{aligned} \tag{6.43}$$

In particular, $\{\Phi_0^{N, \xi^-}[n], \Phi_0^{N-1, \xi^-}[n]\}$ are the minimizing ground-state Slater determinants from which is built the minimizing non-interacting left *N*-centered ensemble density operator, the so-called left *N*-centered Kohn-Sham ensemble density matrix operator

$$\hat{\gamma}_{\text{KS}}^{\xi^-} = (1 - \alpha) \left| \Phi_0^{N, \xi^-}[n] \right\rangle \left\langle \Phi_0^{N, \xi^-}[n] \right| + \frac{N\alpha}{N-1} \left| \Phi_0^{N-1, \xi^-}[n] \right\rangle \left\langle \Phi_0^{N-1, \xi^-}[n] \right|, \tag{6.44}$$

which has the particularity of minimizing the non-interacting ensemble kinetic energy, $\text{Tr}[\hat{\gamma}^{\xi^-} \hat{T}]$, as well as yielding the interacting left *N*-centered ensemble density, $n(\mathbf{r})$, for a given and fixed weight ξ^-

$$\begin{aligned}
 n_{\text{KS}}^{\xi^-}(\mathbf{r}) &= \text{Tr}[\hat{\gamma}_{\text{KS}}^{\xi^-} \hat{n}(\mathbf{r})] \\
 &= (1 - \alpha) n_{\Phi_0^{N, \xi^-}[n]}(\mathbf{r}) + \frac{N\alpha}{N-1} n_{\Phi_0^{N-1, \xi^-}[n]}(\mathbf{r}) \\
 &= n(\mathbf{r}).
 \end{aligned} \tag{6.45}$$

Hence, we see that, in complete analogy with standard Kohn-Sham DFT, left *N*-centered ensemble DFT is based on the mapping of an interacting left *N*-centered ensemble system to a non-interacting left *N*-centered ensemble system that both share a common left *N*-centered ensemble density.

***N*-centered variational ensemble energy and Kohn-Sham molecular orbitals**

For practical reasons, one can express the variational principle for the left *N*-centered ensemble energy in terms of the weight-dependent molecular orbitals $\{\varphi_p^{\xi^-}(\mathbf{r})\}$, which are implicit

functionals of the left *N*-centered ensemble density, from which the non-interacting Kohn-Sham Slater determinants are built,

$$\begin{aligned}
 E_0^{\xi^-} &= \min_{\{\varphi_p^{\xi^-}\}} \left\{ \text{Tr} \left[\hat{\gamma}^{\xi^-} \left(\hat{T} + \hat{V}_{en} \right) \right] + E_{\text{Hxc}}[n_{\hat{\gamma}^{\xi^-}}] \right\} \\
 &= \text{Tr} \left[\hat{\gamma}_{\text{KS}}^{\xi^-} \left(\hat{T} + \hat{V}_{en} \right) \right] + E_{\text{Hxc}}[n_{\text{KS}}^{\xi^-}].
 \end{aligned} \tag{6.46}$$

From now on, we will use the notation $\{\varphi_p^{\xi^-}\}$ to refer to the specific set of minimizing weight-dependent Kohn-Sham orbitals, that is to say the orbitals from which is built the set of single Slater determinantal Kohn-Sham wave functions, $\{\Phi_0^{N,\xi^-}, \Phi_0^{N-1,\xi^-}\} \equiv \{\Phi_0^{N,\xi^-}[n], \Phi_0^{N-1,\xi^-}[n]\}$, that minimize the left *N*-centered ensemble energy and mimic the true interacting left *N*-centered ensemble density $n_0^{\xi^-}(\mathbf{r})$.

For that reason, in the exact theory, we must have

$$\begin{aligned}
 n_{\text{KS}}^{\xi^-}(\mathbf{r}) &= (1 - \alpha)n_{\Phi_0^{N,\xi^-}}(\mathbf{r}) + \frac{N\alpha}{N-1}n_{\Phi_0^{N-1,\xi^-}}(\mathbf{r}) \\
 &= (1 - \alpha)n_{\Psi_0^N}(\mathbf{r}) + \frac{N\alpha}{N-1}n_{\Psi_0^{N-1}}(\mathbf{r}) \\
 &= n_0^{\xi^-}(\mathbf{r})
 \end{aligned} \tag{6.47}$$

where $\{n_{\Psi_0^N}(\mathbf{r}) \equiv n_0^N(\mathbf{r}), n_{\Psi_0^{N-1}}(\mathbf{r}) \equiv n_0^{N-1}(\mathbf{r})\}$ are the exact individual ground-state electron densities generated by the exact eigenstates $\{\Psi_0^N, \Psi_0^{N-1}\}$ of the interacting *N*- and (*N* - 1)-electron systems.

We stress that, for a given ensemble DFT calculation, all the individual states of the ensemble are built from the same set of weight-dependent Kohn-Sham orbitals.

Hence, the individual Kohn-Sham densities can be obtained by summation over all occupied Kohn-Sham orbitals for the given state

$$n_{\Phi_0^{N,\xi^-}}(\mathbf{r}) = \sum_{p=1}^N \left| \varphi_p^{\xi^-}(\mathbf{r}) \right|^2 \tag{6.48} \quad \left| \quad n_{\Phi_0^{N-1,\xi^-}}(\mathbf{r}) = \sum_{p=1}^{N-1} \left| \varphi_p^{\xi^-}(\mathbf{r}) \right|^2. \tag{6.49}$$

Based on those definitions, the non-interacting left *N*-centered Kohn-Sham ensemble density can be reformulated in terms of the occupied weight-dependent Kohn-Sham molecular

orbitals

$$\begin{aligned}
 n_{\text{KS}}^{\xi^-}(\mathbf{r}) &= (1 - \alpha) \sum_{p=1}^N \left| \varphi_p^{\xi^-}(\mathbf{r}) \right|^2 + \frac{N\alpha}{N-1} \sum_{p=1}^{N-1} \left| \varphi_p^{\xi^-}(\mathbf{r}) \right|^2 \\
 &= \left(1 + \frac{\alpha}{N-1} \right) \sum_{p=1}^{N-1} \left| \varphi_p^{\xi^-}(\mathbf{r}) \right|^2 + (1 - \alpha) \left| \varphi_N^{\xi^-}(\mathbf{r}) \right|^2 \\
 &= n_0^{\xi^-}(\mathbf{r}).
 \end{aligned} \tag{6.50}$$

Hence, we see that the left N -centered ensemble density of the \mathcal{N} -electron open system does not mimic the true physical PPLB ensemble density which would correspond to having the $(N - 1)$ lowest Kohn-Sham molecular orbitals occupied by exactly one electron while the N th Kohn-Sham molecular orbital, the ‘‘HOMO’’, would be fractionally occupied by $(1 - \alpha)$ electron.

Self-consistent N -centered Kohn-Sham equations

The minimizing left N -centered Kohn-Sham orbitals are the solutions of a set of non-linear equations, the self-consistent left N -centered Kohn-Sham equations

$$\left(-\frac{1}{2}\nabla^2 + v(\mathbf{r}) + v_{\text{Hxc}}^{\xi^-}(\mathbf{r}) \right) \varphi_p^{\xi^-}(\mathbf{r}) = \varepsilon_p^{\xi^-} \varphi_p^{\xi^-}(\mathbf{r}), \tag{6.51}$$

where $v(\mathbf{r})$ is the weight-independent local external nuclear potential and $v_{\text{Hxc}}^{\xi^-}(\mathbf{r})$ is the weight-dependent Hartree-exchange-correlation potential which is, by definition, the functional derivative of the ensemble Hartree-exchange-correlation energy functional $E_{\text{Hxc}}^{\xi^-}[n]$ with respect to the left N -centered ensemble density $n(\mathbf{r})$

$$v_{\text{Hxc}}^{\xi^-}(\mathbf{r}) = \frac{\delta E_{\text{Hxc}}^{\xi^-}[n]}{\delta n(\mathbf{r})}. \tag{6.52}$$

Hence, we see that left N -centered density-functional theory, like GOK-DFT, is very similar to the standard ground-state formulation of Kohn-Sham DFT with the difference that the Kohn-Sham solutions are now a set of weight-dependent molecular orbitals $\{\varphi_p^{\xi^-}(\mathbf{r})\}$ with weight-dependent orbital energies $\{\varepsilon_p^{\xi^-}\}$.

Both PPLB-DFT and N -centered DFT aim to describe the energy and properties of an open-system but the main difference between these two formalisms is that, since N -centered ensemble densities are forced, by the scaling factors, to always integrate to the central integral number of electrons N in place of the true physical fractional number of electrons \mathcal{N} , it is a canonical formalism and, thus, the exact N -centered Hartree-exchange-correlation functionals must be weight-dependent in order to recover all the information about the ensemble, that is to say the weight configuration.

Indeed, in PPLB-DFT, the ensemble density changes accordingly to the physical charge deviation α of the open system, which has been chosen to be the PPLB ensemble weight and, consequently, the exact PPLB Hartree-exchange-correlation functional is not required to possess a weight-dependency, unlike its *N*-centered counterpart.

6.2.5 Practical Extraction of Individual-State Properties and Excitation Energies

Levy-Zahariev shift-in-potential

Like in GOK-DFT, one may find appealing to have a more convenient formulation of the left *N*-centered ensemble energy and of the individual-state properties encompassed in the ensemble, directly expressed in terms of the non-interacting Kohn-Sham orbital energies.

In that spirit, one can choose to apply the Levy-Zahariev (LZ) shift-in-potential in order to rewrite the left *N*-centered ensemble energy into the form of weighted sums of LZ-shifted Kohn-Sham orbital energies only. The LZ shift-in potential procedure is defined as follows

$$\bar{v}_{\text{Hxc}}^{\xi^-}(\mathbf{r}) = v_{\text{Hxc}}^{\xi^-}(\mathbf{r}) + \frac{E_{\text{Hxc}}^{\xi^-}[n] - \int v_{\text{Hxc}}^{\xi^-}(\mathbf{r})n(\mathbf{r})d\mathbf{r}}{\int n(\mathbf{r})d\mathbf{r}}, \quad (6.53)$$

where $\bar{v}_{\text{Hxc}}^{\xi^-}(\mathbf{r})$ is the LZ-shifted Hartree-exchange-correlation potential and $v_{\text{Hxc}}^{\xi^-}(\mathbf{r})$ is the originally unshifted potential, the definition of which is hereby recalled

$$v_{\text{Hxc}}^{\xi^-}(\mathbf{r}) = \frac{\delta E_{\text{Hxc}}^{\xi^-}[n]}{\delta n(\mathbf{r})}. \quad (6.54)$$

Let us define the weight-dependent Kohn-Sham auxiliary (total) energies of the *N*- and (*N* − 1)-electron ground-states of the left *N*-centered ensemble

$$\mathcal{E}_0^{N,\xi^-} = \sum_{p=1}^N \varepsilon_p^{\xi^-} \quad (6.55) \quad \left| \quad \mathcal{E}_0^{N-1,\xi^-} = \sum_{p=1}^{N-1} \varepsilon_p^{\xi^-}. \quad (6.56)$$

Analogous to standard KS-DFT where the total ground-state energy of the system is not the sum of the energy of the occupied Kohn-Sham orbitals, the exact left *N*-centered ensemble energy does not reduce to a weighted sum of occupied Kohn-Sham orbital energies

$$E_0^{\xi^-} = (1 - \alpha)\mathcal{E}_0^{N,\xi^-} + \frac{N\alpha}{N-1}\mathcal{E}_0^{N-1,\xi^-} + E_{\text{Hxc}}^{\xi^-}[n_{\text{KS}}^{\xi^-}] - \int v_{\text{Hxc}}^{\xi^-}(\mathbf{r})n_{\text{KS}}^{\xi^-}(\mathbf{r})d\mathbf{r}, \quad (6.57)$$

where the non-interacting left *N*-centered Kohn-Sham ensemble density $n_{\text{KS}}^{\xi^-}(\mathbf{r})$ mimics the true interacting left *N*-centered ensemble density $n_0^{\xi^-}(\mathbf{r})$.

When one applies the Levy-Zahariev shift-in-potential procedure, one obtains a more compact formulation of the exact left *N*-centered ensemble energy of the system

$$E_0^{\xi^-} = (1 - \alpha)\bar{\mathcal{E}}_0^{N,\xi^-} + \frac{N\alpha}{N-1}\bar{\mathcal{E}}_0^{N-1,\xi^-}, \quad (6.58)$$

where

$$\begin{cases} \bar{\mathcal{E}}_0^{N, \xi^-} &= \mathcal{E}_0^{N, \xi^-} + \left(E_{\text{Hxc}}^{\xi^-} [n_{\text{KS}}^{\xi^-}] - \int \frac{\delta E_{\text{Hxc}}^{\xi^-} [n_{\text{KS}}^{\xi^-}]}{\delta n(\mathbf{r})} n_{\text{KS}}^{\xi^-}(\mathbf{r}) d\mathbf{r} \right) \\ \bar{\mathcal{E}}_0^{N-1, \xi^-} &= \mathcal{E}_0^{N-1, \xi^-} + \frac{N-1}{N} \left(E_{\text{Hxc}}^{\xi^-} [n_{\text{KS}}^{\xi^-}] - \int \frac{\delta E_{\text{Hxc}}^{\xi^-} [n_{\text{KS}}^{\xi^-}]}{\delta n(\mathbf{r})} n_{\text{KS}}^{\xi^-}(\mathbf{r}) d\mathbf{r} \right) \end{cases} \quad (6.59)$$

are the weight-dependent LZ-shifted Kohn-Sham auxiliary energies of the individual states included in the ensemble. This corresponds to applying the following shift to each Kohn-Sham molecular orbital energy

$$\bar{\varepsilon}_p^{\xi^-} = \varepsilon_p^{\xi^-} + \frac{E_{\text{Hxc}}^{\xi^-} [n_{\text{KS}}^{\xi^-}] - \int v_{\text{Hxc}}^{\xi^-}(\mathbf{r}) n_{\text{KS}}^{\xi^-}(\mathbf{r}) d\mathbf{r}}{\int n_{\text{KS}}^{\xi^-}(\mathbf{r}) d\mathbf{r}}. \quad (6.60)$$

Individual energies and excitation energies

Once the LZ-shift-in-potential procedure applied, one obtains much practical formulations of the individual-state properties and excitation energies of the physical system in terms of Kohn-Sham ensemble quantities and derivatives of the ensemble Hxc-energy functional with respect to the ensemble weights

$$\begin{array}{l|l} E_0^{\xi^-} = (1 - \alpha) \bar{\mathcal{E}}_0^{N, \xi^-} + \frac{N\alpha}{N-1} \bar{\mathcal{E}}_0^{N-1, \xi^-} & E_0^{\xi^+} = (1 - \alpha) \bar{\mathcal{E}}_0^{N, \xi^+} + \frac{N\alpha}{N+1} \bar{\mathcal{E}}_0^{N+1, \xi^+} \\ E_0^N = \bar{\mathcal{E}}_0^{N, \xi^-} - \alpha \frac{\partial E_{\text{Hxc}}^{\xi^-}}{\partial \alpha} \Big|_{n_{\text{KS}}^{\xi^-}} & E_0^N = \bar{\mathcal{E}}_0^{N, \xi^+} - \alpha \frac{\partial E_{\text{Hxc}}^{\xi^+}}{\partial \alpha} \Big|_{n_{\text{KS}}^{\xi^+}} \\ E_0^{N-1} = \bar{\mathcal{E}}_0^{N-1, \xi^-} + \frac{(N-1)}{N} (1 - \alpha) \frac{\partial E_{\text{Hxc}}^{\xi^-}}{\partial \alpha} \Big|_{n_{\text{KS}}^{\xi^-}} & E_0^{N+1} = \bar{\mathcal{E}}_0^{N+1, \xi^+} + \frac{(N+1)}{N} (1 - \alpha) \frac{\partial E_{\text{Hxc}}^{\xi^+}}{\partial \alpha} \Big|_{n_{\text{KS}}^{\xi^+}} \\ I_0^N = -\bar{\varepsilon}_N^{\xi^-} - \frac{1}{N} (1 - \alpha - N) \frac{\partial E_{\text{Hxc}}^{\xi^-}}{\partial \alpha} \Big|_{n_{\text{KS}}^{\xi^-}} & A_0^N = -\bar{\varepsilon}_{N+1}^{\xi^+} - \frac{1}{N} (1 - \alpha + N) \frac{\partial E_{\text{Hxc}}^{\xi^+}}{\partial \alpha} \Big|_{n_{\text{KS}}^{\xi^+}} \end{array} \quad (6.61) \quad (6.62)$$

These are the key results upon which our numerical implementation of N -centered density-functional theory was based in order to perform N -centered ensemble DFT calculations on real simple atomic and molecular systems.

6.3 Numerical Implementation of *N*-centered Density-Functional Theory

In order to explore the performance and subtleties of *N*-centered ensemble DFT when applied to real physical systems, we have implemented various *N*-centered formalisms in our ensemble DFT Fortran software which enables us to perform *N*-centered calculations at both Hartree-Fock and DFT levels with commonly used weight-independent approximate exchange-correlation functionals and with weight-dependent approximate xc-functionals especially designed for the occasion.

6.3.1 With Standard Weight-Independent Exchange-Correlation Functionals

First, let us explore how commonly used approximate xc-functionals that were originally designed for ground-state applications in standard DFT behave when extended to the *N*-centered ensemble DFT framework.

Left *N*-centered ensembles

As a first concrete example, we chose to apply the left *N*-centered ensemble DFT formalism to a small set of simple atomic systems in order to assess the capability of commonly used approximate functionals to yield accurate ionization potentials through the self-consistent variational minimization of a canonical auxiliary quantity, the left *N*-centered ensemble energy.

Let us recall that a left *N*-centered ensemble energy/density consists of a statistical mixture of both *N*- and (*N* − 1)-electron ground-state energies/densities where the fixed ensemble weights assigned to those states are scaled so that the overall fictitious number of electrons associated with the auxiliary ensemble system remains artificially constant and equal to the central integral value *N* while the true number of electrons of the real open system $\mathcal{N} = N - \alpha$ continuously varies in the range $\mathcal{N} \in [N - 1, N]$, relative to the physical charge deviation α ,

$$E_0^{\xi^-} = (1 - \alpha)E_0^N + \frac{N\alpha}{N - 1}E_0^{N-1}. \quad (6.63)$$

As an illustrative example, details of the electronic configurations used in order to perform practical calculations of left *N*-centered ensemble DFT in the case of the lithium atom are reported in Table 6.1. Since our intent was to draw a direct parallel between the performance of left *N*-centered and left PPLB ensembles, the exact same electronic configurations were used for both ensemble formalisms.

Table 6.1: Electronic configurations of the individual states of the left N -centered biensemble associated with the removal of the highest spin-up electron from the electronic configuration of the Lithium ground state. Only the occupation numbers of the six lowest molecular orbitals of each spin are depicted.

State of the ensemble	Weight	Spin	Occupation numbers					
1	$1 - \alpha$	\uparrow	1	1	0	0	0	0
		\downarrow	1	0	0	0	0	0
2	$\frac{N\alpha}{N-1}$	\uparrow	1	0	0	0	0	0
		\downarrow	1	0	0	0	0	0

In the exact theory, the exact left N -centered ensemble energy, that one would obtain with the exact left N -centered ensemble functional, should be perfectly linear with respect to the ensemble weight, and thus to the physical charge deviation of the number of electrons of the real open system \mathcal{N} .

Conversely to the exact left PPLB ensemble energy which must yield the exact ground-state energies of the neutral and cationic systems when $\alpha = 0$ and $\alpha = 1$, respectively, the exact left N -centered ensemble energy must yield the exact ground-state energy of the N -electron system for the weight configuration $\alpha = 0$ but must yield a specific fraction, pre-established by the left N -centered scaling factor, of the exact ground-state energy of the cationic system when $\alpha = 1$. Hence, in the exact theory, one must have

$$E_0^{\xi^-=0} = E_0^N \quad (6.64) \quad \left| \quad E_0^{\xi^-=\frac{N}{N-1}} = \frac{N}{N-1} E_0^{N-1}. \quad (6.65)$$

In the left PPLB framework, we have seen that the use of approximate xc-functionals in place of the unknown exact functional would result in two practical observations: approximate ground-state energies for the neutral and cationic systems, when $\alpha = 0$ and $\alpha = 1$, respectively, plus additional curvature in the ensemble energy for any other weight configuration, $0 < \alpha < 1$. Left PPLB and left N -centered ensemble energies of the lithium atom obtained within various levels of approximation are reported in Figure 6.1 for illustrative purposes.

In the left N -centered framework, similar observations can be made. For a given approximate functional, the resulting left N -centered ensemble energy will exhibit additional curvature but, most of all, it will significantly deviate from its theoretical endpoint value which should be equal to a specific fraction of the ground-state energy of the cationic system obtained in standard ground-state DFT with the same level of approximation, as depicted in Figure 6.1. Hence, when a density-functional approximation (DFA) is used in place of the elusive and unknown exact functional, the resulting ensemble energy will exhibit the following properties

$$E^{\text{DFA}, \xi^-=0} = E_0^{N, \text{DFA}} \quad (6.66) \quad \left| \quad E^{\text{DFA}, \xi^-=\frac{N}{N-1}} \neq \frac{N}{N-1} E_0^{N-1, \text{DFA}}. \quad (6.67)$$

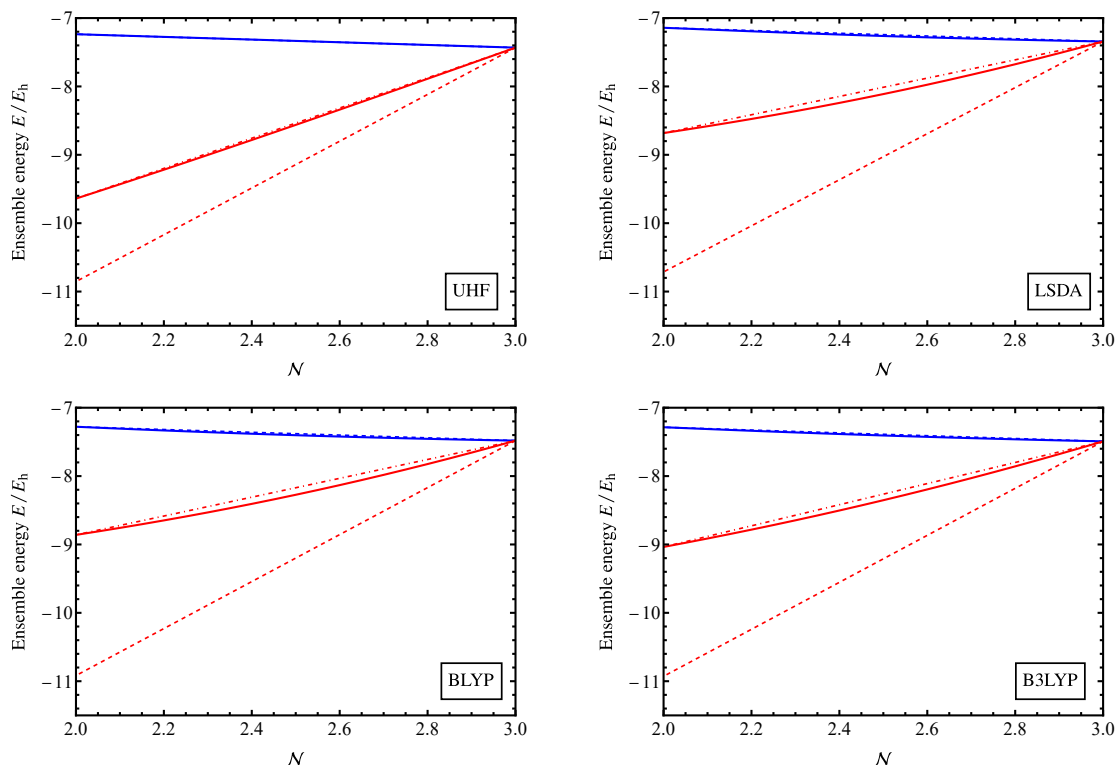


Figure 6.1: Comparison between the left PPLB (blue, solid line) and left N -centered (red, solid line) ensemble energies of Li obtained with different levels of approximations in the cc-pVDZ basis set. Linear interpolations of the PPLB (blue, dashed line) and N -centered (red, dot-dashed line) ensemble energies are reported to highlight the additional curvature arising from the use of approximate functionals as well as the endpoint deviation of the N -centered ensemble energy relative to its theoretical value (red, dashed line).

This endpoint deviation can be explained by the fact that most approximate functionals are not linear relative to the quantity that they must apply to, the electron density for instance. Indeed, when $\alpha = 1$, because of the multiplicative scaling factor $\frac{N}{N-1}$, the left N -centered ensemble density does not reduce to a single ground-state density and because of the nonlinearity of the approximate functional, applying a nonlinear functional to a scaled density fails to yield the corresponding scaled ground-state energy that one would obtain if the functional were linear,

$$E^{\text{DFA}, \xi^-} \left[\frac{N}{N-1} n \right] \neq \frac{N}{N-1} E^{\text{DFA}, \xi^-} [n]. \quad (6.68)$$

In order to have a much substantial overview of the performance of standard weight-independent functionals in the left N -centered ensemble DFT framework, we have performed left N -centered ensemble DFT calculations for a small set of simple atomic systems consisting of elements of the first two rows of the periodic table plus the first three noble gases. For each element, we have computed two specific features of the left N -centered ensemble

energy curve: the curvature of the ensemble energy relative to its linear interpolation with “wrong” endpoint value, and its total deviation relative to its theoretical linear interpolation with “correct” endpoint value (see Figure 6.1).

These two aspects of the total error were computed by use of the trapezoidal rule which consists in approximating the area under a curve. By subtracting those areas, percent errors of the “curvature-only” and “total” deviations were computed for various atomic systems and within various levels of approximation, the results are reported in Table 6.2.

Regarding the curvature, it seems that Hartree-Fock results tend to yield positive curvatures and thus concave left N -centered ensemble energies while LSDA and BLYP functionals tend to yield negative, and quite similar, curvatures and thus convex left N -centered ensemble energies. As for the B3LYP hybrid functional, the results seem to be more subtle in the sense that for some systems the resulting left N -centered ensemble energy will exhibit negative curvature while positive curvature for others. Nevertheless, B3LYP seems to yield left N -centered energy with the lesser curvature.

Turning now to the total deviation of the left N -centered ensemble energy relative to its theoretical linear interpolation. It appears that for all considered systems and within all considered levels of approximations, the total deviation of the left N -centered ensemble energy is positive, resulting in an overestimation of the ensemble energy. Moreover, given the order of magnitude of the curvature percent errors compared to the one of the total percent errors, one can presume that the use of a standard weight-independent functional in the scope of left N -centered ensemble DFT may have significant impact on the “quality” of the resulting left N -centered ensemble energy, and thus, on the accuracy of the physical properties that one aims to extract from it. Hence, at this point, one can assume that standard weight-independent functionals will show significantly different efficiencies in the scope of N -centered ensemble DFT, as opposed to their well-established notorieties in standard ground-state DFT.

Table 6.2: Estimation of the “curvature-only” and “total” deviation errors of the left *N*-centered biensemble energies obtained by computing the area, using the trapezoidal rule, between the curves of the ensemble energy and the corresponding linear interpolations with wrong and correct endpoint values (see text for details). The calculations were performed in Dunning’s correlation-consistent cc-pVDZ basis set, using different range of exchange-correlation approximations. The blanks correspond to calculations that did not converge throughout the whole ensemble process, that is to say for the full range of the ensemble weight.

	Left <i>N</i> -centered: $N \rightarrow N - 1$											
	UHF		LSDA		BLYP		B3LYP					
	Curvature (%)	Total (%)	Curvature (%)	Total (%)	Curvature (%)	Total (%)	Curvature (%)	Total (%)	Curvature (%)	Total (%)	Curvature (%)	Total (%)
He	5.296	5.296	1.070	13.908	0.953	14.023	1.801	12.264				
Li	-0.201	6.450	-0.822	10.519	-0.834	10.442	-0.710	9.633				
Be	0.068	4.304	-0.253	6.317	-0.256	6.303	-0.194	5.890				
B	0.071	3.422	-0.122	4.636	-0.120	4.631	-0.081	4.382				
C	0.085	2.951	-0.057	3.772	-0.056	3.771	-0.027	3.603				
N	0.081	2.655	-	-	-0.030	3.253	-0.007	3.129				
O	0.070	2.441	-0.015	2.903	-0.015	2.904	0.002	2.808				
F	0.066	2.397	-	-	-0.008	2.642	0.005	2.567				
Ne	0.057	2.145	-	-	-0.005	2.440	0.007	2.379				
Ar	0.001	1.093	-	-	-	-	-0.005	1.179				
Mean	0.559	3.315	-0.033	7.009	-0.041	5.601	0.079	4.783				

As previously mentioned in this chapter, N -centered ensembles were designed to extract physical properties of real systems from an auxiliary canonical ensemble energy by taking simple derivatives with respect to the ensemble weight. Furthermore, we have seen that those physical properties could be reformulated in terms of the weight-dependent Kohn-Sham orbital energies with an additional contribution arising from the weight derivative of the ensemble Hartree-exchange-correlation energy (see equations (6.61) and (6.62)). In particular, left N -centered ensembles were specifically designed to extract ionization potentials in a single ensemble calculation.

Since standard approximations, originally designed for ground-state applications, do not possess any explicit dependency on the ensemble weight, it is straightforward to see that the only ensemble contribution to the prediction of physical properties will come from the weight-dependent Kohn-Sham orbital energies. For instance, in the scope of left N -centered ensemble DFT, ionization potentials will be directly approximated by the opposite of the LZ-shifted highest occupied molecular orbital (HOMO) of the neutral system, unlike in the PPLB framework where ionization potentials were associated instead with the unshifted HOMO energy of the neutral system.

$$I_0^N = -\bar{\varepsilon}_N^{\xi^-} - \frac{1}{N}(1 - \alpha - N) \left. \frac{\partial E_{\text{Hxc}}^{\xi^-}}{\partial \alpha} \right|_{n_{\text{KS}}^{\xi^-}} \quad (6.69)$$

Once more, we would like to stress the fact that unlike in standard DFT, in any ensemble DFT formalism, Kohn-Sham orbitals and orbital energies are weight-dependent and thus may differ from one ensemble DFT calculation to another, accordingly to the variation of the ensemble weight. Nevertheless, for sake of simplification, we will lose the superscript notation “ ξ^- ” of the Kohn-Sham orbital energies whose purpose was to highlight their weight-dependency.

In order to compare the performance of left PPLB ensembles and left N -centered ensembles in the prediction of ionization potentials with a given weight-independent approximation, the left PPLB unshifted HOMO energy of the neutral system as well as the left N -centered LZ-shifted and unshifted HOMO energy of the neutral system are reported in Figure 6.2. Additionally, Δ SCF ionization potentials obtained with the same level of approximation are also reported in order to assess the quality of the ensemble Kohn-Sham predictions compared to the ones obtained by total energy differences, which require multiple DFT calculations. Let us recall that in the left PPLB framework, when the xc-functional has no explicit dependence on the weight ensemble, ionization potentials are solely approximated by the opposite of the weight-dependent unshifted HOMO energy of the neutral system while, in the scope of left N -centered theory, it is the opposite of the weight-dependent LZ-shifted HOMO energy that becomes an approximation for the ionization potential of the neutral system (see equation (6.69)).

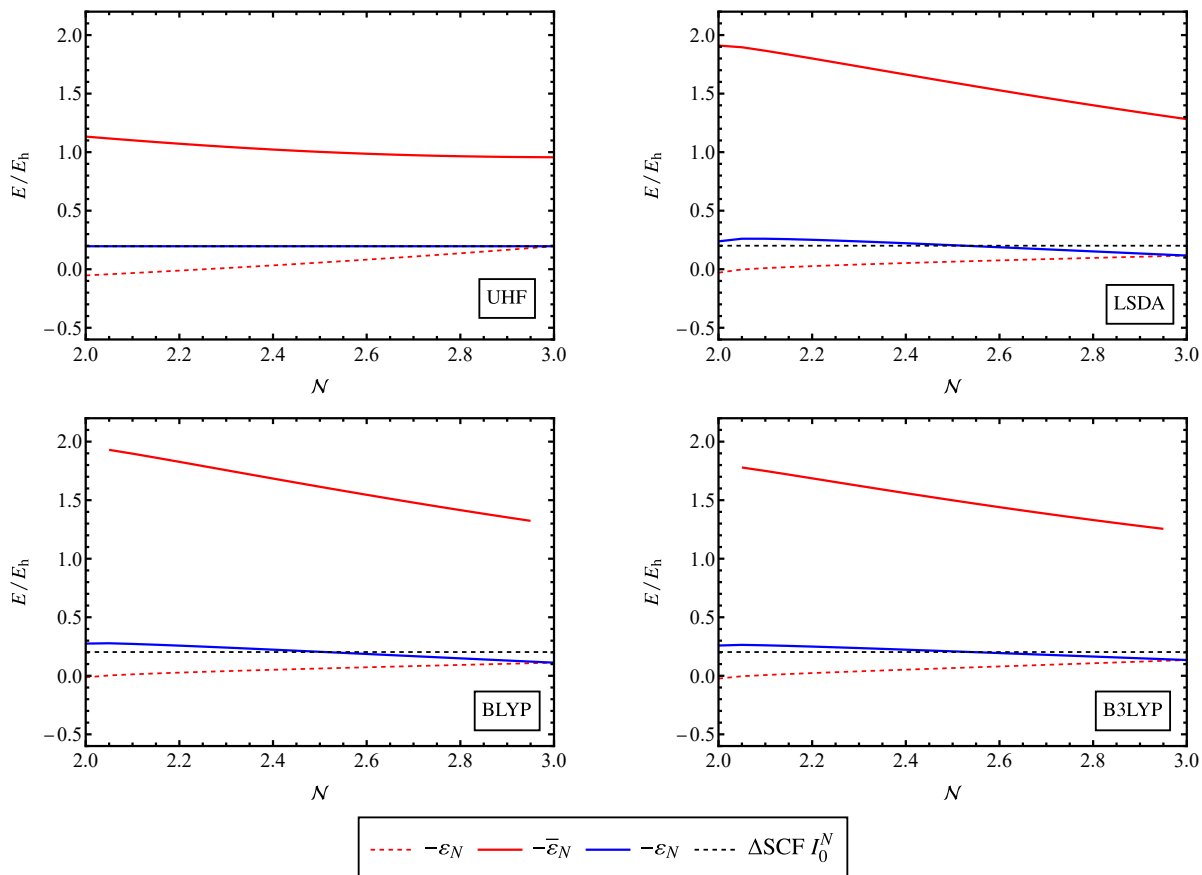


Figure 6.2: Variation of the ionization potential of Li with respect to the fractional number of electrons of the open system, obtained within various ensemble formalisms and with various weight-independent exchange-correlation functionals in the cc-pVDZ basis set. Opposite of the left PPLB weight-dependent HOMO energy of the neutral system (blue solid line) is reported as well as the opposite of the left N -centered weight-dependent unshifted (red dashed line) and LZ-shifted (red solid line) HOMO energies. For each level of approximations, Δ SCF ionization potentials (black dashed line) are also reported for comparison.

Turning back to Figure 6.2, we see that in the zero-weight limit (for $\mathcal{N} = N = 3$), the opposites of the left PPLB and N -centered unshifted HOMO energies are identical, which was expected since both ensemble calculations reduce to the same standard ground-state calculation in that limit. Whereas one electron is continuously removed from Li, through the variation of the ensemble weights, both PPLB and N -centered ensemble HOMO energies vary accordingly. While the opposite of the PPLB HOMO energy increases and manages to match halfway, for $\alpha = 0.5$, the Δ SCF ionization potential reference obtained within the same level of approximation, its N -centered counterpart decreases with a similar order of magnitude, departing from the Δ SCF reference.

In left N -centered theory, we have seen that it is not the unshifted HOMO energy that will be used as a first approximation to the ionization potential of the neutral system but, instead, the LZ-shifted HOMO energy, as depicted in Figure 6.2. Hence, we see that, for all con-

sidered approximations, the impact of the weight-dependent LZ-shift on the HOMO energy is quite significant and will be responsible for yielding significantly overestimated ionization potentials relative to PPLB predictions and Δ SCF references. For instance, with the B3LYP functional, the ionization potential is significantly overestimated, with respect to the Δ SCF reference, by about 1.5 hartrees, which is highly detrimental in terms of accuracy.

In order to offer a more complete overview of the “poor” performance of standard weight-independent xc-functionals in the scope of left N -centered ensemble DFT, we have applied the theory to a set of small atomic systems in order to assess the behavior as well as the quality of the weight-dependent unshifted and LZ-shifted HOMO energies relative to the corresponding Δ SCF ionization potentials, for a small variation of the ensemble weight. The results were computed in terms of percent errors and are reported in Table 6.3.

Table 6.3: Percent errors of the opposite of the unshifted and Levy-Zahariev shifted N th Kohn-Sham orbital energies compared to the ionization potential obtained from Δ SCF calculations for simple atomic systems. The left N -centered calculations were performed for a small charge deviation, $\alpha = 0.05$, in Dunning’s correlation-consistent cc-pVDZ basis set and using different range of exchange-correlation approximations, in the scope of both Hartree-Fock and DFT theories. The blanks correspond to calculations that did not converge.

	$\Delta(\%)$ Left N -centered at $\alpha = 0.05$							
	UHF		LSDA		BLYP		B3LYP	
	$-\varepsilon_N$	$-\bar{\varepsilon}_N$	$-\varepsilon_N$	$-\bar{\varepsilon}_N$	$-\varepsilon_N$	$-\bar{\varepsilon}_N$	$-\varepsilon_N$	$-\bar{\varepsilon}_N$
He	-0.796	58.623	-38.456	57.782	-38.383	58.495	-30.927	56.989
Li	-7.925	387.766	-44.335	552.518	-47.126	552.135	-38.180	507.456
Be	-2.940	379.063	-39.465	442.576	-40.523	449.713	-32.996	420.682
B	-1.486	531.705	-54.949	607.644	-55.457	615.473	-44.164	582.404
C	1.915	539.186	-	-	-51.046	607.122	-40.081	579.213
N	3.604	551.882	-	-	-47.779	610.743	-37.164	586.210
O	7.226	818.062	-52.880	792.719	-52.473	792.428	-40.769	771.797
F	7.842	779.842	-	-	-47.538	774.864	-36.582	755.088
Ne	7.969	757.247	-	-	-43.907	763.389	-30.927	56.989
Mean	1.712	533.708	-46.017	490.647	-47.136	580.484	-36.865	479.647

For a given atomic system and within a given level of approximation, if we compare the percent errors associated with the opposite of the HOMO energy of the neutral system obtained in left N -centered ensemble DFT compared to its left PPLB counterpart (see Table 4.5), we can see that the order of magnitude obtained with both ensemble formalisms, relative to the corresponding Δ SCF reference, are similar, in the range 30 to 50% for DFAs. However, in the N -centered framework, once the LZ-shift is applied to the weight-dependent Kohn-Sham orbital energies, the order of magnitude of the resulting percent error associated with the opposite of the LZ-shifted HOMO energy is significantly increased up to several hundreds percent, yielding significantly worse ionization potentials than in the PPLB framework. Thus, highlighting the fact that besides the general observation that standard weight-independent xc-functionals are rather inadequate to be used in the scope of ensemble-DFT,

they are even more inadequate when they are applied to a completely fictitious auxiliary ensemble with no direct physical reality whatsoever. Hence the need to dedicate a lot of effort in the development of approximate functionals intentionally designed for ensemble applications.

As a small aside, note that in an ensemble formalism, especially in an unrestricted one where spins are treated distinctly, the highest occupied molecular orbital (HOMO) of the ensemble, which can be interpreted as a fictitious average system, is not necessarily the same orbital than the HOMO of the neutral system because the overall ensemble does not necessarily share the same set of occupation numbers than the one associated with a given individual state included in this ensemble. By “not the same”, we mean that they can be orbitals labeled with different numbers. Indeed, a given orbital can be occupied for the description of a given individual state of the ensemble while unoccupied for the description of the ensemble. Since *N*-centered ensembles are canonical ensembles associated with a fixed integral number *N* of electrons, the orbital designated as HOMO of those types of ensembles will always be the same orbital used as the HOMO of the neutral *N*-electron system but this will not necessarily be the case for other types of ensembles, especially grand canonical ensembles. Of course, the same logic holds for the LUMO denomination.

Right *N*-centered ensembles

Now that we have explored the capability of left *N*-centered ensembles to yield accurate predictions for ionization potentials of atomic systems when combined with standard weight-independent exchange-correlation functionals, we will proceed with the extraction of electron affinities from right *N*-centered ensembles.

First, let us recall the generic expression of right *N*-centered ensemble energies associated with an open system arising from the addition of an electron to a neutral *N*-electron system in its ground-state electronic configuration,

$$E_0^{\xi^+} = (1 - \alpha)E_0^N + \frac{N\alpha}{N + 1}E_0^{N+1}. \quad (6.70)$$

As an illustrative example, Table 6.4 reports the details of the electronic configurations that have been used in order to perform practical calculations of right *N*-centered ensemble DFT applied to the lithium atom. Again, in the interest of establishing a parallel between right PPLB and right *N*-centered results, both ensembles were built with the same individual electronic configurations, that is to say that for a given system, the same electron has been added to the neutral system within both formalisms.

Table 6.4: Electronic configurations of the individual states of the right N -centered biensemble mimicing the addition of a spin-down electron to the electronic configuration of the lithium ground state. Only the occupation numbers of the six lowest molecular orbitals of each spin are depicted.

State of the ensemble	Weight	Spin	Occupation numbers					
1	$1 - \alpha$	\uparrow	1	1	0	0	0	0
		\downarrow	1	0	0	0	0	0
2	$\frac{N\alpha}{N+1}$	\uparrow	1	1	0	0	0	0
		\downarrow	1	1	0	0	0	0

Similarly to the exact left N -centered ensemble, in the exact theory, the exact right N -centered ensemble energy must be perfectly linear with respect to the ensemble weight and must obey the following specific boundary conditions,

$$E_0^{\xi^+=0} = E_0^N \quad (6.71) \quad \left| \quad E_0^{\xi^+=\frac{N}{N+1}} = \frac{N}{N+1} E_0^{N+1}. \quad (6.72)$$

Hence, the exact right N -centered ensemble energy, which is an auxiliary canonical quantity with no direct physical meaning, must reduce to the exact ground-state energy of the neutral system in the zero-weight limit and yield a scaled exact ground-state energy of the anionic system, with the right N -centered scaling factor $\frac{N}{N+1}$, when $\alpha = 1$.

In practice, when a density-functional approximation (DFA) is used in place of the unknown exact functional, the resulting boundary conditions will be more subtle because of the non-linearity of most approximate functionals, as discussed for the left N -centered framework.

$$E^{\text{DFA}, \xi^+=0} = E_0^{N, \text{DFA}} \quad (6.73) \quad \left| \quad E^{\text{DFA}, \xi^+=\frac{N}{N+1}} \neq \frac{N}{N+1} E_0^{N+1, \text{DFA}}. \quad (6.74)$$

Indeed, approximate weight-independent functionals will yield non-linear right N -centered ensemble energies with an additional endpoint deviation compared to the theoretical result that would have been obtained if the functional were perfectly linear, as depicted in Figure 6.3. For a more complete overview of right N -centered ensemble energy features, percent errors of curvature-only and total deviation of right N -centered ensemble energies applied to a small set of atomic systems are reported in Table 6.5, within several levels of approximations.

Conversely to left N -centered ensemble energies, we observe that right N -centered ensemble energies obtained with approximate functionals tend to be underestimated compared to their theoretical counterparts. This may be a direct consequence of the fact that the right N -centered scaling factor is, by construction, a positive number less than unity while its left N -centered counterpart is greater than unity, resulting in overestimated left N -centered ensemble energies.

As for the sign of the curvature, and thus the convex or concave nature of the ensemble

energy, it does not seem to be affected by the left or right nature of the N -centered ensemble but much more by the choice of approximation.

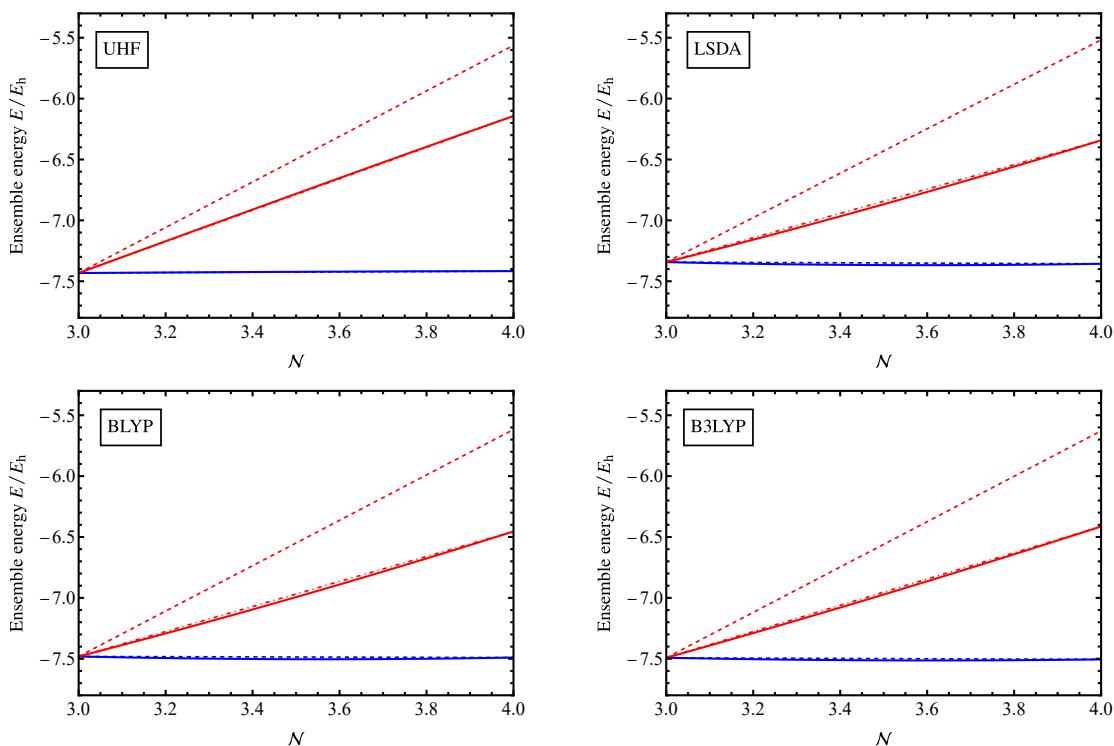


Figure 6.3: Comparison between the right PPLB (blue, solid line) and right N -centered (red, solid line) ensemble energies of Li obtained with different levels of approximations in the cc-pVDZ basis set. Linear interpolations of the PPLB (blue, dashed line) and N -centered (red, dot-dashed line) ensemble energies are reported to highlight the additional curvature arising from the use of approximate functionals as well as the endpoint deviation of the N -centered ensemble energy relative to its theoretical value (red, dashed line).

Turning now to electron affinities and how they can be extracted from right N -centered ensembles. We recall the key-result derived in right N -centered ensemble DFT formalism which enables one to express the electron affinity of a neutral N -electron system in terms of the weight-dependent LUMO energy plus an additional contribution arising from the derivative of the ensemble Hartree-exchange-correlation functional,

$$A_0^N = -\bar{\epsilon}_{N+1}^{\xi^+} - \frac{1}{N}(1 - \alpha + N) \left. \frac{\partial E_{\text{Hxc}}^{\xi^+}}{\partial \alpha} \right|_{n_{\text{KS}}^{\xi^+}}. \quad (6.75)$$

Hence, we see that, just like in standard ground-state DFT, in N -centered ensemble DFT theory the HOMO and LUMO of the neutral N -electron system, the so-called frontier orbitals, play a key-role in approximating ionization potentials and electron affinities with the crucial

Table 6.5: Estimation of the “curvature-only” and “total” deviation errors of the right N -centered biensemble energies obtained by computing the area, using the trapezoidal rule, between the curves of the ensemble energy and the corresponding linear interpolations with wrong and correct endpoint values (see text for details). The calculations were performed in Dunning’s correlation-consistent cc-pVDZ basis set, using different range of exchange-correlation approximations. The blanks correspond to calculations that did not converge throughout the whole ensemble process, that is to say for the full range of the ensemble weight.

	Right N -centered: $N \rightarrow N + 1$											
	UHF			LSDA			BLYP			B3LYP		
	Curvature (%)	Total (%)	Total (%)	Curvature (%)	Total (%)	Total (%)	Curvature (%)	Total (%)	Total (%)	Curvature (%)	Total (%)	Total (%)
He	1.618	-12.009	-19.906	0.111	-19.906	-19.553	0.108	-19.553	-19.553	0.384	-17.860	-17.860
Li	0.060	-4.403	-6.674	-0.243	-6.674	-6.649	-0.245	-6.649	-6.649	-0.187	-6.179	-6.179
Be	0.072	-3.493	-4.955	-0.114	-4.955	-4.946	-0.111	-4.946	-4.946	-0.074	-4.642	-4.642
B	0.084	-3.004	-4.015	-0.054	-4.015	-4.042	-0.052	-4.042	-4.042	-0.024	-3.829	-3.829
C	0.081	-2.706	-	-	-	-3.495	-0.027	-3.495	-3.495	-0.006	-3.335	-3.335
N	0.071	-2.493	-3.116	-0.014	-3.116	-3.113	-0.013	-3.113	-3.113	0.003	-2.986	-2.986
O	0.064	-2.322	-	-	-	-2.825	-0.007	-2.825	-2.825	0.006	-2.721	-2.721
F	0.057	-2.184	-	-	-	-	-	-	-	-	-	-
Ne	-0.039	-2.143	-2.409	-0.006	-2.409	-2.407	-0.006	-2.407	-2.407	0.001	-2.338	-2.338
Ar	0.002	-1.031	-1.142	-0.007	-1.142	-1.142	-0.007	-1.142	-1.142	-0.005	-1.119	-1.119
Mean	0.207	-3.578	-6.031	-0.046	-6.031	-5.352	-0.040	-5.352	-5.352	0.0108	-5.001	-5.001

difference that, in ensemble DFT, the orbitals resulting from the calculation are weight-dependent and are not optimized with respect to the ground-state of the neutral N -electron system but to the whole ensemble system instead.

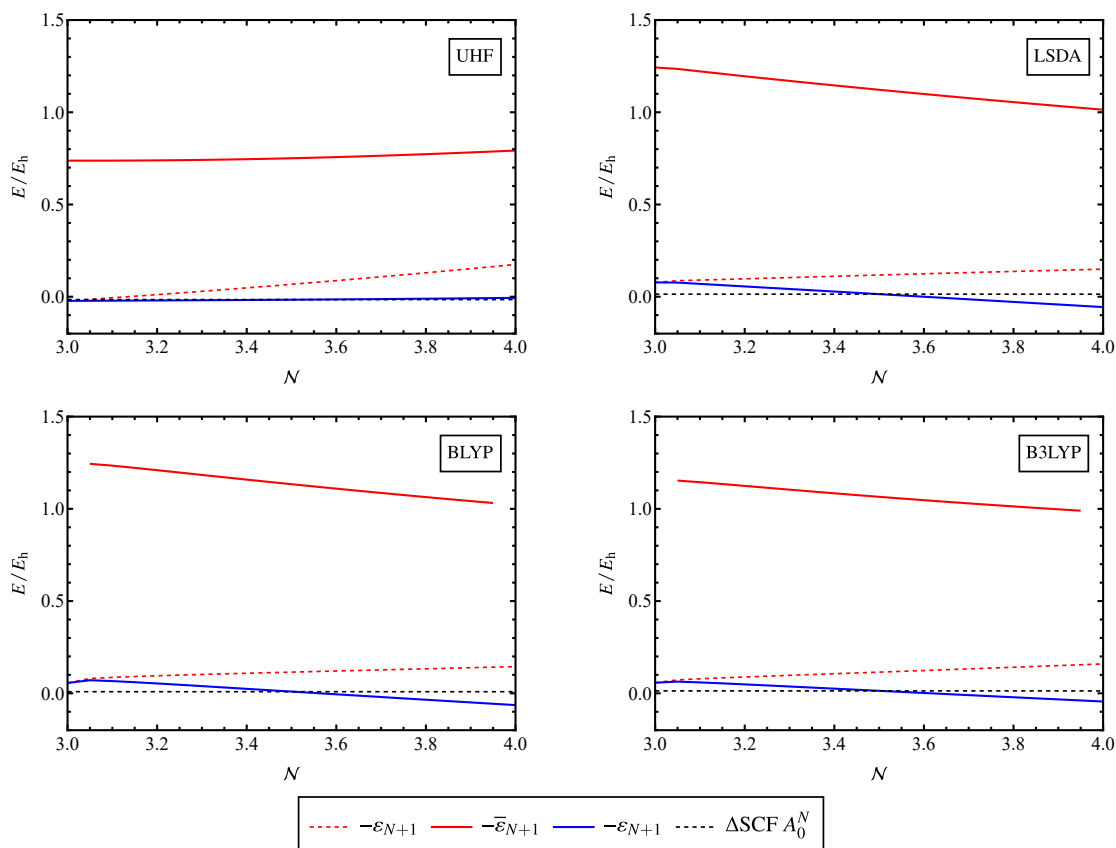


Figure 6.4: Variation of the electron affinity of Li with respect to the fractional number of electrons of the open system, obtained within various ensemble formalisms and with various weight-independent exchange-correlation functionals in the cc-pVDZ basis set. Opposite of the right PPLB weight-dependent LUMO energy of the neutral system (blue solid line) is reported as well as the opposite of the right N -centered weight-dependent unshifted (red dashed line) and LZ-shifted (red solid line) LUMO energies. For each level of approximations, ΔSCF electron affinities (black dashed line) are also reported for comparison.

Since we only consider weight-independent approximations for now, the resulting electron affinity will solely be determined by the opposite of the weight-dependent LZ-shifted LUMO energy of the neutral system, as depicted in Figure 6.4.

Once again, we observe that, in the zero-weight limit, the opposite of the right PPLB and right N -centered unshifted LUMO energies reduce to the same quantity but start departing from each other while the ensemble weight increases, that is to say while a new electron is added to the physical open system. We see that in both left and right N -centered ensemble DFT the LZ-shift-in-potential procedure has significant impact on the quality of the prediction of ionization potentials and electron affinities. Indeed, once the LZ-shift applied

to the LUMO energy of the neutral system, the opposite of the resulting LZ-shifted LUMO energy is moved far above the Δ SCF reference, yielding significantly overestimated electron affinities, by around one hartree for the lithium atom.

Percent errors of the opposite of right N -centered unshifted and LZ-shifted LUMO energies of various atomic systems within various levels of approximation are reported in Table 6.6. The calculations were performed for a small variation of the ensemble weight.

Table 6.6: Percent errors of the opposite of the unshifted and Levy-Zahariev shifted ($N + 1$)th Kohn-Sham orbital energies compared to the electron affinities obtained from Δ SCF calculations for simple atomic systems. The right N -centered calculations were performed for a small charge deviation, $\alpha = 0.05$, in Dunning’s correlation-consistent cc-pVDZ basis set and using different range of exchange-correlation approximations, in the scope of both Hartree-Fock and DFT theories. The blanks correspond to calculations that did not converge.

	$\Delta(\%)$ Right N -centered at $\alpha = 0.05$							
	UHF		LSDA		BLYP		B3LYP	
	$-\varepsilon_{N+1}$	$-\bar{\varepsilon}_{N+1}$	$-\varepsilon_{N+1}$	$-\bar{\varepsilon}_{N+1}$	$-\varepsilon_{N+1}$	$-\bar{\varepsilon}_{N+1}$	$-\varepsilon_{N+1}$	$-\bar{\varepsilon}_{N+1}$
He	-1.011	37.373	20.014	83.211	20.316	86.607	16.109	76.869
Li	8.338	4831.135	528.638	8850.237	820.745	14 190.784	453.614	8690.216
Be	-0.342	2367.638	371.425	5741.472	306.665	4796.656	284.420	5243.750
B	-27.375	5132.238	-	-	841.821	13 176.832	1037.817	19 532.833
C	-267.345	33 269.129	-	-	3122.446	49 429.494	1048.642	20 221.910
N	-17.827	2282.024	312.917	5454.507	313.207	5495.939	257.886	5548.179
O	-46.529	4996.777	-	-	1196.761	22 501.888	1275.353	29 784.450
F	-506.966	49 838.080	-	-	751.706	14 901.682	480.963	11 963.366
Ne	15.126	291.815	-	-	16.157	421.713	12.687	405.308
Mean	-93.770	11 449.578	308.248	5032.356	821.091	13 889.066	540.832	11 274.097

Once more, we see that right PPLB and N -centered ensemble DFT LUMO energies are associated with percent errors of similar orders of magnitude, about a few hundreds percent. Nevertheless, in right N -centered ensemble DFT, the additional LZ-shift-in-potential applied to the LUMO energy will significantly increase the magnitude of the error relative to the Δ SCF reference. While it is well-known that LUMO energies yield poor predictions for physical properties such as electron affinities, we see that this infamous deficiency is even more detrimental in the N -centered framework because of the additional contribution of the LZ-shift to the prediction of electron affinities.

Therefore, without an explicit weight-dependence of the Hxc-functional, it seems unreachable to obtain accurate predictions for charged excitation energies such as ionization potentials and electron affinities through an N -centered ensemble DFT formalism. Hence the need to dedicate significant efforts to designing explicit weight-dependent approximate functionals which encompasses subtleties arising from the scope of both ground-state DFT and ensemble DFT.

Single-weight *N*-centered triensembles

Now that we have seen how ionization potentials and electron affinities can be extracted from left and right *N*-centered ensembles, respectively, in a single DFT-like calculation, we will explore the capability of *N*-centered ensembles to enable direct extraction of fundamental gaps. As a matter of fact, the original formulation of *N*-centered ensemble DFT proposes to design a three-state ensemble which includes the ground states of the neutral, cationic and anionic forms of a *N*-electron system,

$$E^\xi = (1 - 2\xi)E_0^N + \xi E_0^{N-1} + \xi E_0^{N+1}, \quad (6.76)$$

with $0 \leq \xi \leq 0.5$.

In this work, we will focus on the single-weight *N*-centered triensemble which has the specificity of assigning the same ensemble-weight to both cationic and anionic contributions of the ensemble. Since ground-state energies are physical quantities, they must have no dependency on the ensemble weight and, therefore, the single-weight *N*-centered ensemble energy must be linear with respect to the ensemble weight. As a consequence, the variation of the ensemble weight must have no impact on the slope of the exact *N*-centered ensemble energy which must remain constant for any weight-configuration. The practical advantage of such ensemble is to enable direct extraction of fundamental gaps through the derivative of the ensemble energy with respect to the ensemble weight,

$$\begin{aligned} \Omega_0^N &\equiv I_0^N - A_0^N \\ &= E_0^{N-1} + E_0^{N+1} - 2E_0^N \\ &= \frac{dE^\xi}{d\xi}. \end{aligned} \quad (6.77)$$

Based on that definition, we can derive in the same manner that we did for the left and right *N*-centered biensemble formulations for ionization potentials and electron affinities, fundamental gap formulations based on the weight-dependent *N*-centered ensemble Kohn-Sham orbital energies and on the derivative of the Hartree-exchange-correlation functional with respect to the ensemble weight. Hence, we derive the following *N*-centered formulation for the fundamental gap of the *N*-electron system,

$$\Omega_0^N = \varepsilon_{N+1}^\xi - \varepsilon_N^\xi + \left. \frac{\partial E_{\text{Hxc}}^\xi}{\partial \xi} \right|_{n_{\text{KS}}^\xi}. \quad (6.78)$$

Hence we see that, in the single-weight *N*-centered triensemble framework defined previously, we obtain that the fundamental gap of the *N*-electron system can be approximated by the traditional HOMO-LUMO gap of the neutral system, obtained from the unshifted weight-dependent ensemble Kohn-Sham orbital energies, plus an additional contribution arising from the explicit dependence of the exact ensemble Hartree-exchange-correlation functional on the ensemble weight.

Of course, if standard weight-independent approximate Hxc-functionals were to be used in place of the exact unknown functional, the resulting fundamental gap prediction would solely be determined by the ensemble HOMO-LUMO gap of the neutral system which may turn out to be insufficient, in complete analogy with standard-DFT Kohn-Sham HOMO-LUMO gaps.

In order to test the theory, we have performed single-weight N -centered triensemble ensemble DFT calculations for various simple atomic systems (see Table 6.8) in order to evaluate the accuracy and behaviour of the weight-dependent Kohn-Sham approximation for the fundamental gap compared to what one would obtain when performing standard Δ SCF calculations with the same level of Hxc approximation. Note that computing fundamental gaps from Δ SCF calculations would require three standard-DFT calculations while a single-weight N -centered triensemble fundamental gap would only require a single calculation with a DFT-like computational cost.

As an illustrative example, Table 6.7 reports details of the electronic configurations that have been used to apply the single-weight N -centered triensemble eDFT theory to the lithium atom. We stress that the N -centered HOMO-LUMO formulation of fundamental gaps derived in equation (6.78) is only valid if the electronic configurations used to build the individual states of the ensemble are chosen accordingly.

Table 6.7: Electronic configurations of the individual states of the single-weight N -centered triensemble applied to the lithium atom.

State of the ensemble	Weight	Spin	Occupation numbers					
1	$1 - 2\xi$	\uparrow	1	1	0	0	0	0
		\downarrow	1	0	0	0	0	0
2	ξ	\uparrow	1	0	0	0	0	0
		\downarrow	1	0	0	0	0	0
3	ξ	\uparrow	1	1	0	0	0	0
		\downarrow	1	1	0	0	0	0

As expected, assessing the performance of standard weight-independent xc-functionals in the scope of single-weight N -centered triensemble eDFT theory has led us to the same conclusions already drawn in the left and right N -centered frameworks. The use of inadequate weight-independent approximations results in non-linear N -centered ensemble energies and, thus, associated with non-constant slopes, resulting in unphysical weight-dependent fundamental gaps, as depicted in Figure 6.5. Indeed, the lack of explicit weight-dependence in the xc-functionals results in the absence of the weight-derivative additional term in the prediction of fundamental gaps, which appears to have significant impact on the quality of the result.

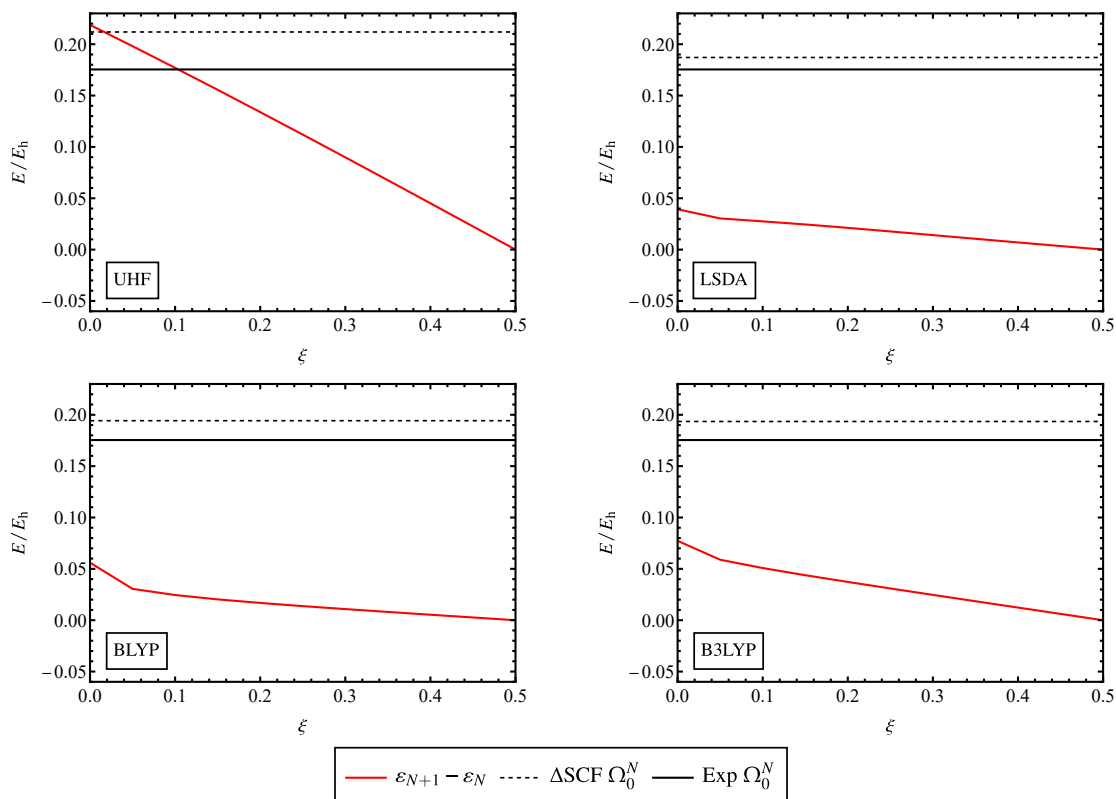


Figure 6.5: Variation of the fundamental gap of Li with respect to the ensemble weight, extracted from the single-weight N -centered triensemble and for various weight-independent exchange-correlation functionals in the cc-pVDZ basis set. Δ SCF fundamental gaps (black dashed line) and experimental fundamental gaps (black solid line) are also reported for comparison (see Appendix A).

In the zero-weight limit, the single-weight N -centered calculation reduces to a standard ground-state DFT calculation for the neutral system, yielding significantly underestimated Kohn-Sham fundamental gaps and slightly overestimated Hartree-Fock fundamental gaps, compared to Δ SCF references obtained within the same level of approximations. Experimental fundamental gaps are also reported in Figure 6.5 to highlight the very poor quality of Kohn-Sham fundamental gaps in both ground-state DFT and N -centered eDFT. In addition, percent errors of single-weight N -centered fundamental gap predictions relative to Δ SCF fundamental gaps obtained with standard weight-independent approximations are reported in Table 6.8 for various atomic systems and various weight configurations.

Table 6.8: Percent errors of the single-weight N -centered triensemble eDFT Kohn-Sham fundamental gap compared to the Δ SCF reference for simple atomic systems. The single-weight N -centered triensemble calculations were performed for a small charge deviation, $\xi = 0.05$ and for the equitriensemble configuration $\xi = 1/3$, in Dunning’s correlation-consistent cc-pVDZ basis set and with different level of exchange-correlation approximations. The blanks correspond to calculations that did not converge.

	$\Delta(\%)$ single-weight N -centered $\varepsilon_{N+1} - \varepsilon_N$							
	UHF		LSDA		BLYP		B3LYP	
	$\xi = 0.05$	$\xi = 1/3$	$\xi = 0.05$	$\xi = 1/3$	$\xi = 0.05$	$\xi = 1/3$	$\xi = 0.05$	$\xi = 1/3$
He	1.322	-14.823	-26.749	-27.256	-27.011	-27.522	-21.489	-25.065
Li	-6.526	-64.596	-83.759	-93.728	-84.297	-95.379	-69.571	-89.389
Be	-0.099	-39.231	-64.182	-65.289	-64.229	-66.491	-51.664	-61.020
B	2.249	-61.840	-98.089	-99.421	-94.148	-97.994	-75.058	-90.797
C	6.776	-60.273	-	-	-95.385	-98.424	-75.188	-90.851
N	6.582	-46.112	-	-	-77.984	-87.614	-60.833	-80.785
O	13.768	-57.928	-	-	-94.811	-98.185	-73.741	-90.299
F	16.279	-56.951	-	-	-95.675	-98.492	-73.815	-90.328
Ne	-9.039	-27.396	-	-	-25.379	-27.596	-19.662	-25.434
Mean	3.479	-47.683	-68.194	-71.423	-73.213	-77.521	-57.891	-71.552

Furthermore, the increase of the N -centered single weight fails to improve the results, yielding even more underestimated fundamental gap predictions with DFAs.

At the Hartree-Fock level, the variation of the ensemble weight will result in a much significant decrease of the gap, compared to the rather slow decrease provided by DFAs. While Hartree-Fock theory is known to yield overestimated fundamental gaps in standard DFT, this overestimation will gradually give way to a much significant underestimation of the gap, as the N -centered ensemble weight increases.

6.3.2 With Weight-dependent Exchange-Correlation Functionals

Building weight-dependent N -centered exchange functionals

Thus far, we have highlighted the poor performance of standard weight-independent xc-functionals when used in the scope of N -centered ensemble DFT, characterised by a deviation of the N -centered ensemble energies from the theoretical ensemble energies that one would expect based on the well-known performance of such approximate functionals within their original framework, ground-state KS-DFT. Indeed, we have seen that the use of inadequate weight-independent and non-linear approximate functionals may cause two notable features of the N -centered ensemble energies, curvature and wrong endpoint energy values, that may have significant impact on the ability of such functionals to provide accurate predictions for physical properties such as ionization potentials and electron affinities.

Therefore, our interest is to build a weight-dependent functional that would aim at correcting both curvature and wrong endpoint features of left and right N -centered ensemble energies in order to explore the impact that such functionals may have on the quality of the physical properties extracted from those ensembles.

Since the order of magnitude of exchange energies is much more significant than for correlation energies, we assume that injecting an explicit weight-dependency into the exchange part of the total ensemble energy functional may correct most of the incorrect features of left and right *N*-centered ensemble energies.

Hence, to design our weight-dependent approximate exchange functional we will start by removing the standard weight-independent exchange energy functional from the total *N*-centered ensemble energy functional and replace it with a weight-dependent exchange energy functional,

$$E^{\xi^\pm, \text{eDFA}}[n] = E^{\xi^\pm, \text{DFA}}[n] - E_x^{\xi^\pm, \text{DFA}}[n] + E_x^{\xi^\pm, \text{eDFA}}[n], \quad (6.79)$$

with the weight-dependent *N*-centered ensemble density-functional approximation (eDFA) for the exchange energy

$$E_x^{\xi^\pm, \text{eDFA}}[n] \equiv F_x^{\xi^\pm} E_x^{\xi^\pm, \text{DFA}}[n], \quad (6.80)$$

where $F_x^{\xi^\pm}$ is the explicitly weight-dependent *N*-centered exchange scaling factor and $\xi^\pm = \frac{N}{N \pm 1}$ are the left (-) or right (+) *N*-centered ensemble weight.

The eDFA exchange approximate functional defined in equation (6.80) must correct both curvature and endpoint deviation errors of the *N*-centered ensemble energy stemming from the use of inadequate standard ground-state density-functional approximations (DFAs). Thereby, the eDFA ensemble energy functional defined in equation (6.79) must recover the same pure-state individual ground-state energy of the neutral system obtained with standard DFAs in ground-state DFT, when $\alpha = 0$, as well as the scaled ground-state energy of the cationic/anionic system, when $\alpha = 1$, in addition to yielding a perfectly linear *N*-centered ensemble energy between those two boundary conditions

$$E^{\xi^\pm, \text{eDFA}} = E_0^{N, \text{DFA}} + \alpha \left(\frac{N}{N \pm 1} E_0^{N \pm 1, \text{DFA}} - E_0^{N, \text{DFA}} \right). \quad (6.81)$$

Combining equations (6.79), (6.80) and (6.81), we deduce the analytical expression of the weight-dependent *N*-centered CC-exchange multiplicative scaling factors

$$F_x^{\xi^\pm} = \frac{E_0^{N, \text{DFA}} + \alpha \left(\frac{N}{N \pm 1} E_0^{N \pm 1, \text{DFA}} - E_0^{N, \text{DFA}} \right) - (E^{\xi^\pm, \text{DFA}} - E_x^{\xi^\pm, \text{DFA}})}{E_x^{\xi^\pm, \text{DFA}}}. \quad (6.82)$$

In order to explore separately the impact of the curvature and endpoint deviation of the *N*-centered ensemble energy, we have designed weight-dependent exchange functionals so that only the linearity of the *N*-centered ensemble energy would be restored, with no alteration of the endpoint energy value. Hence, the analytical expression of the ‘‘curvature’’ weight-dependent *N*-centered CC-exchange multiplicative scaling factors

$$F_{x, \text{curv}}^{\xi^\pm} = \frac{E_0^{N, \text{DFA}} + \alpha (E^{\xi^\pm = \frac{N}{N \pm 1}, \text{DFA}} - E_0^{N, \text{DFA}}) - (E^{\xi^\pm, \text{DFA}} - E_x^{\xi^\pm, \text{DFA}})}{E_x^{\xi^\pm, \text{DFA}}}. \quad (6.83)$$

Since the weight-dependent eDFA exchange functional must reduce to its weight-independent counterparts in the zero-weight limit $\alpha = 0$ but not for $\alpha = 1$, we choose to approximate the N -centered exchange scaling factor with a 4th order polynomial expression that reduces to unity when $\alpha = 0$ (see Figure 6.6),

$$F_x^{\xi\pm} \approx 1 + a\alpha + b\alpha^2 + c\alpha^3 + d\alpha^4. \quad (6.84)$$

As for the ‘‘curvature’’ weight-dependent N -centered CC-exchange multiplicative scaling factors, they must yield no corrections at weight $\alpha = 0$ and $\alpha = 1$, with no correction of the N -centered endpoint energy value. Therefore, we choose to approximate the ‘‘curvature’’ scaling factor with a 4th order polynomial expression centered on $\alpha = \frac{1}{2}$ and which reduces to 1 when $\alpha = 0$ and $\alpha = 1$ (see Figure 6.7)

$$F_{x,\text{curv}}^{\xi\pm} \approx 1 - \alpha(1 - \alpha) \left[a + b \left(\alpha - \frac{1}{2} \right) + c \left(\alpha - \frac{1}{2} \right)^2 \right], \quad (6.85)$$

with $\{a, b, c, d\}$ a set of real parameters.

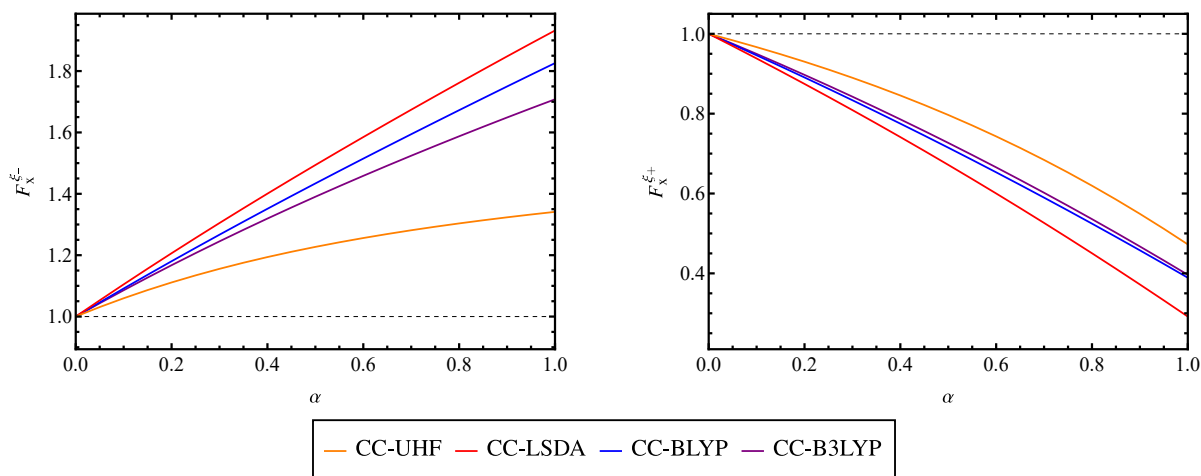


Figure 6.6: Comparison between weight-dependent left (left panel) and right (right panel) N -centered ‘‘total deviation’’ exchange scaling factors of Li, obtained from various weight-dependent approximations in the cc-pVDZ basis set.

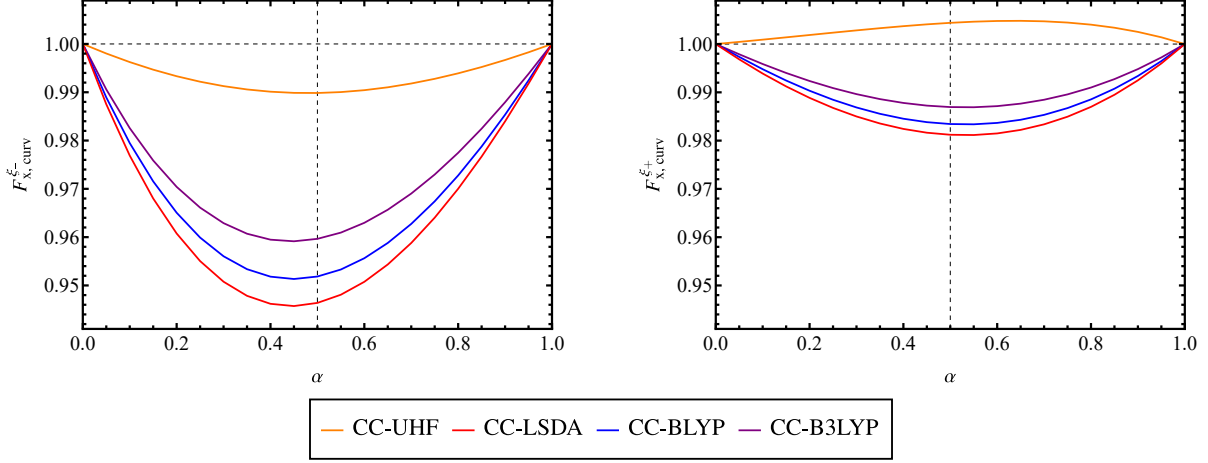


Figure 6.7: Comparison between weight-dependent left (left panel) and right (right panel) N -centered “curvature-only” exchange scaling factors of Li, obtained from various weight-dependent approximations in the cc-pVDZ basis set.

Hence, the following decomposition for the weight-dependent eDFA N -centered total-energy functional

$$E^{\xi^\pm, \text{eDFA}}[n] = T_s[n] + E_H[n] + E_x^{\xi^\pm, \text{eDFA}}[n] + E_c^{\text{DFA}}[n] + E_{\text{en}}[n], \quad (6.86)$$

where we choose to put all the explicit weight-dependency of the Hartree-exchange-correlation functional into its exchange part and to use the classical weight-independent Hartree functional $E_H[n]$ and a standard weight-independent DFA correlation functional $E_c^{\text{DFA}}[n]$. Additionally to the ensemble energy functional, the explicit weight-dependency will be included as well in the ensemble Hartree-exchange-correlation potential

$$v_{\text{Hxc}}^{\xi^\pm, \text{eDFA}}(\mathbf{r}) = v_H(\mathbf{r}) + v_x^{\xi^\pm, \text{eDFA}}(\mathbf{r}) + v_c^{\text{DFA}}(\mathbf{r}), \quad (6.87)$$

where $v_H(\mathbf{r})$ and $v_c^{\text{DFA}}(\mathbf{r})$ are the weight-independent Hartree and correlation potentials, respectively, and

$$\begin{aligned} v_x^{\xi^\pm, \text{eDFA}}(\mathbf{r}) &= \frac{\delta E^{\xi^\pm, \text{eDFA}}[n]}{\delta n(\mathbf{r})} \\ &= F_x^{\xi^\pm} v_x^{\text{DFA}}(\mathbf{r}), \end{aligned} \quad (6.88)$$

is the weight-dependent N -centered exchange potential.

In this work, the use of a weight-dependent exchange functional will enable us to extract more stable individual-state properties and excitation energies from N -centered ensembles, that is to say more constant with respect to the variation of the ensemble weight, due to the additional contribution stemming from its derivative with respect to the ensemble weight,

$$\frac{\partial E_{\text{Hxc}}^{\xi^\pm, \text{eDFA}}[n]}{\partial \xi^\pm} = \frac{\partial E_x^{\xi^\pm, \text{eDFA}}[n]}{\partial \xi^\pm} = \frac{\partial F_x^{\xi^\pm}}{\partial \xi^\pm} E_x^{\text{DFA}}[n]. \quad (6.89)$$

The N -centered weight-dependent eDFAs will be referred to by use of the same denomination already used in this work for the weight-dependent approximate functionals that have been designed in the scope of PPLB and GOK ensemble formalisms. Hence, each weight-independent DFA considered in this work will serve as starting point for the design of its weight-dependent counterpart, the CC-DFA functional. Total and “curvature-only” weight-dependent N -centered CC-exchange multiplicative scaling factors have been computed within the scope of both left and right N -centered biensembles applied to a small set of atomic systems and for various levels of xc-approximation, as depicted in Figure 6.8.

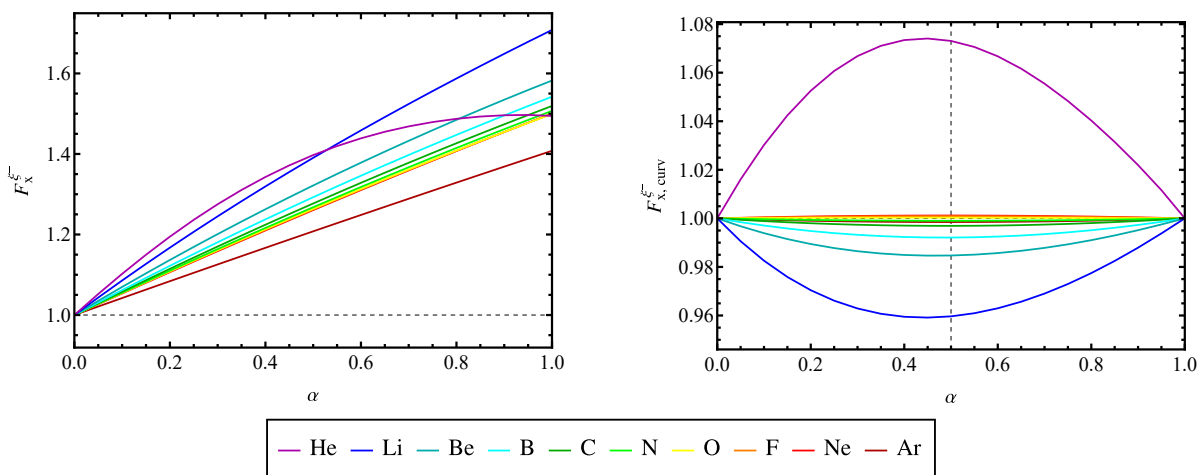


Figure 6.8: Comparison between weight-dependent “total deviation” (left panel) and “curvature-only” (right panel) left N -centered exchange scaling factors of a set of simple atomic systems, obtained from the weight-dependent xc-functional CC-B3LYP in the cc-pVDZ basis set.

Left N -centered ensembles

We have performed self-consistent left N -centered calculations with the above-mentioned weight-dependent CC xc-functionals in order to assess to what extent the curvature and endpoint deviations of N -centered ensemble energies obtained with standard DFAs would affect the quality of the ensemble predictions of physical properties such as charged excitations. Regarding the left N -centered ensemble energies obtained with weight-dependent CC-functionals (see Figure E.7), we see that such functionals managed to recover the “correct” ensemble energies, with no curvature and with correct endpoint energy values, for all considered levels of approximation, as they were intended to. Nevertheless, despite the good behaviour of the CC ensemble energies for almost the full range of the ensemble weight, a small endpoint deviation still subsists. This may be because the CC-functionals are still non-linear with respect to the quantity they are applied to and even enforcing a predefined endpoint value on such functionals doesn’t ensure the final self-consistent results.

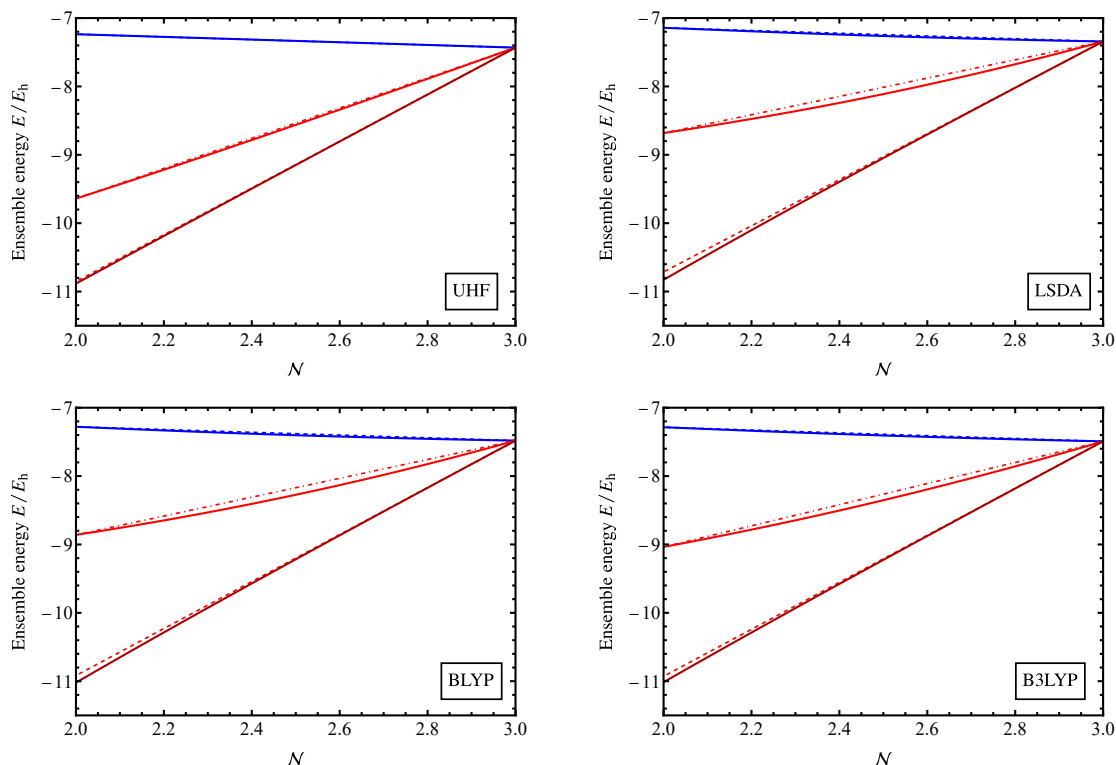


Figure 6.9: Comparison between the left PPLB (blue solid line) and left N -centered (red solid line) ensemble energies of Li obtained with standard weight-independent xc-functionals and their weight-dependent CC-analogs in the cc-pVDZ basis set. Linear interpolations of the PPLB (blue dashed line) and N -centered (red dot-dashed line) ensemble energies are reported to highlight the additional curvature arising from the use of weight-independent approximate functionals as well as the endpoint deviation of the N -centered ensemble energy relative to its theoretical value (red dashed line). For each level of approximation, the left N -centered ensemble energy obtained with the corresponding weight-dependent CC-functional is also reported (dark-red solid line).

Turning now to the ensemble predictions of the ionization potential of Li obtained with CC-functionals, we see that by correcting the total deviation of the left N -centered ensemble energies, the weight-dependent CC-functionals managed to yield much satisfactory ionization potentials than the weight-independent DFAs, as depicted in Figure E.8.

As a matter of fact, the weight-dependent orbital energies obtained from a given DFA and the ones provided by its CC-counterpart are very similar and the same observation stands for the LZ-shifted orbital energies (see Table D.1). Moreover, most of the improvement of the results is due to the additional contribution of the weight derivative of the CC-functionals, illustrated by the “DD” term.

Nevertheless, because of the residual endpoint deviation of the CC left N -centered ensemble energies, the prediction of ionization potentials tends to depart from the Δ SCF references as the ensemble weight increases, that is to say as the electron is gradually removed and the number of electrons of the open system decreases, yielding more and more underestimated predictions. For that reason, left N -centered calculations in the zero-weight limit seems to

be the best option to obtain satisfactory results.

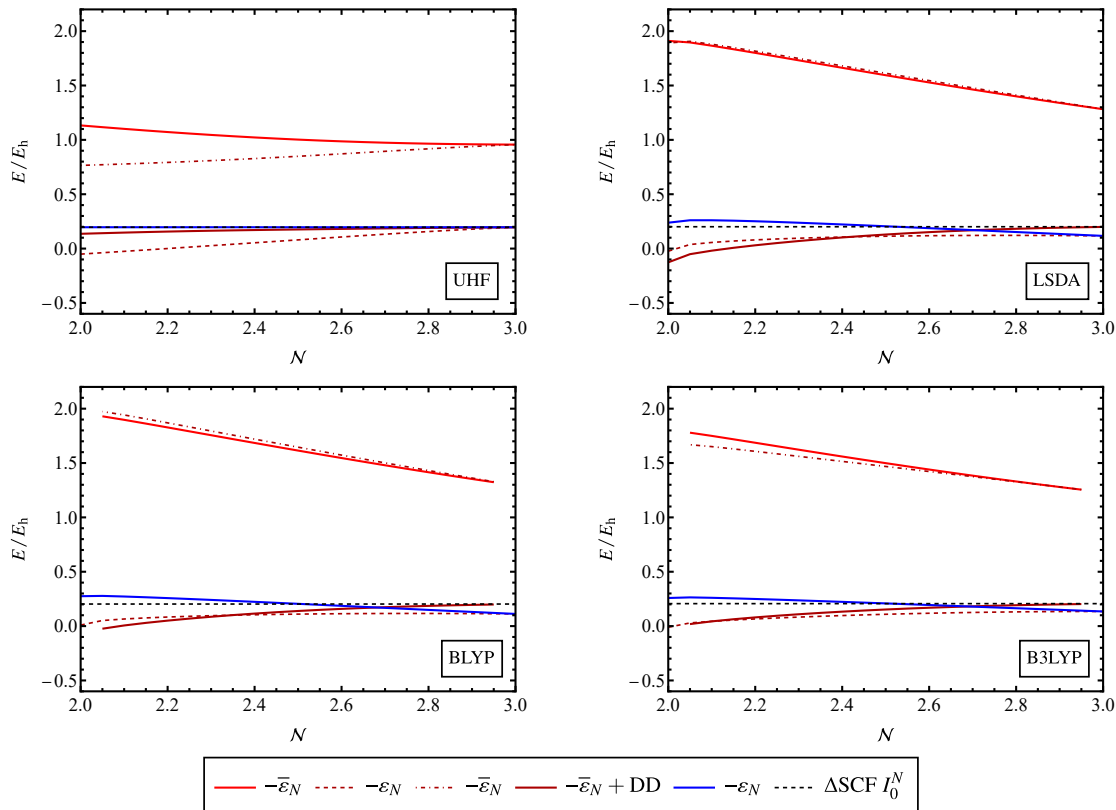


Figure 6.10: Variation of the ionization potential of Li with respect to the fractional number of electrons of the open system, obtained within left PPLB and left N -centered ensemble formalisms with various weight-independent and weight-dependent exchange-correlation functionals in the cc-pVDZ basis set. For each weight-independent approximation, opposite of the left PPLB weight-dependent HOMO energy (blue solid line) of the neutral system is reported as well as the opposite of the left N -centered weight-dependent LZ-shifted HOMO energy (red solid line). Opposites of the left N -centered weight-dependent unshifted (dark-red dashed line) and LZ-shifted (dark-red dot-dashed line) HOMO energies obtained with weight-dependent CC xc-functionals are also reported for comparison along with the total ionization potential prediction (dark-red solid line) arising from the additional weight-derivative contribution of the CC xc-functional. ΔSCF ionization potentials (black dashed line) obtained with weight-independent approximations are also reported for comparison.

Right N -centered ensembles

Similarly, we have performed self-consistent right N -centered eDFT calculations with the CC-functionals that were designed to correct the curvature and endpoint deviations exhibited by standard weight-independent approximations in right N -centered ensemble energies. We draw the same conclusions that for the performance of CC-functionals when applied to left N -centered ensembles. Indeed, CC-functionals succeed as well to restore the “correct” (theoretical) right N -centered ensemble energies for each considered levels of xc-approximations

despite of a marginal endpoint deviation that subsists for final ensemble-weight values, as depicted in Figure 6.11. Note that these residual endpoint deviations of the CC-functionals appear to be smaller than the ones exhibited by left N -centered ensembles with CC-functionals. This may be connected to the fact that the N -centered scaling factor of the ensemble weight is, by construction, larger than unity for left ensembles whereas smaller than unity for right ensembles. Hence, the residual endpoint deviation of the left N -centered ensembles would be emphasized compared to its right counterpart.

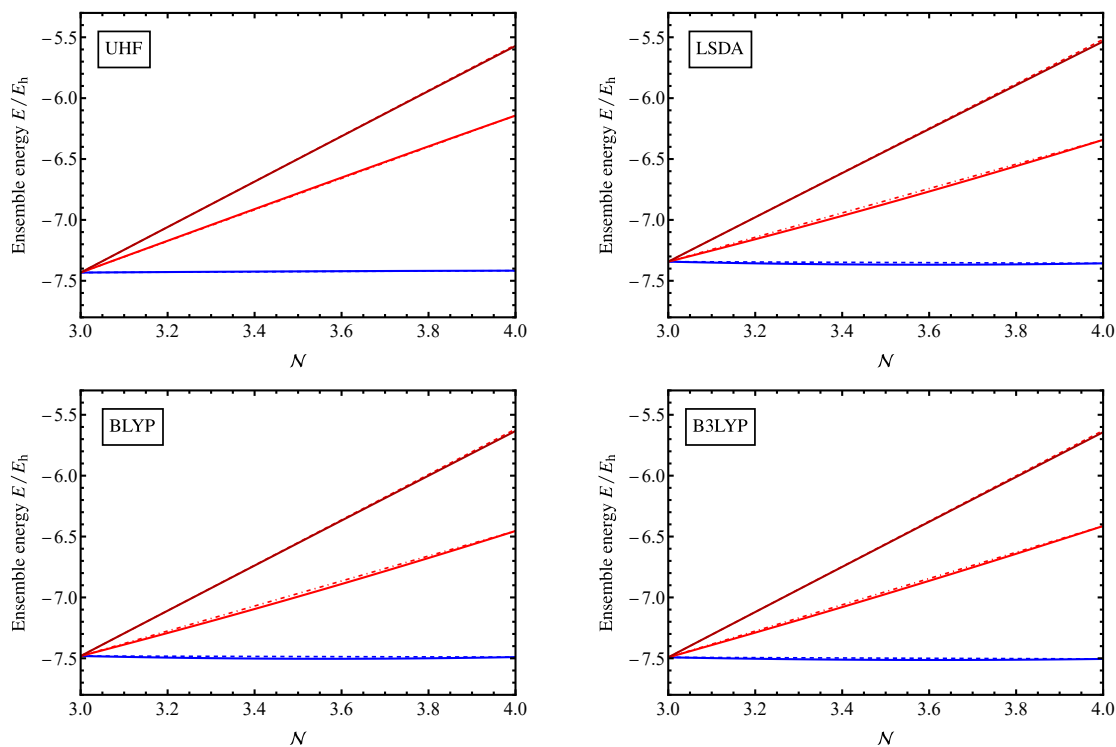


Figure 6.11: Comparison between the right PPLB (blue solid line) and right N -centered (red solid line) ensemble energies of Li obtained with standard weight-independent xc-functionals and their weight-dependent analogs (CC xc-functionals) in the cc-pVDZ basis set. Linear interpolations of the PPLB (blue dashed line) and N -centered (red dot-dashed line) ensemble energies are reported to highlight the additional curvature arising from the use of weight-independent approximate functionals as well as the endpoint deviation of the N -centered ensemble energy with respect to its theoretical value (red dashed line). For each level of approximation, the right N -centered ensemble energy obtained with the corresponding weight-dependent CC-functional is also reported (dark-red solid line).

As for the extraction of electron affinities from right N -centered ensembles with the CC-functionals (see Figure 6.12), we see that, for a given CC-functional, the unshifted and LZ-shifted orbital energies are almost unchanged compared to their counterparts provided by the corresponding weight-independent xc-functional (see Table D.2). Indeed, most of the improvement in the prediction of electron affinities will arise from the additional weight-derivative of the CC-functionals, the “DD” contribution.

Finally, because of the residual endpoint deviation in the ensemble energies provided by the CC-functionals, the resulting electron affinity predictions ensemble will succeed in matching the Δ SCF references for small ensemble-weight values but will become slightly overestimated as the ensemble-weight increases. Hence, we see that for both left and right N -centered ensembles, the zero-weight limits appear to be the most judicious choice for extracting physical properties from such ensembles.

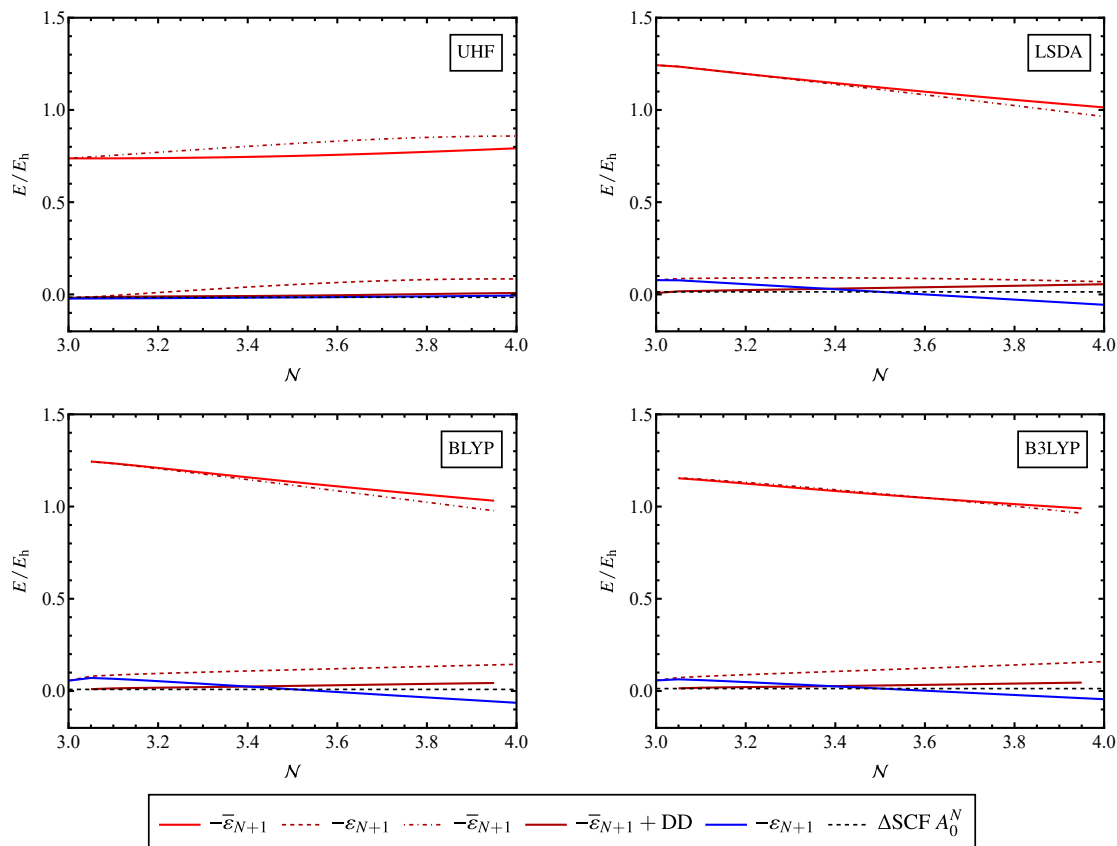


Figure 6.12: Variation of the electron affinity of Li with respect to the fractional number of electrons of the open system, obtained within right PPLB and right N -centered ensemble formalisms with various weight-independent and weight-dependent exchange-correlation functionals in the cc-pVDZ basis set. For each weight-independent approximation, opposite of the right PPLB weight-dependent LUMO energy of the neutral system (blue solid line) is reported as well as the opposite of the right N -centered weight-dependent LZ-shifted LUMO energy (red solid line). Opposites of the right N -centered weight-dependent unshifted (dark-red dashed line) and LZ-shifted (dark-red dot-dashed line) LUMO energies obtained with weight-dependent CC xc-functionals are also reported for comparison along with the electron affinity prediction arising from the additional weight-derivative contribution of the CC xc-functional (dark-red solid line). Δ SCF electron affinities (black dashed line) obtained with weight-independent approximations are also reported for comparison.

6.4 Extended *N*-centered Ensembles: Combining Charged and Neutral Excitation Energies

Very recently, work has been done to benefit from the strong analogy between GOK-DFT and *N*-centered eDFT by designing hybrid GOK/*N*-centered ensembles that would incorporate *N*-electron neutrally excited states into regular *N*-centered ensembles, thus allowing for the extraction of both charged and neutral excitation energies from a single ensemble DFT calculation. Such ensembles, proposed by Fromager et al., are referred to as extended *N*-centered (e*N*-centered) ensembles.

6.4.1 Left Extended *N*-centered Triensemble

First, let us introduce the following left extended *N*-centered (left e*N*cent) triensemble, which is obtained by mixing a left *N*-centered ensemble with a conventional GOK biensemble

$$E^\eta = (1 - \alpha - w)E_0^N + \frac{N\alpha}{N-1}E_0^{N-1} + wE_1^N, \quad (6.90)$$

where $\boldsymbol{\eta} \equiv \{\xi^-; w\} = \{\frac{N\alpha}{N-1}; w\}$ gathers the positive left *N*-centered and GOK ensemble weights. Note that, by definition of both GOK and *N*-centered ensembles, extended *N*-centered ensembles are canonical ensembles associated with ensemble densities that integrate to the central integral number *N* of electrons.

To ensure that the variational minimization of the left e*N*-centered ensemble energy yield a lower bond of the energy, the positive left e*N*-centered ensemble weights must obey convexity constraints in addition to the GOK constraint, thus leading to the following restricted domains

$$0 \leq w \leq \frac{1}{2} - \frac{\alpha}{2} \leq \frac{1}{2} \iff 0 \leq \alpha \leq 1 - 2w \leq 1. \quad (6.91)$$

In complete analogy with the work presented in the GOK chapter, we chose to apply the left e*N*-centered eDFT formalism to a small set of two-electron systems in order to assess the performance of commonly-used weight-independent xc-approximations within this new framework. Hence, the theory was applied to the helium atom He, the hydrogen molecule H₂ in its equilibrium geometry and the helium hydride cation HeH⁺ in its equilibrium geometry. Details of the electronic configurations that were used to build the left e*N*-centered ensemble are reported in Table 6.9.

Table 6.9: Electronic configurations of the individual states of the left extended N -centered triensemble applied to two-electron systems. All individual states of the ensemble are built from a common set of orbitals associated with specific occupation numbers.

State of the ensemble	Weight	Spin	Occupation numbers					
1	$1 - \alpha - w$	\uparrow	1	0	0	0	0	0
		\downarrow	1	0	0	0	0	0
2	$\frac{N\alpha}{N-1}$	\uparrow	0	0	0	0	0	0
		\downarrow	1	0	0	0	0	0
3	w	\uparrow	0	1	0	0	0	0
		\downarrow	1	0	0	0	0	0

Note that, for the particular settings displayed in Table 6.9, the weight-dependent HOMO and LUMO energies of the neutral (ground-state) system are defined as

$$\begin{cases} \varepsilon_N^\eta &= \varepsilon_1^{\uparrow, \eta} \\ \varepsilon_{N+1}^\eta &= \varepsilon_2^{\uparrow, \eta}. \end{cases} \quad (6.92)$$

Variations of the left eN -centered ensemble energy of He with respect to both left N -centered and GOK ensemble weights, obtained within the LSDA approximation, are depicted in Figure 6.13. The variation of the left N -centered weight does not seem to have much impact on the left eN -centered ensemble energy whereas the variation of the GOK weight results in a substantial positive shift of the eN -centered ensemble energy. Moreover, the left N -centered nature of the left eN -centered ensemble seems to induce most of the curvature of the left eN -centered ensemble energy, compared to the GOK contribution.

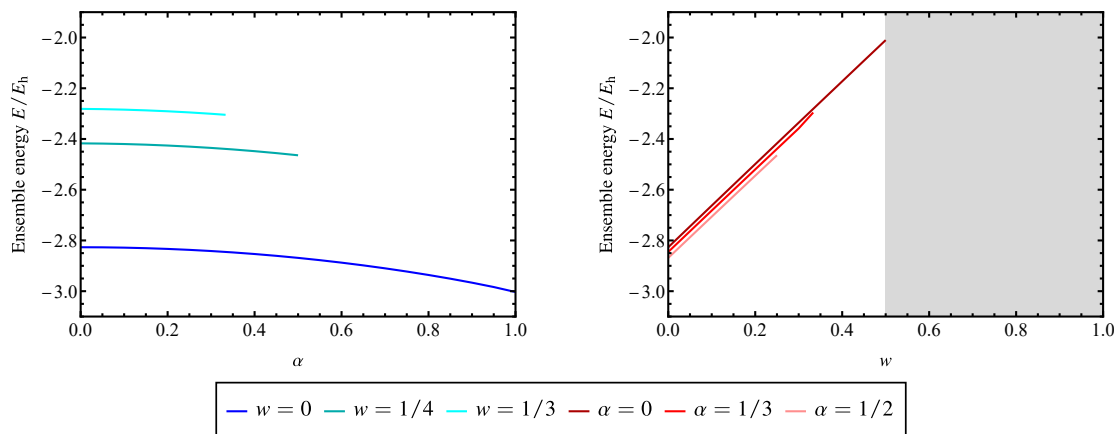


Figure 6.13: Variation of the left extended N -centered ensemble energy of He with respect to the physical charge deviation α of the left N -centered ensemble weight (left panel) and the GOK weight w (right panel) for various weight configurations, obtained with the weight-independent LSDA xc-functional in the cc-pVDZ basis set.

Although the left eN -centered ensemble energy is a fictitious auxiliary quantity, it gives access to all individual energies included in the ensemble and, therefore, to all excitation energies involving those states.

For instance, an exact formulation of the first ionization potential of the N -electron system, defined as

$$I_0^N \equiv E_0^{N-1} - E_0^N, \quad (6.93)$$

can be derived from quantities arising from the left eN -centered eDFT calculation. Indeed, one can derive the following exact formulation for the ground-state ionization potential

$$I_0^N = -\bar{\varepsilon}_N^\eta - \frac{1}{N} \left(1 - \alpha - N\right) \left. \frac{\partial E_{\text{Hxc}}^\eta}{\partial \alpha} \right|_{n_{\text{KS}}^\eta} + \frac{w}{N} \left. \frac{\partial E_{\text{Hxc}}^\eta}{\partial w} \right|_{n_{\text{KS}}^\eta}. \quad (6.94)$$

Additionally, one can extract the first ionization potential of the lowest N -electron excited state, defined as

$$I_1^N \equiv E_0^{N-1} - E_1^N, \quad (6.95)$$

for which an exact formulation can also be derived from the left eN -centered ensemble energy

$$I_1^N = -\bar{\varepsilon}_{N+1}^\eta - \frac{1}{N} \left(1 - \alpha - N\right) \left. \frac{\partial E_{\text{Hxc}}^\eta}{\partial \alpha} \right|_{n_{\text{KS}}^\eta} + \left(\frac{w}{N} - 1\right) \left. \frac{\partial E_{\text{Hxc}}^\eta}{\partial w} \right|_{n_{\text{KS}}^\eta}. \quad (6.96)$$

Finally, the inclusion of neutrally excited states in the left eN -centered ensemble enables the extraction of neutral excitation energies, such as the optical gap of the N -electron system, defined as

$$\begin{aligned} \Omega_1^N &\equiv E_1^N - E_0^N \\ &= I_0^N - I_1^N, \end{aligned} \quad (6.97)$$

for which the following formulation can be derived

$$\Omega_1^N = \varepsilon_{N+1}^\eta - \varepsilon_N^\eta + \left. \frac{\partial E_{\text{Hxc}}^\eta}{\partial w} \right|_{n_{\text{KS}}^\eta}. \quad (6.98)$$

We stress that the fact that we managed to express all excitation energies of equations 6.94, 6.96 and 6.98 in terms of the HOMO and LUMO energies of the neutral (ground-state) system defined in equation 6.92 is a direct consequence of the electronic configurations that we chose to use to build the individual states of the left eN -centered ensemble. Different choices may lead to different formulations for the excitation energies.

Thereby, we see that approximate functionals with no explicit weight-dependence will yield ionization potentials through the sole contribution of the opposite of the weight-dependent LZ-shifted HOMO energy of the neutral N -electron system, with no additional

contributions arising from the derivatives of the Hxc functional with respect to both ensemble weights. As expected, the poor performance of standard weight-independent functionals in yielding accurate ionization potentials in the scope of left N -centered eDFT is extended to the left eN -centered framework, as depicted in Figure 6.14.

Similarly, with weight-independent approximations, the “excited” first ionization potential will solely be approximated by the opposite of the weight-dependent LZ-shifted LUMO energy of the neutral N -electron system, yielding very unsatisfactory results (see Figure 6.15).

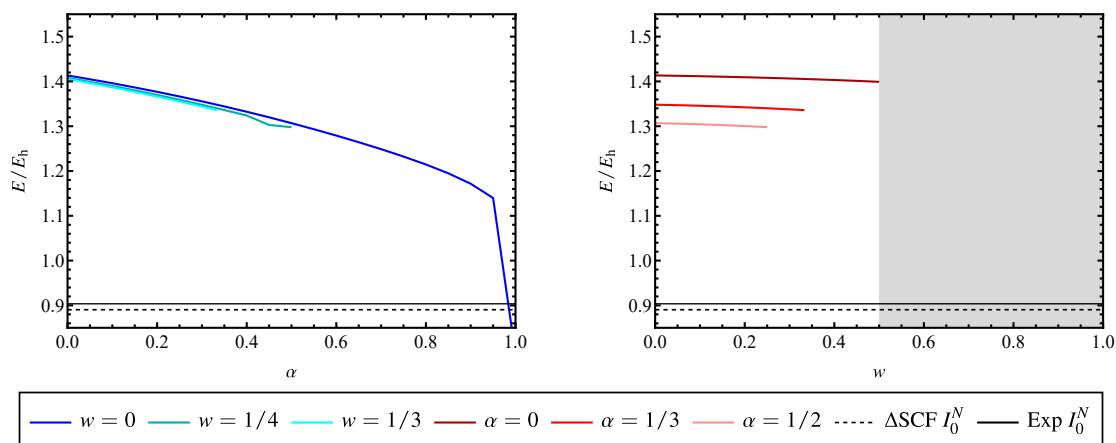


Figure 6.14: Variation of the left extended N -centered first ionization potential of He with respect to the physical charge deviation α of the left N -centered ensemble weight (left panel) and the GOK weight w (right panel) for various weight configurations, obtained with the weight-independent LSDA xc-functional in the cc-pVDZ basis set. ΔSCF and experimental first ionization potentials are reported for comparison (see Appendix A).

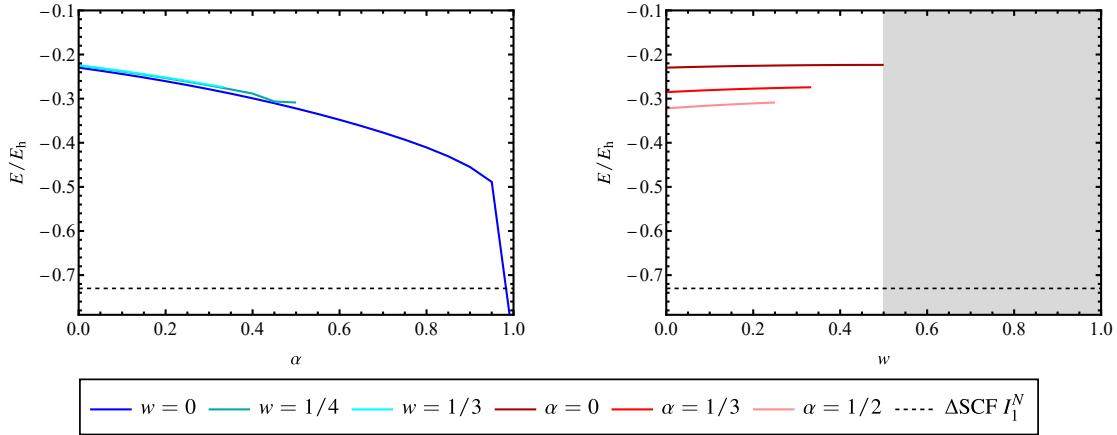


Figure 6.15: Variation of the left extended N -centered “excited” first ionization potential of He with respect to the physical charge deviation α of the left N -centered ensemble weight (left panel) and the GOK weight w (right panel) for various weight configurations, obtained with the weight-independent LSDA xc-functional in the cc-pVDZ basis set. The Δ SCF “excited” ionization potential is reported for comparison.

As a matter of fact, predictions of excitation energies that involve individual states associated with the scaled left N -centered ensemble weight tend to be of significantly poor quality whereas excitation energies, such as the optical gap, that arise from the GOK part of the ensemble seem to yield much acceptable results (see Figure 6.16).

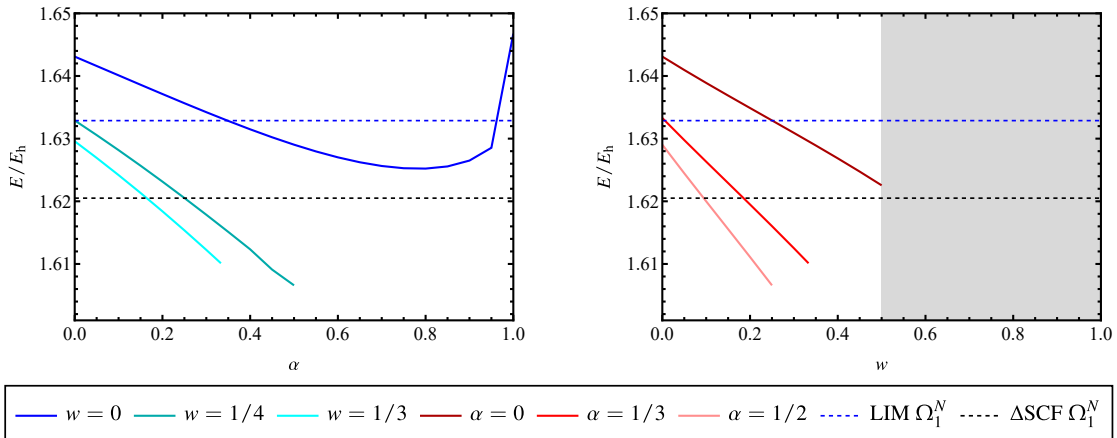


Figure 6.16: Variation of the left extended N -centered optical gap of He with respect to the physical charge deviation α of the left N -centered ensemble weight (left panel) and the GOK weight w (right panel) for various weight configurations, obtained with the weight-independent LSDA xc-functional in the cc-pVDZ basis set. Optical gaps obtained in GOK-DFT with the linear interpolation method (LIM) and Δ SCF method are reported for comparison.

In view of these mitigated results, finding an optimal weight configuration that would yield satisfactory excitation energies in a single eDFT calculation, independently of the system it is

applied to or the choice of approximation seems to be even more challenging when the nature of the ensemble involves two different ensemble formalisms with two specific ensemble weights (see Table 6.10). Hence, the left eN -centered ensemble framework seems to have inherited the deficiencies of its left N -centered counterpart in the scope of weight-independent approximations, emphasizing the necessity to design much adequate weight-dependent functionals to harness properly the potential offered by such new eDFT formalisms.

Table 6.10: Percent errors of the Kohn-Sham predictions compared to the Δ SCF predictions for the first ionization potential I_0^N , the “excited” first ionization potential I_1^N and the optical gap Ω_1^N of He, H_2 and HeH^+ , extracted from left extended N -centered calculations in the cc-pVDZ basis set and using the weight-independent LSDA xc-functional. For the sake of simplicity, we chose to lose the superscript “ η ” that highlighted the weight-dependence of the orbital energies.

	α	w	$-\bar{\epsilon}_N$	$-\bar{\epsilon}_{N+1}$	$\epsilon_{N+1} - \epsilon_N$
He	0	1/2	57.134	69.394	0.126
	1/3	1/3	50.036	62.441	-0.641
	1/2	1/4	45.760	57.709	-0.858
	1/2	0	46.771	55.867	0.526
H_2	0	1/2	51.838	189.293	0.293
	1/3	1/3	44.651	186.184	-8.424
	1/2	1/4	40.859	183.756	-12.726
	1/2	0	44.455	189.445	-9.916
HeH^+	0	1/2	30.203	65.926	-0.151
	1/3	1/3	25.668	66.314	-8.871
	1/2	1/4	23.275	65.829	-12.885
	1/2	0	25.461	68.244	-10.894

6.4.2 Right Extended N -centered Triensemble

For the sake of completeness, we explored as well the possibility of mixing a right N -centered ensemble with a conventional GOK biensemble in order to extract electron affinities and neutral excitation energies from the same eDFT calculation.

In this context, we define the following right extended N -centered (right eN -centered) triensemble

$$E^\eta = (1 - \alpha - w)E_0^N + \frac{N\alpha}{N+1}E_0^{N+1} + wE_1^N, \quad (6.99)$$

where $\eta \equiv \{\xi^+; w\} = \{\frac{N\alpha}{N+1}; w\}$ gathers the positive right N -centered and GOK ensemble weights which must obey the following restricted constraints to ensure the variational minimization of the right eN -centered ensemble energy,

$$0 \leq w \leq \frac{1}{2} - \frac{\alpha}{2} \leq \frac{1}{2} \iff 0 \leq \alpha \leq 1 - 2w \leq 1. \quad (6.100)$$

Table 6.11 displays the details of the electronic configurations that were used to apply the right eN -centered formalism to two-electron systems. Note that, within this context, the

frontier-orbital energies of the neutral (ground-state) N -electron system are still consistent with equation (6.92).

Table 6.11: Electronic configurations of the individual states of the right extended N -centered triensemble applied to two-electron systems. All individual states of the ensemble are built from a common set of orbitals associated with specific occupation numbers.

State of the ensemble	Weight	Spin	Occupation numbers					
1	$1 - \alpha - w$	\uparrow	1	0	0	0	0	0
		\downarrow	1	0	0	0	0	0
2	$\frac{N\alpha}{N+1}$	\uparrow	1	1	0	0	0	0
		\downarrow	1	0	0	0	0	0
3	w	\uparrow	0	1	0	0	0	0
		\downarrow	1	0	0	0	0	0

Such right eN -centered ensembles allow for the extraction of the first electron affinity, defined as

$$A_0^N \equiv E_0^N - E_0^{N+1}, \quad (6.101)$$

as well as the “excited” first electron affinity,

$$A_1^N \equiv E_1^N - E_0^{N+1}, \quad (6.102)$$

and finally the optical gap,

$$\Omega_1^N \equiv E_1^N - E_0^N. \quad (6.103)$$

Once more, when using weight-independent Hxc-functionals, those three excitation energies will be solely approximated by the weight-dependent LZ-shifted kohn-Sham auxiliary excitation energies with no additional contributions arising from the derivatives of the functional with respect to the ensemble weights. As a direct consequence, we derive the following first approximations for the above-mentioned excitation energies

$$\begin{cases} A_0^N & \approx \bar{\mathcal{E}}_0^N - \bar{\mathcal{E}}_0^{N+1} = -\bar{\varepsilon}_{N+1} \\ A_1^N & \approx \bar{\mathcal{E}}_1^N - \bar{\mathcal{E}}_0^{N+1} = -\bar{\varepsilon}_N \\ \Omega_1^N & \approx \bar{\mathcal{E}}_1^N - \bar{\mathcal{E}}_0^N = \bar{\varepsilon}_{N+1} - \bar{\varepsilon}_N = \varepsilon_{N+1} - \varepsilon_N \end{cases} \quad (6.104)$$

Hence, due to the electronic configurations used to build the ensemble, we see that the frontier orbitals of the neutral (ground-state) system play a key-role in our attempt to predict excitation energies from right eN -centered ensemble DFT calculations.

Unfortunately, in complete analogy with the conclusions drawn within the left eN -centered framework, right eN -centered eDFT suffers as well of the inability of right N -centered eDFT to yield satisfactory electron affinity predictions (see Table 6.12) with an order of magnitude

significantly worse than the one obtained for ionization potential predictions in the scope of left eN -centered ensembles, whereas the order of magnitude associated with the predictions of the optical gap are relatively similar in both formalisms.

Table 6.12: Percent errors of the Kohn-Sham predictions compared to the Δ SCF predictions for the electron affinity A_0^N , the “excited” electron affinity A_1^N and the optical gap Ω_1^N of He, H_2 and HeH^+ , extracted from right extended N -centered calculations in the cc-pVDZ basis set and using the weight-independent LSDA xc-functional. For the sake of simplicity, we chose to lose the superscript “ η ” that highlighted the weight-dependence of the orbital energies.

	α	w	$-\bar{\epsilon}_N$	$-\bar{\epsilon}_{N+1}$	$\epsilon_{N+1} - \epsilon_N$
He	0	1/2	416.859	83.445	0.126
	1/3	1/3	423.439	84.390	0.437
	1/2	1/4	426.526	84.814	0.599
	1/2	0	429.289	84.807	1.067
H_2	0	1/2	246.410	373.049	0.293
	1/3	1/3	251.459	373.620	3.109
	1/2	1/4	253.908	373.847	4.495
	1/2	0	256.427	382.506	2.573
HeH^+	0	1/2	84.805	364.966	-0.151
	1/3	1/3	86.860	363.698	2.912
	1/2	1/4	87.871	362.917	4.467
	1/2	0	88.577	378.483	0.666

Chapter 7

Fractional-Charge Error, Fractional-Spin Error and How They Can Emerge from Dissociation Processes

Contents

7.1 Introduction: Fractional-Charge and Fractional-Spin Errors . . .	209
7.2 Fractional-Dissociation Problem	210
7.2.1 Fractional-Charge Error of Atomic Systems	210
7.2.2 Impact of the Fractional-Charge Error on Dissociation Limits . . .	212
7.3 Fractional-Spin Error	217
7.3.1 Fractional-Spin Formalism	217
7.3.2 Application to Fractional-Spin One-electron Systems	223

7.1 Introduction: Fractional-Charge and Fractional-Spin Errors

The undeniable success of DFT is due, to a large extent, to the possibility to resort to approximate xc-functionals, as the exact functional remains out of reach. Paradoxically, the approximate nature of the functionals is also responsible for some of the most massive failures of DFT. Interestingly, such failures are not exclusive to large or complicated systems or to a given class of approximations, but are rather large systematic errors that occur even for the description of the simplest one- or two-electron systems, with either the simplest or the more elaborated approximation.

The inability of approximate functionals to obey the piecewise linearity exact-condition for the energy of systems with fractional charge has been formalized into the concept of localization and delocalization errors [61] (or fractional charge errors) and has shown to be responsible for much of the deviation of calculated DFT properties from experimental results such as band gap predictions or dissociation limits.

As for the violation of the constancy condition for fractional spins, it has led to the static-correlation error [15] (or fractional spin error) and reflects the incapacity of approximate functionals to properly describe systems with degenerate ground states associated with different spin configurations.

Static correlation (or strong correlation) encompasses situations where single-determinantal (single-particle) approaches, such as HF and KS-DFT, fail to provide a proper description of quantum matter. Static-correlation errors have shown to be significant in situations involving degeneracies and near-degeneracies, in strongly correlated systems where electron interactions are particularly difficult to describe, or in situations involving the breaking of chemical bonds.

As a matter of fact, most of the methods exhibiting small fractional-charge errors tend to yield large fractional-spin errors, and vice-versa. For instance, while second-order Møller-Plesset (MP2) perturbation theory provides very low fractional-charge errors, it also exhibits infinite fractional-spin errors. Hence, a method or approximation which would be able to provide marginal errors for both descriptions of fractional charge and fractional spin concepts still constitutes a challenge for electronic-structure calculations.

The concept of fractional charge and fractional spin and their formal and practical implications on real systems have been extensively studied by Mori-Sánchez, Cohen and Yang [14, 16] whose work have provided enlightening insights into the intrinsic nature of some massive systematic errors of approximate xc-functionals within the scope of HF and KS-DFT. Moreover, they proposed a unified formulation of both concepts leading to the “flat-plan condition” [60] for the exact energy of systems with both fractional charges and fractional spins.

These considerations may be essential to the future development of DFT and the elaboration of new approximate functionals which would overcome both basic errors.

7.2 Fractional-Dissociation Problem

7.2.1 Fractional-Charge Error of Atomic Systems

Before addressing the asymptotic fractional-dissociation problem, we recall that the “piecewise linearity” exact property, derived by Perdew, Parr, Levy and Balduz (PPLB) [70], states that, as the number of electrons \mathcal{N} of an open system continuously varies, the exact total energy of such a system, $E^{\mathcal{N}}(\mathcal{N})$, must consist of a series of straight lines between integral electron numbers N . In Chapter 4, we have highlighted the inability of standard methods and functionals to behave in accordance with the “piecewise linearity” exact requirement for

the energy.

We have seen that Hartree-Fock energy is known to depict a concave behaviour, that is to say a positive curvature, which means that fractional configurations of the open system will be given a greater energy than integral configurations and, thus, will be less energetically favourable. Hence, in an Hartree-Fock calculation, the “delocalization” of the charge will erroneously raise the energy of the system. Such functionals that tend to favor too localized charge distributions over much delocalized ones are associated with “localization errors”. Conversely, commonly-used DFA functionals are known to deviate from the piecewise linearity exact condition with negative curvatures, thus, yielding convex energy curves, as depicted in Figure 7.1. In that case, fractional configurations, that is to say delocalized charge distributions, will be given a lower, and thus more stable, energy than integral configurations, or pure states. These observations have led to the concept of “fractional-charge error” or “delocalization error” which is a direct consequence of the negative deviation of the approximate energy of an open system from the piecewise linear exact energy.

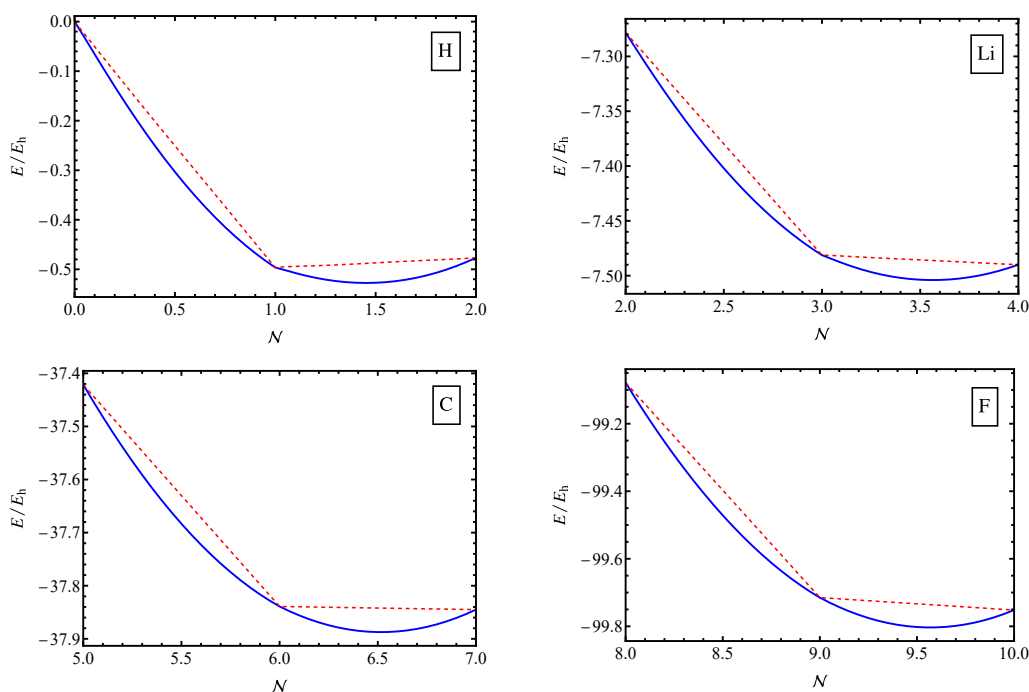


Figure 7.1: Energy versus fractional number of electrons \mathcal{N} for H, Li, C and F with weight-independent BLYP (blue solid line) and weight-dependent CC-BLYP (red dashed line) xc-functionals in cc-pVDZ basis set.

Regarding this matter, we have designed for each considered approximation explicitly weight-dependent alter-egos, “curvature corrected” (CC) xc-functionals, that were intended to correct the energy curvature exhibited by the weight-independent functional, in order to

restore the piecewise linearity exact condition of the energy. A major asset of such weight-dependent ensemble functionals arises from the fact that their elaboration does not necessarily require to step outside the DFT framework or to resort to methods with a higher degree of complexity such as an optimized effective potential method, for instance.

We have performed self-consistent PPLB-DFT ensemble calculations in order to confirm the correct functioning of the CC-functionals in yielding piecewise linear energies for open systems, as depicted in Figure 7.1. We stress that such functionals are not intended for routine applications on a wide range of systems since their elaboration is, by construction, highly specific in the sense that it depends on the system-of-interest, the nature of the ensemble, the choice of basis set, the choice of xc-approximation. . . The CC-functionals presented in this work only aim to highlight the possibility to benefit from explicit weight-dependency into xc-functionals to correct and improve deficiencies of standard approximations within the scope of ensemble DFT.

Fractional charges are not, at first, real phenomena but can arise from dissociation processes of real systems [14], such as stretched molecules where the electron density will delocalize over all dissociated fragments, and may cause significant errors throughout binding curves in their dissociation limits, exhibiting too low or too high predictions of binding energies, as we shall see below.

Moreover, the concept of fractional charge is not specific to atoms and molecules but is a more general problem that may arise from any delocalized charge distribution. Indeed, the inability of commonly used approximate functionals to properly predict the energy for fractional charges in small finite systems will lead to significant systematic errors in the prediction of properties of larger systems, like larger molecules or solid-state calculations [61]. For instance, poor description of fractional charges may have major implications on band-gap predictions, as discussed in Chapter 4.

Hence, evaluating the performance and limitations of approximate functionals when applied to fictitious systems, like fractionally charged systems, can help to better apprehend their physical consequences on real systems.

7.2.2 Impact of the Fractional-Charge Error on Dissociation Limits

A practical consequence of the principle of “integer preference”, derived by Perdew [66], is that, upon stretching, a neutral molecule must dissociate into neutral atoms with integral numbers of electrons on each. As a matter of fact, many approximations fail to obey this simple exact property and erroneously predict that many-electron systems dissociate into fractionally charged fragments, instead. This asymptotic fractional dissociation is highly unphysical and has practical implications.

From energetic considerations, this means that with DFAs an unphysical minimum of the energy of the overall dissociated system is reached when the total charge is delocalized upon all dissociated fragments. This erroneous result stems from the inability of standard approximations to yield proper descriptions of charge-transfer processes, in both molecular and

solid-state systems. It is a direct consequence of the violation of the piecewise linearity exact-condition for the energy, which has been formalized into localization and delocalization errors of approximate functionals. Many systems and approximations are known to exhibit such erroneous behaviour, yielding well-separated atoms with fractional number of electrons on each.

Following the work of Kraisler and Kronik [44], we address the fractional-dissociation problem by employing both standard weight-independent approximations and our weight-dependent CC-functionals, designed within the PPLB framework. By restoring the piecewise linearity of the energy of the dissociated fragments, the weight-dependent CC-functionals may be able to prevent spurious charge transfer between the well-separated atoms and to yield proper descriptions of dissociation limits of molecular systems, as opposed to standard approximations, as we shall see.

Neutral diatomic molecules

We chose to proceed in the same manner as Kraisler and Kronik did to assess the performance of their OEP-based “ensemble generalization” when addressing the fractional-dissociation problem. Hence, we start by considering dissociation limits of neutral diatomic molecules AB whose proper dissociation limit $A \dots B$ must yield well-separated atoms A and B , with respective integer numbers of electrons N_A and N_B .

We will consider the total energy $E_{A\dots B}(q)$ of any dissociation limit involving the transfer of a fractional charge q from one atom to the other, with $-1 \leq q \leq 1$. With that definition, $q = 0$ corresponds to the correct dissociation limit $A \dots B$ with no spurious charge-transfer, while $q = 1$ and $q = -1$ correspond to the transfer of a whole electron from atom B to atom A , and vice-versa.

The total energy of such a dissociated system is dictated by another exact principle, the “separability” principle [66] which states that the total energy of a system composed of well-separated subsystems can be obtained by summation of the energies of the underlying compounds. As a result, the total energy of a well-separated neutral diatomic molecule is given as

$$E_{A\dots B}(q) = E_A(N_A + q) + E_B(N_B - q). \quad (7.1)$$

For the diatomic model system AB , the configurations $q = -1$, $q = 0$ and $q = 1$ correspond to dissociated fragments $A^+ \dots B^-$, $A \dots B$ and $A^- \dots B^+$, respectively.

We have performed self-consistent PPLB ensemble DFT calculations for a small set of atomic systems within various levels of approximation in order to obtain the atomic energy curves $E(\mathcal{N})$ (see Figure 7.1) as functions of the fractional number of electrons \mathcal{N} that are needed in equation (E.30). By summation of these atomic energies, we have built dissociation limits of a small set of neutral diatomic molecules: LiF, CF and FH, as depicted in Figures E.9 and 7.3.

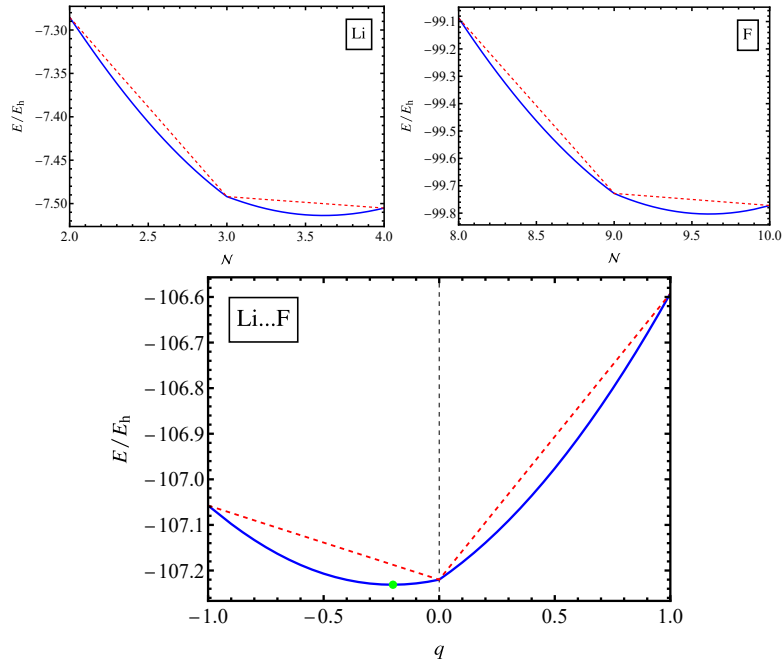


Figure 7.2: Energy $E(N)$ versus fractional number of electrons N for Li (top left panel) and F (top right panel) and dissociation limit $E(q)$ versus fractional charge q for Li...F (bottom), with weight-independent B3LYP (blue solid line) and weight-dependent CC-B3LYP (red dashed line) in cc-pVDZ basis set. The green dot highlights the unphysical spurious minimum of the energy exhibited by standard approximations. For the diatomic model system AB , the configurations $q = -1$, $q = 0$ and $q = 1$ correspond to dissociated fragments $A^+ \dots B^-$, $A \dots B$ and $A^- \dots B^+$, respectively.

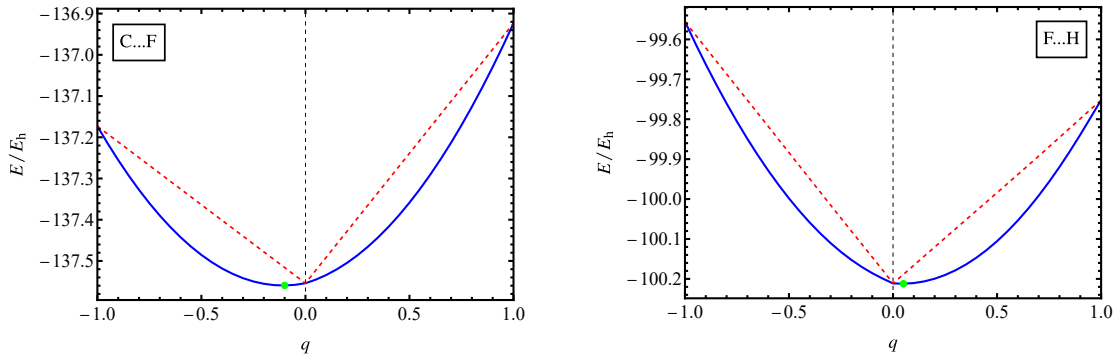


Figure 7.3: Dissociation limit $E(q)$ versus fractional charge q for C...F (left panel) and F...H (right panel), with weight-independent BLYP (blue solid line) and weight-dependent CC-BLYP (red dashed line) in cc-pVDZ basis set. The green dots highlight the unphysical spurious minima of the energy exhibited by standard approximations. For the diatomic model system AB , the configurations $q = -1$, $q = 0$ and $q = 1$ correspond to dissociated fragments $A^+ \dots B^-$, $A \dots B$ and $A^- \dots B^+$, respectively.

For the dissociated LiF molecule the weight-independent B3LYP xc-functional yields a convex energy curve with a spurious minimum at $q = -0.20$. In contrast, the weight-

dependent CC-B3LYP xc-functional yields an energy in much more accordance with the piecewise linearity condition and with a correct minimum at $q = 0$.

Similarly, the weight-independent BLYP xc-functional provides convex energies for the dissociated CF and FH molecules, with unphysical minima at $q = -0.10$ and $q = 0.05$, respectively, whereas the weight-dependent CC-BLYP xc-functional yields much more piecewise-linear energies, with correct minima at $q = 0$ for both systems.

Hence, restoring piecewise linearity of the atomic energies ensures proper dissociation limits of larger systems, such as molecules.

Singly-ionized diatomic molecules

Again, departing from the work of Kraisler and Kronik, we have applied our CC-functionals to a small set of singly ionized diatomic molecules of the type $(A \dots B)^+$ in order to assess the consistency of the dissociation limits obtained with weight-independent and weight-dependent functionals. For such system, the total energy of the dissociated system can be obtained as follows

$$E_{(A \dots B)^+}(q) = E_A(N_A - q) + E_B(N_B - (1 - q)), \quad (7.2)$$

with $0 \leq q \leq 1$ and $1 - q$ the fractions of the electron removed from atom A and B , respectively, such that a single electron is removed from the overall system.

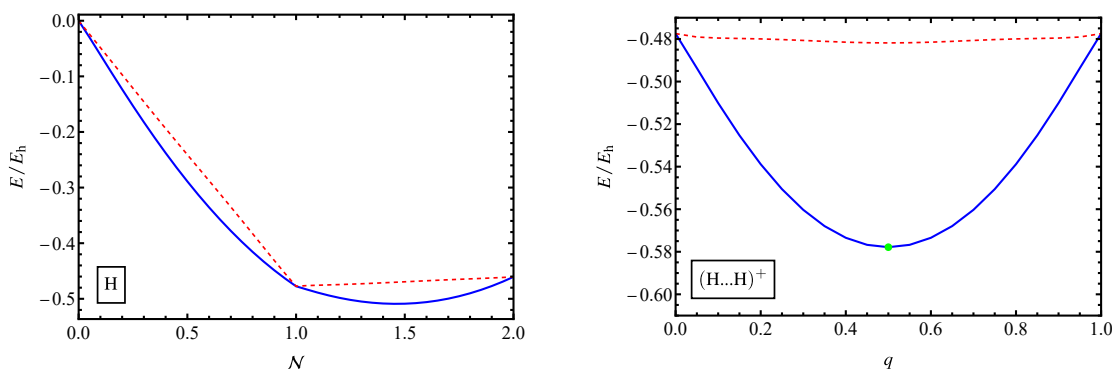


Figure 7.4: Energy $E(\mathcal{N})$ versus fractional number of electrons \mathcal{N} for H (left panel) and dissociation limit $E(q)$ versus fractional charge q for $(H \dots H)^+$ (right panel), with weight-independent LSDA (blue solid line) and weight-dependent CC-LSDA (red dashed line) in cc-pVDZ basis set. The green dot highlights the unphysical spurious minimum of the energy exhibited by standard approximations.

In the case of the symmetric homoatomic $(H \dots H)^+$, the correct dissociation limit must correspond to having an hydrogen atom H and cation H^+ for all values of q but, in practice, many convex approximate functionals, such as the LSDA, favor an unphysical dissociation limit with half of the electron delocalized on each hydrogen center, corresponding to $q = 0.5$, as depicted in Figure 7.4. Indeed, we see that the LSDA yields an underestimated spurious minimum for the dissociation limits of $(H \dots H)^+$ by around 0.10 hartree.

Once more, by restoring the piecewise linearity exact condition for the atomic energy curves,

the weight-dependent CC-LSDA functional succeeds in providing an almost perfectly constant energy curve for the dissociated system, as required.

As for the singly ionized heteroatomic diatomic molecules, $(C \dots H)^+$, $(F \dots H)^+$ and $(C \dots F)^+$, the BLYP functional also predict erroneous convex energies, underestimated by around 0.07, 0.07 and 0.04 hartree, respectively, with corresponding spurious minima at $q = 0.40$, $q = 0.60$ and $q = 0.30$, as depicted in Figure 7.5.

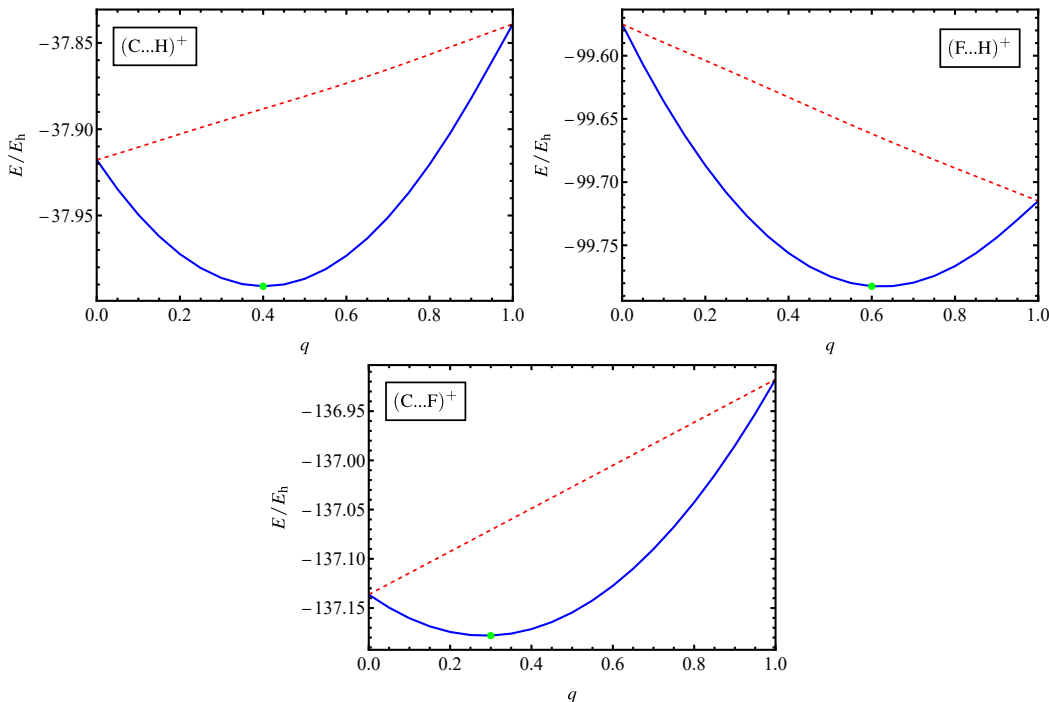


Figure 7.5: Dissociation limit $E(q)$ versus fractional charge q for $(C \dots H)^+$, $(F \dots H)^+$ and $(C \dots F)^+$, with weight-independent BLYP (blue solid line) and weight-dependent CC-BLYP (red dashed line) in cc-pVDZ basis set. The green dots highlight the unphysical spurious minima of the energy exhibited by standard approximations. The true minima obtained at $q = 0$, $q = 1$ and $q = 0$ with CC-BLYP correspond to dissociation limits $C^+ \dots H$, $F \dots H^+$ and $C^+ \dots F$, respectively.

The weight-dependent CC-BLYP xc-functional manages to restore the linearity feature for the energy and thus remedy the spurious fractional dissociation, yielding proper dissociation limits corresponding to well-separated fragments $C^+ \dots H$, $F \dots H^+$ and $C^+ \dots F$. This result is consistent with the ionization potentials of the atomic subsystems (see Appendix A), which represent the cost-in-energy for removing an electron from neutral atomic systems,

$$I_0^C < I_0^H < I_0^F. \quad (7.3)$$

In conclusion, regarding the asymptotic fractional-dissociation problem, designing approximate functionals which are capable of restoring piecewise linearity of the atomic energies ensures proper dissociation limits of larger systems, such as molecules. Explicitly weight-dependant xc-functionals may therefore offer such an appealing alternative within a DFT-like framework.

7.3 Fractional-Spin Error

7.3.1 Fractional-Spin Formalism

Spin-pure electron

An electron can only be in two specific spin-configurations, the spin-up or spin-down configurations (also known as the high- and low-spin configurations), corresponding to specific values of the spin magnetic quantum number $m_s = \pm\frac{1}{2}$ and frequently denominated as α and β spins, respectively.

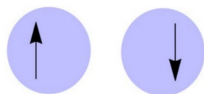


Figure 7.6: Illustrative representations of the spin-up ($m_s = +\frac{1}{2}$) and spin-down ($m_s = -\frac{1}{2}$) configurations of a single electron.

As we have seen, the wave function associated with the description of a single electron is called an orbital. For one-electron systems, the exact ground-state wave function will be determined by a single occupied spatial orbital $\varphi_0(\mathbf{r})$ from which one can derive the exact ground-state spatial electron density

$$n_0(\mathbf{r}) = |\varphi_0(\mathbf{r})|^2 \quad (7.4)$$

with the normalization constraint

$$\int n_0(\mathbf{r})d\mathbf{r} = N = 1, \quad (7.5)$$

where N is the number of electrons of the system.

The exact energy of such one-electron system is solely determined by the kinetic energy $T[n_0]$ of the electron and its potential energy $V_{\text{ext}}[n_0]$ arising from the interaction between the single electron and an external potential such as the one provided by an atomic nucleus. The kinetic and potential energies of an electron are usually conveniently combined to form a one-body component of the energy, the core energy $h[n_0]$,

$$E_0 = T[n_0] + V_{\text{ext}}[n_0] \equiv h[n_0]. \quad (7.6)$$

Fractional-spin electron

Conversely to spin-pure electrons, a fractional-spin electron is associated with unphysical spin configurations, $-\frac{1}{2} < m_s < \frac{1}{2}$.



Figure 7.7: Illustrative representations of various fractional-spin configurations of a single electron ($-\frac{1}{2} < m_s < \frac{1}{2}$) with conservation of the overall norm of the spin.

As a result, the electron density of a fractional-spin electron can be modeled by use of the ensemble formalism. Indeed, by mixing individual spin-up, $n^\alpha(\mathbf{r})$, and spin-down, $n^\beta(\mathbf{r})$, electron densities in accordance with specific ensemble weights, $(1 - w)$ and w , respectively, one obtains a two-state ensemble density that allows for the description and the study of such unconventional electronic system

$$n^w(\mathbf{r}) = (1 - w)n^\alpha(\mathbf{r}) + w n^\beta(\mathbf{r}), \quad (7.7)$$

with the ensemble weight $0 \leq w \leq 1$. Note that $n^\sigma(\mathbf{r})$ (with $\sigma = \{\alpha, \beta\}$) are spatial electron densities associated with spin-pure one-electron systems and thus should be normalized accordingly

$$\int n^\sigma(\mathbf{r})d\mathbf{r} = 1. \quad (7.8)$$

As a consequence, the ensemble density introduced in equation (E.31) is also associated with the description of a single electron and is therefore normalized as well, for any variation of the ensemble weight

$$\int n^w(\mathbf{r})d\mathbf{r} = 1. \quad (7.9)$$

By construction of the ensemble, the description of spin-pure electrons is encompassed within the fractional-spin formalism and are recovered when $w = 0$ and $w = 1$.

Note that when $w = \frac{1}{2}$, which corresponds to the so-called equiweight ensemble (or equiensemble), the overall system mimicked by the ensemble electron density corresponds to a closed-shell system containing exactly half a spin-up and half a spin-down electron.

Constancy condition

Analogously to the piecewise-linearity of the energy for open-systems [61], Cohen, Mori-Sánchez and Yang [15, 14, 16] have shown the existence of another exact-condition that should be satisfied by exchange-correlation functionals for the energy of fractional-spin systems. This exact-condition, known as the constancy-condition for fractional spins, involves systems with degenerate ground-states associated with different spin-configurations and states that, for a given one-electron system, any fractional-spin configurations must be degenerate in energy with a normal spin-pure system.

In complete analogy with the delocalization error for fractional charges, the deviation of the energy of a fractional-spin system from the constancy-condition requirement with a given approximate functional is known as the fractional-spin error or static correlation error. As a matter of fact, many quantum chemistry methods, including Hartree-Fock theory and

density-functional theory, struggle to provide proper description and energies of fractional-spin systems in accordance with the constancy-condition, even for the simplest system, as we shall see.

Unrestricted and restricted Hartree-Fock energies

One can derive analytic expressions of the Hartree-Fock energy of a fractional-spin one-electron system by use of the ensemble density introduced in equation (E.31). We shall see that even in the scope of Hartree-Fock theory, which is known to be exact for one-electron systems, the energy of a fractional-spin one-electron system will differ from the energy of a spin-pure one-electron system.

Let us start by considering a two-state ensemble composed of spin-up and spin-down fractions of a single electron, in their respective lowest spatial orbitals $\varphi_1^\alpha(\mathbf{r})$ and $\varphi_1^\beta(\mathbf{r})$ with ensemble weights $(1 - w)$ and w , respectively, yielding the normalized spin-pure electron densities

$$n^\sigma(\mathbf{r}) = |\varphi_1^\sigma(\mathbf{r})|^2, \quad (7.10)$$

with $\sigma = \{\alpha, \beta\}$.

Furthermore, let us recall the definition of the (spin-resolved) one-particle density matrix for the electrons of spin σ ,

$$\gamma_1^\sigma(\mathbf{r}, \mathbf{r}') = \sum_{i_\sigma}^{N_{\text{occ}}^\sigma} n_{i_\sigma} \varphi_{i_\sigma}^*(\mathbf{r}) \varphi_{i_\sigma}(\mathbf{r}'), \quad (7.11)$$

where $\{n_{i_\sigma}\}$ are the occupation numbers of the N_{occ}^σ occupied spatial orbitals of the spin channel σ .

Finally, one can derive the weight-dependent (spin-resolved) one-particle ensemble density matrix

$$\begin{aligned} \gamma_1^w(\mathbf{r}, \mathbf{r}') &= \gamma_1^{\alpha, w}(\mathbf{r}, \mathbf{r}') + \gamma_1^{\beta, w}(\mathbf{r}, \mathbf{r}') \\ &= (1 - w)\gamma_1^\alpha(\mathbf{r}, \mathbf{r}') + w\gamma_1^\beta(\mathbf{r}, \mathbf{r}') \\ &= (1 - w)\varphi_1^\alpha(\mathbf{r})\varphi_1^\alpha(\mathbf{r}') + w\varphi_1^\beta(\mathbf{r})\varphi_1^\beta(\mathbf{r}'). \end{aligned} \quad (7.12)$$

Note that the diagonal element of equation (7.12) recovers the ensemble density defined in equation (E.31)

$$\gamma_1^w(\mathbf{r}, \mathbf{r}) = (1 - w)\varphi_1^\alpha(\mathbf{r})^2 + w\varphi_1^\beta(\mathbf{r})^2 = n^w(\mathbf{r}) \quad (7.13)$$

Based on that definition, one can derive the weight-dependent ensemble analogues of the Hartree-Fock core energy

$$\begin{aligned} E_{\text{core}}^w &= (1 - w) \int \varphi_1^\alpha(\mathbf{r}) \hat{h}(\mathbf{r}) \varphi_1^\alpha(\mathbf{r}) \mathbf{d}\mathbf{r} + w \int \varphi_1^\beta(\mathbf{r}) \hat{h}(\mathbf{r}) \varphi_1^\beta(\mathbf{r}) \mathbf{d}\mathbf{r} \\ &= (1 - w)h_1^\alpha + wh_1^\beta, \end{aligned} \quad (7.14)$$

Hartree energy

$$\begin{aligned}
 E_{\text{H}}^w &= \frac{1}{2} \iint \frac{\gamma_1^w(\mathbf{r}, \mathbf{r})\gamma_1^w(\mathbf{r}', \mathbf{r}')}{|\mathbf{r} - \mathbf{r}'|} d\mathbf{r}d\mathbf{r}' \\
 &= \frac{1}{2} \iint \frac{n^w(\mathbf{r})n^w(\mathbf{r}')}{|\mathbf{r} - \mathbf{r}'|} d\mathbf{r}d\mathbf{r}' \\
 &= \frac{1}{2} \iint \frac{[(1-w)\varphi_1^\alpha(\mathbf{r})^2 + w\varphi_1^\beta(\mathbf{r})^2][(1-w)\varphi_1^\alpha(\mathbf{r}')^2 + w\varphi_1^\beta(\mathbf{r}')^2]}{|\mathbf{r} - \mathbf{r}'|} d\mathbf{r}d\mathbf{r}' \\
 &= \frac{1}{2} [(1-w)^2 J_{11}^{\alpha\alpha} + 2w(1-w) J_{11}^{\alpha\beta} + w^2 J_{11}^{\beta\beta}],
 \end{aligned} \tag{7.15}$$

and exchange energy for a fractional-spin system

$$\begin{aligned}
 E_{\text{x}}^w &= -\frac{1}{2} \iint \frac{\gamma_1^{\alpha,w}(\mathbf{r}, \mathbf{r}')\gamma_1^{\alpha,w}(\mathbf{r}', \mathbf{r}) + \gamma_1^{\beta,w}(\mathbf{r}, \mathbf{r}')\gamma_1^{\beta,w}(\mathbf{r}', \mathbf{r})}{|\mathbf{r} - \mathbf{r}'|} d\mathbf{r}d\mathbf{r}' \\
 &= -\frac{1}{2} \iint \frac{(1-w)^2 \varphi_1^\alpha(\mathbf{r})\varphi_1^\alpha(\mathbf{r}')\varphi_1^\alpha(\mathbf{r}')\varphi_1^\alpha(\mathbf{r}) + w^2 \varphi_1^\beta(\mathbf{r})\varphi_1^\beta(\mathbf{r}')\varphi_1^\beta(\mathbf{r}')\varphi_1^\beta(\mathbf{r})}{|\mathbf{r} - \mathbf{r}'|} d\mathbf{r}d\mathbf{r}' \\
 &= -\frac{1}{2} [(1-w)^2 J_{11}^{\alpha\alpha} + w^2 J_{11}^{\beta\beta}],
 \end{aligned} \tag{7.16}$$

where h_1^σ and $J_{11}^{\sigma\sigma'}$ are the one-electron and Coulomb matrix elements in the UHF spatial-orbital basis $\{\varphi_1^\alpha, \varphi_1^\beta\}$.

Summation of the above-mentioned contributions yields the unrestricted Hartree-Fock total energy of the fractional-spin system

$$\boxed{
 \begin{aligned}
 E_{\text{UHF}}^w &= E_{\text{core}}^w + E_{\text{H}}^w + E_{\text{x}}^w \\
 &= (1-w)h_1^\alpha + wh_1^\beta + w(1-w)J_{11}^{\alpha\beta}.
 \end{aligned}
 } \tag{7.17}$$

Of course, in case where a single common set of spatial orbitals is used for both spin fragments, such that

$$\varphi_1^\alpha(\mathbf{r}) = \varphi_1^\beta(\mathbf{r}) = \varphi_1(\mathbf{r}), \tag{7.18}$$

the restricted Hartree-Fock energy is recovered

$$\boxed{E_{\text{RHF}}^w = h_1 + w(1-w)J_{11}}. \tag{7.19}$$

If one compares the expressions of the UHF and RHF ensemble energy of the fractional-spin system, one can see that they drastically differ from the expression of the energy of a spin-pure

one-electron system in the sense that they do not reduce to a single one-body contribution due to the unphysical presence of an additional weight-dependent artificial coulombic interaction with no additional exchange counterpart.

Moreover, it is straightforward to see that the UHF and RHF yield equivalent energies for the spin-pure states at $w = 0$ and $w = 1$, with no spurious coulombic interaction, and the spin-unpolarized state at $w = 1/2$, which corresponds to a singlet state with a single electron with half a spin-up and half a spin-down.

Minimization of the unrestricted and restricted Hartree-Fock energies yields the UHF and RHF ground-state energies of the fractional-spin one-electron system.

Generalized Hartree-Fock energy

As a matter of fact, Hartree-Fock theory exists in many different formalisms depending on the symmetry restrictions imposed to the electronic state [26], and each of these approximations may yield different fractional-spin errors [10].

Whereas restricted Hartree-Fock uses the same spatial orbitals for both spin-up and spin-down electrons, conserving \hat{S}^2 and \hat{S}_z (squared-magnitude and z -component operators of the spin angular-momentum vector) spin symmetry, the unrestricted approach uses different spatial orbitals for different spins, allowing broken \hat{S}^2 symmetry but enforcing \hat{S}_z symmetry. More constraints on the wave function can only raise the energy of a variational optimized solution. If we eliminate symmetry constraints related to spin and time reversal, we get the generalized Hartree-Fock (GHF) solutions which allows mixed-spin descriptions, as well as complex wave functions.

The GHF formalism uses a single-determinantal wave function with no restrictions on the one-electron orbitals other than orthonormality. The more familiar restricted and unrestricted Hartree-Fock methods can be regarded as special cases of the generalized HF method in which additional restrictions are imposed on the orbitals. In practice, GHF allows each orbital to have spin-up and spin-down components and is not guaranteed to conserve either \hat{S}^2 or \hat{S}_z symmetry. Fukutome [25] classifies these three Hartree-Fock formalisms as time-reversal invariant closed-shell, axial spin density waves and torsional spin density waves, respectively.

A GHF two-state ensemble is an extension of the UHF ensemble with an additional flexibility stemming from the fact that every orbital can include both a spin-up and a spin-down component so that

$$\varphi_I(\mathbf{x}) = \varphi_I^\alpha(\mathbf{r}) |\alpha\rangle + \varphi_I^\beta(\mathbf{r}) |\beta\rangle, \quad (7.20)$$

where $\mathbf{x} = \{\mathbf{r}, \sigma\}$ is the combined space-spin coordinate associated with the single electron, and the index $I = \{1, 2\}$ labels the states belonging to the two-state GHF ensemble.

In this work, we used the two-component spinor basis

$$|\alpha\rangle = \begin{pmatrix} 1 \\ 0 \end{pmatrix}, \quad |\beta\rangle = \begin{pmatrix} 0 \\ 1 \end{pmatrix}, \quad (7.21)$$

such that

$$\varphi_I = \begin{pmatrix} \varphi_I^\alpha \\ \varphi_I^\beta \end{pmatrix}. \quad (7.22)$$

Hence, the corresponding GHF ensemble density

$$n_{\text{GHF}}^w(\mathbf{r}) = (1 - w)n_1(\mathbf{r}) + w n_2(\mathbf{r}), \quad (7.23)$$

where the two-component density is defined as

$$n_I(\mathbf{r}) = \begin{pmatrix} n_I^{\alpha\alpha}(\mathbf{r}) & n_I^{\alpha\beta}(\mathbf{r}) \\ n_I^{\beta\alpha}(\mathbf{r}) & n_I^{\beta\beta}(\mathbf{r}) \end{pmatrix}, \quad (7.24)$$

with

$$n_I^{\sigma\sigma'}(\mathbf{r}) = \varphi_I^\sigma(\mathbf{r})\varphi_I^{\sigma'}(\mathbf{r}). \quad (7.25)$$

With those definitions, one can derive an analytic expression of the generalized Hartree-Fock energy of a fractional-spin one-electron system

$$\boxed{E_{\text{GHF}}^w = (1 - w)h[n_1] + wh[n_2] + w(1 - w) \sum_{\sigma, \sigma'} \left[(\varphi_1^\sigma \varphi_1^\sigma | \varphi_2^{\sigma'} \varphi_2^{\sigma'}) - (\varphi_1^\sigma \varphi_2^\sigma | \varphi_2^{\sigma'} \varphi_1^{\sigma'}) \right]}. \quad (7.26)$$

In the RHF and UHF formalisms, the fractional-spin error arises from the lack of exchange interaction between spin-up and spin-down densities in both ensembles. This missing term in the restricted and unrestricted frameworks leads to a fractional-spin error because the artificial coulomb interaction between the two fragments of the spin of the single electron is not sufficiently cancelled, leading to the static-correlation error for fractional-spin systems. In that sense, the fractional-spin ensemble behaves as a two-body problem.

Conversely, when the two individual GHF densities and their corresponding orbitals are equivalent, the exact energy is recovered, for all weight-configurations,

$$E_{\text{GHF}}^w = E_0, \quad (7.27)$$

with $\varphi_1 = \varphi_2 = \varphi_0$.

As a matter of fact, the spin expectation values can be used to understand how GHF succeeds in providing the correct exchange energy to fully cancel the fractional-spin error [10], as opposed to RHF and UHF. Additional flexibility of the GHF approximation conserves the overall norm of the spin vector and results in an exchange interaction that cancels out the spurious Coulomb interaction. As a consequence, a fractional-spin one-electron ensemble built from GHF densities must be independent of the ensemble weight and thus always exact. Since the GHF representation of a one-electron system with either a spin-pure or a fractional-spin electron must always be exact, variational optimization of the two-state GHF ensemble will reduce to a single GHF state with exact energy and density.

7.3.2 Application to Fractional-Spin One-electron Systems

Hydrogen atom

We first consider the hydrogen atom in a minimal spatial basis comprising the lowest-energy (and exact ground-state of H) 1s and 2s atomic orbitals

$$\phi_{1s}(\mathbf{r}) = \sqrt{\frac{1}{4\pi}} \exp(-r) \quad (7.28) \quad \left| \quad \phi_{2s}(\mathbf{r}) = \sqrt{\frac{1}{32\pi}} (2-r) \exp\left(-\frac{r}{2}\right), \quad (7.29)$$

with $r = |\mathbf{r}|$ the electron-nucleus distance.

Note that the same physics occurs in larger basis sets, as we shall see below.

By use of these two basis functions, one can form a parametrized generic expression for the single occupied orbital for the fractional-spin RHF ensemble

$$\varphi(\mathbf{r}) = \cos \theta \phi_{1s}(\mathbf{r}) + \sin \theta \phi_{2s}(\mathbf{r}), \quad (7.30)$$

with θ an orbital-rotation angle to be optimized.

Similarly, the UHF orbitals of the spin-up and spin-down fractions of the single electron can be built using different orbital-rotation angles for each spin, θ^α and θ^β , such that

$$\varphi^\alpha(\mathbf{r}) = \cos \theta^\alpha \phi_{1s}(\mathbf{r}) + \sin \theta^\alpha \phi_{2s}(\mathbf{r}) \quad (7.31) \quad \left| \quad \varphi^\beta(\mathbf{r}) = \cos \theta^\beta \phi_{1s}(\mathbf{r}) + \sin \theta^\beta \phi_{2s}(\mathbf{r}). \quad (7.32)$$

Let us recall the analytical solutions for the ground-state of H, with exact ground-state density

$$n_0(\mathbf{r}) = |\phi_{1s}(\mathbf{r})|^2, \quad (7.33)$$

and exact ground-state energy

$$E_0 = -\frac{1}{2} E_h. \quad (7.34)$$

We have computed optimized RHF and UHF energies built from the above-mentioned RHF and UHF parametrized orbitals. As expected, in the 1s2s basis set, both formalisms are equivalent at the spin-pure configurations $w = 0$ and $w = 1$, yielding the exact ground-state energy of the hydrogen atom, as depicted in Figure 7.8.

Nevertheless, for any other fractional-spin configuration, $0 < w < 1$, both formalisms exhibit a non-zero weight-dependent deviation from the exact energy, the fractional-spin error, whose maximum is reached when the fractional-spin system is in the spin-unpolarized state, at $w = 0.5$. As expected, RHF and UHF calculations yield equivalent results for this particular closed-shell configuration.

For intermediate weight configurations, the greater flexibility of the unrestricted orbitals compared to their restricted counterparts enables an additional marginal energetic relaxation of the UHF energy in an attempt to reduce the overall fractional-spin error. As a matter

of fact, spatial separation of the different spin components is essential for providing the additional relaxation of the unrestricted ensemble relative to the restricted ensemble [10].

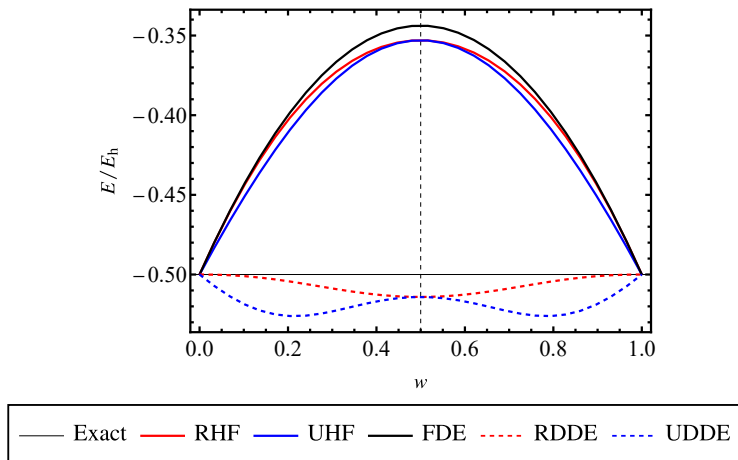


Figure 7.8: Restricted and unrestricted Hartree-Fock ensemble energies for the fractional-spin H atom in the 1s2s basis set compared to the exact energy. The functional-driven error (FDE) and the RHF and UHF density-driven errors (DDE) are also represented for completeness.

The total fractional-spin error of the HF formalisms can be decomposed into two contributions, the error stemming from the use of an incorrect approximate functional and the error arising from the use of an incorrect approximate electron density. To study and compare the impact of both errors on the overall fractional-spin error, calculations were performed by fixing the spatial electron density at its exact value $n_0(\mathbf{r})$ and computing the energy via the incorrect HF energy functional, yielding the functional-driven error (FDE) and, by construction, the density-driven error (DDE) defined as the remaining part of the total fractional-spin error obtained by injection of incorrect approximate RHF and UHF densities into the exact functional $h[n]$.

We find that, for both formalisms, the magnitude of the fractional-spin DDE is very small in the H atom compared to the much significant FDE. Furthermore, the magnitude of the unrestricted DDE is always larger than its restricted counterpart, reaching maximum magnitude when the unrestricted energetic relaxation is most significant, which is consistent with the broader observation than in HF theory, lower electronic energies can be reached at the expense of less accurate electronic densities.

Indeed, while the restricted ensemble provides a greater energy error but a more accurate density, the unrestricted framework offers energetic stabilization with a detrimental impact on the quality of the electron density.

The performance of five commonly used functionals is shown in Figure E.11 for the fractional-spin H atom in a larger basis set. The left-hand side shows the energy of the fractional-spin H atom and the right-hand side shows the fractional-spin error defined as the difference in energy of the H atom with a fractional-spin electron compared to the energy of

the H atom with a spin-pure electron, obtained with a given approximate functional.

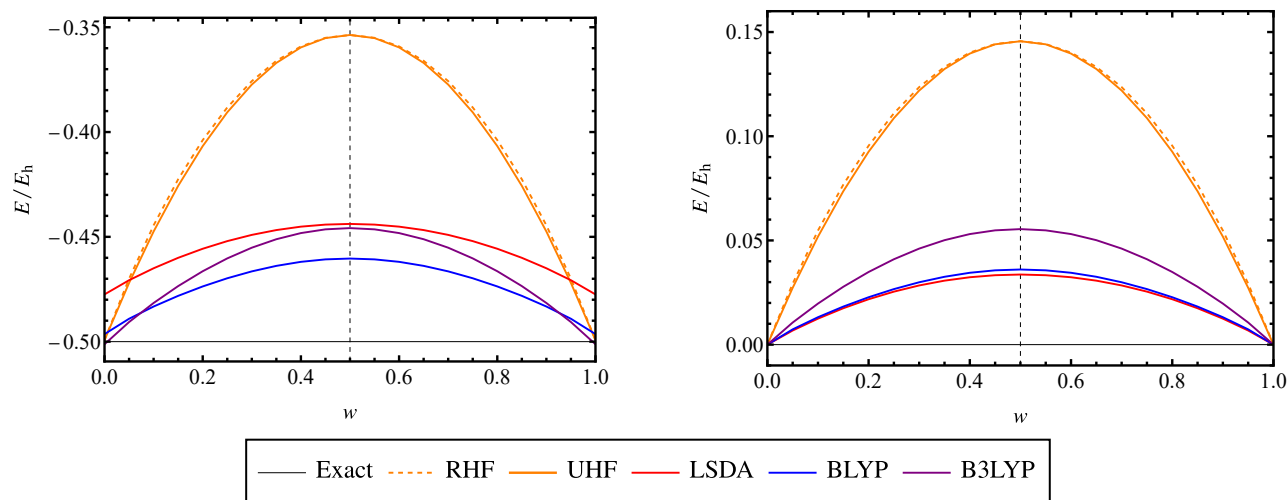


Figure 7.9: Ensemble energies (left panel) and fractional-spin errors (right panel) for the fractional spin H atom at the restricted and unrestricted Hartree-Fock levels and with various unrestricted DFAs in the cc-pVDZ basis set, compared to the exact results.

Such self-consistent calculations reveal important deficiencies in the approximate functionals for fractional-spin ensembles. Note that even functionals which are exact for the spin-pure H atom such as Hartree-Fock exhibit large errors for fractional-spin systems. Hartree-Fock has the largest error while LSDA has the smallest error, but both functionals overestimate the energy for fractional-spin systems.

GGA functionals, such as BLYP, perform roughly the same as LSDA despite their varied forms and more sophisticated hybrid functionals, such as B3LYP, have a behaviour in-between LSDA and HF [15].

Hydrogen molecule cation

From now on, our interest is to study the behaviour of a fractional-spin one-electron molecular system upon dissociation at the HF level. As a matter of fact, the error in some stretched molecules has been shown to stem from the inability of approximate functionals to satisfy the exact fractional-spin constancy condition [15, 14, 63].

Indeed, incorrect molecular dissociations are normally attributed to the lack of static correlation, which can be connected to the violation of the constancy condition for the fractional-spin states of the dissociating atoms. For example, complete dissociation of the H_2 molecule yields a singlet system, which consists of two fractional-spin H atoms separated by a large distance. For that particular system, spin-restricted DFT calculations yield significantly overestimated energy and this overestimation has been shown to match exactly twice the fractional-spin error for the H atom with fractional-spin configuration $w = 0.5$, corresponding to an electron with half a spin-up and half a spin-down.

For that reason we now turn to the one-electron homonuclear diatomic H_2^+ which is a one-electron system with two sites. We want to study the behaviour of the ground-state of a fractional-spin H_2^+ upon stretching. In the case of H_2^+ , the dissociation limit should yield an isolated H atom with an additional single proton which should not energetically contribute because of the infinite spatial separation of the two dissociated fragments.

We will use the same STO-3G basis of atomic orbitals and restricted spatial molecular orbitals than the ones used for the description of the hydrogen molecule. Therefore, we will use a minimal basis formalism comprising two contracted s -type gaussian functions $\phi_L(\mathbf{r})$ and $\phi_R(\mathbf{r})$ to build the one-electron spatial orbitals, or molecular orbitals, of our system. We choose to center these two atomic orbitals on the left and right H atoms, respectively, with bond length R . One practical advantage of such a small basis set is to allow for the derivation of analytic expressions of the ground-state energy of such a system and to study its behaviour in the dissociation limit [84].

We obtain two delocalized, symmetry-determined, orthonormal restricted molecular orbitals, one occupied orbital with lower energy and one virtual orbital with higher energy

$$\varphi_1(\mathbf{r}) = \frac{\phi_L(\mathbf{r}) + \phi_R(\mathbf{r})}{\sqrt{2(1 + S_{LR})}} \quad (7.35) \quad \left| \quad \varphi_2(\mathbf{r}) = \frac{\phi_L(\mathbf{r}) - \phi_R(\mathbf{r})}{\sqrt{2(1 - S_{LR})}}, \quad (7.36)$$

where $S_{LR} = \langle \phi_L | \phi_R \rangle$ defines the overlap of the non-orthogonal atomic orbitals at a given bond length R .

The ground-state unrestricted occupied molecular orbitals can be conveniently built as linear combinations of the restricted symmetry-determined orbitals, benefiting from additional flexibility through the use of a single parameter, an orbital rotation angle θ , such that

$$\varphi_1^\alpha(\mathbf{r}) = \cos \theta \varphi_1(\mathbf{r}) + \sin \theta \varphi_2(\mathbf{r}) \quad (7.37) \quad \left| \quad \varphi_1^\beta(\mathbf{r}) = \cos \theta \varphi_1(\mathbf{r}) - \sin \theta \varphi_2(\mathbf{r}). \quad (7.38)$$

Similarly, one can build the corresponding unrestricted virtual molecular orbitals

$$\varphi_2^\alpha(\mathbf{r}) = -\sin \theta \varphi_1(\mathbf{r}) + \cos \theta \varphi_2(\mathbf{r}) \quad (7.39) \quad \left| \quad \varphi_2^\beta(\mathbf{r}) = \sin \theta \varphi_1(\mathbf{r}) + \cos \theta \varphi_2(\mathbf{r}). \quad (7.40)$$

Note that the symmetric RHF orbitals are recovered for $\theta = 0$, while $\theta = \pm\pi/4$ corresponds to full spatial-separation of the spin-up and spin-down orbitals, localized on opposite H atoms.

The UHF ensemble energy can then be derived as

$$E_{\text{UHF}}^w = \cos^2 \theta h_1 + \sin^2 \theta h_2 + w(1-w) \left[\cos^4 \theta J_{11} + \sin^4 \theta J_{22} + 2 \cos^2 \theta \sin^2 \theta (J_{12} - K_{12}) \right], \quad (7.41)$$

where the one-electron, Coulomb and exchange matrix elements in the RHF orthogonal basis are denoted

$$h_i = (\varphi_i | \hat{h} | \varphi_i), \quad J_{ij} = (\varphi_i \varphi_i | \varphi_j \varphi_j), \quad K_{ij} = (\varphi_i \varphi_j | \varphi_j \varphi_i). \quad (7.42)$$

By differentiating equation (7.41) with respect to the orbital-rotation angle θ and solving

$$\frac{dE_{\text{UHF}}^w}{d\theta} = 0, \quad (7.43)$$

one obtains the stationary points of the ensemble energy of fractional-spin H_2^+ and, therefore, the ground-state RHF and UHF solutions whose existence can be formalized by the following stationary conditions,

$$\cos \theta_{\text{RHF}} = 0 \quad (7.44)$$

and

$$\cos^2 \theta_{\text{UHF}} = \frac{h_1 - h_2 + 2w(1-w)(J_{12} - J_{22} - 2K_{12})}{-2w(1-w)(J_{11} - 2J_{12} + J_{22} + 4K_{22})}. \quad (7.45)$$

Note that solutions of equation (7.43) are not guaranteed to be true minimum of the energy as we shall see.

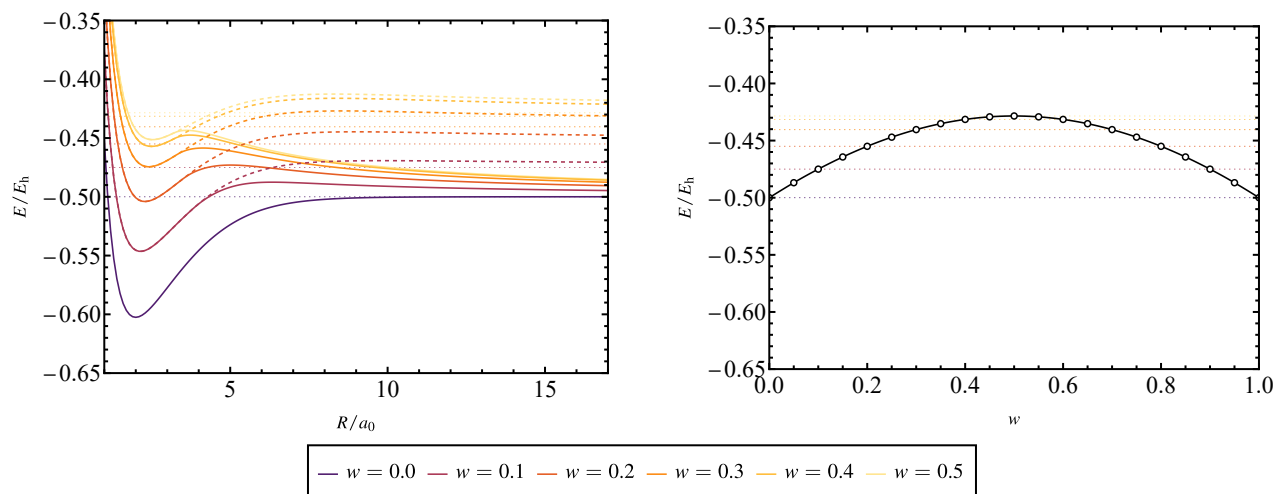


Figure 7.10: Restricted (dashed lines) and unrestricted (solid lines) energy of H_2^+ as functions of the bond length R for various fractional-spin configurations (left panel) and restricted dissociation limits (right panel) of a fractional-spin H_2^+ as a function of the ensemble weight, at the Hartree-Fock level in cc-pVQZ basis set. For all fractional-spin configurations considered, dissociation limits of H_2^+ (dotted lines) are also reported for clarity.

We find that at short bond-length, for each value of the weight (or fractional-spin configuration), there exists a single stationary solution which always corresponds to the restricted solution $\theta = 0$ and is a true minimum of the energy, and no unrestricted solution exists.

On increasing the bond length, up to a weight-dependent critical value R_c^w , the restricted solution will no longer be a true minimum of the energy but will become instead a saddle point of the energy while a lower-energy unrestricted solution will emerge if the ensemble weight allows it ($w \neq 0$ or 1). This transition point can be seen as a weight-dependent analogue to the Coulson–Fischer point [18] of H_2 and can be determined by solving $\theta_{\text{RHF}} = \theta_{\text{UHF}}$.

Figure E.12 reveals that the critical bond-length R_c^w decreases as w increases between 0 and 1, reaching a minimum at $w = 1/2$. As a result, the shortest bond length for UHF symmetry breaking of fractional-spin H_2^+ occurs when the fractional-spin error of the dissociating fragments is largest.

Whereas restricted solutions yield weight-dependent overestimated dissociation limits, unrestricted solutions go smoothly to the proper limit of one single spin-pure H atom, calculated with the same level of approximation and basis set. Therefore, at the HF level, in complete analogy with the dissociation of H_2 , it becomes more energetically favorable for the spatial symmetry of fractional-spin H_2^+ to be broken by localizing the high-spin and low-spin orbitals on opposite centers.

As a matter of fact, like for the H atom, spatial separation of the spin-up and spin-down densities minimizes the fractional-spin error, leading to more accurate UHF energies. It is worth mentioning that the UHF energetic relaxation is more significant for H_2^+ than for the H atom as the two atomic centers increase the possible extent of spatial separation [10]. Hence, increase of the negative unrestricted density-driven error lower the overall unrestricted energy and fractional-spin system.

In the minimal basis, one can derive analytical expressions for the dissociation limits of fractional-spin H_2^+ within both RHF and UHF formalisms by expanding the expressions of the RHF and UHF ensemble energies in the atomic-orbital basis set and by considering that, in the large- R limit, the overlap between the two AOs decays to zero as R grows as well as all integrals mixing the two atom-centered basis functions.

Therefore, the RHF and UHF dissociation limits are given as

$$\begin{aligned}
 \lim_{R \rightarrow +\infty} E_{\text{RHF}}^w &= \lim_{R \rightarrow +\infty} (h_1 + w(1-w)J_{11}) \\
 &= (1-w)h_{\text{L}} + wh_{\text{R}} + \frac{w(1-w)}{4}(J_{\text{LL}} + J_{\text{RR}}) \\
 &= h_{\text{L}} + \frac{w(1-w)}{2}J_{\text{LL}}
 \end{aligned} \tag{7.46}$$

and

$$\begin{aligned}
 \lim_{R \rightarrow +\infty} E_{\text{UHF}}^w &= \lim_{R \rightarrow +\infty} \left((1-w)h_1^\alpha + wh_1^\beta + w(1-w)J_{11}^{\alpha\beta} \right) \\
 &= \lim_{R \rightarrow +\infty} \left((1-w)h_L + wh_R + w(1-w)J_{LR} \right) \\
 &= h_L,
 \end{aligned} \tag{7.47}$$

with $h_L = h_R$, $J_{LL} = J_{RR}$ and $J_{LR} = J_{RL}$ the one-body and Coulomb matrix elements in the atomic-orbital basis.

We find that the error in the RHF energy of a dissociated fractional-spin H_2^+ is exactly half the fractional-spin error of a H atom with spin-up and spin-down configurations of respective weights $(1-w)$ and w while the UHF ensemble energy decays to the correct energy. As a result, delocalization of the electron density over two dissociated atomic centers reduces the overall RHF fractional-spin error in one-electron models by a factor 2.

As a matter of fact, the reduction in the RHF fractional-spin error is even more pronounced for larger numbers of atomic centers as delocalizing the RHF electron density over multiple sites further reduces the fictitious Coulomb repulsion between the spin-up and spin-down densities.

Conclusion

Various ensemble formalisms have been extensively discussed throughout this thesis within the scope of both Hartree-Fock and density-functional theories. The performance of such methods based on ensemble densities as a basic variable has been investigated regarding the prediction of charged and neutral excitation energies.

In particular, the generalization of standard ground-state KS-DFT to electronic states with fractional occupation numbers, PPLB-DFT, has been studied by use of the ensemble formalism to describe the behaviour of the ground-state energy of an open system upon continuous variation of its total number of electrons. In this context, the so-called left and right PPLB ground-state ensemble energies have been self-consistently computed in order to extract ionization potentials and electron affinities, respectively, for simple atomic systems with standard weight-independent exchange-correlation approximations. This has highlighted the inability of standard approximations to recover the infamous derivative discontinuity of the exact potential and therefore to obey the piecewise-linearity exact condition for the total energy of an open system, with massive implications on band-gap predictions. The fundamental gap has been addressed as well as the possibility to resort to explicitly weight-dependent approximations to mimic the elusive derivative discontinuity through their weight-derivatives in order to restore the piecewise-linearity condition for the energy and to yield much satisfactory predictions for physical properties.

The second issue we focused on was to what extent DFT can give access to (neutrally) excited states through its time-independent in-principle-exact ensemble extension, GOK-DFT. Regarding this matter, we considered various two-state and three-state GOK ensembles, intentionally designed to extract single and double excitation energies of two-electron systems. The curvature of GOK ensemble energies has been studied as well as the construction of curvature-corrected weight-dependent exchange-correlation functionals. Excitation energies have been extracted from GOK ensembles in various manners: by differentiation of the GOK ensemble energies with respect to the ensemble weights, through multiple choices of ensemble weights, such as the equiweight configuration, or by use of the Linear Interpolation Method. In the present work, although we only discussed the use of weight-dependent approximations within the scope of elementary GOK ensembles, we believe that exploring much larger and sophisticated ensembles, built from multiple states and weights, along with the development of xc-approximations with multiple weight-dependencies could turn GOK-DFT into a routinely practical procedure for neutrally excited states and excitation energies. In this

respect, within the scope of GOK-DFT, standard ground-state approximations could be used as starting points for the future development of weight-dependent approximations specifically designed for ensemble applications. As a matter of fact, very recently, exact conditions for ensemble functionals have been investigated and may offer crucial and instructive insights regarding this matter.

Then, we addressed the fundamental gap problem through its recent canonical reformulation proposed by Senjean and Fromager, in which the challenging task of mimicking the infamous derivative discontinuity of the exact potential is entirely transposed into the modeling of the weight dependency of the Hxc functional. This offers an in-principle-exact time-independent unified formulation of charged and neutral excitation energies within ensemble DFT. Practical self-consistent calculations of left and right N -centered ensembles have been performed for the extraction of ionization potentials and electron affinities of real atomic systems, respectively, as well as the two-weight and single-weight original formulations of N -centered ensembles, especially designed for the direct extraction of fundamental gaps. Curvatures and total deviations of the N -centered ensemble energies with respect to the theoretical values, obtained with standard ground-state weight-independent approximations, have been investigated and have shed light on the detrimental impact that nonlinear density functionals may have on the self-consistent results within the scope of N -centered theory. Regarding this matter, we have shown how explicitly weight-dependent approximate functionals could benefit from their weight derivatives to circumvent limitations of standard ground-state approximations and provide much satisfactory ensemble predictions for physical properties. Finally, newly developed GOK/ N -centered combined ensembles, which allow for the extraction of charged and neutral excitation energies from the same DFT-like self-consistent calculation, have been explored as well and applied to real two-electron systems.

The final issue that we have chosen to address in this thesis is the concepts of fractional-charge and fractional-spin errors, which stem from the inability of standard approximations to obey the piecewise-linearity and the constancy exact conditions for the energy. We have shown that fractional-charge errors, also known as localization and delocalization errors, may have significant impact on band-gap predictions and may be responsible for erroneous descriptions of dissociation processes. As for the fractional-spin error, or static-correlation error, we have shown that even approximations that are known to be exact for one-electron systems, like Hartree-Fock theory, fail to provide physically relevant descriptions of systems with fractional spins. Weight-dependent approximations may be a solution to palliate these deficiencies, as well.

In view of these considerations, we believe that it is necessary to go beyond ground-state DFAs in order to fully exploit the potential of eDFT and turn it into a reliable and low-cost computational method, for a wide range of applications. With regard to this matter, the development of a new class of approximate exchange-correlation functionals with explicit weight-dependencies and specifically designed for ensemble applications should be further investigated.

Appendix A

Experimental Ionization Potentials, Electron Affinities and Fundamental Gaps of Neutral Atomic Systems

Table A.1: Experimental ionization potentials, electron affinities and fundamental gaps of neutral atomic systems [19, 50]. All energy values are given in atomic Hartree units.

Atom	Ionization Potential	Electron Affinity	Fundamental Gap
H	0.499 734	0.027 716	0.472 017
He	0.903 570	-	-
Li	0.198 142	0.022 712	0.175 429
Be	0.342 603	-	-
B	0.304 947	0.010 279	0.294 667
C	0.413 808	0.046 381	0.367 426
N	0.534 118	-	-
O	0.500 454	0.053 694	0.446 759
F	0.640 276	0.124 991	0.515 285
Ne	0.792 482	-	-
Ar	0.579 155	-	-

Appendix B

PPLB-DFT Supplementary Material

B.1 PPLB-DFT Code Testing

In order to ensure the proper functioning of our eDFT Fortran code within the scope of PPLB-DFT, we managed to verify the consistency of the data extracted from the self-consistent eDFT calculation, such as individual-state energies and excitation energies.

Indeed, in PPLB-DFT we have seen that once the calculation has reached convergence, yielding the minimizing molecular orbitals with corresponding minimum ensemble energy, excitation energies and individual energies can be extracted from the ensemble calculation in two different manners: from the ensemble energy and its derivatives with respect to the ensemble weights

$$\left. \begin{aligned} E_0^N &= E^\alpha - \alpha \frac{\partial E^\alpha}{\partial \alpha} \\ E_0^{N-1} &= E^\alpha + (1 - \alpha) \frac{\partial E^\alpha}{\partial \alpha} \\ I_0^N &= E_0^{N-1} - E_0^N = \frac{\partial E^\alpha}{\partial \alpha} \end{aligned} \right| \quad (B.1)$$

$$\begin{aligned} E_0^N &= E^\alpha - \alpha \frac{\partial E^\alpha}{\partial \alpha} \\ E_0^{N+1} &= E^\alpha + (1 - \alpha) \frac{\partial E^\alpha}{\partial \alpha} \\ A_0^N &= E_0^N - E_0^{N+1} = -\frac{\partial E^\alpha}{\partial \alpha}. \end{aligned} \quad (B.2)$$

or from the (Hartree-Fock or Kohn-Sham) auxiliary energies and the derivative of the weight-dependent Hartree-exchange-correlation functional

$$\begin{aligned}
 E_0^N &= \mathcal{E}_0^{N,\alpha} \\
 &+ E_{\text{Hxc}}^\alpha[n_{\text{KS}}^\alpha] - \int \frac{\delta E_{\text{Hxc}}^\alpha[n_{\text{KS}}^\alpha]}{\delta n(\mathbf{r})} n_{\text{KS}}^\alpha(\mathbf{r}) d\mathbf{r} \\
 &- \alpha \frac{\partial E_{\text{Hxc}}^\alpha[n_{\text{KS}}^\alpha]}{\partial \alpha} \\
 E_0^{N-1} &= \mathcal{E}_0^{N-1,\alpha} \\
 &+ E_{\text{Hxc}}^\alpha[n_{\text{KS}}^\alpha] - \int \frac{\delta E_{\text{Hxc}}^\alpha[n_{\text{KS}}^\alpha]}{\delta n(\mathbf{r})} n_{\text{KS}}^\alpha(\mathbf{r}) d\mathbf{r} \\
 &+ (1 - \alpha) \frac{\partial E_{\text{Hxc}}^\alpha[n_{\text{KS}}^\alpha]}{\partial \alpha} \\
 I_0^N &= -\varepsilon_N^\alpha + \frac{\partial E_{\text{Hxc}}^\alpha[n_{\text{KS}}^\alpha]}{\partial \alpha}
 \end{aligned} \tag{B.3}$$

$$\begin{aligned}
 E_0^N &= \mathcal{E}_0^{N,\alpha} \\
 &+ E_{\text{Hxc}}^\alpha[n_{\text{KS}}^\alpha] - \int \frac{\delta E_{\text{Hxc}}^\alpha[n_{\text{KS}}^\alpha]}{\delta n(\mathbf{r})} n_{\text{KS}}^\alpha(\mathbf{r}) d\mathbf{r} \\
 &- \alpha \frac{\partial E_{\text{Hxc}}^\alpha[n_{\text{KS}}^\alpha]}{\partial \alpha} \\
 E_0^{N+1} &= \mathcal{E}_0^{N+1,\alpha} \\
 &+ E_{\text{Hxc}}^\alpha[n_{\text{KS}}^\alpha] - \int \frac{\delta E_{\text{Hxc}}^\alpha[n_{\text{KS}}^\alpha]}{\delta n(\mathbf{r})} n_{\text{KS}}^\alpha(\mathbf{r}) d\mathbf{r} \\
 &+ (1 - \alpha) \frac{\partial E_{\text{Hxc}}^\alpha[n_{\text{KS}}^\alpha]}{\partial \alpha} \\
 A_0^N &= -\varepsilon_{N+1}^\alpha - \frac{\partial E_{\text{Hxc}}^\alpha[n_{\text{KS}}^\alpha]}{\partial \alpha}.
 \end{aligned} \tag{B.4}$$

Nevertheless, quantities obtained from either methods should be identical.

Derivatives of the ensemble energy with respect to the ensemble weights were computed by use of a finite difference approximation in its symmetric difference quotient formulation.

B.1.1 PPLB-DFT with Weight-Independent Functionals

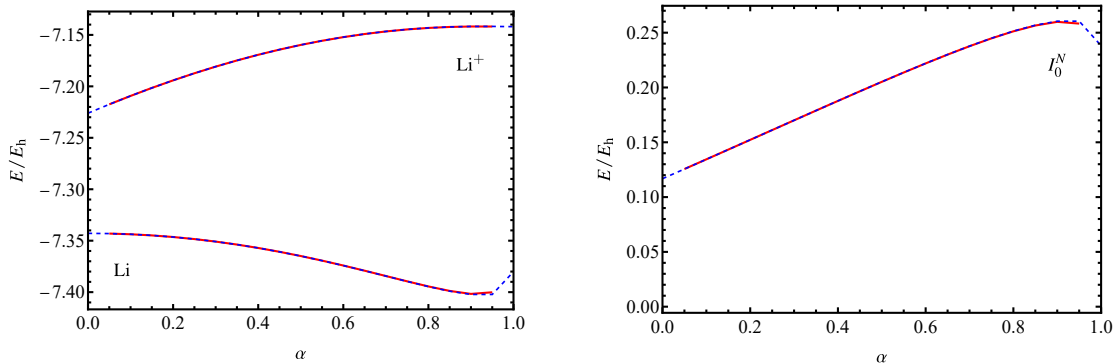


Figure B.1: Checking the validity of left PPLB-DFT calculations with the weight-independent LSDA xc-functional in the cc-pVDZ basis set. Individual energies and excitation energies obtained with equations (B.3) (blue dashed lines) are compared to the same quantities obtained with equations (E.4) (red solid lines).

When weight-independent approximate functionals are used, excitation energies and individual energies obtained from equations (B.3) and (B.4) will include no additional contribution arising from the explicit weight-dependency of the approximate functional, as depicted in Figures B.1 and B.4.

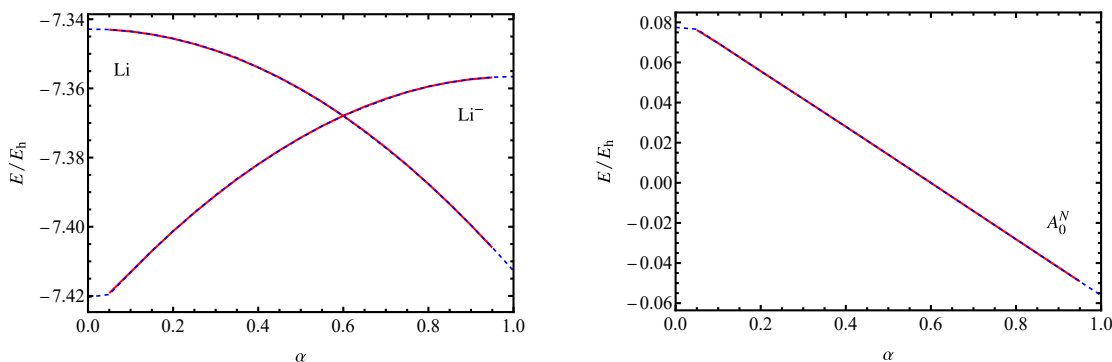


Figure B.2: Checking the validity of right PPLB-DFT calculations with weight-independent LSDA xc-functional in the cc-pVDZ basis set. Individual energies and excitation energies obtained with equations (B.4) (blue dashed lines) are compared to the same quantities obtained with equations (E.5) (red solid lines).

B.1.2 PPLB-DFT with Weight-Dependent Functionals

Conversely, when a weight-dependent approximate functional is used, the weight derivative of the Hxc-functional will contribute to improving predictions of excitation energies and individual energies, as depicted in Figures B.3 and B.4.

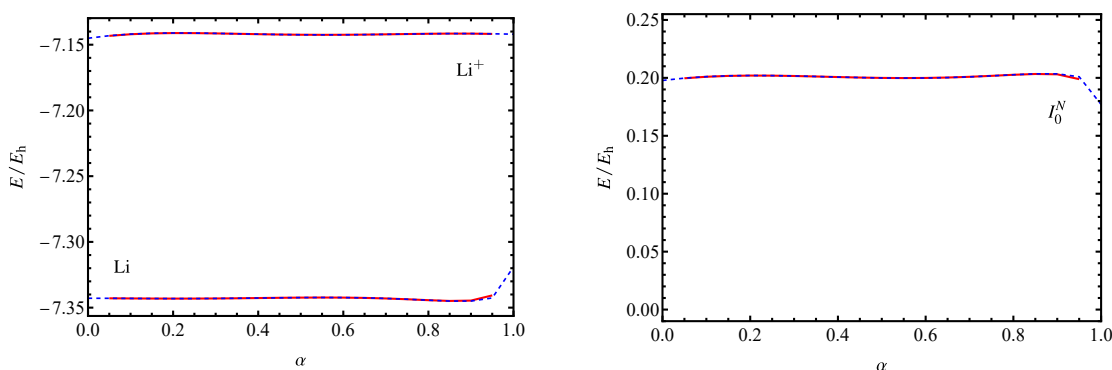


Figure B.3: Checking the validity of left PPLB-DFT calculations with the weight-dependent CC-LSDA xc-functional in the cc-pVDZ basis set. Individual energies and excitation energies obtained with equations (B.3) (blue dashed lines) are compared to the same quantities obtained with equations (E.4) (red solid lines).

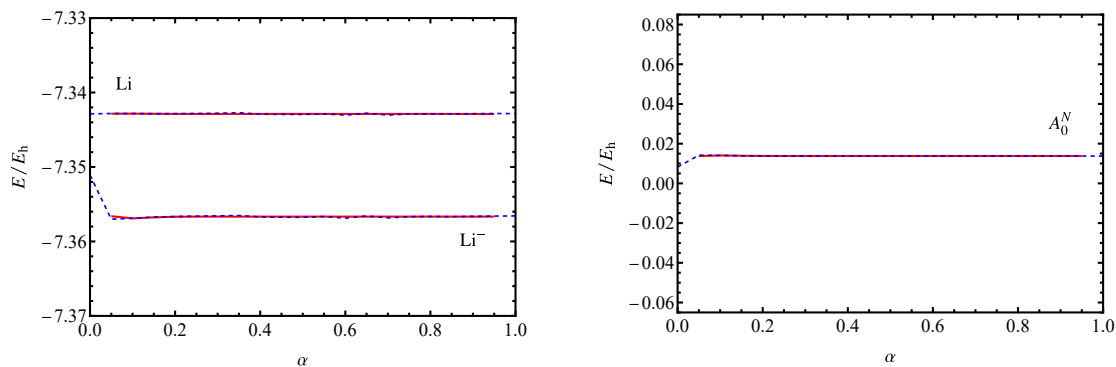


Figure B.4: Checking the validity of right PPLB-DFT calculations with the weight-dependent CC-LSDA xc-functional in the cc-pVDZ basis set. Individual energies and excitation energies obtained with equations (B.4) (blue dashed lines) are compared to the same quantities obtained with equations (E.5) (red solid lines).

B.2 Overview of PPLB-DFT Results with CC-functionals

B.2.1 Individual-State Energies

In this subsection, we show that the CC-functionals succeed in providing more stable and accurate PPLB predictions for the ground-state energies of the neutral, cationic and anionic forms of Li, as depicted in Figures B.5 and B.6. By accurate, we mean more in accordance with the ground-state energies obtained with multiple self-consistent calculations within the scope of standard ground-state DFT with the same level of approximations.

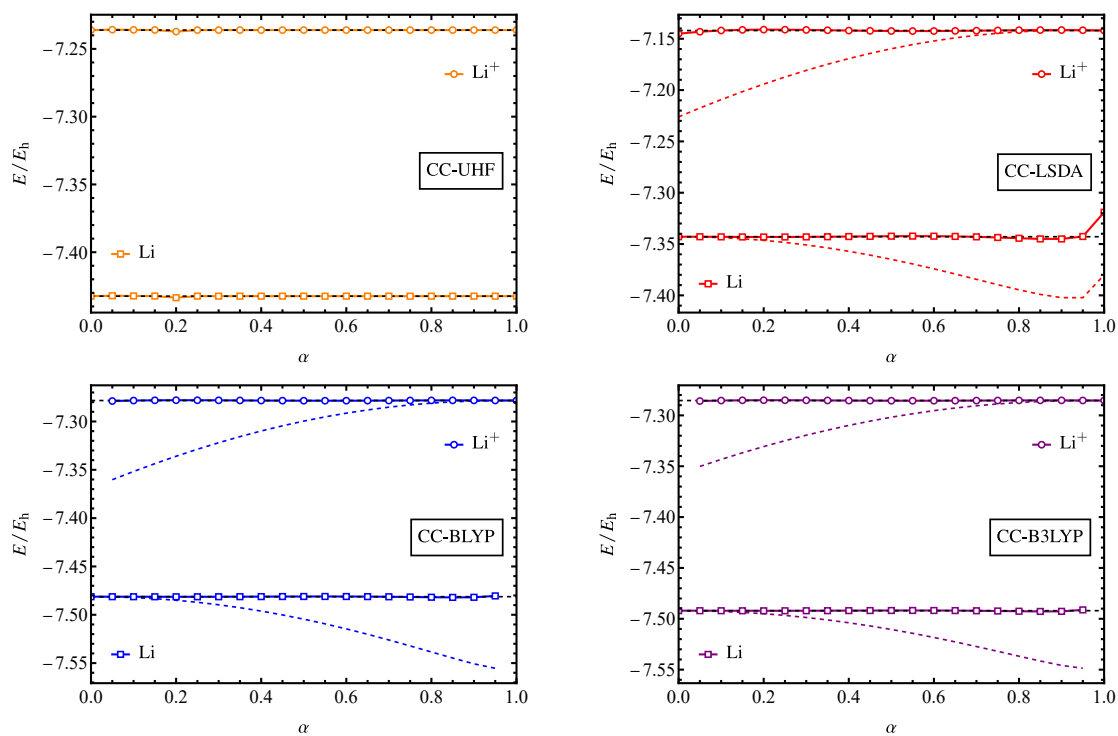


Figure B.5: Comparison between left PPLB-DFT neutral and cationic ground-state energies of Li, obtained with weight-independent xc-functionals (colored dashed lines) and their weight-dependent CC-counterparts (colored solid lines), as functions of the fractional-charge deviation α , in the cc-pVDZ basis set. SCF (black dashed line) individual-state energies obtained with the same level of approximation are reported for comparison.

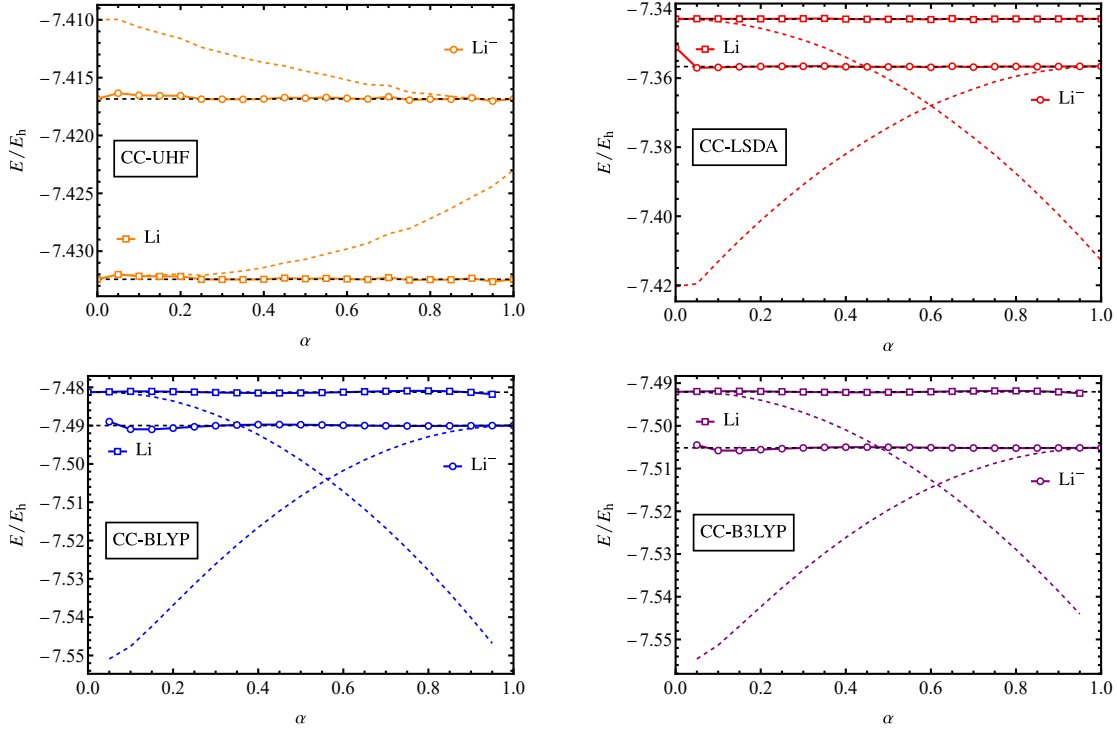


Figure B.6: Comparison between right PPLB-DFT neutral and anionic ground-state energies of Li, obtained with weight-independent xc-functionals (colored dashed lines) and their weight-dependent CC-counterparts (colored solid lines), as functions of the fractional-charge deviation α , in the cc-pVDZ basis set. SCF (black dashed line) individual-state energies obtained with the same level of approximation are reported for comparison.

B.2.2 Excitation Energies

In this subsection, we show that the CC-functionals succeed in providing more stable and accurate PPLB predictions for the ionization potential and electron affinity of Li, as depicted in Figures B.7 and B.8. By accurate, we mean more in accordance with the ionization potentials and electron affinities obtained with the Δ SCF method within the scope of standard ground-state DFT with the same level of approximations.

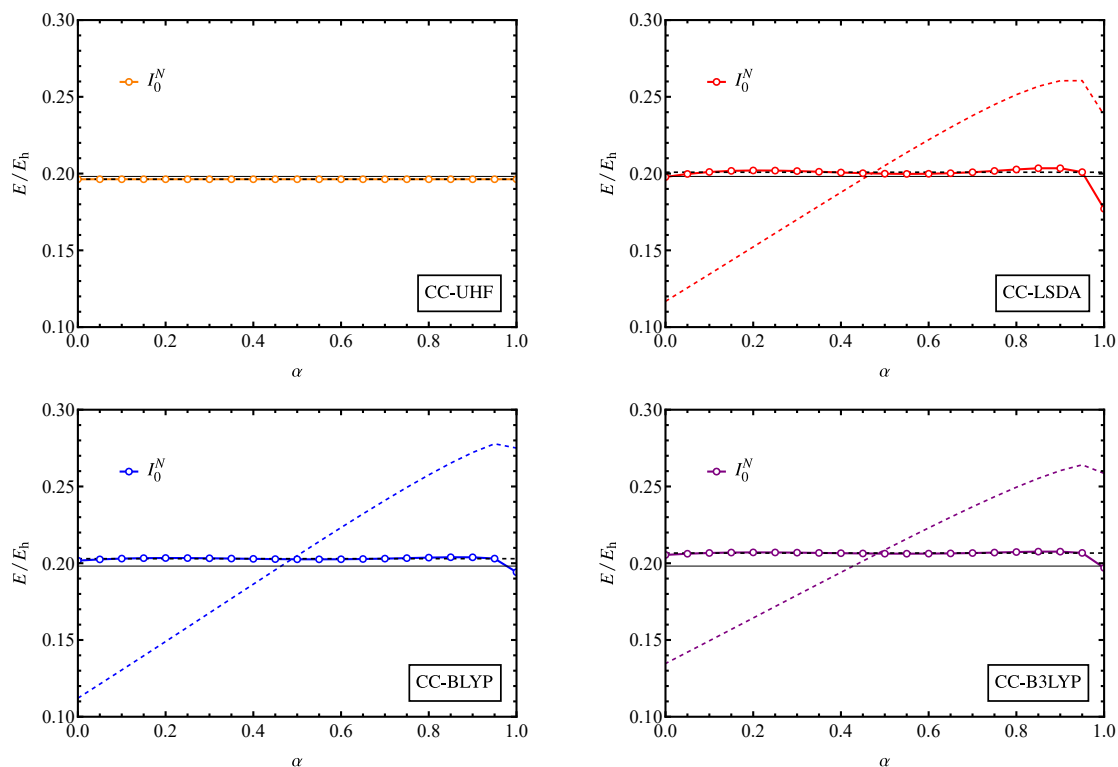


Figure B.7: Comparison between left PPLB-DFT ionization potentials of Li, obtained with weight-independent xc-functionals (colored dashed lines) and their weight-dependent CC-counterparts (colored solid lines), as functions of the fractional-charge deviation α , in the cc-pVDZ basis set. Δ SCF (black dashed line) ionization potentials obtained with the same level of approximation are reported for comparison as well as the experimental (black solid lines) ionization potential of Li (see Appendix A).

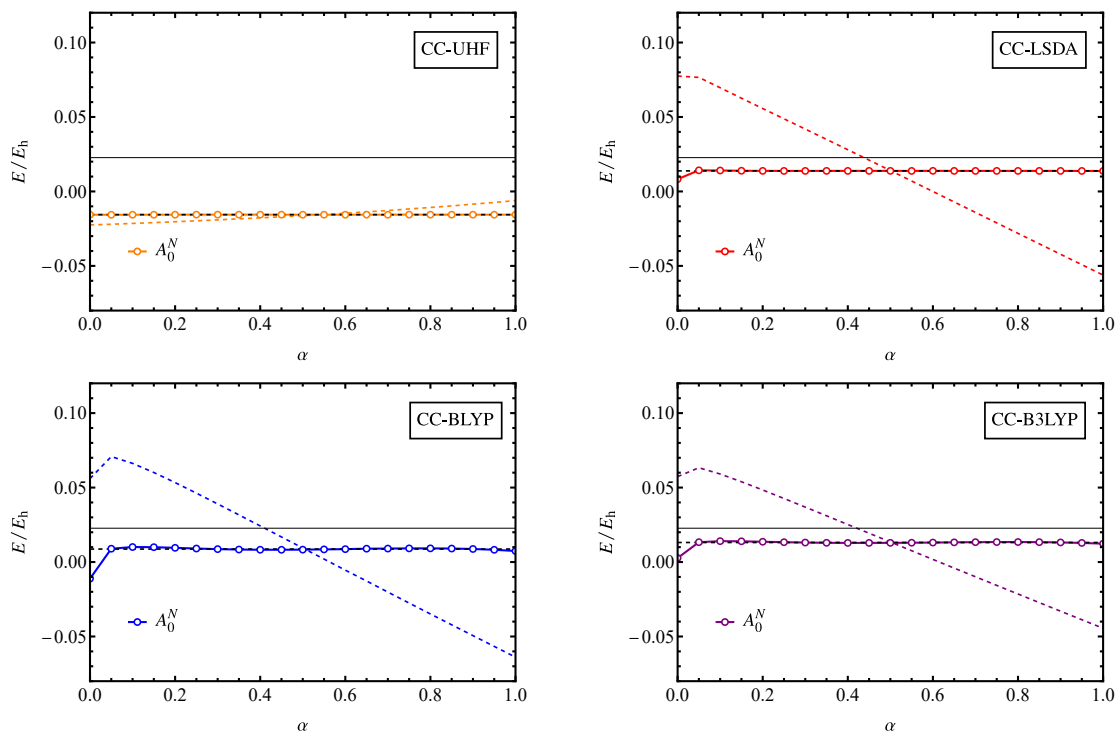


Figure B.8: Comparison between right PPLB-DFT electron affinities of Li, obtained with weight-independent xc-functionals (colored dashed lines) and their weight-dependent CC-counterparts (colored solid lines), as functions of the fractional-charge deviation α , in the cc-pVDZ basis set. Δ SCF (black dashed line) electron affinities obtained with the same level of approximation are reported for comparison as well as the experimental (black solid lines) electron affinity of Li (see Appendix A).

Appendix C

GOK-DFT Supplementary Material

C.1 GOK-DFT Code Testing

In order to ensure the proper functioning of our eDFT Fortran code within the scope of GOK-DFT, we managed to verify the consistency of the data extracted from the self-consistent eDFT calculation, such as individual-state energies and excitation energies.

Indeed, in GOK-DFT we have seen that once the calculation has reached convergence yielding the minimizing molecular orbitals with corresponding minimum ensemble energy, excitation energies can be extracted from the ensemble calculation in two different manners: from the ensemble energy and its derivatives with respect to the ensemble weights

$$\Omega_I = \frac{\partial E^{\mathbf{w}}}{\partial w_I}, \quad (\text{C.1})$$

or from the (Hartree-Fock or Kohn-Sham) auxiliary excitation energies and the derivative of the weight-dependent Hartree-exchange-correlation functional

$$\Omega_I = \mathcal{E}_I^{\mathbf{w}} - \mathcal{E}_0^{\mathbf{w}} + \left. \frac{\partial E_{\text{Hxc}}^{\mathbf{w}}[n]}{\partial w_I} \right|_{n=n_{\text{KS}}^{\mathbf{w}}}. \quad (\text{C.2})$$

Nevertheless, excitation energies obtained from equations (C.1) and (C.2) should be identical. Derivatives of the ensemble energy with respect to the ensemble weights of equation (C.1) were computed by use of a finite difference approximation in its symmetric difference quotient formulation.

C.1.1 GOK-DFT with Weight-Independent Functionals

When weight-independent approximate functionals are used, excitation energies obtained from equation (C.2) reduce to weight-dependent auxiliary excitation energies built from the molecular orbital energies, with no additional contribution arising from the explicit weight-dependency of the approximate functional, as depicted in Figure C.1.

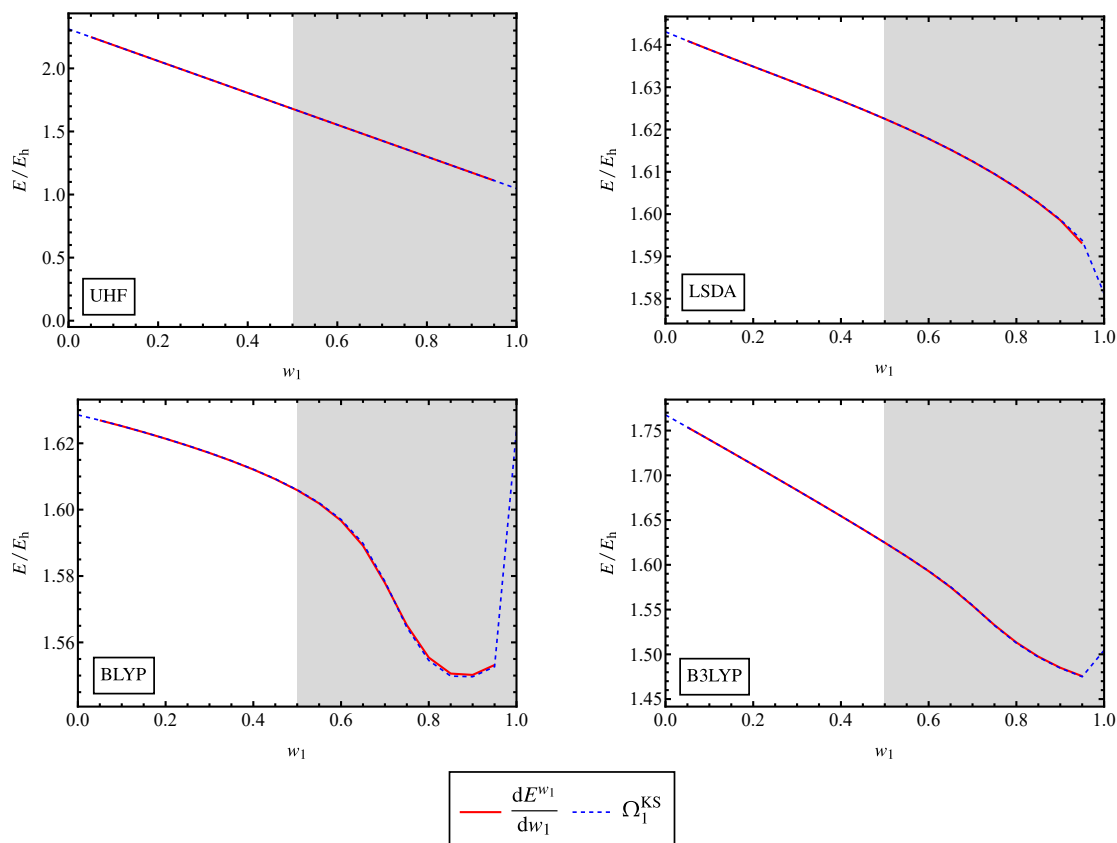


Figure C.1: Checking the validity of GOK-DFT “single” biensemble calculations with weight-independent approximations in the cc-pVDZ basis set.

C.1.2 GOK-DFT with Weight-Dependent Functionals

Conversely, when a weight-dependent approximate functional is used, the weight derivative of the Hxc-functional will contribute to improving predictions of excitation energies, as depicted in Figure C.2.

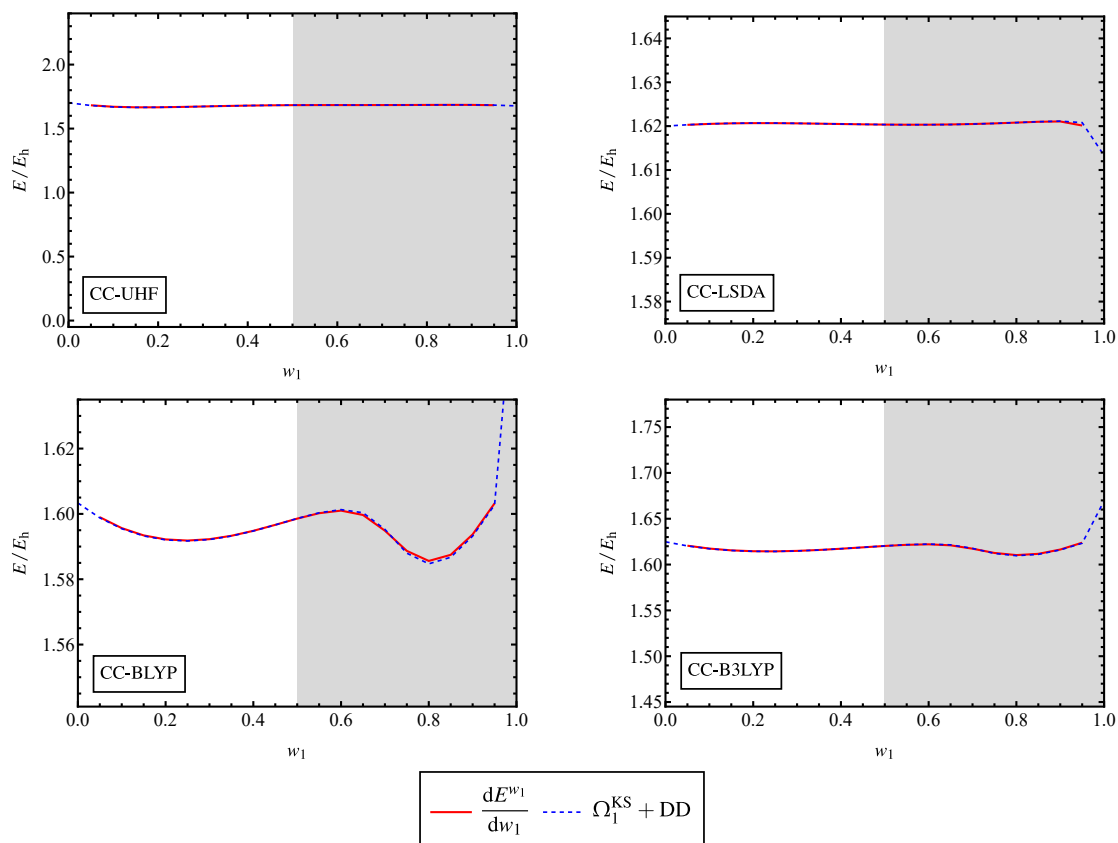


Figure C.2: Checking the validity of GOK-DFT “single” biensemble calculations with weight-dependent approximations in the cc-pVDZ basis set. The “DD” term refers to the additional contribution arising from the weight-derivative of the approximate functional (see equation (C.2)).

C.2 Proof of Correctness of the GOK-DFT Numerical Results

Table C.1: Ground-state energy and two lowest singly excited-state energies (with spin multiplicity 1S and 3S) of He, for various exchange-correlation functionals and basis sets. Δ SCF excitation energies for the electronic transition between the ground state and the 1S and 3S excited state are reported along with calculated and accurate references. All energies are in hartree.

	cc-pVDZ		d-aug-cc-pVTZ
	BLYP	B3LYP	BLYP
$E_0(^1S)$	-2.897 849 407	-2.907 051 315	-2.906 547 599
Accurate ^a			-2.903 724 377
$E_1(^1S)$	-1.302 502 815	-1.289 467 230	-2.162 683 358
Accurate ^a			-2.145 974 046
$E_1(^3S)$	-1.412 962 984	-1.418 071 546	-2.169 847 699
Accurate ^a			-2.175 229 378
Δ SCF $\Omega_1(^3S)$	1.484 886 423	1.488 979 769	0.736 699 899
Calculated ^b	1.484 882 330	1.488 978 475	0.736 645 506
Accurate ^a			0.728 494 998
Δ SCF $\Omega_1(^1S)$	1.595 346 592	1.617 584 085	0.743 864 241
Accurate ^a			0.757 750 331

^a obtained from [8].

^b obtained from [40].

Appendix D

N -centered eDFT Supplementary Material

D.1 N -centered eDFT Code Testing

In order to ensure the proper functioning of our eDFT Fortran code within the scope of N -centered eDFT, we managed to verify the consistency of the data extracted from the self-consistent eDFT calculation, such as individual-state energies and excitation energies.

Indeed, in N -centered eDFT we have seen that once the calculation has reached convergence yielding the minimizing molecular orbitals with corresponding minimum ensemble energy, ionization potentials can be extracted from the left N -centered ensemble calculation in two different manners: from the ensemble energy and its derivatives with respect to the ensemble weights

$$I_0^N = -\bar{\varepsilon}_N^{\xi^-} - \frac{1}{N}(1 - \alpha - N) \left. \frac{\partial E_{\text{Hxc}}^{\xi^-}}{\partial \alpha} \right|_{n_{\text{KS}}^{\xi^-}}, \quad (\text{D.1})$$

or from the weight-dependent LZ-shifted (Hartree-Fock or Kohn-Sham) molecular orbital energies and the derivative of the weight-dependent Hartree-exchange-correlation functional

$$I_0^N = -\frac{1}{N} \left[E^{\xi^-} + (1 - \alpha - N) \frac{dE^{\xi^-}}{d\alpha} \right]. \quad (\text{D.2})$$

In the same manner, electron affinities can be extracted from right N -centered eDFT calculation in two different ways,

$$A_0^N = -\frac{1}{N} \left[E^{\xi^+} + (1 - \alpha + N) \frac{dE^{\xi^+}}{d\alpha} \right], \quad (\text{D.3})$$

or

$$A_0^N = -\bar{\varepsilon}_{N+1}^{\xi^+} - \frac{1}{N}(1 - \alpha + N) \left. \frac{\partial E_{\text{Hxc}}^{\xi^+}}{\partial \alpha} \right|_{n_{\text{KS}}^{\xi^+}}. \quad (\text{D.4})$$

Nevertheless, ionization potentials and electron affinities obtained from equations (D.1) and (D.2), and (D.3) and (D.4), respectively, should be identical.

Derivatives of the ensemble energies with respect to the ensemble weights of equation (D.1) and (D.3) were computed by use of a finite difference approximation in its symmetric difference quotient formulation.

D.1.1 Left and Right *N*-centered eDFT with Weight-Independent LSDA

When weight-independent approximate functionals are used, excitation energies obtained from equation (D.2) and (D.4) reduce to weight-dependent LZ-shifted molecular orbital energies, with no additional contribution arising from the explicit weight-dependency of the approximate functional, as depicted in Figure D.1.

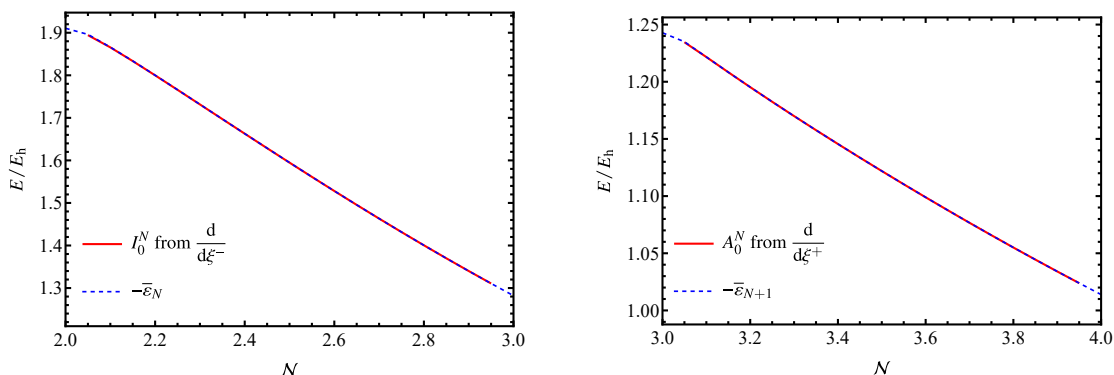


Figure D.1: Checking the validity of left (left panel) and right (right panel) *N*-centered ensemble eDFT calculations with the weight-independent LSDA functional in the cc-pVDZ basis set..

D.1.2 Left and Right *N*-centered eDFT with Weight-Dependent CC-LSDA

Conversely, when a weight-dependent approximate functional is used, the weight derivative of the Hxc-functional will contribute to improving predictions of excitation energies, as depicted in Figure D.2.

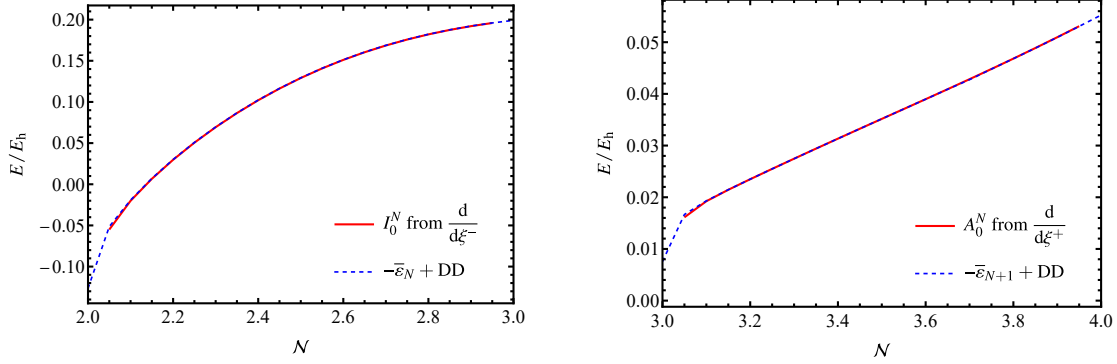


Figure D.2: Checking the validity of left (left panel) and right (right panel) N -centered ensemble eDFT calculations with weight-dependent CC-LSDA functionals in the cc-pVDZ basis set. The “DD” term refers to the additional contribution arising from the weight-derivative of the approximate functional (see equations (D.2) and (D.4)).

D.1.3 Single-Weight N -centered eDFT with Weight-Independent Functionals

In the single-weight triensemble formulation of N -centered eDFT, fundamental gaps can be extracted either from the derivative of the ensemble energy with respect to the ensemble weight

$$\Omega_0^N = \frac{dE^\xi}{d\xi}, \quad (\text{D.5})$$

or from

$$\Omega_0^N = \varepsilon_{N+1}^\xi - \varepsilon_N^\xi + \left. \frac{\partial E_{\text{Hxc}}^\xi}{\partial \xi} \right|_{n_{\text{KS}}^\xi}, \quad (\text{D.6})$$

as depicted in Figure D.3.

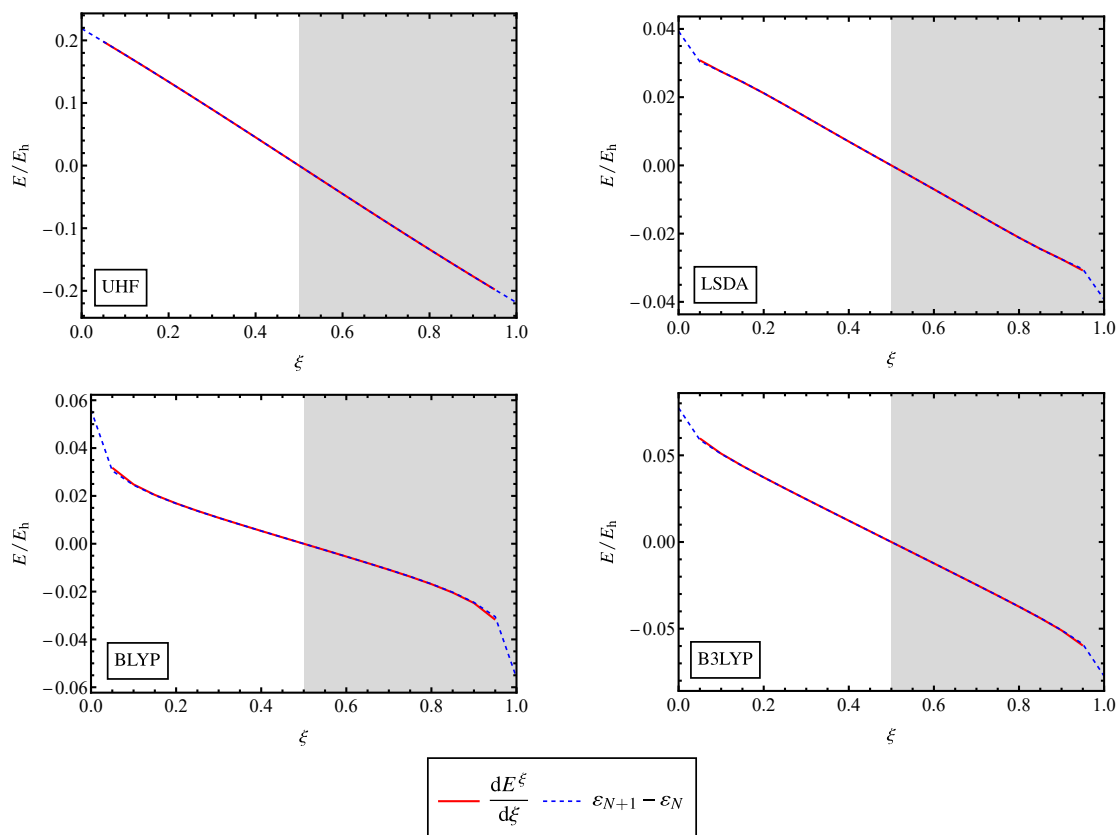


Figure D.3: Checking the validity of single-weight *N*-centered triensemble eDFT calculations with weight-independent approximations in the cc-pVDZ basis set.

D.2 Overview of Left and Right *N*-centered Results with CC-Functionals

This section provides more detailed overviews of the left (see Table D.1) and right (see Table D.2) *N*-centered eDFT results obtained with the weight-dependent CC-functionals compared to the results obtained with standard weight-independent xc-functionals.

Table D.1: Comparison between the left N -centered predictions for the ionization potential of Li and the Δ SCF references obtained with standard weight-independent and weight-dependent (CC) xc-functionals in the cc-pVDZ basis set, for various weight-configurations. The “DD” notation refers to the additional weight-derivative contributions of the CC-functionals to the ionization potential predictions. The blanks are left to highlight the fact that, unlike CC-functionals, standard weight-independent functionals do not benefit from the additional “DD” term. The “ \times ” notations correspond to quantities that could not be computed in the zero-weight limit for the BLYP and B3LYP sets of functionals. Percent errors ($\Delta(\%)$ notations) of the quantity in the line above, with respect to the Δ SCF ionization potentials, are reported. All energies are in hartree and experimental references are available in Appendix A.

Left N -centered: $N \rightarrow N - 1$									
	UHF	CC-UHF	LSDA	CC-LSDA	BLYP	CC-BLYP	B3LYP	CC-B3LYP	
Δ SCF I_0	0.19631	0.19631	0.20087	0.20087	0.20295	0.20295	0.20661	0.20661	0.20661
$\alpha = 0.00$									
$-\epsilon_N$	0.19632	0.19632	0.11678	0.11678	0.11210	0.11210	0.13466	0.13466	0.13466
$\Delta(\%)$	0.005	0.005	-41.862	-41.862	-44.764	-44.764	-34.824	-34.824	-34.824
$-\bar{\epsilon}_N$	0.95643	0.95643	1.28210	1.28210	\times	\times	\times	\times	\times
$\Delta(\%)$	387.203	387.203	538.273	538.273	\times	\times	\times	\times	\times
$-\bar{\epsilon}_N + \text{DD}$	-	0.19479	-	0.19911	-	\times	-	\times	\times
$\Delta(\%)$	-	-0.774	-	-0.876	-	\times	-	\times	\times
$\alpha = 0.05$									
$-\epsilon_N$	0.18075	0.18789	0.11181	0.11853	0.10731	0.11366	0.12772	0.13454	0.13454
$\Delta(\%)$	-7.926	-4.289	-44.337	-40.991	-47.124	-43.996	-38.183	-34.882	-34.882
$-\bar{\epsilon}_N$	0.95754	0.94813	1.31074	1.31427	1.32354	1.32802	1.25511	1.25576	1.25576
$\Delta(\%)$	387.769	382.975	552.531	554.288	552.150	554.358	507.477	507.792	507.792
$-\bar{\epsilon}_N + \text{DD}$	-	0.19422	-	0.19598	-	0.19865	-	0.20270	0.20270
$\Delta(\%)$	-	-1.064	-	-2.434	-	-2.118	-	-1.892	-1.892
$\alpha = 0.50$									
$-\epsilon_N$	0.05675	0.08001	0.06451	0.113661	0.06219	0.11026	0.06613	0.10870	0.10870
$\Delta(\%)$	-71.091	-59.243	-67.884	-43.415	-69.356	-45.671	-67.992	-47.388	-47.388
$-\bar{\epsilon}_N$	1.00247	0.84881	1.59482	1.61271	1.61453	1.64581	1.49902	1.46846	1.46846
$\Delta(\%)$	410.656	332.382	693.956	702.862	695.530	710.943	625.531	610.740	610.740
$-\bar{\epsilon}_N + \text{DD}$	-	0.17598	-	0.12925	-	0.13905	-	0.15267	0.15267
$\Delta(\%)$	-	-10.356	-	-35.654	-	-31.485	-	-26.107	-26.107

Table D.2: Comparison between the right *N*-centered predictions for the electron affinity of Li and the Δ SCF references obtained with standard weight-independent and weight-dependent (CC) xc-functionals in the cc-pVDZ basis set, for various weight-configurations. The "DD" notation refers to the additional weight-derivative contributions of the CC-functionals to the electron affinity predictions. The blanks are left to highlight the fact that, unlike CC-functionals, standard weight-independent functionals do not benefit from the additional "DD" term. The "x" notations correspond to quantities that could not be computed in the zero-weight limit for the BLYP and B3LYP sets of functionals. Percent errors ($\Delta(\%)$ notations) of the quantity in the line above, with respect to the Δ SCF electron affinities, are reported. All energies are in hartree and experimental references are available in Appendix A.

Right <i>N</i>-centered: $N \rightarrow N + 1$									
	UHF	CC-UHF	LSDA	CC-LSDA	BLYP	CC-BLYP	B3LYP	CC-B3LYP	
Δ SCF A_0	-0.015 58	-0.015 58	0.013 79	0.013 79	0.008 70	0.008 70	0.013 11	0.013 11	
$\alpha = 0.00$									
$-\epsilon_{N+1}$	-0.022 45	-0.022 45	0.077 49	0.077 49	0.056 06	0.056 06	0.057 35	0.057 35	
$\Delta(\%)$	-44.031	-44.031	461.620	461.620	544.049	544.049	337.242	337.242	
$-\bar{\epsilon}_{N+1}$	0.737 65	0.737 65	1.242 82	1.242 82	×	×	×	×	
$\Delta(\%)$	4831.969	4831.969	8907.046	8907.046	×	×	×	×	
$-\bar{\epsilon}_{N+1} + \text{DD}$	-	-0.018 412	-	-	0.007 56	×	×	×	
$\Delta(\%)$	-	-18.178	-	-45.140	-	×	-	×	
$\alpha = 0.05$									
$-\epsilon_{N+1}$	-0.014 28	-0.014 21	0.086 74	0.085 57	0.080 15	0.078 72	0.072 62	0.071 65	
$\Delta(\%)$	8.338	8.784	528.638	520.211	820.745	804.320	453.614	446.200	
$-\bar{\epsilon}_{N+1}$	0.737 52	0.745 73	1.234 98	1.235 62	1.244 09	1.243 69	1.153 13	1.155 43	
$\Delta(\%)$	4831.135	4883.814	8850.237	8854.900	14 190.784	14 186.244	8690.216	8707.732	
$-\bar{\epsilon}_{N+1} + \text{DD}$	-	-0.015 55	-	0.016 66	-	0.010 07	-	0.014 40	
$\Delta(\%)$	-	0.164	-	20.757	-	15.843	-	9.877	
$\alpha = 0.50$									
$-\epsilon_{N+1}$	0.067 20	0.053 09	0.117 61	0.088 65	0.114 79	0.086 57	0.114 77	0.089 28	
$\Delta(\%)$	531.104	440.572	752.387	542.488	1218.582	894.515	774.905	580.645	
$-\bar{\epsilon}_{N+1}$	0.750 62	0.817 46	1.121 92	1.110 79	1.133 62	1.115 73	1.065 21	1.069 83	
$\Delta(\%)$	4915.160	5343.943	8030.859	7950.161	12 921.804	12 716.876	8019.978	8055.189	
$-\bar{\epsilon}_{N+1} + \text{DD}$	-	-0.000 691	-	0.035 16	-	0.027 69	-	0.029 93	
$\Delta(\%)$	-	55.633	-	154.855	-	218.341	-	128.375	

Appendix E

Résumé substantiel en français

Introduction

Cette thèse est consacrée à l'étude de la théorie de la fonctionnelle de la densité d'ensemble (eDFT) à travers différents formalismes et leur application à des systèmes atomiques et moléculaires : les ensembles PPLB pour la description de systèmes avec un nombre fractionnaire d'électrons, les ensembles GOK pour accéder aux états excités, et les ensembles N -centrés qui permettent d'extraire des énergies d'excitation chargée, sans altération du nombre d'électrons. Nous évaluerons la performance des fonctionnelles standard d'échange-corrélation vis-à-vis de l'extraction d'énergies d'excitation à travers l'eDFT. En particulier, nous discuterons certaines des limitations les plus connues de ces approximations standard, telles que l'absence de dérivée discontinue, la violation de la condition exacte de linéarité par morceaux, la description des systèmes avec charge ou spin fractionnaires et leur impact dans les processus de dissociation.

De la DFT à la DFT d'ensemble

Au cours des dernières décennies, la théorie de la fonctionnelle de la densité (DFT) s'est imposée comme une approche rigoureuse pour la description de l'état fondamental des systèmes électroniques. Grâce à son faible coût computationnel et à l'élaboration d'approximations sophistiquées pour la fonctionnelle d'échange-corrélation (xc-DFA), la DFT est devenue la méthode de choix pour le calcul de structure électronique. Néanmoins, il subsiste nombre de défis que la DFT ne parvient pas à surmonter. En réalité, ces carences ne sont pas le fruit de la théorie elle-même mais plutôt du fait de défauts intrinsèques des approximations utilisées. Il existe une formulation plus générale de la DFT pour les nombres fractionnaires d'occupation qui permet la description de systèmes avec nombre fractionnaire d'électrons, la PPLB-DFT. Cette formulation grand canonique de la DFT peut être mise en place à l'aide d'un formalisme d'ensemble et permet une extraction directe d'énergies d'excitation chargée et d'autres propriétés à partir d'un seul calcul de type DFT. Malheureusement, l'incapacité des DFAs à reproduire la fameuse dérivée discontinue (DD) s'est avérée être par-

ticulièrement préjudiciable pour la prédiction d'énergies d'excitation chargée, telles que les potentiels d'ionisation et les affinités électroniques, donnant lieu à des erreurs conséquentes, et connue comme le problème du gap fondamental. Dans ce contexte, la DFT d'ensemble (eDFT) offre une alternative très attrayante du fait de sa capacité à user de DFAs dépendantes du poids de l'ensemble pour reproduire la DD via leur dérivée. La DFT est connue pour montrer des limites vis-à-vis du calcul d'énergies d'excitation chargée et neutre. La procédure standard pour accéder aux états excités neutralement dans le cadre de la DFT est à travers son extension dépendante du temps, la TD-DFT. En effet, l'usage est de recourir à la TD-DFT pour obtenir des prédictions acceptables pour les énergies de transition des niveaux excités les plus bas, cela avec un coût computationnel relativement modéré. Bien que la TD-DFT se soit avérée incroyablement fructueuse pour accéder aux énergies d'excitation neutre, elle a également montré certaines limites lors de la description de certains phénomènes et propriétés physiques. En cela, l'eDFT constitue une alternative prometteuse à la TD-DFT pour le calcul des énergies d'excitation électroniques. En eDFT, il est possible d'extraire n'importe quelle énergie d'excitation neutre d'un système électronique en un seul calcul à l'aide d'un ensemble Gross-Oliveira-Kohn (GOK), et cela avec un coût computationnel et un niveau d'approximation pour la fonctionnelle d'xc, similaires à ceux de la DFT standard. La GOK-DFT est une alternative moins connue mais tout autant rigoureuse que la TD-DFT, où le large choix de poids de l'ensemble et la dépendance en poids de la fonctionnelle xc peuvent significativement influencer sur la qualité des énergies calculées. En temps normal, accéder aux énergies d'excitation chargée nécessite de faire varier le nombre d'électrons du système, ce qui peut s'avérer problématique dans certains cas. Très récemment, un nouveau formalisme canonique a été développé, l'eDFT N -centrée, rendant possible l'extraction d'énergies d'excitation chargée sans altération du nombre d'électrons. Le comportement des DFAs standard dans le cadre de l'eDFT peut offrir une compréhension plus poussée de la nature intrinsèque des erreurs systématiques dont elles souffrent, telles que la violation des conditions exactes de linéarité par morceaux et de constance de l'énergie. En outre, la mauvaise description des systèmes avec charge et spin fractionnaires a prouvé avoir un impact majeur dans la description des systèmes fortement corrélés ainsi que dans les processus de dissociation et la prédiction de gaps d'énergie. Tout cela pourrait donner un nouvel essor au développement futur de la DFT et à des applications émergentes jusqu'alors inaccessibles.

Le formalisme PPLB : la DFT généralisée aux systèmes à nombres fractionnaires d'électrons

Lorsqu'un électron est continuellement retiré ou ajouté de/à un système à N électrons, ce dernier se comporte comme un système ouvert avec un nombre fractionnaire d'électrons $\mathcal{N} = N \pm \alpha$, avec α l'écart fractionnaire de charge par rapport à la valeur entière centrale N

$$\alpha \equiv |\mathcal{N} - N|. \quad (\text{E.1})$$

De plus, les densités et énergies électroniques exactes de l'état fondamental de tels systèmes dits ouverts consistent en des combinaisons linéaires des densités et des énergies, respective-

ment, des états fondamentaux, sur lesquels sont basées les excitations chargées correspondantes, c'est-à-dire les grandeurs physiques à N et $(N \pm 1)$ électrons.

Rappelons les expressions compactes des densités et énergies d'ensemble exactes associées aux ensembles de type PPLB

$$n^\alpha(\mathbf{r}) = (1 - \alpha)n_0^N(\mathbf{r}) + \alpha n_0^{N\pm 1}(\mathbf{r}) \quad (\text{E.2}) \quad \left| \quad E^\alpha = (1 - \alpha)E_0^N + \alpha E_0^{N\pm 1}, \quad (\text{E.3})$$

où $0 \leq \alpha \leq 1$ est le poids de l'ensemble PPLB décrivant, pour les deux processus, l'écart de charge physique par rapport au nombre entier central d'électron N .

Dans ce contexte, la configuration de poids $\alpha = 0$ correspond au système neutre initial de N électrons, tandis que le cas $\alpha = 1$ correspond au système cationique/anionique, selon la nature "gauche" ($-$) ou "droite" ($+$) de l'ensemble PPLB. Dans ces trois scénarios particuliers, les calculs de DFT d'ensemble PPLB-DFT se réduisent à des calculs de DFT standard pour état fondamental.

Une caractéristique importante du cadre PPLB-DFT est que le poids de l'ensemble et la densité d'ensemble ne sont pas des quantités indépendantes. En effet, puisque le résultat de l'intégration de la densité d'ensemble doit correspondre au nombre fractionnaire d'électrons $\mathcal{N} = N \pm \alpha$ du système ouvert, un changement de poids α entraînera automatiquement un changement dans la densité. Ainsi, toutes les informations qui définissent l'ensemble sont donc déjà englobées dans la densité d'ensemble, ce qui signifie que la fonctionnelle exacte, c'est-à-dire la fonctionnelle garantissant la linéarité par morceaux de l'énergie d'ensemble, n'a pas besoin de posséder une dépendance explicite en poids de l'ensemble pour calculer les propriétés exactes du système ouvert. Bien évidemment, puisque la fonctionnelle exacte n'est pas connue, nul n'est obligé de restreindre son cadre de travail au seul domaine des fonctionnelles standards indépendantes du poids, et il est toujours possible d'explorer la faisabilité et la pertinence de construire de meilleures approximations basées sur des fonctionnelles incluant une dépendance explicite en poids de l'ensemble, comme cela a été fait au cours de cette thèse.

Puisque l'énergie d'ensemble exacte de l'état fondamental du système à \mathcal{N} électrons est supposée être linéaire par rapport au poids d'ensemble α , il est possible d'extraire facilement les énergies individuelles des différents état fondamentaux $\{E_0^N; E_0^{N\pm 1}\}$ ainsi que les diverses énergies d'excitation, telles que le potentiel d'ionisation I_0^N et l'affinité électronique A_0^N du système référence à N électrons, et ce, directement à partir des énergies d'ensemble PPLB "gauche" et "droite", respectivement, E^α et de leurs dérivées respectives par rapport au poids α , tel que

$$\begin{aligned}
 E_0^N &= E^\alpha - \alpha \frac{\partial E^\alpha}{\partial \alpha} \\
 E_0^{N-1} &= E^\alpha + (1 - \alpha) \frac{\partial E^\alpha}{\partial \alpha} \\
 I_0^N &= E_0^{N-1} - E_0^N = \frac{\partial E^\alpha}{\partial \alpha}
 \end{aligned} \tag{E.4}$$

$$\begin{aligned}
 E_0^N &= E^\alpha - \alpha \frac{\partial E^\alpha}{\partial \alpha} \\
 E_0^{N+1} &= E^\alpha + (1 - \alpha) \frac{\partial E^\alpha}{\partial \alpha} \\
 A_0^N &= E_0^N - E_0^{N+1} = -\frac{\partial E^\alpha}{\partial \alpha}.
 \end{aligned} \tag{E.5}$$

En pratique, lorsque l'on effectue des calculs DFT ou eDFT, certaines des quantités primaires auxquelles on a accès une fois la convergence obtenue sont les énergies orbitales de Kohn-Sham $\{\varepsilon_i\}$. Par conséquent, il serait très pratique de pouvoir extraire les énergies individuelles et les énergies d'excitation mentionnées ci-dessus, directement à partir des quantités d'ensemble de Kohn-Sham. Encore une fois, nous insistons sur le fait que, pour un calcul de DFT d'ensemble, le set d'orbitales de Kohn-Sham sera dépendant du poids de l'ensemble et sera optimisé par rapport à l'ensemble entier, et non pour un état spécifique inclus dans l'ensemble. Pour cette raison, les prédictions d'énergies individuelles et d'énergies d'excitations seront toutes obtenues à partir du même système d'ensemble de Kohn-Sham. Rappelons les formules clés qui seront utilisées pour prédire les propriétés physiques des états individuels et ainsi que les énergies d'excitation lors de calculs pratiques de type PPLB-DFT

$$\begin{aligned}
 E_0^N &= \mathcal{E}_0^{N,\alpha} \\
 &+ E_{\text{Hxc}}^\alpha[n_{\text{KS}}^\alpha] - \int \frac{\delta E_{\text{Hxc}}^\alpha[n_{\text{KS}}^\alpha]}{\delta n(\mathbf{r})} n_{\text{KS}}^\alpha(\mathbf{r}) d\mathbf{r} \\
 &- \alpha \frac{\partial E_{\text{Hxc}}^\alpha[n_{\text{KS}}^\alpha]}{\partial \alpha} \\
 E_0^{N-1} &= \mathcal{E}_0^{N-1,\alpha} \\
 &+ E_{\text{Hxc}}^\alpha[n_{\text{KS}}^\alpha] - \int \frac{\delta E_{\text{Hxc}}^\alpha[n_{\text{KS}}^\alpha]}{\delta n(\mathbf{r})} n_{\text{KS}}^\alpha(\mathbf{r}) d\mathbf{r} \\
 &+ (1 - \alpha) \frac{\partial E_{\text{Hxc}}^\alpha[n_{\text{KS}}^\alpha]}{\partial \alpha} \\
 I_0^N &= -\varepsilon_N^\alpha + \frac{\partial E_{\text{Hxc}}^\alpha[n_{\text{KS}}^\alpha]}{\partial \alpha}
 \end{aligned} \tag{E.6}$$

$$\begin{aligned}
 E_0^N &= \mathcal{E}_0^{N,\alpha} \\
 &+ E_{\text{Hxc}}^\alpha[n_{\text{KS}}^\alpha] - \int \frac{\delta E_{\text{Hxc}}^\alpha[n_{\text{KS}}^\alpha]}{\delta n(\mathbf{r})} n_{\text{KS}}^\alpha(\mathbf{r}) d\mathbf{r} \\
 &- \alpha \frac{\partial E_{\text{Hxc}}^\alpha[n_{\text{KS}}^\alpha]}{\partial \alpha} \\
 E_0^{N+1} &= \mathcal{E}_0^{N+1,\alpha} \\
 &+ E_{\text{Hxc}}^\alpha[n_{\text{KS}}^\alpha] - \int \frac{\delta E_{\text{Hxc}}^\alpha[n_{\text{KS}}^\alpha]}{\delta n(\mathbf{r})} n_{\text{KS}}^\alpha(\mathbf{r}) d\mathbf{r} \\
 &+ (1 - \alpha) \frac{\partial E_{\text{Hxc}}^\alpha[n_{\text{KS}}^\alpha]}{\partial \alpha} \\
 A_0^N &= -\varepsilon_{N+1}^\alpha - \frac{\partial E_{\text{Hxc}}^\alpha[n_{\text{KS}}^\alpha]}{\partial \alpha}.
 \end{aligned} \tag{E.7}$$

Il est connu que les coûts énergétiques pour le retrait ou l'ajout d'un électron de/vers l'état fondamental d'un système électronique neutre sont différents. Par conséquent, l'énergie d'ensemble exacte E^N d'un système ouvert doit être linéaire par morceaux par rapport à la

variation continue du nombre d'électrons \mathcal{N} .

Dans ce contexte, Perdew, Parr, Levy et Balduz ont dérivé deux propriétés fondamentales exactes auxquelles une théorie en principe exacte, telle que la formulation Kohn-Sham de la DFT, doit obéir lorsqu'elle est appliquée à un système dit ouvert.

- La courbe de l'énergie totale exacte par rapport au nombre d'électrons du système ouvert, $E^{\mathcal{N}}(\mathcal{N})$, doit être constituée d'une série de lignes droites entre nombres entiers successifs d'électrons N .
- Lors du franchissement d'un nombre entier d'électrons, le potentiel exact d'échange-corrélation doit subir un "saut", connu sous le nom de "dérivée discontinue", Δ_{xc} .

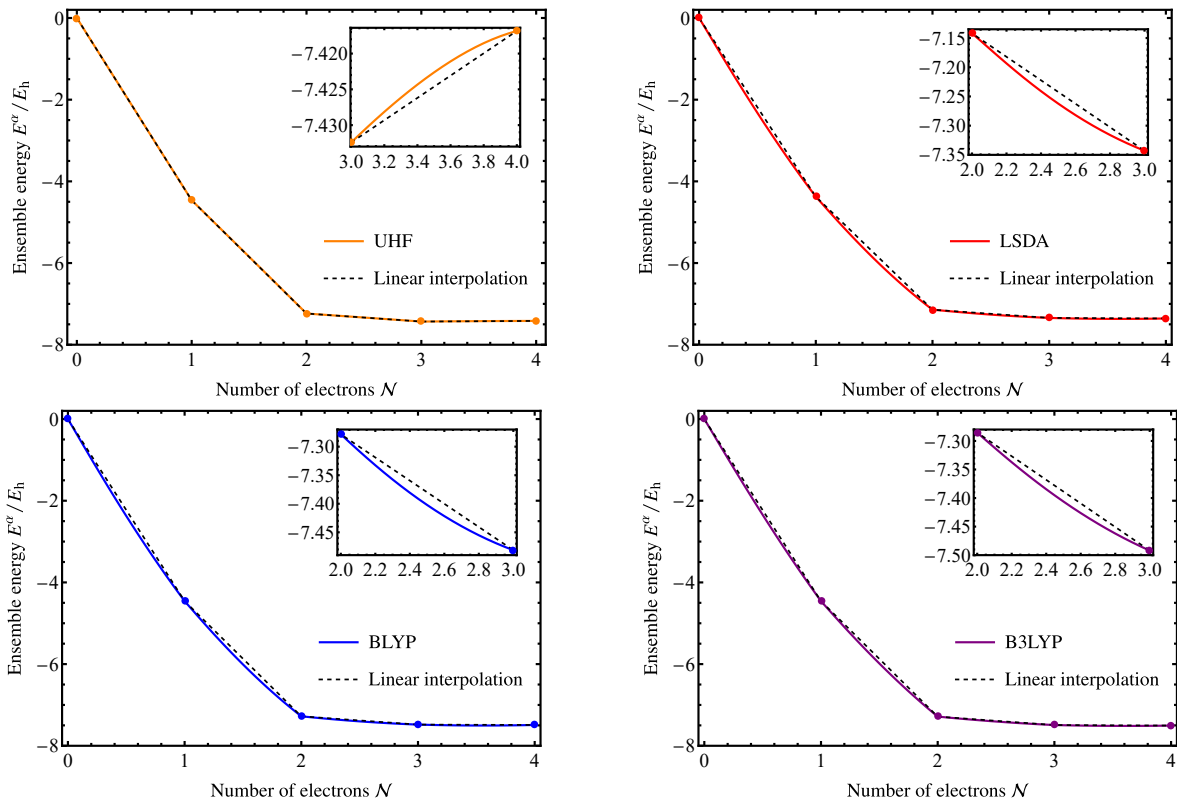


Figure E.1: Violation de la condition exacte de linéarité par morceaux de l'énergie d'ensemble PPLB exacte de Li par rapport au nombre d'électrons du système ouvert avec diverses méthodes et fonctionnelles d'xc, dans la base cc-pVDZ. Les énergies d'ensemble PPLB auto-cohérentes obtenues sont comparées aux énergies d'interpolation linéaire correspondantes, obtenues avec les mêmes méthodes et fonctionnelles et basées sur les énergies fondamentales des états dits "purs" correspondants (points).

Ces deux contraintes exactes sont en fait intrinsèquement liées et la violation de l'une entraînera des conséquences immédiates sur l'autre, comme démontré dans ce travail. En effet, l'utilisation d'une fonctionnelle approchée d'échange-corrélation dépourvue de dérivée

discontinue engendrera un écart par rapport à la condition exacte de linéarité par morceaux de l'énergie totale (voir Figures E.1 et E.2).

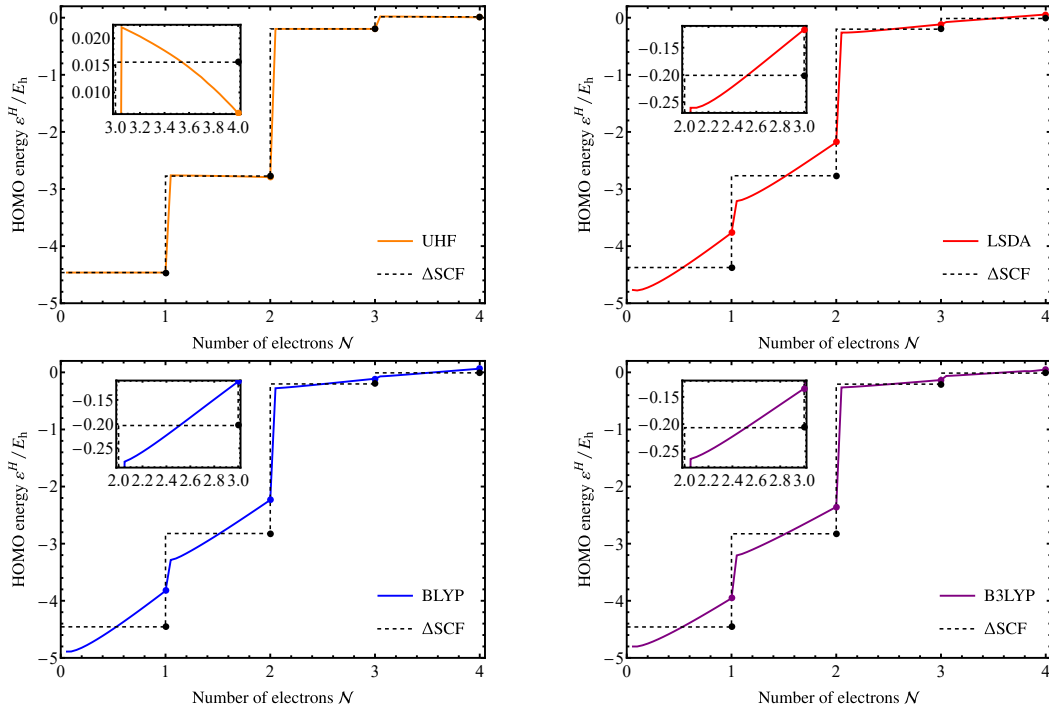


Figure E.2: Violation de la condition exacte de constance par morceaux de l'énergie HOMO de Li par rapport au nombre d'électrons \mathcal{N} , en utilisant diverses méthodes et niveaux d'approximation d'xc, dans la base cc-pVDZ. Les énergies orbitales HF/KS dépendantes du poids sont comparées à l'opposé des potentiels d'ionisation et des affinités électroniques correspondants obtenus par différences d'énergie totales (méthode Δ SCF) entre les énergies fondamentales des états purs successifs.

Compte tenu de cette problématique, nous explorons dans cette thèse la faisabilité de concevoir une fonctionnelle d'échange-corrélation explicitement dépendante du poids de l'ensemble et qui serait à même de corriger la courbure parasite des énergies d'ensemble de type PPLB obtenues par les fonctionnelles standard indépendantes du poids en PPLB-DFT. Ces fonctionnelles dénommées “CC” (Courbure-Corrigée) sont de la forme suivante

$$E_x^{\alpha, \text{eDFA}}[n] \equiv F_x^\alpha E_x^{\alpha, \text{DFA}}[n], \quad (\text{E.8})$$

avec F_x^α un facteur multiplicatif d'échange explicitement dépendant du poids de l'ensemble.

Ainsi, la conception de fonctionnelles possédant une propriété de dérivée discontinue, ou capables de l'imiter artificiellement, peut permettre dans un premier temps de restaurer le comportement linéaire par morceaux de l'énergie totale du système et d'améliorer du même coup la prédiction de propriétés physiques telles que les énergies d'excitation (voir Figure E.3).

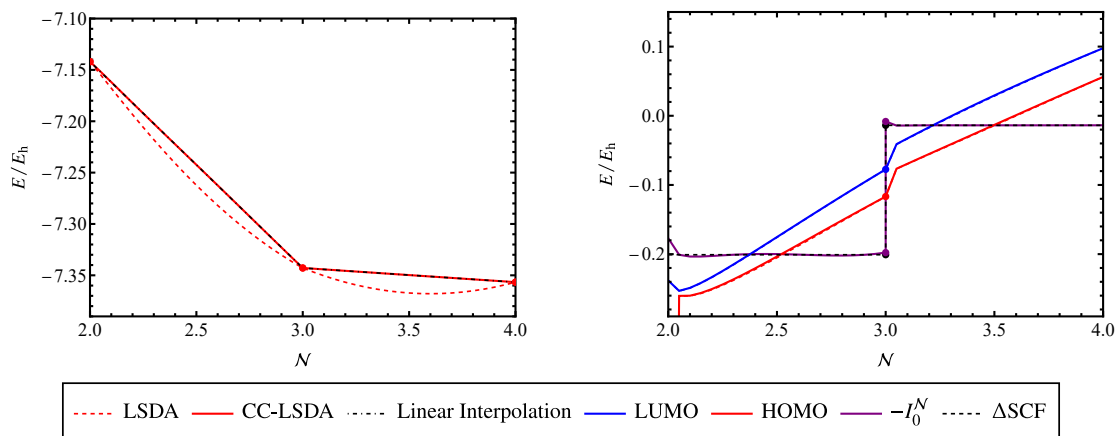


Figure E.3: Impact de la capacité des fonctionnelles CC à restaurer la condition exacte de linéarité par morceaux de l'énergie totale d'un système ouvert sur la pertinence physique de la prédiction du gap fondamental à partir de quantités d'ensemble. Les calculs ont été effectués sur Li dans la base cc-pVDZ avec la fonctionnelle d'xc LSDA et son alter-ego CC dépendant du poids de l'ensemble. Un parallèle est établi entre le rétablissement de la condition de linéarité par morceaux de l'énergie totale du système ouvert (Figure de gauche) et l'amélioration de la prédiction du gap fondamental (Figure de droite). Le gap fondamental correspondant obtenu par différences d'énergie totales (méthode ΔSCF) entre les états purs correspondants avec le même niveau d'approximation est également reporté à des fins de comparaison.

La GOK-DFT pour les états excités et les excitations électroniques neutres

La DFT est une théorie de l'état fondamental conçue à l'origine pour décrire les systèmes statiques (indépendants du temps) associés à un potentiel externe indépendant du temps $v(r)$. Néanmoins, à l'instar du théorème de Hohenberg-Kohn, le théorème de Runge-Gross a prouvé l'existence d'une correspondance unique entre un potentiel externe $v(r, t)$ et la densité électronique $n(r, t)$ d'un système évoluant dans un tel potentiel. Par conséquent, la DFT a été généralisée pour inclure des potentiels externes dépendants du temps qui permettent la description des états dits excités (neutralement) et de donner accès aux excitations qui vérifient la conservation du nombre d'électrons du système, telles que les excitations optiques à effets excitoniques. Il est à noter que, dans le même esprit, il existe également une extension dépendante du temps de la théorie de Hartree-Fock, la TD-HF.

En pratique, l'application la plus courante de la TD-DFT se fait dans le régime de réponse linéaire, qui évite de devoir résoudre l'équation de Schrödinger dépendante du temps. La TD-DFT est très similaire à la DFT standard pour le calcul de l'état fondamental et consiste à résoudre de manière auto-cohérente un ensemble de problèmes Kohn-Sham dépendants du temps avec une difficulté supplémentaire provenant du fait que le potentiel d'échange-corrélation est beaucoup plus subtil qu'en DFT standard en raison du fait qu'il doit englober un effet "mémoire" dans sa dépendance à la densité électronique.

En général, un moyen de contourner cette difficulté est d'utiliser la TD-DFT dans le cadre de l'approximation adiabatique qui consiste à négliger cette caractéristique temporelle du potentiel d'xc en utilisant à la place son analogue indépendant du temps utilisé en DFT pour l'état fondamental. Malheureusement, l'approximation adiabatique, qui implique le recours à un noyau d'échange-corrélation statique, restreint le domaine d'application de la TD-DFT à la seule description d'états à excitation unique et, par conséquent, manque complètement les excitations multiples dont la description nécessiterait un noyau d'xc dépendant de la fréquence. La TD-DFT, dans le régime de la réponse linéaire et dans sa formulation adiabatique, s'est imposée comme l'une des alternatives les plus prometteuses pour la description et le calcul d'excitations neutres. Bien qu'elle puisse prédire avec une précision satisfaisante les énergies d'excitation, elle souffre néanmoins de nombreuses carences qualitatives qui doivent encore être surmontées. La TD-DFT a été très largement utilisée avec succès au cours des dernières décennies, mais ne parvient pas à fournir une description appropriée d'un certain nombre de phénomènes et de propriétés intéressantes telles que la description des états de Rydberg, des excitations à transfert de charge ou des intersections coniques qui jouent un rôle clé dans les mécanismes photochimiques. De plus, les excitations multiples sont complètement absentes des spectres obtenus par la TD-DFT. D'où la nécessité de développer une approche plus générale applicable à tous types d'états excités et capable d'accéder à l'ensemble du spectre énergétique d'un système électronique via un formalisme indépendant du temps et nécessitant un faible coût de calcul.

En cela, le formalisme Gross-Oliveira-Kohn de la DFT d'ensemble peut constituer une alternative attrayante. En effet, la GOK-DFT est une théorie exacte et indépendante du temps qui peut non seulement accéder à toutes sortes d'énergies d'excitation mais aussi aux énergies et aux densités des états excités et, ce, à travers un seul calcul de type DFT grâce à l'utilisation du formalisme d'ensemble. Néanmoins, un tel formalisme soulève un certain nombre de questions qui restent encore sans réponse et doivent être investigués afin de pouvoir exploiter pleinement cette méthode. Par exemple, les questions du choix optimal des valeurs de poids de l'ensemble à utiliser et la nécessité de concevoir de nouvelles fonctionnelles approchées d'xc dépendantes du poids demeurent cruciales. Par ailleurs, nous abordons également dans ce travail la nécessité d'aller au-delà des fonctionnelles standard d'xc indépendantes du poids et explorons la possibilité d'user de la méthode d'interpolation linéaire (LIM) comme alternative pour obtenir des prédictions suffisamment précises pour les énergies d'excitation d'atomes et de systèmes moléculaires.

Dans ce travail, nous avons tout d'abord considéré des ensemble à deux états incluant l'état fondamental $E_0^N \equiv E_0$ de systèmes électronique à $N = 2$ électrons ainsi que l'état excité de type singulet le plus bas obtenu par excitation unique $E_1^N \equiv E_1$ que nous avons supposé être l'état excité de plus basse énergie. L'énergie associée à ce type de bienensemble GOK prend la forme suivante

$$E^{w_1} = (1 - w_1)E_0 + w_1E_1. \quad (\text{E.9})$$

De même, nous avons également considéré un deuxième bienensemble incluant cette fois l'état fondamental du système ainsi que l'état excité de type singulet le plus bas obtenu par double

excitation $E_2^N \equiv E_2$. L'énergie de ce deuxième type de biensemble GOK s'écrit alors

$$E^{w_2} = (1 - w_2)E_0 + w_2E_2. \quad (\text{E.10})$$

Enfin, nous avons défini et étudié le “triensemble” GOK incluant cette fois les trois états électroniques les plus bas du système à N électrons, que nous avons supposé être l'état fondamental, l'état singulet le plus bas obtenu par excitation unique et l'état singulet le plus bas obtenu par double excitation.

Basé sur cette définition, nous avons tout d'abord distingué la configuration à deux poids distincts

$$E^{\mathbf{w}} = (1 - w_1 - w_2)E_0 + w_1E_1 + w_2E_2, \quad (\text{E.11})$$

où $\mathbf{w} = \{w_1; w_2\}$, et la configuration à poids unique qui est un cas particulier du triensemble GOK précédant où $w_1 = w_2 = w$

$$E^w = (1 - 2w)E_0 + wE_1 + wE_2. \quad (\text{E.12})$$

Il faut noter que, afin de garantir la validité du principe variationnel GOK, les poids de l'ensemble doivent vérifier

$$0 \leq w_2 \leq \frac{1}{3} \quad (\text{E.13}) \quad \left| \quad w_2 \leq w_1 \leq \frac{1}{2}(1 - w_2). \quad (\text{E.14})$$

Par application du théorème de Hellmann-Feynman à la définition de l'énergie d'ensemble GOK, les énergies d'excitation peuvent être exprimées, en principe exactement, en termes d'énergies Kohn-Sham et de dérivées de la fonctionnelle d'échange-corrélation par rapport aux poids de l'ensemble.

$$\frac{\partial E^{\mathbf{w}}}{\partial w_I} = E_I - E_0 = \mathcal{E}_I^{\mathbf{w}} - \mathcal{E}_0^{\mathbf{w}} + \left. \frac{\partial E_{\text{Hxc}}^{\mathbf{w}}[n]}{\partial w_I} \right|_{n=n_{\text{KS}}^{\mathbf{w}}}. \quad (\text{E.15})$$

Dans cette définition, $\mathcal{E}_I^{\mathbf{w}}$ est la I ème énergie totale auxiliaire Kohn-Sham dépendante du poids, obtenue par sommation des énergies orbitales Kohn-Sham qui sont occupées dans la description du I ème état de l'ensemble

$$\mathcal{E}_I^{\mathbf{w}} = \sum_p n_p^I \varepsilon_p^{\mathbf{w}}. \quad (\text{E.16})$$

Du fait que les fonctionnelles d'xc approchées indépendantes du poids de l'ensemble ne parviennent pas à fournir des énergies d'ensemble GOK parfaitement linéaires (voir la Figure E.4), les énergies d'excitation associées aux états simplement et doublement excités obtenues par dérivation des énergies des biensembles et triensembles GOK par rapport aux poids w_1 et w_2 , respectivement, varient considérablement avec les poids, ce qui est très peu physique, par opposition avec les références Δ SCF obtenues dans en DFT standard avec le même niveau d'approximations, comme illustré dans la Figure E.5.

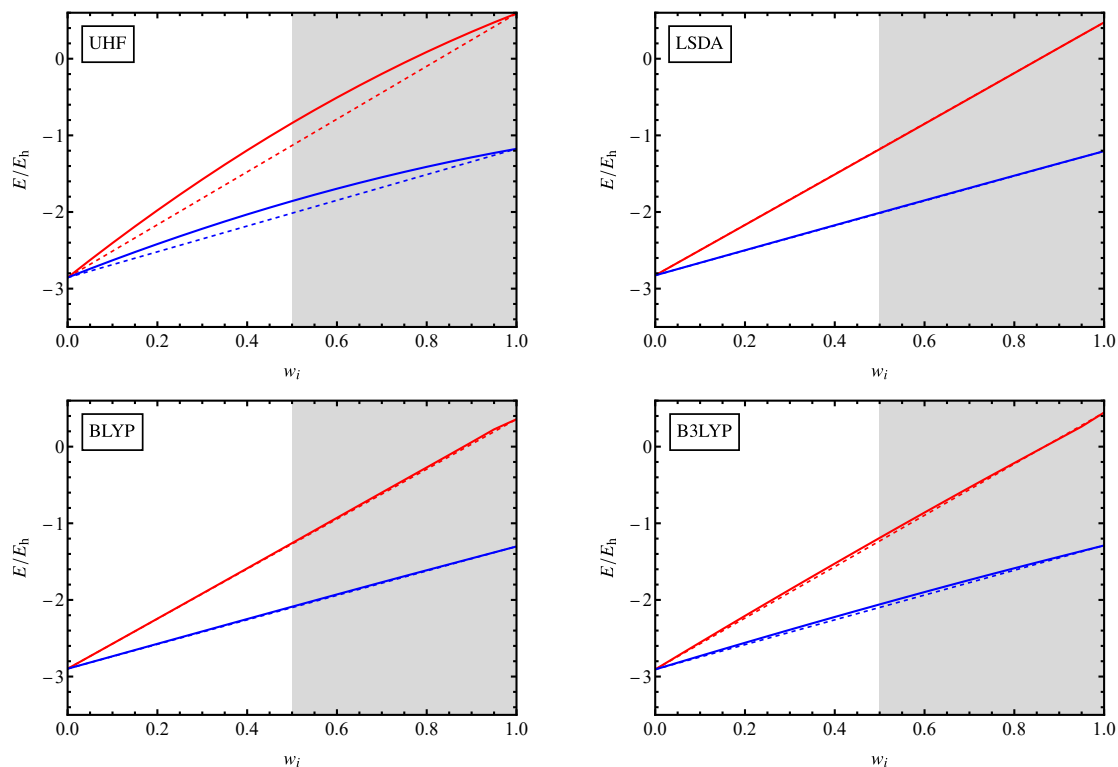


Figure E.4: Violation de la condition exacte de linéarité des énergies d'ensemble GOK de He obtenus pour les biensembles GOK "simples" (traits continus bleus) et "doubles" (traits continus rouges) par diverses méthodes et niveaux d'approximation d'xc dans la base cc-pVDZ. Les énergies d'ensemble GOK auto-cohérentes (traits continus) sont comparées aux interpolations linéaires correspondantes (traits discontinus). Les zones ombrées mettent en évidence le domaine de validité restreint du principe variationnel GOK.

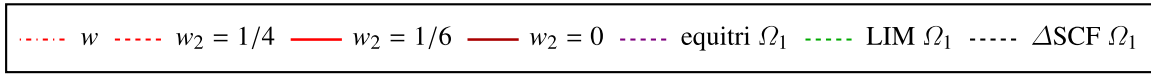
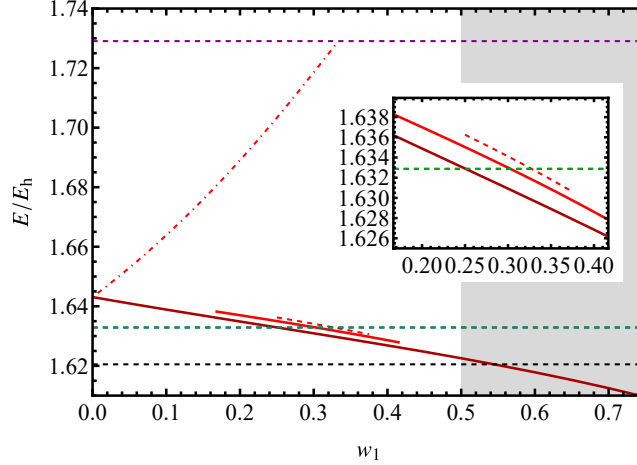


Figure E.5: Variation de l'énergie d'excitation simple la plus basse de He en fonction du poids de l'ensemble, obtenue à partir des triensembles GOK. Les énergies Kohn-Sham d'excitation simple obtenues à partir des triensembles GOK sont reportées pour la configuration à poids unique ($w_1 = w_2 = w$), pour différentes configurations de poids du triensemble à deux poids distincts ainsi que pour la configuration équiensemble ($w_1 = w_2 = \frac{1}{3}$), et sont comparées aux énergies d'excitation simple obtenues à partir du biensemble GOK "simple" ($w_2 = 0$), celle obtenue par la méthode d'interpolation linéaire (LIM) appliquée au biensemble ou au triensemble, de manière équivalente, ainsi que la prédiction Δ SCF obtenue avec le même niveau d'approximation. Les calculs ont été effectués dans le cadre de l'approximation d'xc LSDA et dans la base cc-pVDZ.

En parfaite analogie avec ce qui a été fait dans le cas des ensembles PPLB, nous avons conçu des fonctionnelles approchées d'échange dépendantes du poids et basées sur certaines des fonctionnelles approchées standard conçues pour la DFT pour les états fondamentaux. Cela, afin de corriger les erreurs de courbure des énergies d'ensemble GOK et d'améliorer la qualité des énergies d'excitation.

$$E_x^{w_i, \text{eDFA}}[n] \equiv F_x^{w_i} E_x^{w_i, \text{DFA}}[n], \quad (\text{E.17})$$

En parvenant à rétablir la condition exacte de linéarité de l'énergie des biensembles GOK et, ainsi, la constance de leurs dérivées respectives par rapport aux poids, les fonctionnelles CC parviennent à produire des prédictions beaucoup plus stables et précises des énergies d'excitation, en accord avec les références Δ SCF correspondantes (voir la Figure E.6).

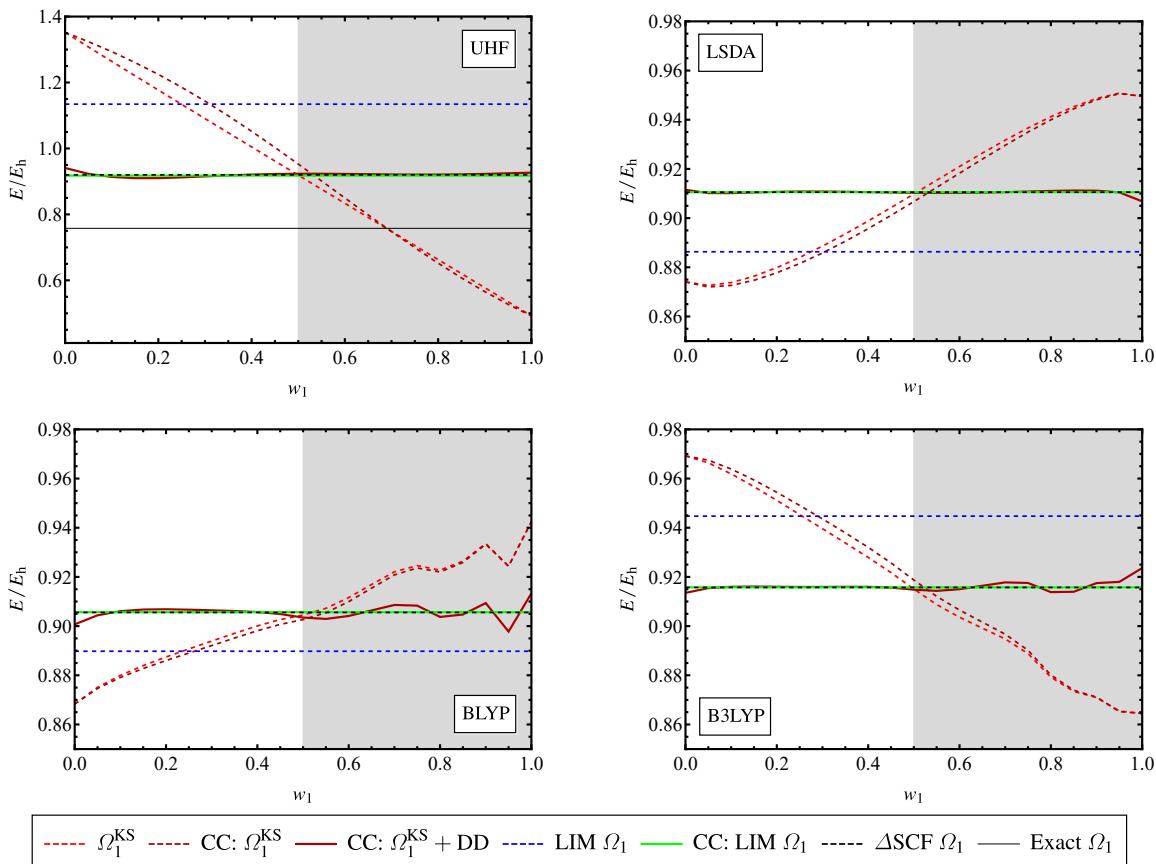


Figure E.6: Variation de l'énergie d'excitation simple la plus basse de He en fonction de la variation du poids de l'ensemble, obtenue à partir du bienensemble GOK "simple". Les énergies Kohn-Sham d'excitation fournies par les fonctionnelles standards indépendantes du poids et leurs analogues CC dépendantes du poids sont reportées. Les énergies d'excitation simples complètes, incluant les contributions supplémentaires "DD" venant des dérivées des fonctionnelles CC par rapport aux poids, sont également reportées. À titre de comparaison, les prédictions LIM des approximations indépendantes et dépendantes du poids sont également reportées. Enfin, les énergies d'excitation simple ΔSCF obtenues avec le même niveau d'approximation sont reportées ainsi que l'énergie d'excitation simple exacte. Les calculs ont été effectués dans la base cc-pVQZ avec diverses méthodes et niveaux d'approximations.

Le formalisme N -centré pour les excitations électroniques chargées

Bien que la DFT soit aujourd'hui largement applicable à une grande variété de systèmes à plusieurs électrons, principalement du fait des efforts considérables qui ont été consacrés à la conception d'un large panel d'approximations, et bien qu'elle se soit imposée au cours des dernières décennies comme une méthode fiable et relativement facile à mettre en oeuvre avec un coût de calcul relativement faible dans de nombreux domaines scientifiques tels que la physique, la chimie et la science des matériaux, elle souffre encore néanmoins de certaines limi-

tations conséquentes. En effet, il existe encore quelques quantités spécifiques dont l'extraction directe depuis des quantités Kohn-Sham (KS) obtenues par un calcul DFT ne parvient pas à atteindre une précision satisfaisante par rapport aux références expérimentales de ces mêmes quantités physiques. Par exemple, les potentiels d'ionisation, les affinités électroniques et, par construction, les gaps fondamentaux sont quelques exemples de propriétés qui demeurent insaisissables du fait qu'elles soient mal prédites par les quantités Kohn-Sham résultant d'un calcul DFT. Cependant, ces quantités peuvent toujours être évaluées au moyen de la méthode Δ SCF sous la forme de différences d'énergies totales des états fondamentaux des différentes espèces neutres, anioniques et cationiques. En fait, ces propriétés physiques résultant de processus impliquant une altération du nombre total d'électrons du système d'intérêt peuvent s'avérer assez difficiles à calculer dans certaines situations. Par exemple, dans le cas de systèmes périodiques, tels que les solides cristallins, induire une variation du nombre total d'électrons de l'édifice cristallin constitue une difficulté supplémentaire à surmonter en raison du caractère périodique de tels systèmes. En effet, en raison des conditions aux limites périodiques, un changement infinitésimal de la charge d'une cellule primitive impliquerait un changement identique dans chaque réplique de la cellule primitive, entraînant ainsi une variation infinie du nombre total d'électrons de l'ensemble du système. D'où la nécessité de surmonter cette difficulté technique et de trouver une alternative pour extraire les excitations chargées tels que les gaps fondamentaux basés sur des quantités résultant de calculs faisant uniquement intervenir le système neutre, sans qu'il soit impératif de faire varier la charge totale du système. Bien sûr, de nombreux efforts ont été fournis jusqu'à présent pour améliorer la précision des prévisions des gaps fondamentaux fournis par les fonctionnelles semi-locales conventionnelles dans le cadre de la KS-DFT. Par exemple, l'utilisation de la fonctionnelle d'échange exact (EXX) combinée au potentiel effectif optimisé (OEP) pour restaurer la fameuse dérivée discontinue manquante des fonctionnelles approchées standard ou encore la possibilité d'aller au-delà du cadre Kohn-Sham et de recourir plutôt au formalisme Kohn-Sham généralisé (GKS), où le système d'électrons en interaction est associé à un système fictif en interaction mais qui peut néanmoins être décrit par un unique déterminant de Slater et associé à un opérateur non local dépendant des orbitales. Bien que le cadre GKS ait permis une amélioration significative de la prédiction des gaps fondamentaux de solides par rapport au schéma KS standard, pour les systèmes de taille finie, comme les atomes et les molécules, elle reste malheureusement inefficace en raison de son incapacité à prendre en compte suffisamment de contributions d'échange à longue distance.

Une autre alternative, suggérée par Kraisler et Kronik, consisterait en une généralisation à l'aide d'un formalisme d'ensemble des termes de Hartree, d'échange et de corrélation. Néanmoins, une idée très intéressante serait de pouvoir extraire des énergies d'excitation chargées à l'aide d'une approche fondée sur les premiers principes et qui ne nécessiterait qu'un faible coût de calcul de type DFT et l'utilisation exclusive de grandeurs associées au système neutre, évitant ainsi toute altération du nombre d'électrons, ce qui le rendrait largement applicable à des systèmes finis ou périodiques. Dans ce chapitre, nous avons étudié une reformulation canonique exacte du problème du gap fondamental en DFT et nous l'avons mise en pratique dans le cadre de systèmes atomiques simples.

Tout récemment, Senjean et Fromager ont introduit le concept d'ensembles N -centrés pour obtenir des descriptions précises des processus d'excitation chargée à travers un formalisme canonique qui maintient constant artificiellement le nombre total d'électrons du système et égal à une valeur entière spécifique dans le cadre de la DFT d'ensemble (eDFT). Contrairement à l'approche grand canonique standard PPLB où le nombre d'électrons du système physique ouvert est censé varier de manière continue, ce qui engendre un saut discontinu du potentiel exact d'échange-corrélation, connu sous le nom de dérivée discontinue, à chaque franchissement d'un nombre entier d'électrons, dans le cadre canonique N -centré, le potentiel exact d'xc n'est pas astreint à présenter une telle discontinuité.

Par conséquent, bien que l'absence de dérivée discontinue dans les approximations de l'énergie d'xc couramment utilisées soit très préjudiciable pour la prédiction précise des excitations chargées telles que le gap fondamental en PPLB-DFT standard et entraîne souvent des erreurs conséquentes, en DFT d'ensemble N -centrée, cela reste sans conséquence et la capacité des fonctionnelles approchées à produire des prédictions suffisamment précises pour les excitations chargées sera plutôt du fait de la dépendance explicite au poids de l'ensemble de ces fonctionnelles.

Dans ce chapitre, nous avons exploré différents choix d'ensembles N -centrés dans le but de décrire les propriétés résultant des fluctuations de charge autour du nombre entier central d'électrons N d'un système atomique neutre.

En cela, nous avons commencé par étudier les ensembles N -centrés "gauche" ($-$) et "droit" ($+$) de densités et d'énergies d'ensemble

$$n^{\xi^\pm}(\mathbf{r}) = (1 - \alpha)n_0^N(\mathbf{r}) + \frac{N\alpha}{N \pm 1}n_0^{N\pm 1}(\mathbf{r}) \quad \left| \quad E^{\xi^\pm} = (1 - \alpha)E_0^N + \frac{N\alpha}{N \pm 1}E_0^{N\pm 1}, \quad (\text{E.19}) \right.$$

qui permettent d'extraire respectivement le potentiel d'ionisation et l'affinité électronique d'un système électronique selon

$$I_0^N = -\bar{\varepsilon}_N^{\xi^-} - \frac{1}{N}(1 - \alpha - N) \frac{\partial E_{\text{Hxc}}^{\xi^-}}{\partial \alpha} \Bigg|_{n_{\text{KS}}^{\xi^-}} \quad \left| \quad A_0^N = -\bar{\varepsilon}_{N+1}^{\xi^+} - \frac{1}{N}(1 - \alpha + N) \frac{\partial E_{\text{Hxc}}^{\xi^+}}{\partial \alpha} \Bigg|_{n_{\text{KS}}^{\xi^+}}. \quad (\text{E.21}) \right.$$

Dans la théorie exacte, les énergies d'ensemble exactes N -centrées, que l'on obtiendrait avec la fonctionnelle exacte, devraient être parfaitement linéaires par rapport au poids de l'ensemble, et donc du nombre d'électrons du système ouvert réel \mathcal{N} .

Contrairement aux énergies d'ensemble PPLB exactes qui doivent produire les énergies exactes des états fondamentaux des systèmes neutre et cationique (ou anionique) lorsque $\alpha = 0$ et $\alpha = 1$, respectivement, les énergies d'ensemble N -centrées exactes doivent correspondre à l'énergie exacte de l'état fondamental du système à N -électrons pour la configuration de poids $\alpha = 0$ mais doivent correspondre à des fractions spécifiques, préétablies par les fac-

teurs d'échelle des poids N -centrés, des énergies exactes des états fondamentaux des systèmes cationique ou anionique lorsque $\alpha = 1$. Ainsi, selon la théorie exacte, l'énergie d'ensemble N -centrée doit vérifier

$$E_0^{\xi^\pm=0} = E_0^N \quad (\text{E.22}) \quad \left| \quad E_0^{\xi^\pm=\frac{N}{N\pm 1}} = \frac{N}{N\pm 1} E_0^{N\pm 1}. \quad (\text{E.23})$$

Dans la théorie PPLB-DFT, nous avons vu que l'utilisation de fonctionnelles d'xc approchées à la place de la fonctionnelle exacte inconnue engendre deux conséquences : l'obtention d'énergies approchées des états fondamentaux des systèmes neutre et cationique (ou anionique), lorsque $\alpha = 0$ et $\alpha = 1$, respectivement, et une courbure supplémentaire dans l'énergie d'ensemble obtenue pour toute autre configuration de poids, $0 < \alpha < 1$. Les énergies d'ensemble PPLB et N -centrées "gauche" de l'atome de lithium obtenues avec différents niveaux d'approximation sont reportées dans la Figure E.7 à des fins d'illustration.

En N -centré, des observations similaires peuvent être faites. Pour une fonctionnelle approchée donnée, l'énergie d'ensemble N -centrée obtenue présentera une courbure additionnelle mais, surtout, elle présentera une déviation conséquente de sa valeur finale théorique qui devrait théoriquement être égale à une fraction spécifique de l'énergie de l'état fondamental du système cationique (ou anionique) obtenue en DFT standard avec le même niveau d'approximation, comme illustré sur la Figure E.7. Par conséquent, lorsqu'une fonctionnelle approchée (DFA) est utilisée à la place de la fonctionnelle exacte, l'énergie d'ensemble N -centrée résultante présentera les propriétés suivantes

$$E^{\text{DFA}, \xi^\pm=0} = E_0^{N, \text{DFA}} \quad (\text{E.24}) \quad \left| \quad E^{\text{DFA}, \xi^\pm=\frac{N}{N\pm 1}} \neq \frac{N}{N\pm 1} E_0^{N\pm 1, \text{DFA}}. \quad (\text{E.25})$$

Cette déviation parasite peut s'expliquer par le fait que la plupart des fonctionnelles approchées s'avèrent ne pas être des opérations linéaires par rapport à la quantité à laquelle elles s'appliquent, la densité électronique par exemple. En effet, lorsque $\alpha = 1$, en raison du facteur d'échelle multiplicatif $\frac{N}{N\pm 1}$, les densités d'ensemble N -centrée "gauche" et "droite" ne se réduisent pas à une simple densité d'état fondamental et du fait de la non-linéarité de la fonctionnelle approchée, l'application d'une fonctionnelle non linéaire à une densité à laquelle est appliqué un facteur multiplicatif ne résulte pas en l'application de ce même facteur à l'énergie associée à cette densité, comme cela serait le cas si la fonctionnelle était linéaire,

$$E^{\text{DFA}, \xi^\pm} \left[\frac{N}{N\pm 1} n \right] \neq \frac{N}{N\pm 1} E^{\text{DFA}, \xi^\pm} [n]. \quad (\text{E.26})$$

En conséquence, la qualité des prédictions d'énergies fondamentales et d'énergies d'excitation chargée obtenues par des calculs d'eDFT N -centrée "gauche" et "droite" vont s'avérer fortement impactées par ces considérations, comme illustré dans la Figure E.8.

Là encore, la construction et le recours à des fonctionnelles approchées explicitement dépendantes

du poids de l'ensemble peuvent permettre de corriger et d'améliorer la qualité des estimations des grandeurs physiques calculées.

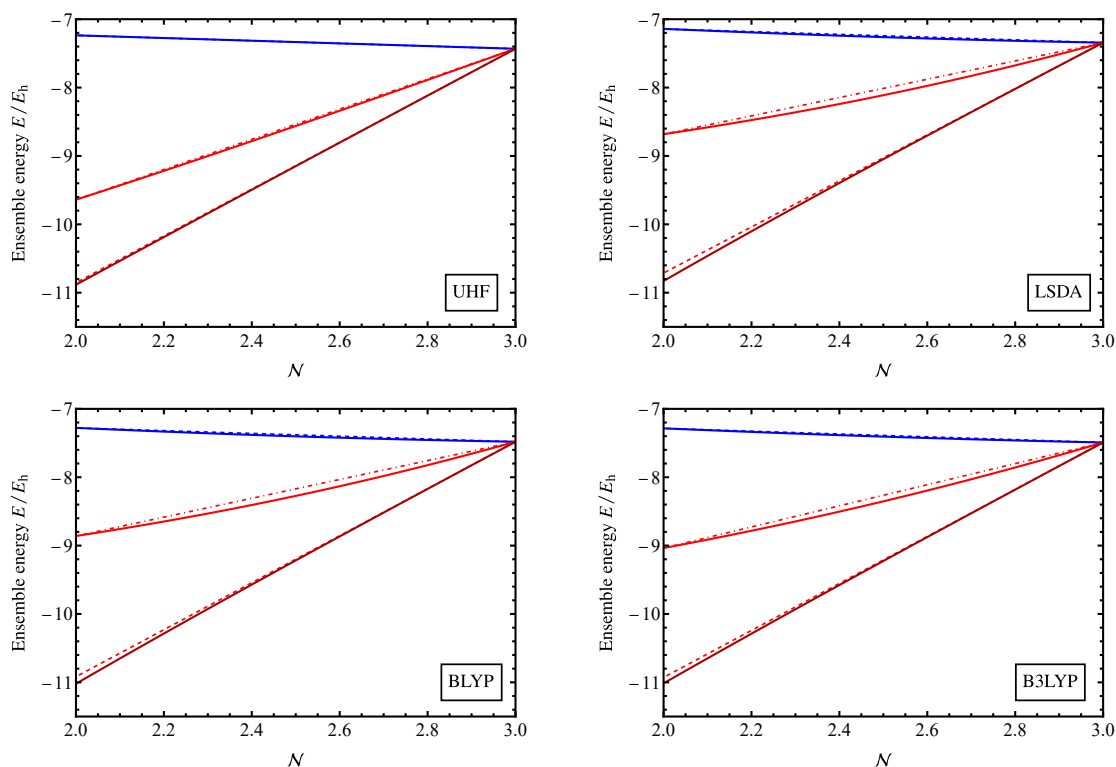


Figure E.7: Comparaison entre les énergies d'ensemble PPLB "gauche" (trait continu bleu) et N -centrée "gauche" (trait continu rouge) de Li obtenues avec des fonctionnelles d'xc standard indépendantes du poids dans la base cc-pVDZ. Les interpolations linéaires des énergies d'ensemble PPLB (trait discontinu bleu) et N -centrées (trait mixte rouge) mettent en évidence la courbure supplémentaire résultant de l'utilisation de fonctionnelles approchées indépendantes du poids ainsi que la déviation finale de l'énergie d'ensemble N -centrée par rapport à sa valeur théorique (trait discontinu rouge). Pour chaque niveau d'approximation, l'énergie d'ensemble N -centrée "gauche" obtenue avec la fonctionnelle CC correspondante dépendante du poids est également indiquée (trait continu rouge foncé).

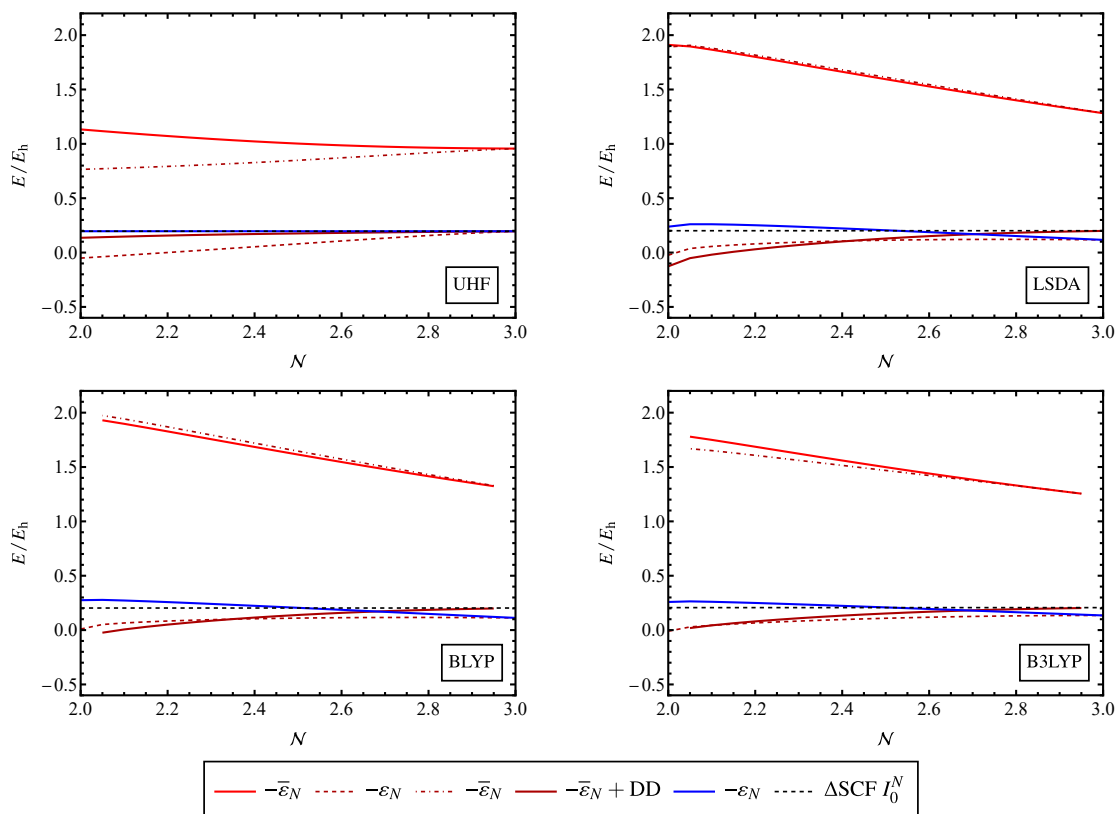


Figure E.8: Variation du potentiel d’ionisation de Li en fonction du nombre fractionnaire d’électrons du système ouvert, extrait à partir d’un ensemble PPLB “gauche” et d’un ensemble N -centré “gauche” avec diverses fonctionnelles d’échange-corrélation indépendantes et dépendantes du poids de l’ensemble dans la base cc-pVDZ. Pour chaque approximation indépendante du poids, l’opposé de l’énergie HOMO PPLB dépendante du poids (trait continu bleu) du système neutre est reporté, de même que l’opposé de l’énergie HOMO N -centrée LZ-shiftée (trait continu rouge). L’opposé des énergies HOMO N -centrée non shiftée (trait discontinu rouge foncé) et shiftée (trait mixte rouge foncé) obtenues avec des fonctionnelles CC d’xc explicitement dépendantes du poids sont également reportées à des fins de comparaison. Enfin, la prédiction complète du potentiel d’ionisation (trait continu rouge foncé) incluant la contribution additionnelle de la dérivée (DD) de la fonctionnelle CC par rapport au poids de l’ensemble est également reportée. Les potentiels d’ionisation obtenus par la méthode Δ SCF (trait discontinu noir) pour chaque approximation standard indépendante du poids sont également reportés à des fins de comparaison.

Enfin, d’autres types d’ensemble N -centrés ont également été étudiés et mis en pratique, parmi lesquels le triensemble à poids unique

$$E^\xi = (1 - 2\xi)E_0^N + \xi E_0^{N-1} + \xi E_0^{N+1}, \quad (\text{E.27})$$

avec $0 \leq \xi \leq 0.5$. Cet ensemble N -centré à trois états possède la particularité de permettre une extraction directe du gap fondamental du système à N électrons en un unique calcul

selon l'expression suivante

$$\Omega_0^N = \frac{dE^\xi}{d\xi} = \varepsilon_{N+1}^\xi - \varepsilon_N^\xi + \left. \frac{\partial E_{\text{Hxc}}^\xi}{\partial \xi} \right|_{n_{\text{KS}}^\xi}. \quad (\text{E.28})$$

Encore très récemment, des travaux ont été réalisés afin de bénéficier de la forte analogie entre les formalismes de GOK-DFT et d'eDFT N -centrée en concevant des ensembles hybrides GOK/ N -centré qui incorporeraient à la fois des états à N électrons excités neutralement et des états excités résultant d'excitations chargées. De tels ensembles permettraient ainsi l'extraction simultanée d'énergies d'excitation chargée et neutre à partir d'un unique calcul de DFT d'ensemble. Ces ensembles, proposés par Fromager et al., sont appelés ensembles N -centrés étendus.

$$E^{\eta=\{\alpha,w\}} = (1 - \alpha - w)E_0^N + \frac{N\alpha}{N-1}E_0^{N-1} + wE_1^N, \quad (\text{E.29})$$

Les erreurs de charge et spin fractionnaires et leurs implications dans les processus de dissociation asymptotiques

Le succès indéniable de la DFT est dû, dans une très large mesure, à la possibilité de recourir à des fonctionnelles d'échange-corrélation approchées compte tenu du fait que la fonctionnelle exacte demeure inconnue et hors de portée. Paradoxalement, la nature approchée des fonctionnelles utilisées en pratique est également responsable de certaines des défaillances les plus massives des calculs de DFT. Il est intéressant de noter que de telles défaillances ne sont pas exclusives aux systèmes électroniques à grand nombre d'électrons ou complexes ou encore à une classe donnée d'approximations, mais il s'agit en réalité d'erreurs systématiques assez conséquentes qui se produisent même lors de la description de systèmes les plus élémentaires présentant un ou deux électrons, que ce soit avec le niveau d'approximation le plus simple ou le plus élaboré.

Par exemple, l'incapacité des fonctionnelles approchées à respecter la condition exacte de linéarité par morceaux de l'énergie des systèmes à charge fractionnaire a été formalisée par le concept d'erreurs de localisation et de délocalisation (ou erreurs de charge fractionnaire) et s'est avéré être responsable d'une grande partie des déviations des propriétés calculées en DFT par rapport aux résultats expérimentaux, telles que les prédictions de bande interdite ou les limites de dissociation. Quant à la violation de la condition de constance pour les spins fractionnaires, elle a donné lieu à l'erreur de corrélation statique (ou erreur de spin fractionnaire) et reflète l'incapacité d'une fonctionnelle approchée à décrire correctement les systèmes possédant des états fondamentaux dégénérés associés à différentes configurations de spin. La corrélation statique (ou corrélation forte) englobe les situations où l'utilisation d'un unique déterminant, telles que les théories Hartree-Fock et KS-DFT, ne parvient pas à fournir une description appropriée de la matière et des comportements quantiques. Les

erreurs de corrélation statique se sont révélées significatives dans les situations impliquant des dégénérescences et quasi-dégénérescences, dans des systèmes dits fortement corrélés où les interactions électroniques sont particulièrement difficiles à décrire, ou dans des situations de rupture de liaisons chimiques. Il a été observé que la plupart des méthodes présentant de petites erreurs de charge fractionnaire ont paradoxalement tendance à générer de grandes erreurs de spin fractionnaire, et vice-versa. Par exemple, alors que l'ordre 2 de la théorie des perturbations de Møller-Plesset (MP2) fournit de très faibles erreurs de charge fractionnaire, elle présente également des erreurs de spin fractionnaire infinies. Ainsi l'élaboration d'une méthode ou d'une approximation qui permettrait de fournir à la fois des erreurs marginales pour la description des deux concepts de charge fractionnaire et de spin fractionnaire constitue encore aujourd'hui un véritable défi pour les calculs de structures électroniques.

Les concepts de charge fractionnaire et de spin fractionnaire et leurs implications formelles et pratiques sur les systèmes réels ont été largement étudiés par Mori-Sánchez, Cohen et Yang dont les travaux ont fourni des informations éclairantes sur la nature intrinsèque de certaines erreurs systématiques massives des fonctionnelles d'xc approchées dans le cadre des théories HF et KS-DFT. De plus, ils sont parvenu à proposer une formulation unifiée de ces deux concepts conduisant à la condition de "plan plat" que doit respecter l'énergie exacte des systèmes électroniques présentant à la fois des charges fractionnaires et des spins fractionnaires. Ces considérations peuvent s'avérer essentielles au développement futur de la DFT et à l'élaboration d'une nouvelle gamme de fonctionnelles approchées qui permettraient de pallier à ces deux erreurs fondamentales.

L'erreur de charge fractionnaire

Une conséquence concrète du principe de "préférence entière", énoncé par Perdew, est que, lors de l'étirement d'une molécule électriquement neutre celle-ci doit se dissocier en un ensemble d'atomes neutres possédant un nombre entier d'électrons sur chacun. En pratique, de nombreuses approximations échouent à obéir à cette propriété exacte très simple et prédisent à tort que les systèmes moléculaires à plusieurs électrons se dissocient en des fragments possédant des charges fractionnaires. Cette dissociation asymptotique fractionnaire bien que dépourvue de réalité physique s'avère avoir des implications très concrètes.

D'un point de vue énergétique, cela signifie qu'avec les DFAs, un minimum global non physique de l'énergie totale du système dissocié est atteint lorsque la charge totale est délocalisée sur les divers fragments dissociés. Ce résultat erroné découle de l'incapacité des approximations standards à fournir des descriptions appropriées des processus de transfert de charge, aussi bien pour les systèmes moléculaires que pour les systèmes de l'état solide. Il s'agit d'une conséquence directe de la violation de la condition exacte de linéarité par morceaux de l'énergie, qui a été formalisée en termes d'erreurs de localisation et de délocalisation des fonctionnelles approchées. De nombreux systèmes et approximations sont connus pour présenter un tel comportement erroné, décrivant des atomes bien séparés mais avec un nombre fractionnaire d'électrons sur chacun.

En nous inspirant des travaux de Kraisler et Kronik, nous avons abordé le problème de

dissociation asymptotique fractionnaire en employant à la fois les approximations standard indépendantes du poids de la DFT ainsi que nos fonctionnelles CC explicitement dépendantes du poids et conçues pour le formalisme PPLB. En rétablissant la linéarité par morceaux de l'énergie des fragments dissociés, les fonctionnelles CC dépendantes du poids pourraient être en mesure d'empêcher les transferts de charge parasites entre les atomes bien séparés et de fournir des descriptions appropriées des limites de dissociation des systèmes moléculaires. L'énergie totale d'un tel système dissocié est dictée par un autre principe exact, le principe de "séparabilité" qui stipule que l'énergie totale d'un système composé de sous-systèmes bien séparés peut être obtenue par sommation des énergies des composés sous-jacents. En conséquence, l'énergie totale d'une molécule diatomique neutre parfaitement dissociée est donnée par

$$E_{A\dots B}(q) = E_A(N_A + q) + E_B(N_B - q). \quad (\text{E.30})$$

Ainsi, dans le cas du système modèle diatomique AB , les configurations $q = -1$, $q = 0$ et $q = 1$ correspondent aux fragments dissociés $A^+ \dots B^-$, $A \dots B$ et $A^- \dots B^+$, respectivement.

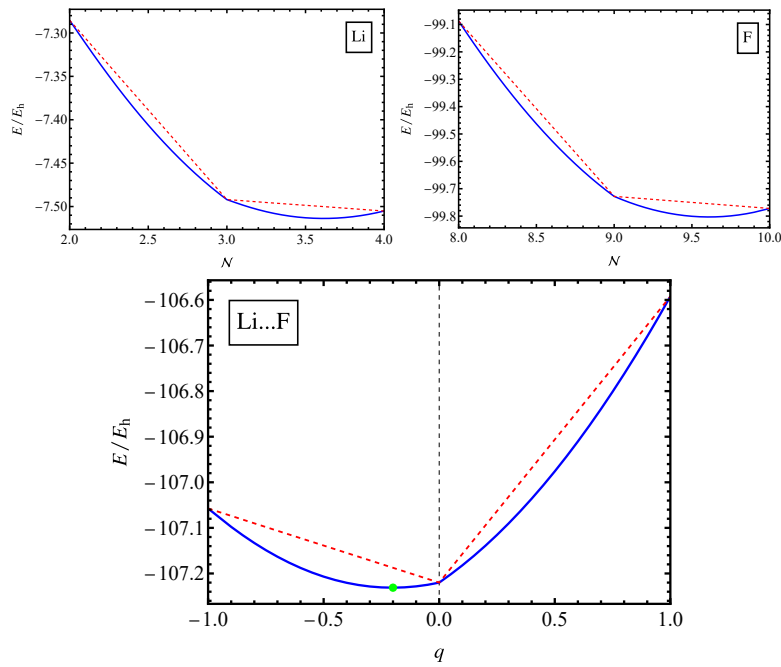


Figure E.9: Énergie $E(\mathcal{N})$ en fonction de la variation du nombre fractionnaire d'électrons \mathcal{N} pour Li (Figure en haut à gauche) et F (Figure en haut à droite) et limite de dissociation $E(q)$ en fonction de la charge fractionnaire q pour Li...F (Figure du bas), avec B3LYP (trait continu bleu) et CC-B3LYP (trait discontinu rouge) dans la base cc-pVDZ. Le point vert met en évidence le minimum parasite non physique de l'énergie obtenue par les approximations standard de DFT.

Nous avons ainsi effectué des calculs auto-cohérents de DFT d'ensemble de type PPLB pour un petit ensemble de systèmes atomiques avec différents niveaux d'approximation afin d'obtenir les courbes d'énergie des systèmes atomiques $E(\mathcal{N})$ en fonction de la variation continue du nombre d'électrons \mathcal{N} , ces courbes étant nécessaires à la construction de l'équation

(E.30). Par sommation de ces énergies atomiques, nous avons pu reconstruire les limites de dissociation d’un petit ensemble de molécules diatomiques telles que LiF, CF et FH, comme le montre la Figure E.9.

Dans le cas de la dissociation de la molécule LiF, la fonctionnelle d’xc B3LYP indépendante du poids produit une courbe d’énergie convexe avec un minimum d’énergie parasite placé en $q = -0,20$. En revanche, la fonctionnelle d’xc dépendante du poids CC-B3LYP parvient elle à produire une énergie beaucoup plus en accord avec la condition exacte de linéarité par morceaux et possède un minimum correct localisé en $q = 0$, fournissant ainsi une description physiquement conforme du processus de dissociation de la molécule.

L’erreur de spin fractionnaire

Contrairement aux électrons possédant un spin dit “pur”, les électrons à spin fractionnaire sont associés à des configurations de spin non physiques, $-\frac{1}{2} < m_s < \frac{1}{2}$.



Figure E.10: Illustration de diverses configurations fractionnaires du spin d’un électron ($-\frac{1}{2} < m_s < \frac{1}{2}$) vérifiant la conservation de la norme du spin total.

Il se trouve que la densité électronique d’un électron à spin fractionnaire peut être modélisée à l’aide d’un formalisme d’ensemble. En effet, en mélangeant des densités électroniques de spin “up”, $n^\alpha(\mathbf{r})$, et de spin “down”, $n^\beta(\mathbf{r})$, associées à des poids spécifiques et complémentaires dans l’ensemble, $(1-w)$ et w , respectivement, il est possible d’obtenir une densité d’ensemble à deux états qui permet la description et l’étude d’un tel système électronique non conventionnel

$$n^w(\mathbf{r}) = (1-w)n^\alpha(\mathbf{r}) + wn^\beta(\mathbf{r}), \quad (\text{E.31})$$

avec le poids de l’ensemble vérifiant la condition $0 \leq w \leq 1$.

De manière analogue à la condition exacte de linéarité par morceaux de l’énergie pour les systèmes ouverts, Cohen, Mori-Sánchez et Yang ont prouvé l’existence d’une autre condition exacte qui devrait être satisfaite par les fonctionnelles d’échange-corrélation dans le cadre du calcul d’énergie des systèmes à spin fractionnaire. Cette condition exacte, connue sous le nom de “condition de constance” pour les spins fractionnaires, s’applique notamment aux systèmes possédant des états fondamentaux dégénérés en énergie associés à différentes configurations de spin et indique que, pour un système donné à un électron, toute configuration de spin fractionnaire doit être dégénérée en énergie avec les configurations associées à des spins “purs”.

En complète analogie avec l’erreur de délocalisation pour les charges fractionnaires, la déviation de l’énergie d’un système à spin fractionnaire par rapport à la condition exacte de constance avec une fonctionnelle approchée donnée est connue sous le nom d’erreur de spin fractionnaire

ou d'erreur de corrélation statique. En fait, de nombreuses méthodes de chimie quantique, parmi lesquelles la théorie de Hartree-Fock et la théorie de la fonctionnelle de la densité, échouent à livrer une description et des énergies conformes à la condition exacte de constance pour les systèmes à spin fractionnaire, même dans le cas des systèmes les plus simples, comme illustré dans la Figure E.11.

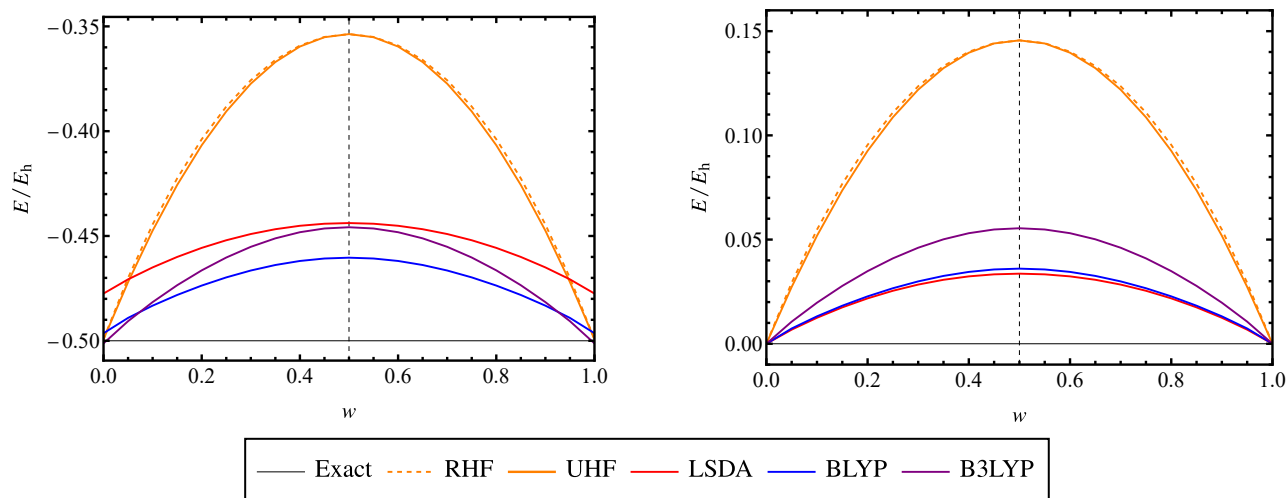


Figure E.11: Énergies d'ensemble (Figure de gauche) et erreurs de spin fractionnaire (Figure de droite) de l'atome d'hydrogène obtenues avec les formalismes "restricted" et "unrestricted" d'Hartree-Fock ainsi qu'avec diverses fonctionnelles "unrestricted" standard de DFT, calculées dans la base cc-pVDZ.

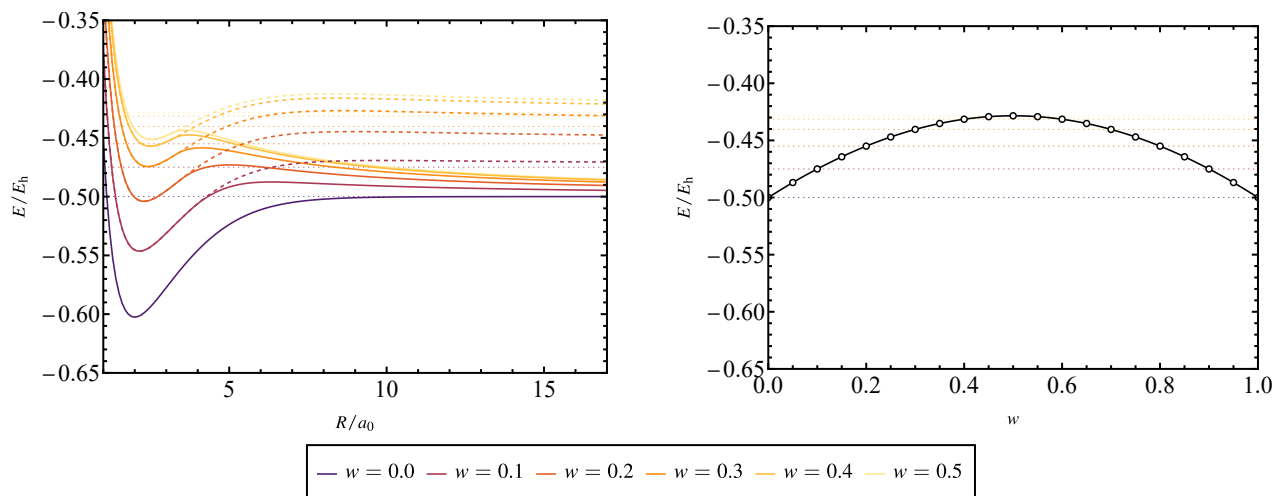


Figure E.12: Énergies restrictées (traits discontinus) et unrestrictées (traits continus) de H_2^+ en fonction de la longueur de liaison R pour diverses configurations de spin fractionnaire (Figure de gauche) et limites de dissociation restrictées (Figure droite) de H_2^+ avec un spin fractionnaire en fonction de la variation du poids de l'ensemble, au niveau Hartree-Fock dans la base cc-pVQZ. Pour toutes les configurations à spin fractionnaire considérées, les limites de dissociation de H_2^+ (traits pointillés) sont également indiquées.

Les calculs auto-cohérents de DFT d'ensemble mettent en lumière des défaillances significatives des fonctionnelles approchées dans le cas de systèmes à spin fractionnaire. Il faut noter que même les approximations et méthodes connues pour être exactes lorsque appliquées à l'atome d'hydrogène avec un spin pur, tel que la méthode d'Hartree-Fock, souffrent d'erreurs importantes lorsque appliquées à des systèmes à spin fractionnaire.

Dans un deuxième temps, nous avons choisi d'étudier le comportement d'un système moléculaire à un électron avec un spin fractionnaire lors de sa dissociation au niveau HF. En fait, il a été démontré que l'erreur de dissociation de certaines molécules étirées était une conséquence directe de l'incapacité des fonctionnelles approchées à satisfaire la condition exacte de constance pour les spins fractionnaires, comme illustré dans la Figure E.12 .

Conclusion

Divers formalismes d'ensemble ont été très largement discutés tout au long de cette thèse à travers les formalismes de de Hartree-Fock et de la théorie de la fonctionnelle de la densité. La performance des méthodes basées sur la densité d'ensemble en tant que variable de base a été étudiée dans le cadre de la prédiction des énergies d'excitation chargée et neutre.

En particulier, la généralisation du formalisme KS-DFT aux états fondamentaux électroniques avec des nombres d'occupation fractionnaires, la PPLB-DFT, a été étudiée en utilisant le formalisme d'ensemble pour décrire le comportement de l'énergie de l'état fondamental d'un système ouvert en fonction de la variation continue du nombre d'électrons. Dans ce contexte, les énergies d'ensemble PPLB ont été calculées de manière auto-cohérente afin d'extraire des potentiels d'ionisation et affinités électroniques de systèmes atomiques simples avec les approximations standard d'échange-corrélation indépendantes du poids. Cela a mis en évidence l'incapacité des approximations standard à reproduire la fameuse dérivée discontinue du potentiel exact, et par la même occasion d'obéir à la condition exacte de linéarité par morceaux de l'énergie totale d'un système ouvert, avec des implications massives sur les prévisions de bande interdite. Le problème du gap fondamental a été adressé de même que la possibilité de recourir à des approximations explicitement dépendantes du poids de l'ensemble pour reproduire la fameuse dérivée discontinue à travers leurs dérivées. Cela, afin de restaurer la condition exacte de linéarité par morceaux de l'énergie et d'obtenir des prédictions plus satisfaisants pour les propriétés physiques du système.

La deuxième question sur laquelle nous nous sommes concentrés était de savoir dans quelle mesure la DFT pouvait permettre d'accéder aux états excités neutralement à travers sa formulation d'ensemble exacte et indépendante du temps, la GOK-DFT. À cet égard, nous avons considéré divers ensembles GOK à deux et trois états, intentionnellement conçus pour extraire les énergies d'excitation simples et doubles de systèmes à deux électrons. La courbure des énergies d'ensemble GOK a ainsi été étudiée ainsi que la construction de fonctionnelles d'échange-corrélation dépendantes du poids destinées à corriger cette courbure. Dans ce contexte, les énergies d'excitation ont été extraites des ensembles GOK de diverses manières :

par différenciation des énergies d'ensembles GOK par rapport aux poids des ensembles, pour diverses valeurs de poids des ensembles, ou encore en utilisant la méthode d'interpolation linéaire.

Dans ce travail, l'utilisation d'approximations dépendantes du poids de l'ensemble n'a été discutée que dans le cadre d'ensembles élémentaires, néanmoins, nous pensons qu'explorer des ensembles plus sophistiqués, incluant un plus grand nombre d'états et de poids, ainsi que le développement d'approximations d'xc basées sur de multiples dépendances en poids pourraient permettre de transformer la GOK-DFT en une méthode plus couramment utilisée pour le calcul d'états excités neutralement et les énergies d'excitation neutres associées. Dans ce contexte, les approximations standard de la DFT pour les états fondamentaux pourraient servir de points de départ dans le développement futur d'approximations dépendantes du poids, spécifiquement conçues pour des applications sur les ensembles d'états. En effet, très récemment, des conditions exactes spécifiques aux fonctionnelles d'ensemble ont été démontrées ont livré des informations cruciales et très instructives à ce sujet.

Le problème du gap fondamental a ensuite été abordé à travers sa récente reformulation canonique proposée par Senjean et Fromager, dans laquelle la difficulté de reproduire la fameuse dérivée discontinue du potentiel exact est entièrement transposée dans la modélisation de la dépendance en poids de la fonctionnelle H_{xc} , offrant ainsi une formulation unifiée, indépendante du temps et en principe exacte de DFT d'ensemble plus les excitations chargées et neutres. Des calculs auto-cohérents d'ensembles N -centrés ont ainsi été réalisés afin d'extraire les potentiels d'ionisation et les affinités électroniques de systèmes réels. De même, les formulations N -centrées originales à deux poids distincts et à poids unique, spécialement conçues pour l'extraction directe de gaps fondamentaux ont également été étudiées. Les Courbures et déviations des énergies d'ensemble N -centrées par rapport aux valeurs théoriques, obtenues avec des approximations standard de DFT indépendantes du poids ont été mises en lumière, révélant l'impact néfaste de la non linéarité des fonctionnelles approchées. Face à cette problématique, nous avons montré dans quelle mesure les approximations explicitement dépendantes du poids de l'ensemble pouvaient bénéficier de leurs dérivées pour pallier aux limitations des approximations standard et pour fournir des prévisions plus satisfaisantes pour les propriétés physiques obtenues par un calcul de DFT d'ensemble. Enfin, des ensembles hybrides GOK/ N -centré récemment développés et permettant l'extraction d'énergies d'excitation chargée et neutre à partir d'un même calcul auto-cohérent de type DFT, ont également été étudiés et appliqués à des systèmes réels à deux électrons.

La dernière problématique que nous avons choisi d'aborder dans cette thèse concerne les erreurs liées à la description des charges fractionnaires et les erreurs de spin fractionnaire, qui proviennent de l'incapacité des approximations standard à obéir aux conditions exactes de linéarité par morceaux et de constance de l'énergie. Ainsi, nous avons montré que les erreurs de charge fractionnaire, également appelées erreurs de localisation et de délocalisation, peuvent avoir un impact significatif sur les prévisions de bande interdite et peuvent être responsables d'erreurs dans la description de processus de dissociation. Quant à l'erreur de

spin fractionnaire, ou erreur de corrélation statique, nous avons montré que même dans le cadre d'approximations connues pour être exactes pour les systèmes à un électron, telles que la théorie de Hartree-Fock, elles échouaient à fournir des descriptions physiquement pertinentes des systèmes à spin fractionnaire. Les approximations dépendantes du poids peuvent là encore fournir une alternative pour pallier à ces carences systématiques.

Au vu de ces considérations, nous pensons qu'il est nécessaire d'aller au-delà des approximations élaborées dans le cadre de la DFT pour les états fondamentaux, afin d'exploiter pleinement le potentiel de l'eDFT et d'en faire une méthode de calcul fiable et pertinente pour une large gamme d'applications. Dans cette optique, le développement de nouvelles classes de fonctionnelles approchées d'échange-corrélation incluant des dépendances explicites en poids de l'ensemble, et spécifiquement conçues pour les calculs d'ensemble mériterait d'être davantage étudié.

Bibliography

- [1] A. Kramida et al. NIST Atomic Spectra Database (ver. 5.10), [Online]. Available: <https://physics.nist.gov/asd> [2023, September 16]. National Institute of Standards and Technology, Gaithersburg, MD. 2022.
- [2] E. J. Baerends, O. V. Gritsenko, and R. van Meer. “The Kohn–Sham gap, the fundamental gap and the optical gap: the physical meaning of occupied and virtual Kohn–Sham orbital energies”. In: *Phys. Chem. Chem. Phys.* 15 (39 2013), pp. 16408–16425. DOI: [10.1039/C3CP52547C](https://doi.org/10.1039/C3CP52547C). URL: <http://dx.doi.org/10.1039/C3CP52547C>.
- [3] A. D. Becke. “Density-functional exchange-energy approximation with correct asymptotic behavior”. In: *Phys. Rev. A* 38 (6 Sept. 1988), pp. 3098–3100. DOI: [10.1103/PhysRevA.38.3098](https://doi.org/10.1103/PhysRevA.38.3098). URL: <https://link.aps.org/doi/10.1103/PhysRevA.38.3098>.
- [4] Axel D. Becke. “Density-functional thermochemistry. III. The role of exact exchange”. In: *The Journal of Chemical Physics* 98.7 (1993), pp. 5648–5652. DOI: [10.1063/1.464913](https://doi.org/10.1063/1.464913). eprint: <https://doi.org/10.1063/1.464913>. URL: <https://doi.org/10.1063/1.464913>.
- [5] Sonia Conesa Boj and Simon Groeblicher. *Bound and scattering states*. 2021. URL: https://qm1.quantumtinkerer.tudelft.nl/7_scattering_states/.
- [6] Alex Borgoo, Andy M. Teale, and Trygve Helgaker. “Excitation energies from ensemble DFT”. In: *AIP Conference Proceedings* 1702.1 (Dec. 2015). 090049. ISSN: 0094-243X. DOI: [10.1063/1.4938857](https://doi.org/10.1063/1.4938857). eprint: https://pubs.aip.org/aip/acp/article-pdf/doi/10.1063/1.4938857/12908246/090049_1_online.pdf. URL: <https://doi.org/10.1063/1.4938857>.
- [7] Jean-Luc Bredas. “Mind the gap!” In: *Mater. Horiz.* 1 (1 2014), pp. 17–19. DOI: [10.1039/C3MH00098B](https://doi.org/10.1039/C3MH00098B). URL: <http://dx.doi.org/10.1039/C3MH00098B>.
- [8] A Burgers, D Wintgen, and J -M Rest. “Highly doubly excited S states of the helium atom”. In: *Journal of Physics B: Atomic, Molecular and Optical Physics* 28 (1995), pp. 3163–3183. URL: <https://api.semanticscholar.org/CorpusID:250850579>.
- [9] K Burke. *The ABC of DFT*. Apr. 2007. URL: <https://dft.uci.edu/doc/g1.pdf>.

- [10] Hugh G. A. Burton et al. “Variations of the Hartree–Fock fractional-spin error for one electron”. In: *The Journal of Chemical Physics* 155.5 (Aug. 2021), p. 054107. ISSN: 0021-9606. DOI: [10.1063/5.0056968](https://doi.org/10.1063/5.0056968). eprint: https://pubs.aip.org/aip/jcp/article-pdf/doi/10.1063/5.0056968/14112752/054107\1\1_online.pdf. URL: <https://doi.org/10.1063/5.0056968>.
- [11] D. M. Ceperley and B. J. Alder. “Ground State of the Electron Gas by a Stochastic Method”. In: *Phys. Rev. Lett.* 45 (7 Aug. 1980), pp. 566–569. DOI: [10.1103/PhysRevLett.45.566](https://doi.org/10.1103/PhysRevLett.45.566). URL: <https://link.aps.org/doi/10.1103/PhysRevLett.45.566>.
- [12] Filip Cernatic et al. “Ensemble Density Functional Theory of Neutral and Charged Excitations”. In: *Topics in Current Chemistry* 380 (2021).
- [13] M. K. Y. Chan and G. Ceder. “Efficient Band Gap Prediction for Solids”. In: *Phys. Rev. Lett.* 105 (19 Nov. 2010), p. 196403. DOI: [10.1103/PhysRevLett.105.196403](https://doi.org/10.1103/PhysRevLett.105.196403). URL: <https://link.aps.org/doi/10.1103/PhysRevLett.105.196403>.
- [14] Aron J. Cohen, Paula Mori-Sánchez, and Weitao Yang. “Challenges for Density Functional Theory”. In: *Chemical Reviews* 112.1 (2012). PMID: 22191548, pp. 289–320. DOI: [10.1021/cr200107z](https://doi.org/10.1021/cr200107z). eprint: <https://doi.org/10.1021/cr200107z>. URL: <https://doi.org/10.1021/cr200107z>.
- [15] Aron J. Cohen, Paula Mori-Sánchez, and Weitao Yang. “Fractional spins and static correlation error in density functional theory”. In: *The Journal of Chemical Physics* 129.12 (Sept. 2008), p. 121104. ISSN: 0021-9606. DOI: [10.1063/1.2987202](https://doi.org/10.1063/1.2987202). eprint: https://pubs.aip.org/aip/jcp/article-pdf/doi/10.1063/1.2987202/15419668/121104\1\1_online.pdf. URL: <https://doi.org/10.1063/1.2987202>.
- [16] Aron J. Cohen, Paula Mori-Sánchez, and Weitao Yang. “Insights into Current Limitations of Density Functional Theory”. In: *Science* 321.5890 (2008), pp. 792–794. DOI: [10.1126/science.1158722](https://doi.org/10.1126/science.1158722). eprint: <https://www.science.org/doi/pdf/10.1126/science.1158722>. URL: <https://www.science.org/doi/abs/10.1126/science.1158722>.
- [17] Renato Colle and Oriano Salvetti. “Approximate calculation of the correlation energy for the closed shells”. In: *Theoretica chimica acta* 37 (1975), pp. 329–334.
- [18] Prof. C.A. Coulson and Miss I. Fischer. “XXXIV. Notes on the molecular orbital treatment of the hydrogen molecule”. In: *The London, Edinburgh, and Dublin Philosophical Magazine and Journal of Science* 40.303 (1949), pp. 386–393. DOI: [10.1080/14786444908521726](https://doi.org/10.1080/14786444908521726). eprint: <https://doi.org/10.1080/14786444908521726>. URL: <https://doi.org/10.1080/14786444908521726>.
- [19] CRC Handbook. *CRC Handbook of Chemistry and Physics, 85th Edition*. Ed. by David R. Lide. 85th ed. CRC Press, 2004. ISBN: 0849304881. URL: <https://hcbp.chemnetbase.com/>.

-
- [20] Killian Deur and Emmanuel Fromager. “Ground and excited energy levels can be extracted exactly from a single ensemble density-functional theory calculation”. In: *The Journal of Chemical Physics* 150.9 (2019), p. 094106. DOI: [10.1063/1.5084312](https://doi.org/10.1063/1.5084312). eprint: <https://doi.org/10.1063/1.5084312>. URL: <https://doi.org/10.1063/1.5084312>.
- [21] Killian Deur et al. “Exploring weight-dependent density-functional approximations for ensembles in the Hubbard dimer”. In: *The European Physical Journal B* 91 (Mar. 2018). DOI: [10.1140/epjb/e2018-90124-7](https://doi.org/10.1140/epjb/e2018-90124-7).
- [22] P. A. M. Dirac. “Note on Exchange Phenomena in the Thomas Atom”. In: *Mathematical Proceedings of the Cambridge Philosophical Society* 26.3 (1930), pp. 376–385. DOI: [10.1017/S03050004100016108](https://doi.org/10.1017/S03050004100016108).
- [23] V. Fock. “Näherungsmethode zur Lösung des quantenmechanischen Mehrkörperproblems”. In: *Zeitschrift für Physik* 61.1-2 (Jan. 1930), pp. 126–148. DOI: [10.1007/BF01340294](https://doi.org/10.1007/BF01340294).
- [24] Emmanuel Fromager. “Individual Correlations in Ensemble Density Functional Theory: State- and Density-Driven Decompositions without Additional Kohn-Sham Systems”. In: *Phys. Rev. Lett.* 124 (24 June 2020), p. 243001. DOI: [10.1103/PhysRevLett.124.243001](https://doi.org/10.1103/PhysRevLett.124.243001). URL: <https://link.aps.org/doi/10.1103/PhysRevLett.124.243001>.
- [25] Hideo Fukutome. “Unrestricted Hartree–Fock theory and its applications to molecules and chemical reactions”. In: *International Journal of Quantum Chemistry* 20.5 (Nov. 1981), pp. 955–1065. ISSN: 1097-461X. DOI: [10.1002/qua.560200502](https://doi.org/10.1002/qua.560200502). URL: <http://dx.doi.org/10.1002/qua.560200502>.
- [26] Joshua Goings. *Broken Symmetries in Hartree-Fock*. 2014. URL: <https://joshuagoings.com/2014/10/14/broken-symmetries-in-hartree-fock/>.
- [27] Tim Gould, Leeor Kronik, and Stefano Pittalis. “Charge transfer excitations from exact and approximate ensemble Kohn-Sham theory”. In: *The Journal of Chemical Physics* 148.17 (May 2018). 174101. ISSN: 0021-9606. DOI: [10.1063/1.5022832](https://doi.org/10.1063/1.5022832). eprint: https://pubs.aip.org/aip/jcp/article-pdf/doi/10.1063/1.5022832/15540688/174101_1_online.pdf. URL: <https://doi.org/10.1063/1.5022832>.
- [28] Tim Gould, Leeor Kronik, and Stefano Pittalis. “Double excitations in molecules from ensemble density functionals: Theory and approximations”. In: *Phys. Rev. A* 104 (2 Aug. 2021), p. 022803. DOI: [10.1103/PhysRevA.104.022803](https://doi.org/10.1103/PhysRevA.104.022803). URL: <https://link.aps.org/doi/10.1103/PhysRevA.104.022803>.
- [29] Tim Gould and Stefano Pittalis. “Density-Driven Correlations in Many-Electron Ensembles: Theory and Application for Excited States”. In: *Phys. Rev. Lett.* 123 (1 July 2019), p. 016401. DOI: [10.1103/PhysRevLett.123.016401](https://doi.org/10.1103/PhysRevLett.123.016401). URL: <https://link.aps.org/doi/10.1103/PhysRevLett.123.016401>.
- [30] Tim Gould and Stefano Pittalis. “Hartree and Exchange in Ensemble Density Functional Theory: Avoiding the Nonuniqueness Disaster”. In: *Phys. Rev. Lett.* 119 (24 Dec. 2017), p. 243001. DOI: [10.1103/PhysRevLett.119.243001](https://doi.org/10.1103/PhysRevLett.119.243001). URL: <https://link.aps.org/doi/10.1103/PhysRevLett.119.243001>.

- [31] E. K. U. Gross, L. N. Oliveira, and W. Kohn. “Density-functional theory for ensembles of fractionally occupied states. I. Basic formalism”. In: *Phys. Rev. A* 37 (8 Apr. 1988), pp. 2809–2820. DOI: [10.1103/PhysRevA.37.2809](https://doi.org/10.1103/PhysRevA.37.2809). URL: <https://link.aps.org/doi/10.1103/PhysRevA.37.2809>.
- [32] E. K. U. Gross, L. N. Oliveira, and W. Kohn. “Rayleigh-Ritz variational principle for ensembles of fractionally occupied states”. In: *Phys. Rev. A* 37 (8 Apr. 1988), pp. 2805–2808. DOI: [10.1103/PhysRevA.37.2805](https://doi.org/10.1103/PhysRevA.37.2805). URL: <https://link.aps.org/doi/10.1103/PhysRevA.37.2805>.
- [33] G. G. Hall. “The Molecular Orbital Theory of Chemical Valency. VIII. A Method of Calculating Ionization Potentials”. In: *Proceedings of the Royal Society of London Series A* 205.1083 (Mar. 1951), pp. 541–552. DOI: [10.1098/rspa.1951.0048](https://doi.org/10.1098/rspa.1951.0048).
- [34] D. R. Hartree. “The Wave Mechanics of an Atom with a Non-Coulomb Central Field. Part I. Theory and Methods”. In: *Mathematical Proceedings of the Cambridge Philosophical Society* 24.1 (1928), pp. 89–110. DOI: [10.1017/S0305004100011919](https://doi.org/10.1017/S0305004100011919).
- [35] T Helgaker, P Jørgensen, and J Olsen. *Molecular Electronic Structure Theory*. Chichester: John Wiley & Sons, LTD, 2000.
- [36] M. J. P. Hodgson, J. Wetherell, and Emmanuel Fromager. “Exact exchange-correlation potentials for calculating the fundamental gap with a fixed number of electrons”. In: *Phys. Rev. A* 103 (1 Jan. 2021), p. 012806. DOI: [10.1103/PhysRevA.103.012806](https://doi.org/10.1103/PhysRevA.103.012806). URL: <https://link.aps.org/doi/10.1103/PhysRevA.103.012806>.
- [37] P. Hohenberg and W. Kohn. “Inhomogeneous Electron Gas”. In: *Phys. Rev.* 136 (3B Nov. 1964), B864–B871. DOI: [10.1103/PhysRev.136.B864](https://doi.org/10.1103/PhysRev.136.B864). URL: <https://link.aps.org/doi/10.1103/PhysRev.136.B864>.
- [38] J. F. Janak. “Proof that $\frac{\partial E}{\partial n_i} = \epsilon$ in density-functional theory”. In: *Phys. Rev. B* 18 (12 Dec. 1978), pp. 7165–7168. DOI: [10.1103/PhysRevB.18.7165](https://doi.org/10.1103/PhysRevB.18.7165). URL: <https://link.aps.org/doi/10.1103/PhysRevB.18.7165>.
- [39] Frank Jensen. *Introduction to Computational Chemistry*. Hoboken, NJ, USA: John Wiley and Sons, Inc., 2006. ISBN: 0470011874.
- [40] Russell Johnson. *NIST Computational Chemistry Comparison and Benchmark Database*. 2022-05-22 2022. URL: <http://cccbdb.nist.gov/> (visited on 09/16/2023).
- [41] K. Kim and K. D. Jordan. “Comparison of Density Functional and MP2 Calculations on the Water Monomer and Dimer”. In: *The Journal of Physical Chemistry* 98.40 (1994), pp. 10089–10094. DOI: [10.1021/j100091a024](https://doi.org/10.1021/j100091a024). eprint: <https://doi.org/10.1021/j100091a024>. URL: <https://doi.org/10.1021/j100091a024>.
- [42] W. Kohn and L. J. Sham. “Self-Consistent Equations Including Exchange and Correlation Effects”. In: *Phys. Rev.* 140 (4A Nov. 1965), A1133–A1138. DOI: [10.1103/PhysRev.140.A1133](https://doi.org/10.1103/PhysRev.140.A1133). URL: <https://link.aps.org/doi/10.1103/PhysRev.140.A1133>.

- [43] T Koopmans. “Über die Zuordnung von Wellenfunktionen und Eigenwerten zu den Einzelnen Elektronen Eines Atoms”. In: *Physica* 1.1 (1934), pp. 104–113. ISSN: 0031-8914. DOI: [https://doi.org/10.1016/S0031-8914\(34\)90011-2](https://doi.org/10.1016/S0031-8914(34)90011-2). URL: <https://www.sciencedirect.com/science/article/pii/S0031891434900112>.
- [44] Eli Kraisler and Leeor Kronik. “Elimination of the asymptotic fractional dissociation problem in Kohn-Sham density-functional theory using the ensemble-generalization approach”. In: *Phys. Rev. A* 91 (3 Mar. 2015), p. 032504. DOI: [10.1103/PhysRevA.91.032504](https://doi.org/10.1103/PhysRevA.91.032504). URL: <https://link.aps.org/doi/10.1103/PhysRevA.91.032504>.
- [45] Eli Kraisler and Leeor Kronik. “Fundamental gaps with approximate density functionals: The derivative discontinuity revealed from ensemble considerations”. In: *The Journal of Chemical Physics* 140.18 (2014), 18A540. DOI: [10.1063/1.4871462](https://doi.org/10.1063/1.4871462). eprint: <https://doi.org/10.1063/1.4871462>. URL: <https://doi.org/10.1063/1.4871462>.
- [46] Eli Kraisler and Leeor Kronik. “Piecewise Linearity of Approximate Density Functionals Revisited: Implications for Frontier Orbital Energies”. In: *Phys. Rev. Lett.* 110 (12 Mar. 2013), p. 126403. DOI: [10.1103/PhysRevLett.110.126403](https://doi.org/10.1103/PhysRevLett.110.126403). URL: <https://link.aps.org/doi/10.1103/PhysRevLett.110.126403>.
- [47] Eli Kraisler et al. “Effect of ensemble generalization on the highest-occupied Kohn-Sham eigenvalue”. In: *The Journal of Chemical Physics* 143.10 (Sept. 2015), p. 104105. ISSN: 0021-9606. DOI: [10.1063/1.4930119](https://doi.org/10.1063/1.4930119). eprint: https://pubs.aip.org/aip/jcp/article-pdf/doi/10.1063/1.4930119/15502126/104105_1_online.pdf. URL: <https://doi.org/10.1063/1.4930119>.
- [48] Stephan Kümmel and Leeor Kronik. “Orbital-dependent density functionals: Theory and applications”. In: *Rev. Mod. Phys.* 80 (1 Jan. 2008), pp. 3–60. DOI: [10.1103/RevModPhys.80.3](https://doi.org/10.1103/RevModPhys.80.3). URL: <https://link.aps.org/doi/10.1103/RevModPhys.80.3>.
- [49] S. Kurth, M.A.L. Marques, and E.K.U. Gross. “Density-Functional Theory”. In: *Encyclopedia of Condensed Matter Physics*. Ed. by Franco Bassani, Gerald L. Liedl, and Peter Wyder. Oxford: Elsevier, 2005, pp. 395–402. ISBN: 978-0-12-369401-0. DOI: <https://doi.org/10.1016/B0-12-369401-9/00445-9>. URL: <https://www.sciencedirect.com/science/article/pii/B0123694019004459>.
- [50] Sharon Lavie, Yuli Goshen, and Eli Kraisler. “Ionization Potentials and Fundamental Gaps in Atomic Systems from the Ensemble-DFT Approach”. In: (2023). arXiv: [2304.08250](https://arxiv.org/abs/2304.08250) [[cond-mat.mtrl-sci](https://arxiv.org/abs/2304.08250)].
- [51] Chengteh Lee, Weitao Yang, and Robert G. Parr. “Development of the Colle-Salvetti correlation-energy formula into a functional of the electron density”. In: *Phys. Rev. B* 37 (2 Jan. 1988), pp. 785–789. DOI: [10.1103/PhysRevB.37.785](https://doi.org/10.1103/PhysRevB.37.785). URL: <https://link.aps.org/doi/10.1103/PhysRevB.37.785>.
- [52] Mel Levy. “Electron densities in search of Hamiltonians”. In: *Phys. Rev. A* 26 (3 Sept. 1982), pp. 1200–1208. DOI: [10.1103/PhysRevA.26.1200](https://doi.org/10.1103/PhysRevA.26.1200). URL: <https://link.aps.org/doi/10.1103/PhysRevA.26.1200>.

- [53] Mel Levy. “Universal variational functionals of electron densities, first-order density matrices, and natural spin-orbitals and solution of the $\{i_j, v_j\}/i_j$ -representability problem”. In: *Proceedings of the National Academy of Sciences* 76.12 (1979), pp. 6062–6065. DOI: [10.1073/pnas.76.12.6062](https://doi.org/10.1073/pnas.76.12.6062). eprint: <https://www.pnas.org/doi/pdf/10.1073/pnas.76.12.6062>. URL: <https://www.pnas.org/doi/abs/10.1073/pnas.76.12.6062>.
- [54] Elliott H. Lieb. “Density functionals for coulomb systems”. In: *International Journal of Quantum Chemistry* 24.3 (1983), pp. 243–277. DOI: <https://doi.org/10.1002/qua.560240302>. eprint: <https://onlinelibrary.wiley.com/doi/pdf/10.1002/qua.560240302>. URL: <https://onlinelibrary.wiley.com/doi/abs/10.1002/qua.560240302>.
- [55] Pierre-François Loos and Emmanuel Fromager. “A weight-dependent local correlation density-functional approximation for ensembles”. In: *The Journal of Chemical Physics* 152.21 (2020), p. 214101. DOI: [10.1063/5.0007388](https://doi.org/10.1063/5.0007388). eprint: <https://doi.org/10.1063/5.0007388>. URL: <https://doi.org/10.1063/5.0007388>.
- [56] Neepa T. Maitra and Kieron Burke. “Demonstration of initial-state dependence in time-dependent density-functional theory”. In: *Phys. Rev. A* 63 (4 Mar. 2001), p. 042501. DOI: [10.1103/PhysRevA.63.042501](https://link.aps.org/doi/10.1103/PhysRevA.63.042501). URL: <https://link.aps.org/doi/10.1103/PhysRevA.63.042501>.
- [57] Neepa T. Maitra, Kieron Burke, and Chris Woodward. “Memory in Time-Dependent Density Functional Theory”. In: *Phys. Rev. Lett.* 89 (2 June 2002), p. 023002. DOI: [10.1103/PhysRevLett.89.023002](https://link.aps.org/doi/10.1103/PhysRevLett.89.023002). URL: <https://link.aps.org/doi/10.1103/PhysRevLett.89.023002>.
- [58] Richard M. Martin, Lucia Reining, and David M. Ceperley. *Interacting Electrons: Theory and Computational Approaches*. Cambridge University Press, 2016. DOI: [10.1017/CB09781139050807](https://doi.org/10.1017/CB09781139050807).
- [59] Clotilde Marut et al. “Weight dependence of local exchange–correlation functionals in ensemble density-functional theory: double excitations in two-electron systems”. In: *Faraday Discuss.* 224 (0 2020), pp. 402–423. DOI: [10.1039/D0FD00059K](https://dx.doi.org/10.1039/D0FD00059K). URL: <http://dx.doi.org/10.1039/D0FD00059K>.
- [60] Paula Mori-Sánchez, Aron J. Cohen, and Weitao Yang. “Discontinuous Nature of the Exchange-Correlation Functional in Strongly Correlated Systems”. In: *Phys. Rev. Lett.* 102 (6 Feb. 2009), p. 066403. DOI: [10.1103/PhysRevLett.102.066403](https://link.aps.org/doi/10.1103/PhysRevLett.102.066403). URL: <https://link.aps.org/doi/10.1103/PhysRevLett.102.066403>.
- [61] Paula Mori-Sánchez, Aron J. Cohen, and Weitao Yang. “Localization and Delocalization Errors in Density Functional Theory and Implications for Band-Gap Prediction”. In: *Phys. Rev. Lett.* 100 (14 Apr. 2008), p. 146401. DOI: [10.1103/PhysRevLett.100.146401](https://link.aps.org/doi/10.1103/PhysRevLett.100.146401). URL: <https://link.aps.org/doi/10.1103/PhysRevLett.100.146401>.

- [62] Paula Mori-Sánchez, Aron J. Cohen, and Weitao Yang. “Many-electron self-interaction error in approximate density functionals”. In: *The Journal of Chemical Physics* 125.20 (2006), p. 201102. DOI: [10.1063/1.2403848](https://doi.org/10.1063/1.2403848). eprint: <https://doi.org/10.1063/1.2403848>. URL: <https://doi.org/10.1063/1.2403848>.
- [63] Bastien Mussard and Julien Toulouse. “Fractional-charge and fractional-spin errors in range-separated density-functional theory”. In: *Molecular Physics* 115 (2016), pp. 161–173. URL: <https://api.semanticscholar.org/CorpusID:13683991>.
- [64] Robert G. Parr and Libero J. Bartolotti. “Some remarks on the density functional theory of few-electron systems”. In: *The Journal of Physical Chemistry* 87.15 (1983), pp. 2810–2815. DOI: [10.1021/j100238a023](https://doi.org/10.1021/j100238a023). eprint: <https://doi.org/10.1021/j100238a023>. URL: <https://doi.org/10.1021/j100238a023>.
- [65] Robert G. Parr and Weitao Yang. *Density-Functional Theory of Atoms and Molecules*. Oxford University Press, USA, 1989.
- [66] John P. Perdew. “Size-Consistency, Self-Interaction Correction, and Derivative Discontinuity in Density Functional Theory”. In: *Density Functional Theory of Many-Fermion Systems*. Ed. by Per-Olov Löwdin. Vol. 21. Advances in Quantum Chemistry. Academic Press, 1990, pp. 113–134. DOI: [https://doi.org/10.1016/S0065-3276\(08\)60594-8](https://doi.org/10.1016/S0065-3276(08)60594-8). URL: <https://www.sciencedirect.com/science/article/pii/S0065327608605948>.
- [67] John P. Perdew and Mel Levy. “Comment on “Significance of the highest occupied Kohn-Sham eigenvalue””. In: *Phys. Rev. B* 56 (24 Dec. 1997), pp. 16021–16028. DOI: [10.1103/PhysRevB.56.16021](https://link.aps.org/doi/10.1103/PhysRevB.56.16021). URL: <https://link.aps.org/doi/10.1103/PhysRevB.56.16021>.
- [68] John P. Perdew and Mel Levy. “Physical Content of the Exact Kohn-Sham Orbital Energies: Band Gaps and Derivative Discontinuities”. In: *Phys. Rev. Lett.* 51 (20 Nov. 1983), pp. 1884–1887. DOI: [10.1103/PhysRevLett.51.1884](https://link.aps.org/doi/10.1103/PhysRevLett.51.1884). URL: <https://link.aps.org/doi/10.1103/PhysRevLett.51.1884>.
- [69] John P. Perdew and Karla Schmidt. “Jacob’s ladder of density functional approximations for the exchange-correlation energy”. In: *AIP Conference Proceedings* 577.1 (2001), pp. 1–20. DOI: [10.1063/1.1390175](https://doi.org/10.1063/1.1390175). eprint: <https://aip.scitation.org/doi/pdf/10.1063/1.1390175>. URL: <https://aip.scitation.org/doi/abs/10.1063/1.1390175>.
- [70] John P. Perdew et al. “Density-Functional Theory for Fractional Particle Number: Derivative Discontinuities of the Energy”. In: *Phys. Rev. Lett.* 49 (23 Dec. 1982), pp. 1691–1694. DOI: [10.1103/PhysRevLett.49.1691](https://link.aps.org/doi/10.1103/PhysRevLett.49.1691). URL: <https://link.aps.org/doi/10.1103/PhysRevLett.49.1691>.
- [71] J. A. Pople and R. K. Nesbet. “Self-Consistent Orbitals for Radicals”. In: *The Journal of Chemical Physics* 22.3 (1954), pp. 571–572. DOI: [10.1063/1.1740120](https://doi.org/10.1063/1.1740120). eprint: <https://doi.org/10.1063/1.1740120>. URL: <https://doi.org/10.1063/1.1740120>.

- [72] C. C. J. Roothaan. “New Developments in Molecular Orbital Theory”. In: *Rev. Mod. Phys.* 23 (2 Apr. 1951), pp. 69–89. DOI: <https://doi.org/10.1103/RevModPhys.23.69>. URL: <https://link.aps.org/doi/10.1103/RevModPhys.23.69>.
- [73] Erich Runge and E. K. U. Gross. “Density-Functional Theory for Time-Dependent Systems”. In: *Phys. Rev. Lett.* 52 (12 Mar. 1984), pp. 997–1000. DOI: [10.1103/PhysRevLett.52.997](https://doi.org/10.1103/PhysRevLett.52.997). URL: <https://link.aps.org/doi/10.1103/PhysRevLett.52.997>.
- [74] Thais R. Scott et al. *Exact Conditions for Ensemble Density Functional Theory*. 2023. arXiv: [2307.00187](https://arxiv.org/abs/2307.00187) [cond-mat.str-el].
- [75] Bruno Senjean and Emmanuel Fromager. “N-centered ensemble density-functional theory for open systems”. In: *International Journal of Quantum Chemistry* 120.21 (2020), e26190. DOI: <https://doi.org/10.1002/qua.26190>. eprint: <https://onlinelibrary.wiley.com/doi/pdf/10.1002/qua.26190>. URL: <https://onlinelibrary.wiley.com/doi/abs/10.1002/qua.26190>.
- [76] Bruno Senjean and Emmanuel Fromager. “Unified formulation of fundamental and optical gap problems in density-functional theory for ensembles”. In: *Phys. Rev. A* 98 (2 Aug. 2018), p. 022513. DOI: [10.1103/PhysRevA.98.022513](https://doi.org/10.1103/PhysRevA.98.022513). URL: <https://link.aps.org/doi/10.1103/PhysRevA.98.022513>.
- [77] Bruno Senjean et al. “Combining linear interpolation with extrapolation methods in range-separated ensemble density functional theory”. In: *Molecular Physics* 114.7-8 (2016), pp. 968–981. DOI: [10.1080/00268976.2015.1119902](https://doi.org/10.1080/00268976.2015.1119902). eprint: <https://doi.org/10.1080/00268976.2015.1119902>. URL: <https://doi.org/10.1080/00268976.2015.1119902>.
- [78] Bruno Senjean et al. “Linear interpolation method in ensemble Kohn-Sham and range-separated density-functional approximations for excited states”. In: *Phys. Rev. A* 92 (1 July 2015), p. 012518. DOI: [10.1103/PhysRevA.92.012518](https://doi.org/10.1103/PhysRevA.92.012518). URL: <https://link.aps.org/doi/10.1103/PhysRevA.92.012518>.
- [79] J. C. Slater. “A Simplification of the Hartree-Fock Method”. In: *Phys. Rev.* 81 (3 Feb. 1951), pp. 385–390. DOI: [10.1103/PhysRev.81.385](https://doi.org/10.1103/PhysRev.81.385). URL: <https://link.aps.org/doi/10.1103/PhysRev.81.385>.
- [80] J. C. Slater. “The Theory of Complex Spectra”. In: *Phys. Rev.* 34 (10 Nov. 1929), pp. 1293–1322. DOI: [10.1103/PhysRev.34.1293](https://doi.org/10.1103/PhysRev.34.1293). URL: <https://link.aps.org/doi/10.1103/PhysRev.34.1293>.
- [81] Tamar Stein et al. “Curvature and Frontier Orbital Energies in Density Functional Theory”. In: *The Journal of Physical Chemistry Letters* 3.24 (2012). PMID: 26291104, pp. 3740–3744. DOI: [10.1021/jz3015937](https://doi.org/10.1021/jz3015937). eprint: <https://doi.org/10.1021/jz3015937>. URL: <https://doi.org/10.1021/jz3015937>.

-
- [82] Tamar Stein et al. “Fundamental Gaps in Finite Systems from Eigenvalues of a Generalized Kohn-Sham Method”. In: *Phys. Rev. Lett.* 105 (26 Dec. 2010), p. 266802. DOI: [10.1103/PhysRevLett.105.266802](https://doi.org/10.1103/PhysRevLett.105.266802). URL: <https://link.aps.org/doi/10.1103/PhysRevLett.105.266802>.
- [83] P. J. Stephens et al. “Ab Initio Calculation of Vibrational Absorption and Circular Dichroism Spectra Using Density Functional Force Fields”. In: *The Journal of Physical Chemistry* 98.45 (1994), pp. 11623–11627. DOI: [10.1021/j100096a001](https://doi.org/10.1021/j100096a001). eprint: <https://doi.org/10.1021/j100096a001>. URL: <https://doi.org/10.1021/j100096a001>.
- [84] Attila Szabó and Neil S. Ostlund. “Modern quantum chemistry : introduction to advanced electronic structure theory”. In: 1982.
- [85] Andreas K Theophilou. “The energy density functional formalism for excited states”. In: *Journal of Physics C: Solid State Physics* 12 (1979), pp. 5419–5430.
- [86] L. H. Thomas. “The calculation of atomic fields”. In: *Mathematical Proceedings of the Cambridge Philosophical Society* 23.5 (1927), pp. 542–548. DOI: [10.1017/S0305004100011683](https://doi.org/10.1017/S0305004100011683).
- [87] Julien Toulouse. *Introduction to density-functional theory*. Sept. 2019. URL: https://www.lct.jussieu.fr/pagesperso/toulouse/enseignement/introduction_dft.pdf.
- [88] Julien Toulouse. *Introduction to quantum chemistry*. Jan. 2021. URL: https://www.lct.jussieu.fr/pagesperso/toulouse/enseignement/introduction_qc.pdf.
- [89] S. H. Vosko, L. Wilk, and M. Nusair. “Accurate spin-dependent electron liquid correlation energies for local spin density calculations: a critical analysis”. In: *Canadian Journal of Physics* 58.8 (1980), pp. 1200–1211. DOI: [10.1139/p80-159](https://doi.org/10.1139/p80-159). eprint: <https://doi.org/10.1139/p80-159>. URL: <https://doi.org/10.1139/p80-159>.
- [90] Zeng-hui Yang et al. “Exact and approximate Kohn-Sham potentials in ensemble density-functional theory”. In: *Phys. Rev. A* 90 (4 Oct. 2014), p. 042501. DOI: [10.1103/PhysRevA.90.042501](https://doi.org/10.1103/PhysRevA.90.042501). URL: <https://link.aps.org/doi/10.1103/PhysRevA.90.042501>.